UNIVERSITY OF MINNESOTA

This is to certify that I have examined this bound copy of a doctoral dissertation by

Amartya Sankar Banerjee

and have found that it is complete and satisfactory in all respects,
and that any and all revisions required by the final
examining committee have been made.

Richard D. James , Ryan S. Elliott

Names of Faculty Advisers

_____

Signatures of Faculty Advisers

_____

Date

GRADUATE SCHOOL

Density Functional Methods for Objective Structures: Theory and Simulation Schemes

A DISSERTATION
SUBMITTED TO THE FACULTY OF THE GRADUATE SCHOOL
OF THE UNIVERSITY OF MINNESOTA
BY

Amartya Sankar Banerjee

IN PARTIAL FULFILLMENT OF THE REQUIREMENTS
FOR THE DEGREE OF
Doctor of Philosophy

Richard D. James, Adviser
Ryan S. Elliott, Co-Adviser

December 2013

Acknowledgments

I want to take this opportunity to express my gratitude to all those who have helped me and inspired me during my studies. First and foremost, I would like to thank my advisers Prof. Richard D. James and Prof. Ryan S. Elliott for giving me the opportunity to work on the interesting and challenging problem of computing the electronic properties of objective structures. Their help and guidance has been invaluable. I also greatly value their patience and understanding as well as the freedom that they gave me in shaping my research work. It has been an enjoyable journey and at the same time, it has been a great learning experience.

I would like to thank my committee members Prof. Ellad Tadmor and Prof. Traian Dumitrica for their feedback and suggestions. I would like to express special thanks and gratitude to Prof. Phanish Suryanarayana (Georgia Tech.) for his many suggestions, help and discussions during the implementation phase of this project. I would also like to thank Phani Motamarri (U. Michigan) and Prof. Vikram Gavini (U. Michigan) for their help and suggestions and for sharing some of the details of their work which made it easier for me to carry out my own validation studies.

I would like to acknowledge support from the funding agencies (NSF, DOE, AFOSR) over the years. Most of the simulations in this work were carried out using clusters from the Minnesota Supercomputing Institute.

I would like to thank my parents for their love and encouragement. I owe my interest in pursuing a career in science and mathematics to my father, who sparked my curiosity in these subjects as a child.

I have been fortunate to have many talented friends and colleagues at the University of Minnesota. I would like to thank Nikhil Admal, Vincent Jusuf, Amit Singh, Dan Karls, Xian Chen, Vivekanand Dabade, Subrahmanyam Pattamatta, Yintao Song, Henrik van Lengerich and Shameek Bose for our many discussions and for the good times we have shared over the years.

Finally, without the love, encouragment and untiring support of my wife Neha, this work would perhaps not have been possible. This thesis is dedicated to her.

Dedicated to my wife Neha.

Abstract

Objective structures are atomic/molecular configurations which generalize the notion of crystals and are such that all the constituent atoms/molecules of the structure see the same environment up to orthogonal transformations and translations. Objective structures are ubiquitously present in all of materials science, biology and nanotechnology and examples of these structures include nanotubes, buckyballs, tail sheaths and capsids of viruses, graphene sheets and molecular bilayers. Due to their association with large degrees of symmetry, objective structures are likely to be a fertile source of materials with remarkable material properties – particularly, collective material properties such as ferromagnetism and ferroelectricity. A systematic study of objective structures therefore, is likely to lead to the discovery of novel materials. At the same time, formulation of computational methods specifically designed for studying objective structures, is likely to lead to the development of novel nanomechanics simulations methodologies.

Following this line of thought, this thesis deals with the development of Objective Density Functional Theory – a suite of rigorously formulated Density Functional methods and numerical algorithms for carrying out abinitio simulation studies of objective structures. Drawing analogies from the classical plane-wave density functional method of solid state physics, our focus has been on the development of novel spectral schemes for studying objective structures using Kohn-Sham Density Functional Theory. In this work, we demonstrate how the equations of Kohn-Sham Density Functional Theory for objective structures admit interpretation in terms of symmetry adapted cell problems. We propose complete orthonormal basis sets for discretizing these cell problems. Next, we discuss the significant challenges associated with the efficient solution of the discretized cell problems and our progress in addressing these challenges through a variety of numerical and algorithmic strategies. Many of these strategies and methods have been implemented within the framework of a powerful first principles simulation package called ClusterES (Cluster Electronic Structure) that we designed and developed as part of this work.

We end with some examples highlighting the efficiency and accuracy of our numerical methods as well as a brief discussion of ongoing applications of our spectral schemes to the study of some problems in nano-mechanics.

Contents

List of Figures

Chapter 1

Introduction

Prediction of new materials with properties of engineering and scientific interest is the central goal of theoretical materials science.[1] Methods used by the theoretical materials scientist often include sophisticated mathematical tools for modeling and analysis of the physical phenomena associated with materials, as well as the numerical simulation of these phenomena. Most of these phenomena involve multiple temporal and spatial scales and so, the physical theories employed range from continuum to quantum mechanics [Tadmor and Miller, 2011].

Physical symmetry usually plays a very important role in the theories used for the modeling and simulation of materials. Presence of symmetry is usually associated with interesting material properties, or sometimes, symmetry provides an explanation for the lack of such properties. On the continuum scale for instance, one can employ symmetry related ideas to conclude that an isotropic elastic material can have only two independent elastic constants [Gurtin, 1981]. At the molecular level, symmetry related ideas can be used to draw conclusions about the vibrational spectra and optical properties of molecules [Hammermesh, 1989]. In fact, the most widely studied molecular structures in materials science and solid state physics are crystals, whose wide variety of interesting material properties are usually directly related to their underlying space group symmetries [Lax, 2001; Hammermesh, 1989].

The usual manner by which one searches for materials with interesting properties, is what can be called a constitution based search. In this approach, different atomic and molecular

[1] As explained later in this chapter, for maintatining coherence and continuity, portions of the contents of this chapter are adopted verbatim from our earlier work [Banerjee, 2011].

constitutions are envisioned and one tries to systematically verify if the material resulting from such a constitution has any interesting material properties. Given the important role that molecular arrangement and structure play in the determination of material properties, one can adopt a slightly different viewpoint in which the search for new materials is based on probing different atomic and molecular structures satisfying some imposed requirements. In particular, since structural symmetry seems to play a rather important role in the occurrence of interesting material properties, a structure based search for new materials could be organized and made systematic by means of classification based on different symmetry groups. The objective structures frame-work seems to provide a unified approach for systematically carrying out this program.

As defined in James [2006], an *objective atomic structure* is a collection of atoms, represented by mass points or ions, for which every atom sees precisely the same atomic environment up to orthogonal transformation and translation. An *objective molecular structure* is a collection of molecules in which corresponding atoms in each molecule see the same environment up to orthogonal transformation and translation. It is clear from these definitions that objective structures are intrinsically associated with symmetry and therefore, one might hope to make a systematic, structure based search for new materials with interesting properties by looking at all possible objective structures.

Some of the most widely studied atomic/molecular structures in materials science and nanotechnology fall into the category of objective structures [James, 2006]. Indeed, all perfect crystals are objective structures, as are nanotubes of arbitrary chirality. The list of objective structures also includes (but is not limited to) buckyballs, tail sheaths and capsids of viruses, graphene sheets and molecular bilayers. Figure 1.1 shows a collection of some non-crystalline objective structures.

The objective structures framework has already been linked to a variety of materials applications. Dumitrica and James [2007] have developed *objective molecular dynamics*, a natural extension of the classical technique of periodic molecular dynamics [Allen and Tildesley, 1987; Parrinello and Rahman, 1980], to objective structures. Dumitrica and James [2007] have used their method to study instability modes of nanotubes using empirical potentials. There have been extensions of this work to tightbinding calculations as well [Zhang et al., 2009, 2008]. The objective structures framework has also been used, in conjunction with multiscale ideas, for the study of viscometric flows and the design of viscometers [Dayal and James, 2010, 2011]. With the objective structures framework already being used for molecular level and mechanics simulations, it is quite natural to extend the

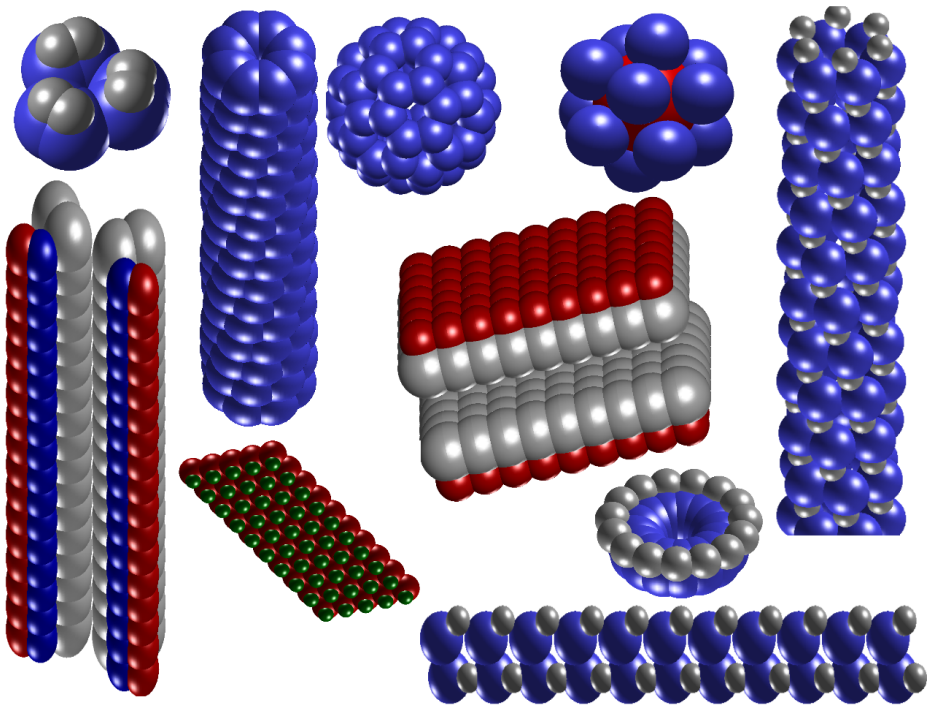

Figure 1.1: A zoology of objective structures: Each atom of the same color "sees" the same environment upto isometries. (Boundary effects for structures of infinite extent are to be ignored)

framework to the electronic structure level and this work is meant to be a step towards that goal. In addition to allowing for novel mechanics , as conjectured in [James, 2006], electronic properties of objective structures are very likely to be interesting in themselves: indeed, the notion of "seeing the same environment" is likely to lead to objective structures which display collective material properties such as ferromagnetism and ferroelectricity. This is depicted schematically in Figure 1.2.

To use the objective structures framework for searching new materials, a key step is to identify all possible objective structures. This question turns out to be intimately related to the derivation of all possible discrete groups of isometries in three dimensions [Dayal et al., 2013]. The derivation of these groups is a classical topic [Opechowski, 1986] and some of the groups are summarized in the International Tables of Crystallography [Hahn, 2003]. Of special interest for objective structures are the subperiodic groups, that is, the ones that do not contain three linearly independent translations. Volume E of the International Tables contains an incomplete listing of the subperiodic groups. Another problem with the listings of these groups is that only the abstract groups are listed, whereas for using the objective structures framework, the explicit isometries, and particularly the allowed

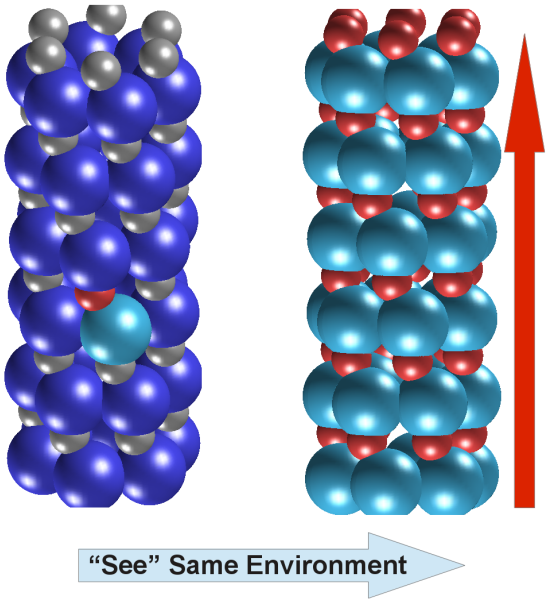

Figure 1.2: Schematic of how collective properties might emerge from objective structres: On the left, an objective strutcture develops a charge separation over its constituent atoms (red and light blue atoms). "Seeing the same environment" would now require every other set of atoms on this structure to deveolp a similar charge separation. This could result an overall polarization to develop in the structure (red arrow).

parameter dependence of these isometries, is needed. Dayal et al. [2013] have calculated from the basic definition, the explicit forms of all subperiodic, discrete groups of isometries and therefore, we now have an exhaustive list of all possible objective structures.

The effects of physical symmetry on electronic structure have been well studied in many cases. The work of F. Bloch on the single electron theory of a crystalline solid [Bloch, 1929], is perhaps one of the earliest works in this direction. In Bouckaert et al. [1936], an explicit connection of the Bloch theory with space group symmetries was made. These works have subsequently led to the formulation of symmetry adapted quadrature and Brillouin zone sampling techniques [te Velde and Baerends, 1992; Evarestov and Smirnov, 1983; Defranceschi and Le Bris, 2000], as well as simplifications in Linear Combination of Atomic Orbital (LCAO) based methods [Slater and Koster, 1954; Roothaan, 1960; Zicovich-Wilson and Dovesi, 1998a,b]. While the above mentioned works are primarily concerned with systems that have periodic and/or point group symmetries, there have been extensions of these works to helical and other quasi one-dimensional systems [Milosević et al., 2006; Dakić et al., 2009; White et al., 1993]. Some popular electronic structure computation codes now have some degrees of symmetry exploitation routines built into them.

Examples of such codes would include the packages CRYSTAL [Noel et al., 2010], turbomole [Ahlrichs et al., 1989], fhi96md [Bockstedte et al., 1997], Gulp [Gale, 1997] and PARSEC [Kronik et al., 2006].

Compared to the existing literature, our methodology is different in two respects. First, our point of view is that the literature on symmetry adapted techniques seems to be missing the unifying theme that the objective structures framework provides. It is also not clear to us, how the symmetry principles that have been employed in some of the aforementioned literature, can be rigorously justified from first principles. For instance, while dealing with point group symmetries, theorems from group representation, in the context of finite dimensional vector spaces, are often cited (see for instance Noel et al. [2010]). The connection between this finite dimensional representation theory, and the solutions of the equations of density functional theory (which represent a nonlinear infinite dimensional problem) are not made clear however. In particular, these works do not demonstrate that much like the case of crystals, there is a natural "cell problem" associated with the electronic structure computation problem of atomic/molecular structures that are associated with non-periodic symmetries.

It is our hope, that this work will take an important step towards addressing some of the above issues, in a mathematically rigorous way. For the purpose of analyzing how the equations of density functional theory interact with underlying symmetry, we have formulated an appropriate representation theory on a general class of Hilbert spaces. This has helped us in establishing clear connections between electronic structure calculation of objective structures and the harmonic analysis of finite groups of isometries. In addition, we have also rigorously formulated a version of the classical Bloch theorem of solids state phsyics, for structures generated by helical groups. In spirit, this work extends the canonical analysis of periodic systems that is carried out using the Fourier transform, to systems with helical and point group symmetries. Our work in this direction first appeared in Banerjee [2011] and it predates the some what similar efforts in Fang et al. [2013] for carrying out symmetry adaptation for eigenvalue problems.

Secondly, as far as numerical implementation is concerened, most of the existing methodologies and computer codes fall either into the category of generic molecular codes which use the Linear Combination of Atomic Orbitals (LCAO) approach or generic periodic codes which use plane-waves. The implementation of symmetry in these codes is ad hoc: neither the basis sets used in the codes nor the numerical schemes used to solve the discretized equations are designed keeping objective structures or the objective structures framework

in mind.

To address this issue, we have specifically formulated basis sets and numerical schemes that integrate well with the objective structures framework. Starting from the observation that one of the most successful methods for solving the Kohn-Sham equations for periodic systems – the plane wave method – is a spectral method based on eigenfunction expansion, we have formulated in this work, spectral methods designed towards solving the Kohn-Sham equations for objective structures generated by finite groups of isometries or by infinite helical groups. This allows for efficient calculation of the electronic structure of these systems with high accuracy and systematic convergence properties without the need for any artifical periodicity. The basis functions in our methods form complete orthonormal sets and therefore, lead to simple discretized expressions. As a specific illustration of the use of our basis sets, we have developed from scratch a powerful code designed for the study of clusters. This code can study objective structures generated by arbitrary point group symmetries. Computation of the occupied eigenstates of the discretized Kohn-Sham Hamiltonian in this code is carried out using a combination of preconditioned block eigensolvers and Chebyshev polynomial filter accelarated subspace iterations. A variety of benchmark calculations employing local and non-local pseudopotentials conclusively demonstrate the ability of our code to handle arbitrary cluster systems efficiently. Adaptation of cyclic symmetry groups in this code allows us to study large nano-systems abinitio. A similar enterprise using the basis sets developed for helical groups currently constitutes on going work.

This work is meant to subsume our earlier efforts in formulating Density Functional Methods for Objective Structures as presented in Banerjee [2011]. As such, for the sake of completeness and for presenting a coherent overview of the entire work, portions of this thesis reproduce the contents of that earlier work either in essence or verbatim. Specifically, the introductory material in this chapter and the next one, as well as the representation theory tools used for formulation of cell problems for finite groups (Chapters 2, 3 and Appendix C) are directly adopted from Banerjee [2011]. The contents of Chapters 4 and 5 follow these earlier developments and they constitute more recent work. They are currently being prepared for submission to peer reviewed journals [Banerjee et al., 2014b,a].

The rest of this work is outlined as follows. Chapter 2 provides some of the basic background material on objective structures and density functional theory. Tools from abstract harmonic analysis / group representation theory that are used later in the work are also presented in this chapter. In Chapter 3, we formulate cell problems arising out of the electronic structure computation of objective structures generated by finite and helical groups. Chap-

ter 4 describes in detail the development of our spectral scheme for clusters. The various computational and algorithmic challenges (including issues about parallelization) associated with the development of this scheme are described in this chapter. Symmetry adapted spectral schemes are described in Chapter 5. Chapter 6 summarises the thesis and discusses ongoing efforts, especially in terms of various applications of the methods developed in this work.

Chapter 2

Background

We use this chapter to provide some background on the theory of objective structures, on some basic ideas from electronic structure calculation theories and also for building important tools from abstract harmonic analysis / group representation theory. This also provides us with a chance to introduce some notation that is employed later in this work. The material in this chapter is directly adopted from our earlier work in Banerjee [2011].

2.1 Isometry Groups and Objective Structures

Following James [2006] and Dayal et al. [2013] we adopt a mathematical definition of objective structures in terms of discrete groups of isometries. This requires that we first introduce a few related ideas. Let $\mathrm{Lin}(3)$ denote the set of linear transformations on $\mathbb{R}^3$ and let $\mathbf{O}(3)$ denote the orthogonal group in three dimensions, that is, $\mathbf{O}(3) = \{\mathbf{R} \in \mathrm{Lin}(3) : \mathbf{R}^T\mathbf{R} = \mathbf{I}\}$. We recall that an isometry is an affine map $\Upsilon : \mathbb{R}^3 \to \mathbb{R}^3$ of the form $\Upsilon = (\mathbf{R}|\mathbf{c})$ with $\mathbf{R} \in \mathbf{O}(3), \mathbf{c} \in \mathbb{R}^3$ such that the point $\mathbf{x} \in \mathbb{R}^3$ is mapped to the point $\mathbf{R}\mathbf{x} + \mathbf{c}$. As the name implies, isometries preserve distances (and hence angles), that is $\forall \mathbf{x}, \mathbf{y} \in \mathbb{R}^3,\ |\Upsilon(\mathbf{x}) - \Upsilon(\mathbf{y})| = |\mathbf{x} - \mathbf{y}|$. The product of two isometries $\Upsilon_1 = (\mathbf{R}_1|\mathbf{c}_1)$ and $\Upsilon_2 = (\mathbf{R}_2|\mathbf{c}_2)$ is defined as a composition of their maps, that is, $(\Upsilon_1 \circ \Upsilon_2)(\mathbf{x}) = \Upsilon_1(\Upsilon_2(\mathbf{x}))$. This implies that $\Upsilon_1 \circ \Upsilon_2$ admits the representation $(\mathbf{R}_1\mathbf{R}_2|\mathbf{R}_1\mathbf{c}_2 + \mathbf{c}_1)$. The identity isometry maps every $\mathbf{x} \in \mathbb{R}^3$ to itself and is represented by $(\mathbf{I}|\mathbf{0})$. It follows that the inverse of the isometry $\Upsilon = (\mathbf{R}|\mathbf{c})$ is the isometry $(\mathbf{R}^T| - \mathbf{R}^T\mathbf{c})$ and this is denoted as Υ^{-1}. A group of isometries is a set of isometries which includes the identity isometry and which forms a group with the product and inverse operations described above.

If $\mathcal{G}$ is a group of isometries, then the orbit of a point $\mathbf{x} \in \mathbb{R}^3$ is the set $\{\Upsilon(\mathbf{x}) : \Upsilon \in \mathcal{G}\}$

and we denote this as $\text{Orb}(\mathcal{G}, \mathbf{x})$. The set $\text{Stab}(\mathcal{G}, \mathbf{x})$ is the set of isometries whose action on $\mathbf{x}$ leave it invariant, that is $\text{Stab}(\mathcal{G}, \mathbf{x}) = \{\Upsilon \in \mathcal{G} : \Upsilon(\mathbf{x}) = \mathbf{x}\}$. We can easily verify that $\text{Stab}(\mathcal{G}, \mathbf{x})$ is in fact always a subgroup of $\mathcal{G}$ for any $\mathbf{x} \in \mathbb{R}^3$. A group of isometries is termed discrete if for every $\epsilon > 0$ and every $\mathbf{x}, \mathbf{y} \in \mathbb{R}^3$, the open ball of radius ϵ centered about $\mathbf{y}$ contains only finitely many points from the orbit of $\mathbf{x}$, that is:

$$\text{Orb}(\mathcal{G}, \mathbf{x}) \cap \mathcal{B}_\epsilon(\mathbf{y}) = \text{a finite set}, \ \forall \epsilon > 0 \text{ and } \forall \mathbf{x}, \mathbf{y} \in \mathbb{R}^3. \tag{2.1}$$

We are now in a position to define objective structures:

Definition 2.1.1. Let $M \subset \mathbb{R}^3$ be a finite collection of distinct points and let $\mathcal{G}$ be a discrete group of isometries such that $\text{Stab}(\mathcal{G}, \mathbf{x}) = \{(\mathbf{I}|\mathbf{0})\}$ or $\mathcal{G}$ for all $\mathbf{x} \in M$. Then

$$\mathcal{S} = \bigcup_{x \in M} \text{Orb}(\mathcal{G}, \mathbf{x}) \tag{2.2}$$

is called an objective structure with $\mathcal{G}$ as its underlying discrete group of isometries provided that there is at least one $\mathbf{x} \in M$ such that $\text{Stab}(\mathcal{G}, \mathbf{x}) = \{(\mathbf{I}|\mathbf{0})\}$. In particular, if $\text{Stab}(\mathcal{G}, \mathbf{x}) = \{(\mathbf{I}|\mathbf{0})\}$ for all $\mathbf{x} \in M$, then we say that the objective structure is fixed point free. If M consists of only one point then the we say that $\mathcal{S}$ is an Objective Atomic Structure and if M consists of more than one point, we say that $\mathcal{S}$ is an Objective Molecular Structure. □

The need for having at least one point which has a nontrivial orbit (that is, a point for which $\text{Stab}(\mathcal{G}, \mathbf{x}) = \{(\mathbf{I}|\mathbf{0})\}$) arises so as to prevent one from associating unrelated groups and structures. We note however, that neither of the above definitions require an objective structure to be of finite extent and so, the group $\mathcal{G}$ can be infinite. An objective structure which is of infinite extent, that is for which $\sup_{\mathbf{x},\mathbf{y} \in \mathcal{S}} |\mathbf{x} - \mathbf{y}| = \infty$ cannot be generated by a finite group of isometries unless M contains points which are an infinite distance apart.

The requirement, that the group of isometries used in generating the objective structure be discrete, is quite essential. Indeed, it follows from this condition that an objective structure generated by such a group would satisfy the physical requirement of having all its points (at which, in a physical setting, mass points or ions would be located) a non zero distance apart:

Proposition 2.1.2. *Let $\mathcal{S}$ be a fixed point free objective molecular structure generated by*

the discrete group of isometries $\mathcal{G}$ acting on the distinct set of points M. Let

$$\delta = \inf_{\mathbf{x}\neq\mathbf{y}} \{|\mathbf{x}-\mathbf{y}|, \mathbf{x}, \mathbf{y} \in \mathcal{S}\}. \tag{2.3}$$

Then it holds that $\delta > 0$.

Proof: Since we are considering the infimum among a set of non-negative real numbers, it can only be that $\delta \geq 0$. If the group $\mathcal{G}$ is finite, then we are considering the infimum among a finite set of positive numbers (this set being the pairwise distances between all points in $\mathcal{S}$) and so δ has to be positive. So the only possibility of having $\delta = 0$ is when $\mathcal{G}$ is an infinite group. We now assume for the sake of contradiction that $\delta = 0$. Since $\mathcal{S}$ is fixed point free, each $\mathbf{x} \in \mathcal{S}$ lies on the orbit of a unique $\mathbf{p} \in M$ and so, we may rewrite (2.3) as:

$$\delta = \inf_{\mathbf{p},\mathbf{q}\in M} \big\{ \inf_{\mathbf{x}\neq\mathbf{y}} \{|\mathbf{x}-\mathbf{y}|;\ \mathbf{x} \in \text{Orb}(\mathcal{G},\mathbf{p}), \mathbf{y} \in \text{Orb}(\mathcal{G},\mathbf{q})\}\big\}. \tag{2.4}$$

Since $\delta = 0$ and the outer minimization in (2.4) is over a finite set, it must be that at least one of the inner minimizations yield zero. Thus, there must exist $\mathbf{p}, \mathbf{q} \in M$ such that

$$\inf_{\mathbf{x}\neq\mathbf{y}} \{|\mathbf{x}-\mathbf{y}|;\ \mathbf{x} \in \text{Orb}(\mathcal{G},\mathbf{p}), \mathbf{y} \in \text{Orb}(\mathcal{G},\mathbf{q})\} = 0 \tag{2.5}$$

This implies that there exist $\{\mathbf{x}_k, \mathbf{y}_k\}, k \in \mathbb{N}$ such that $\mathbf{x}_k \in \text{Orb}(\mathcal{G},\mathbf{p}), \mathbf{y}_k \in \text{Orb}(\mathcal{G},\mathbf{q})$ and $|\mathbf{x}_k - \mathbf{y}_k| \to 0$ as $k \to \infty$. Let $\mathbf{x}_k = \Upsilon_k(\mathbf{p}), \mathbf{y}_k = \tilde{\Upsilon}_k(\mathbf{q})$. The isometries $\Upsilon_k, \tilde{\Upsilon}_k$ are uniquely determined because $\mathcal{S}$ is fixed point free. For each $k \in \mathbb{N}$,

$$\begin{aligned} |\mathbf{x}_k - \mathbf{y}_k| = |\Upsilon_k(\mathbf{p}) - \tilde{\Upsilon}_k(\mathbf{q})| &= |\Upsilon_k^{-1}(\Upsilon_k(\mathbf{p})) - \Upsilon_k^{-1}(\tilde{\Upsilon}_k(\mathbf{q}))| \\ &= |\mathbf{p} - \Upsilon_k^{-1} \circ \tilde{\Upsilon}_k(\mathbf{q})|. \end{aligned} \tag{2.6}$$

Since $|\mathbf{x}_k - \mathbf{y}_k| \to 0$ it follows that $\{\Upsilon_k^{-1} \circ \tilde{\Upsilon}_k(\mathbf{q})\}_{k\in\mathbb{N}} \to \mathbf{p}$. But this contradicts with the discreteness of $\mathcal{G}$ since $\{\Upsilon_k^{-1} \circ \tilde{\Upsilon}_k(\mathbf{q})\}_{k\in\mathbb{N}} \subset \text{Orb}(\mathcal{G},\mathbf{q})$ and a ball of any radius centered around $\mathbf{p}$ would contain infinitely many points from the convergent sequence $\{\Upsilon_k^{-1} \circ \tilde{\Upsilon}_k(\mathbf{q})\}_{k\in\mathbb{N}}$. Hence we can only have $\delta > 0$ in (2.3). ■

A consequence of defining objective structures through discrete groups of isometries (as in Definition 2.1.1 above) is that a study of these structures, in a large part, becomes a study of the isometry groups that generate these structures.[1] We adopt this point of view and

[1] In particular, Objective Atomic Structures and (fixed point free) Objective Molecular Structures need not be studied separately.

attempt to categorize the electronic structure calculation problem of objective structures through the different groups of isometries involved. This raises a natural question about what all possible discrete groups of isometries in three spatial dimensions are and if it is possible precisely identify these groups in terms of formulae and parameters. The answer to these questions is worked out in Dayal, Elliott, and James [2013] where the following important result is derived and it is reproduced here without proof:

Theorem 2.1.3 (Dayal, Elliott and James)**.** *Every discrete group of isometries is either a space group, a net group, a helical group or a discrete group of rotations.*

Certain terms that appear in the above theorem need to be explained so that we are in a position to appreciate the limitations that this theorem places on the morphology of objective structures. A discrete group of isometries $\mathcal{G}$ is called a space group if it contains three translations $(\mathbf{I}|\mathbf{t}_1), (\mathbf{I}|\mathbf{t}_2), (\mathbf{I}|\mathbf{t}_3)$ with $\mathbf{t}_1, \mathbf{t}_2, \mathbf{t}_3$ linearly independent and if every translation in $\mathcal{G}$ is in the group generated by these three translations. Thus, every translation in $\mathcal{G}$ is expressible in the form $(\mathbf{I}|\mu_1\mathbf{t}_1 + \mu_2\mathbf{t}_2 + \mu_3\mathbf{t}_3), \mu_1, \mu_2, \mu_3 \in \mathbb{Z}$. Similarly, a discrete group of isometries $\mathcal{G}$ is called a net group if it contains two translations $(\mathbf{I}|\mathbf{t}_1), (\mathbf{I}|\mathbf{t}_2)$ with $\mathbf{t}_1, \mathbf{t}_2$ linearly independent and every translation in $\mathcal{G}$ is expressible in the form $(\mathbf{I}|\mu_1\mathbf{t}_1 + \mu_2\mathbf{t}_2), \mu_1, \mu_2 \in \mathbb{Z}$. A discrete group of isometries $\mathcal{G}$ is called a rod group if it contains a translation $(\mathbf{I}|\mathbf{t})$ and every translation in $\mathcal{G}$ is expressible in the form $(\mathbf{I}|\mu\mathbf{t}), \mu \in \mathbb{Z}$. Finally, a helical group is a discrete group of isometries if it does not contain a translation and does not consist entirely of rotations. Dayal et al. [2013] also show that a discrete group of rotations can only be a finite group and these consist of the symmetry groups of the Platonic solids as well as the cyclic and dihedral groups that fix an axis.

We may now try to interpret what bearing the above discussion has on the problem of electronic structure computation of objective structures. For objective structures that are generated by a space group, a net group or a rod group, one can exploit translational invariance since the isometry groups associated with these structures contain a group of translations as a normal subgroup. Hence, by proper choice of a periodic unit cell, one may hope to reduce the electronic structure problem posed on the entire objective structure to one posed only on the unit cell and augment this reduced problem with periodic boundary conditions. One should note however that this is not necessarily the most optimum method for performing electronic structure computations on these structures since only a subgroup of the full symmetry group is being exploited.[2] Nevertheless, this has been the canonical approach

[2]An example would be a body centered cubic lattice. A standard periodic unit cell would have 2 atoms per unit cell while a consideration of the complete symmetry group associated with the lattice would lead one to perform all computations on a (symmetry adapted) single atom cell.

of the computational materials science and solid state physics community to perform electronic structure computations on most materials systems[Martin, 2004; Kaxiras, 2003]. On the other hand, for the objective structures associated with helical groups or with discrete groups of rotations, there is no underlying periodicity and so we need to discover methods that are well suited for these symmetry groups. The way these groups are conventionally handled in the computational materials science/computational chemistry community is by use of the so called super-cell method [Martin, 2004]. The idea is to make the structure under study artificially periodic and then to study this periodic problem using methods designed for studying crystals. Thus, the supercell method does not really study the problem associated with the original structure, but only periodic approximations of the problem. One of the goals of this work, is to be able to formulate electronic structure calculation algorithms suited for non-periodic objective structures without resorting to any sort of artificial periodicity.

2.2 Electronic Structure Computation Theories

We discuss the electronic structure computation problem as it applies to a system with a finite number of electrons at absolute zero temperature. We will try to outline only the general principles involved in this discussion - the numerous theoretical and implementation details involved will be brought up in later portions of this work as and when required. The primary focus of our discussion will be on Density Functional Theory. A more detailed discussion of electronic structure computation theories may be found in Parr and Yang [1994]; Szabo and Ostlund [1996] and Martin [2004]. Some of the rigorous mathematical foundations of these theories have been laid out in Kato [1957]; Lieb and Simon [1977a,b]; Lions [1987] and Lieb [1983] among others. Good overviews of the mathematical issues involved can be found in Le Bris [2005, 2003]; Defranceschi and Le Bris [2000] and references therein. Our presentation of the contents of this section, as well as our choice of notation are very much in the light of these more mathematical works. For the purpose of simplicity, we will omit the spin variable in this presentation with complete awareness however, of the great practical significance of spin in practical electronic structure calculations (also see Section 4.2.1). The atomic unit system with $m_e = 1, e = 1, \hbar = 1, \frac{1}{4\pi\epsilon_0} = 1$, is used rest of the work, unless otherwise mentioned.

2.2.1 Born-Oppenheimer Quantum Mechanics

In many quantum chemistry/computational materials science applications, it is legitimate to treat the nuclei of the system of interest as positively charged point masses which behave

classically. So we assign precise positions $(\mathbf{x}_1, \mathbf{x}_2, \ldots, \mathbf{x}_M)$ and charges $(z_1, z_2, \ldots, z_M)$ to the nuclei and treat the electrons as quantum mechanical particles. Under these assumptions,[3] determination of the ground state structure of a molecular system consisting of M nuclei and N electrons takes the following form:

$$\inf_{(\mathbf{x}_1,\ldots,\mathbf{x}_M)\in\mathbb{R}^{3M}} \left\{ W\big(\mathbf{x}_1,\ldots,\mathbf{x}_M\big) = U\big(\mathbf{x}_1,\ldots,\mathbf{x}_M\big) + \sum_{1\le k\le l\le M} \frac{z_k z_l}{|\mathbf{x}_k - \mathbf{x}_l|} \right\}, \tag{2.7}$$

$$\text{where,} \quad U\big(\mathbf{x}_1,\ldots,\mathbf{x}_M\big) = \inf_{\psi_e\in\mathcal{H}_e} \left\{ \langle \psi_e, H_e^{(\mathbf{x}_1,\ldots,\mathbf{x}_M)}\psi_e\rangle_{L^2}, \|\psi_e\|_{L^2} = 1 \right\}, \tag{2.8}$$

with $H_e^{(\mathbf{x}_1,\ldots,\mathbf{x}_M)}$ denoting the (non-relativistic) electronic Hamiltonian and $\mathcal{H}_e$ denoting a suitable function space in which the minimization in (2.8) must be carried out. The minimization in (2.8) corresponds to determining the ground state electronic structure with the nuclei clamped at the positions $(\mathbf{x}_1, \ldots, \mathbf{x}_M)$. Our work will almost entirely focus on this electronic structure computation problem with the added constraint that $(\mathbf{x}_1, \ldots, \mathbf{x}_M)$ should be expressible in such a way that Definition 2.1.1 can be applied. The outer minimization in (2.7) is important while doing structural optimization computations and we should note that even this minimization problem is considerably simplified for the case of objective structures since one needs to optimize over a lower dimensional manifold of $\mathbb{R}^{3M}$.

The ground state electronic structure computation problem (2.8) consists of finding the lowest eigenvalue of the electronic Hamiltonian $H_e^{(\mathbf{x}_1,\ldots,\mathbf{x}_M)}$ parametrized by the positions of the nuclei. This Hamiltonian consists of a term accounting for the kinetic energy of the electrons, a term accounting for the electron-nuclei attraction and a term accounting for the electron-electron repulsion and can be written as:

$$H_e^{(\mathbf{x}_1,\ldots,\mathbf{x}_M)} = -\sum_{i=1}^{N} \frac{1}{2}\Delta_{\mathbf{y}_i} - \sum_{i=1}^{N}\sum_{k=1}^{M} \frac{z_k}{|\mathbf{y}_i - \mathbf{x}_k|} + \sum_{1\le i\le j\le N} \frac{1}{|\mathbf{y}_i - \mathbf{y}_j|}. \tag{2.9}$$

The natural choice for the function space $\mathcal{H}_e$ turns out to be[4] the following subspace of $\mathsf{L}^2(\mathbb{R}^{3N})$:

$$\mathcal{H}_e = \bigwedge_{i=1}^{N} \mathsf{H}^1(\mathbb{R}^3), \tag{2.10}$$

where, the wedge is used to denote the antisymmetrized tensor product and $\mathsf{H}^1(\mathbb{R}^3)$ denotes the Sobolev space of square integrable functions on $\mathbb{R}^3$ whose first order weak derivatives

[3] Referred to as Born Oppenheimer approximation in literature.

[4] This follows from ensuring finiteness of the kinetic energy and fulfillment of the Pauli exclusion principle.

are also square integrable. The Euler-Lagrange equation of the minimization problem (2.8) is the eigenvalue problem:

$$H_e^{(\mathbf{x}_1,\ldots,\mathbf{x}_M)}\psi_e = E_e\psi_e, \tag{2.11}$$

with $E_e = U\big(\mathbf{x}_1,\ldots,\mathbf{x}_M\big)$ the lowest possible eigenvalue of the self-adjoint operator $H_e^{(\mathbf{x}_1,\ldots,\mathbf{x}_M)}$. Equation 2.11 is often referred to as the many-body Schrödinger equation in the literature.

2.2.2 Density Functional Methods

Unfortunately however, for any practical problem, a direct numerical attack on the minimization problem (2.8) or the eigenvalue problem (2.11) is prohibitively expensive due to the large dimensionality involved. To overcome this difficulty, the generic philosophy is to trade the linearity of (2.11) for a reduction in dimensionality. Density functional methods are based on a reformulation of (2.8) in such a way that the unknown function is the electronic density:

$$\rho(\mathbf{y}) = N\int_{\mathbb{R}^{3(N-1)}} |\psi_e(\mathbf{y},\mathbf{y}_2,\ldots,\mathbf{y}_N)|^2\, d\mathbf{y}_2\ldots d\mathbf{y}_N, \tag{2.12}$$

which is a scalar field on $\mathbb{R}^3$ unlike the wavefunction ψ_e which is a scalar field on $\mathbb{R}^{3N}$. The justification behind this reformulation strategy comes from a seminal paper by Hohenberg and Kohn [Hohenberg and Kohn, 1964] who showed that electron-density as a basic variable is sufficient to describe the properties of a material system in its ground state. To see how (2.8) may be reformulated in terms of the density (2.12), we may follow Lieb [1983] and Le Bris [2005] to define:

$$E(\rho) = \inf_{\psi_e\in\mathcal{H}_e}\Bigg\{\langle\psi_e,\Big(-\sum_{i=1}^{N}\frac{1}{2}\Delta_{\mathbf{y}_i} + \sum_{1\le i\le j\le N}\frac{1}{|\mathbf{y}_i-\mathbf{y}_j|}\Big)\psi_e\rangle_{L^2} : \\ \|\psi_e\|_{L^2}=1, \psi_e \text{ has density } \rho\Bigg\} \tag{2.13}$$

$$\text{and}\quad \mathcal{I}_N = \Big\{\rho\ge 0 : \sqrt{\rho}\in \mathsf{H}^1(\mathbb{R}^3), \int_{\mathbb{R}^3}\rho = N\Big\}, \tag{2.14}$$

so that, problem (2.8) reduces to:

$$U\big(\mathbf{x}_1,\ldots,\mathbf{x}_M\big) = \inf_{\rho\in\mathcal{I}_N}\Big\{E(\rho) - \int_{\mathbb{R}^3}\Big(\sum_{k=1}^{M}\frac{z_k}{|\mathbf{y}-\mathbf{x}_k|}\rho(\mathbf{y})\,d\mathbf{y}\Big)\Big\} \tag{2.15}$$

The functional $E : \mathcal{I}_N \to \mathbb{R}^+$ is called a density functional and it is often described as being "universal" in literature (for example, Hohenberg and Kohn [1964]) since it does not depend on any particular material/molecular system. However, an explicit formula for this universal density functional $E(\rho)$ is not known and so, in practice one must construct approximations of this density functional by carefully studying reference systems that are in some sense "close" to the system being studied.

2.2.3 Kohn-Sham Density Functional Theory

A density functional model very widely used today is the one introduced by Kohn and Sham [Kohn and Sham, 1965] who considered a system of N non-interacting electrons as a reference. Under appropriate assumptions, the kinetic energy of such a system can be written as [Le Bris, 2005]:

$$T_{KS}(\rho) = \inf_{\phi_i \in \mathsf{H}^1(\mathbb{R}^3)} \left\{ \frac{1}{2} \sum_{i=1}^{N} \int_{\mathbb{R}^3} |\nabla \phi_i|^2 : \langle \phi_i, \phi_j \rangle_{L^2} = \delta_{ij}, \sum_{i=1}^{N} |\phi_i|^2 = \rho \right\}. \tag{2.16}$$

The Kohn-Sham model first chooses this as an approximation for the kinetic energy for the system of interacting electrons that is being studied. It then adds electrostatic terms to account for the electron-electron repulsion and the electron nuclei attraction. It finally adds an exchange-correlation functional to the model, the purpose of this term being to account for the non-independence of the electrons. The Kohn-Sham model therefore reads as:

$$I_N^{KS} = \inf_{\phi_i \in \mathsf{H}^1(\mathbb{R}^3)} \left\{ \frac{1}{2} \sum_{i=1}^{N} \int_{\mathbb{R}^3} |\nabla \phi_i|^2 + \int_{\mathbb{R}^3} \rho V_{nu} + \frac{1}{2} \int_{\mathbb{R}^3} \int_{\mathbb{R}^3} \frac{\rho(\mathbf{x})\rho(\mathbf{y})}{|\mathbf{x} - \mathbf{y}|} \, d\mathbf{x} \, d\mathbf{y} \right.$$
$$\left. + E_{xc}(\rho) : \langle \phi_i, \phi_j \rangle_{L^2} = \delta_{ij} \right\} \tag{2.17}$$

The exact form of $E_{xc}(\rho)$ is of course, not known since a knowledge of it's exact form would amount to having the knowledge of the elusive density functional $E(\rho)$ that appears in (2.13) and (2.15). One of the common approximations for this term is the so called Local Density Approximation, in which $E_{xc}(\rho(\mathbf{y}))$ is expressed as $\int_{\mathbb{R}^3} F(\rho(\mathbf{y})) \, d\mathbf{y}$. The simplest form of the Local Density Approximation is obtained for the case of a uniform non-interacting electron gas, in which case we have [Le Bris, 2005]:

$$E_{xc}(\rho) = -C_D \int_{\mathbb{R}^3} \rho^{4/3}(\mathbf{y}) \, d\mathbf{y}, \text{ with } C_D = \frac{3}{4} \left(\frac{3}{\pi} \right)^{1/3}. \tag{2.18}$$

The Euler-Lagrange equations of (2.17) are the celebrated Kohn-Sham equations, which for a system with M nuclei are as follows:

$$K(\rho)\phi_i = \lambda_i\phi_i;\ \langle\phi_i,\phi_j\rangle_{L^2} = \delta_{ij} \quad . \tag{2.19}$$

$$K(\rho) = -\frac{1}{2}\Delta - \sum_{i=1}^{M}\frac{z_k}{|\mathbf{y}-\mathbf{x}_k|} + \left(\int_{\mathbb{R}^3}\frac{\rho(\mathbf{x})}{|\mathbf{y}-\mathbf{x}|}\,d\mathbf{x}\right) + V_{xc}(\rho) \quad . \tag{2.20}$$

with,

$$\rho(\mathbf{x}) = \sum_{i=1}^{N}|\phi_i(\mathbf{x})|^2, \text{ and } \quad V_{xc}(\rho) = \frac{\partial E_{xc}(\rho)}{\partial\rho} \quad . \tag{2.21}$$

The λ_i that appear in the (4.1) are the Lagrange multipliers of the orthonormality constraints. Owing to the fact that the Kohn-Sham energy functional (2.17) is invariant with respect to unitary transformations of the ϕ_i, the matrix of Lagrange multipliers may be diagonalized without loss of generality. This transformation also leaves the expression for the density in (2.21) unchanged. They λ_i are taken to be the lowest N eigenvalues of the of the Kohn-Sham operator $K(\rho)$.

The usual method of solution of the Kohn-Sham equations is by a self-consistent approach [Kohn and Sham, 1965; Martin, 2004]. One starts from a guess of the density $\rho(\mathbf{x})$ and evaluates the electrostatic and exchange correlation terms. One then solves the linearized eigenvalue problem with these potentials and computes the lowest N states $\phi_i, i = 1,\ldots,N$. The expression for the density in (2.21) is used to compute the new electronic density from the ϕ_i. The potentials are then computed with this new density and the cycle repeats. It is not obvious however, that this iteration will converge and whether it will converge to the sought minimizer. In practice therefore, "mixing schemes" are employed [Martin, 2004], so that the newly computed density from the present iteration step is combined with densities from earlier iterations and this "mixed" density is used to evaluate the potentials in the current iteration step. See Section 4.3.4.1 for more details on this.

We should mention in passing, that Kohn-Sham calculations for extended systems, such as crystals, involve theoretical and implementation issues that are not originally present in Kohn-Sham Density Functional Theory as presented here. For instance, at the theoretical level, formal extension of the Kohn-Sham theory to such calculations, involves the introduction of a single electron band theory and ideas related to the density of states. At the implementation level, the computation of the electrostatic potentials and energies are done through so called Ewald sums. See Reed and Simon [1978]; Defranceschi and Le Bris

[2000]; Le Bris [2003]; Martin [2004] and Pickett [1989] for more details. In the context of the present work, this means that studies of the electronic structure of infinite objective structures (such as those generated by helical groups), should keep such issues in mind during the formulation and implementation phase.

2.3 Results and tools from Abstract Harmonic Analysis

As mentioned earlier, one of the objectives of this thesis is to investigate how density functional methods can be adapted to study the electronic structure of objective structures. In the Kohn-Sham setting, this translates to investigating how the symmetry group of an objective structure interacts with the Kohn-Sham model (2.19)-(2.21). However, the non-convexity of the functional appearing in (2.17) and the non-linearity of the system (2.19)-(2.21) make it somewhat difficult to answer these questions and in fact, loss of symmetry in self consistent solutions to the Kohn-Sham equations is quite well known [Prodan, 2005].

This is a somewhat generic concern with regard to the analysis of how symmetry interacts with non-linear problems. In such situations, a problem with a certain degree of symmetry may not exhibit solutions with the same degree of symmetry. Hence, the analysis of such problems is mainly focused on efficiently computing solutions which do have the right degree of symmetry should they exist [Healey, 1989], as well as on studying symmetry breaking bifurcating solutions [Healey, 1988; Healey and Kielhöfer, 1991].

On the other hand, the interaction of symmetry with linear problems is well understood and well characterized. The main mathematical tools for the study of such problems are provided by linear representation theory and abstract harmonic analysis. There seems to be a wealth of literature devoted to the analysis of such problems and their applications. A list of references would include Hammermesh [1989] and McWeeny [2002] for applications to problems in physics and chemistry, Bossavit [1986, 1993] and Georg and Tausch [1994] for applications to linear boundary value problems and their solutions by Finite Element and Boundary Element techniques, Healey and Treacy [1991] and Fahmi and Potier-Ferry [1998] for applications to eigenvalue problems arising out of structural analysis, and Allgower et al. [1998]; Ahlander and Munthe-Kaas [2005, 2006]; Allgower and Georg [1999] for applications to numerical algorithms.

We will now focus on developing mathematical tools that will enable us to study the interaction of symmetry groups of objective structures with a broad class of linear problems. Our justification for studying linear problems comes from the fact that the self-consistent iteration scheme for computing solutions of the Kohn-Sham equations basically involves

solution to linear problems at each stage of the iteration. This is elaborated upon in later chapters.

In order to introduce the large number of ideas involved in representation theory in a coherent way, a fair bit of abstraction is needed at this point. The basic theme of the developments that follow is the formulation of a representation theory for a discrete group of isometries $\mathcal{G}$ on a Hilbert space of square integrable functions. The utility of this sort of abstraction is that it allow us to treat finite as well as infinite groups of isometries in a unified way later. Also, the development of these tools in terms of a rather generic Hilbert space has the distinct advantage of allowing us to study both linear partial differential equations as well as numerical discretizations of these equations, with minor modifications. A linear problem may be viewed in terms of a linear operator posed on a suitable space of solutions. Therefore, the question of how the symmetry group $\mathcal{G}$ interacts with a particular linear problem may be formulated in terms of how representations of $\mathcal{G}$ on the space of solutions interact with the linear operator associated with the problem.

The material that we present in the following sections has been largely influenced by Folland [1994]; Barut and Raczka [1986] and Miller [1972]. However, we believe that our presentation is quite original in some respects. In many cases, we have had to adapt the more sophisticated general theory presented in the above references to our somewhat simplified needs. The main source of our simplification arises from the fact that the groups (of isometries) associated with objective structures, are always discrete and hence countable.[5]

2.3.1 Group Actions

The notion of group actions was introduced in Section 2.1 in the context of groups of isometries acting on $\mathbb{R}^3$. We begin by generalizing this idea. Let G be a group with $\circ$ denoting the group operation and let S be an arbitrary set.

Definition 2.3.1. The Left Group Action[6] of G on S is a mapping $\bullet : G \times S \to S$ denoted as $g \bullet x$ for $g \in G, x \in S$ which satisfies:

1. $(g \circ h) \bullet x = g \bullet (h \bullet x), \forall g, h \in G, x \in S$.
2. If e denotes the identity element of G, then $e \bullet x = x, \forall x \in S$. □

[5]The result that discrete groups of isometries are always countable follows quite directly from Dayal et al. [2013, Lemma 5.1, Theorem 5.1].

[6]We may similarly define the right group action of G on S. However, every right group action may be re-interpreted as a left group action and so we only concern ourselves with left group actions here.

As before, we denote $\text{Orb}(G, x) = \{g \bullet x : g \in G\}$ and $\text{Stab}(G, x) = \{g \in G : g \bullet x = x\}$. We extend the notation of actions and orbits to arbitrary subsets $A \subset S$ by denoting $g \bullet A = \{g \bullet x : x \in A\}$ and $\text{Orb}(G, A) = \{g \bullet A : g \in G\}$. In particular, we say that $A \subset S$ is a fundamental set for the action of G on S if $\text{Orb}(G, A) = S$. [7] Fundamental sets are of great importance to us since, broadly speaking, we are interested in reducing a problem posed over a set S with a symmetry group G, to a problem posed on a fundamental set for the action of G on S.

It is useful to note that our definition of group action automatically ensures that the map for the group action $\bullet : G \times S \to S$ is such that for each fixed first argument, it is a bijection in the second argument. [8] [9] The consequence of this is the following simple useful result:

Proposition 2.3.2. *There exists a fundamental set for the action of G on S.*

Proof: The bijection property guarantees that we may define an equivalence relation $\sim$ on $S \times S$ which is as follows: $\forall x, y \in S, x \sim y \Leftrightarrow \exists g \in G$ such that $y = g \bullet x$. By the fundamental property of equivalence relations [Naylor and Sell, 1971], the equivalence relation $\sim$ will partition S into the disjoint union of equivalence classes and in this case, the equivalence class of x will simply be $\text{Orb}(G, x)$. If we now define a set V such that it contains a member from each equivalence class, it is easy to check that $\text{Orb}(G, V) = S$ ensuring that V is a fundamental set. ■

We now consider how group actions on S can be used to define group actions on suitable function spaces on S. We will achieve this through a point-wise redefinition of the functions and so the technical issue of whether specifying a function point-wise actually specifies it uniquely, arises. To circumvent this, we assume that S is equipped with a topology such that for each fixed $g \in G$, the group action is a continuous map from S to S. If we confine our attention to the set of all maps $f : S \to \mathbb{C}$ which are continuous in this topology, we can prove the following result:

[7] In the context of Definition 2.1.1, it is easy to see that if $\mathcal{S}$ is an objective structure generated by a discrete group of isometries $\mathcal{G}$ acting on the set M, then M is in fact a fundamental set for the Objective Structure $\mathcal{S}$.

[8] The proof of this is as follows: The map is an injection because with $g \in G$ fixed, if $g \bullet x_1 = g \bullet x_2$ for any $x_1, x_2 \in S$, then $g^{-1} \bullet (g \bullet x_1) = g^{-1} \bullet (g \bullet x_2)$. Thus, by the laws of group action, we must have $x_1 = x_2$. Now, we assume for the sake of contradiction that the map is not a surjection. Thus there exists $g \in G$ such that $g \bullet S \subsetneq S$. Let $x \in S \backslash g \bullet S$. Now $g^{-1} \bullet x \in S$ and therefore, $g \bullet (g^{-1} \bullet x) \in g \bullet S$. By the laws of group action this implies a contradiction since we have $x \in g \bullet S$ as well as $x \in S \backslash g \bullet S$.

[9] The converse is not true in general since we may find $x \in S$ such that $\text{Stab}(G, x)$ is a non-trivial subgroup of G and so, for each fixed second argument, the group action is not a surjection in its first argument.

Proposition 2.3.3. *Let $\bullet : G \times S \to S$ denote the action of G on S and let $\mathsf{C}(S)$ denote the set of functions $f : S \to \mathbb{C}$ which are continuous (in the aforementioned topology). Then the map $\bullet : \mathcal{G} \times \mathsf{C}(S) \to \mathsf{C}(S) : f(x) \mapsto f(g^{-1} \bullet x)$ defines an action of G on $\mathsf{C}(S)$.*

Proof: First, we note that the pointwise definition of the group action makes sense since we are dealing with continuous functions. Next, we note that for any fixed $g \in G$, $f(g^{-1} \bullet x) \in \mathsf{C}(S)$ since it is the composition of two continuous maps. Now, for any $g, h \in G, x \in S$ and $f \in \mathsf{C}(S)$ we have:

$$\begin{aligned}(g \circ h) \bullet f(x) = f((g \circ h)^{-1} \bullet x) = f((h^{-1} \circ g^{-1}) \bullet x) = f(h^{-1} \bullet (g^{-1} \bullet x)) \\ = h \bullet f(g^{-1} \bullet x) = g \bullet (h \bullet f(x)),\end{aligned} \tag{2.22}$$

which verifies the first law. Also, $e \bullet f(x) = f(e^{-1} \bullet x) = f(x)$ which verifies the second law. This completes the proof. ■

The advantage of introducing group actions on continuous functions is that group actions can be defined on a large class of other function spaces by means of density theorems. A particular example would be the group action of a discrete group of isometries $\mathcal{G}$ on a suitable subset $\Omega \subset \mathbb{R}^3$ as discussed in Chapter 2. We may easily verify that the usual topology on $\mathbb{R}^3$ satisfies the hypotheses of Proposition 2.3.3. Hence, a group action on $\mathsf{C}(\Omega)$ may be defined. Next, by employing density theorems of continuous functions, this action can be extended to suitable function spaces on Ω that are relevant to the study of boundary value problems associated with electronic structure calculation. We carry out such a program in later sections of this work.

2.3.2 Representation Theory

2.3.2.1 Group Representations over Hilbert Spaces

Let $\mathsf{H}, \tilde{\mathsf{H}}$ denote nonzero Hilbert spaces. Let $\mathcal{L}(\mathsf{H}, \tilde{\mathsf{H}})$ denote the space of bounded linear operators from H to $\tilde{\mathsf{H}}$ that is:

$$\mathcal{L}(\mathsf{H}, \tilde{\mathsf{H}}) = \left\{T : \mathsf{H} \to \tilde{\mathsf{H}} : T \text{ is linear and } \exists\, C > 0 \text{ such that } \|Tf\|_{\tilde{\mathsf{H}}} < C\|f\|_{\mathsf{H}},\ \forall f \in \mathsf{H}\right\} \tag{2.23}$$

Further, let $\mathcal{U}(\mathsf{H}, \tilde{\mathsf{H}})$ denote the space of unitary operators from H to $\tilde{\mathsf{H}}$, that is,

$$\mathcal{U}(\mathsf{H}, \tilde{\mathsf{H}}) = \left\{T \in \mathcal{L}(\mathsf{H}, \tilde{\mathsf{H}}) : T \text{ is surjective and } \langle f_1, f_2\rangle_{\mathsf{H}} = \langle Tf_1, Tf_2\rangle_{\tilde{\mathsf{H}}},\ \ \forall f_1, f_2 \in \mathsf{H}\right\}. \tag{2.24}$$

We then introduce:

Definition 2.3.4. A map $\zeta : \mathcal{G} \to \mathcal{L}(\mathsf{H}, \mathsf{H})$ is a linear representation of the discrete group of isometries $\mathcal{G}$ on the carrier space H, provided that ζ is a homomorphism and it preserves the identity, i.e., $\forall g, h \in \mathcal{G}, \zeta(gh) = \zeta(g) \circ \zeta(h)$ and $\zeta(e) = I_{\mathsf{H}}$ (where e and I_{H} denote the identity element in $\mathcal{G}$ and the identity operator on H respectively). The dimension of the Hilbert space H is called the dimension of the representation. If, for a linear representation, the map ζ is a bijection onto it's range, then ζ is in fact an isomorphism and we call it a faithful linear representation of $\mathcal{G}$. If a linear representation is such that for each $g \in \mathcal{G}$, $\zeta(g) \in \mathcal{U}(\mathsf{H}, \mathsf{H})$, we call the map a unitary representation of $\mathcal{G}$. Finally, if all the elements of $\mathcal{G}$ are mapped to I_{H}, then we call the representation trivial. □

Thus, the image of $\mathcal{G}$ under the linear representation is a set of operators which form a group under the operation of composition of operators (denoted here as $\cdot$), and the identity element of this group is the identity operator on H. The condition that $\zeta(e) = I_{\mathsf{H}}$ guarantees that each linear operator in the image of the representation is an isomorphism on H. This observation follows from the fact that:

$$\forall g \in \mathcal{G}, \quad \zeta(g) \cdot \zeta(g^{-1}) = \zeta(g^{-1}) \cdot \zeta(g) = \zeta(g \circ g^{-1}) = \zeta(g^{-1} \circ g) = \zeta(e) = I_{\mathsf{H}}\,, \tag{2.25}$$

and so we must have $\zeta(g)^{-1} = \zeta(g^{-1}) \in \mathcal{L}(\mathsf{H}, \mathsf{H})$. Hence the inverse operator of each $\zeta(g)$ is well defined and bounded and so each $\zeta(g)$ is an isomorphism on H. In particular, for a unitary representation, we have $\zeta(g^{-1}) = \zeta(g)^{-1} = \zeta(g)^*$, where $*$ is used to denote the adjoint.[10] Henceforth, we will be interested in unitary representations for the most part because of the nicer properties of unitary operators. This may seem like a somewhat restrictive choice but as our next result demonstrates, unitary representations can be constructed quite routinely for most of our applications. In particular, this gives us a method of constructing unitary representations on some of the common function spaces associated with partial differential equations of interest to this work as well as finite dimensional spaces associated with discretized versions of those equations. While the theorem itself is quite intuitive and is a direct extension of Proposition 2.3.3, some minor technical details need to be sorted out. First we note that we call a Radon measure ν on a locally compact Hausdorff topological space S group invariant (from the left) if for any measurable subset $A \subseteq S$, $\nu(A) = \nu(g \circ A)$ for every group element g. Here, $g \circ A$ is a notation for $\bigcup_{p \in A} g \circ p$. Next,

[10] For any $T \in \mathcal{L}(\mathsf{H}, \mathsf{H})$, the adjoint of T is the unique operator T^*, that satisfies $\langle Tf_1, f_2 \rangle_{\mathsf{H}} = \langle f_1, T^* f_2 \rangle_{\mathsf{H}}$, $\forall f_1 \in \mathsf{H}, f_2 \in \mathsf{H}$. An operator $T \in \mathcal{U}(\mathsf{H}, \mathsf{H})$ if and only if T is invertible and $T^{-1} = T^*$.

we have:

Lemma 2.3.5. *Let S be a locally compact Hausdorff topological space and let $\mathcal{G}$ be a discrete group of isometries such that the action of $\mathcal{G}$ on S is continuous for each fixed $g \in \mathcal{G}$. Let ν be a group invariant Radon measure on S and let $\mathsf{L}^2_\nu(S)$ denote the Hilbert space of complex valued square integrable functions. Then the following defines an action of $\mathcal{G}$ on any function $f \in \mathsf{L}^2_\nu(S)$:*

$$g \bullet f = \lim_{n\to\infty} f_n(g^{-1} \bullet x), \tag{2.26}$$

where $\{f_n\}_{n\in\mathbb{N}} \subset \mathsf{C_c}(S)$ is a sequence (of continuous functions with compact support in S) that converges to f in the $\|\cdot\|_{\mathsf{L}^2_\nu(S)}$ topology.

Proof: First, we ensure that the definition of the group action makes sense. If $f \in \mathsf{L}^2_\nu(S)$, then by density of $\mathsf{C_c}(S)$ in $\mathsf{L}^2_\nu(S)$ [Folland, 1999], there exists $\{f_n\}_{n\in\mathbb{N}} \subset \mathsf{C_c}(S)$ such that $\|f - f_n\|_{\mathsf{L}^2_\nu(S)} \to 0$ as $n \to \infty$. For each f_n, the function $f_n(g^{-1} \bullet x) \in \mathsf{C_c}(S)$ since the map $x \mapsto f_n(g^{-1} \bullet x)$ is continuous for each fixed g and the continuous image of a compact set (the support of f_n in this case) is compact. Also, $f_n(g^{-1} \bullet x) \in \mathsf{L}^2_\nu(S)$ because, by a change of variables/Radon-Nikodym theorem and the group invariance of the measure ν, we have that:

$$\begin{aligned}\int_S |f_n(g^{-1} \bullet x)|^2 \, d\nu = \int_{g\bullet S} |f_n(g^{-1} \bullet (g \bullet y))|^2 \, d\nu = \int_S |f_n(y)|^2 \, d\nu = \int_{\text{spt.}(f_n)} |f_n(y)|^2 \, d\nu \\ \leq \big(\sup_{y\in\text{spt.}(f_n)} |f_n(y)|^2 \big) \times \nu(\text{spt.}(f_n)) < \infty \end{aligned} \tag{2.27}$$

By a computation very similar to the one above, we also conclude that $\{f_n(g^{-1} \bullet x)\}_{n\in\mathbb{N}}$ is a Cauchy sequence in $\mathsf{L}^2_\nu(S)$ and so, by completeness, the limit in (2.26) and hence the proposed group action is well defined.[11]

We now need to confirm that this limit satisfies the two laws of group action. For the first law, we need to verify that $(g\circ h)\bullet f = g\bullet(h\bullet f)$. So, let $\{f_n(x)\}_{n\in\mathbb{N}} \subset \mathsf{C_c}(S)$ be convergent to $f \in \mathsf{L}^2_\nu(S)$. Then, by definition of the action and the calculations in Proposition 2.3.3, we have:

$$(g \circ h) \bullet f = \lim_{n\to\infty} f_n((g \circ h)^{-1} \bullet x) = \lim_{n\to\infty} f_n((h^{-1} \circ g^{-1}) \bullet x) \quad . \tag{2.28}$$

[11]The action is also unambiguous in the sense that one can choose *any* approximating sequence for the purpose - two different sequences will necessarily produce results that differ from each other only on a set of ν-measure zero.

On the other hand, to evaluate $g \bullet (h \bullet f)$, let $\{\phi_n(x)\}_{n\in\mathbb{N}} \subset \mathsf{C_c}(S)$ converge to $(h \bullet f) \in \mathsf{L}^2_\nu(S)$. So, $g \bullet (h \bullet f) = \lim_{n\to\infty} \phi_n(g^{-1} \bullet x)$. Since $\{f_n(x)\}_{n\in\mathbb{N}} \to f$ in $\mathsf{L}^2_\nu(S)$, by definition of the group action, we must have that $\{f_n(h^{-1} \bullet x)\}_{n\in\mathbb{N}} \to h \bullet f$ in $\mathsf{L}^2_\nu(S)$. Thus, by choosing the sequence $\{\phi_n(x)\}_{n\in\mathbb{N}}$ to be equal to $\{f_n(h^{-1} \bullet x)\}_{n\in\mathbb{N}}$, we get that:

$$g \bullet (h \bullet f) = \lim_{n\to\infty} f_n(h^{-1} \bullet (g^{-1} \bullet x)) = \lim_{n\to\infty} f_n((h^{-1} \circ g^{-1}) \bullet x) \quad . \tag{2.29}$$

Comparing (2.28) and (2.29), the first law of group action is verified. Finally, we also have:

$$e \bullet f(x) = \lim_{n\to\infty} f_n(e^{-1} \bullet x) = \lim_{n\to\infty} f_n(x) = f(x). \tag{2.30}$$

This completes the proof. ■

An immediate corollary of the above is the following result on unitary representations:

Theorem 2.3.6. *With the setting of Lemma 2.3.5, let $\bullet : \mathcal{G} \times \mathsf{L}^2_\nu(S) \to \mathsf{L}^2_\nu(S)$ denote the action of $\mathcal{G}$ on functions in $\mathsf{L}^2_\nu(S)$ as defined by* (2.26)*. For each $g \in \mathcal{G}$ we consider an operator $\mathcal{T}_g : \mathsf{L}^2_\nu(S) \to \mathsf{L}^2_\nu(S)$ such that for any $f \in \mathsf{L}^2_\nu(S)$, $\mathcal{T}_g[f] = g \bullet f$. Let the set $L_\mathcal{G}$ denote the collection $\{\mathcal{T}_g : g \in \mathcal{G}\}$. Then the map $\zeta : \mathcal{G} \to L_\mathcal{G}$ forms a unitary representation of the group $\mathcal{G}$ on the carrier space $\mathsf{L}^2_\nu(S)$.*

Proof: We first note that $\forall g \in \mathcal{G}$, the action of $\mathcal{T}_g$ on any function $f \in \mathsf{L}^2_\nu(S)$ is well defined via Lemma 2.3.5. Each $\mathcal{T}_g$ is easily verified to be a linear operator on $\mathsf{L}^2_\nu(S)$ and $\mathcal{T}_g \in \mathcal{L}(\mathsf{L}^2_\nu(S), \mathsf{L}^2_\nu(S))$ because, by the continuity of the norm and the change of variables calculation in (2.27), we have:

$$\begin{aligned} \|\mathcal{T}_g[f]\|_{\mathsf{L}^2_\nu(S)} = \|g \bullet f\|_{\mathsf{L}^2_\nu(S)} &= \|\lim_{n\to\infty} f_n(g^{-1} \bullet x)\|_{\mathsf{L}^2_\nu(S)} = \lim_{n\to\infty} \|f_n(g^{-1} \bullet x)\|_{\mathsf{L}^2_\nu(S)} \\ &= \lim_{n\to\infty} \|f_n(x)\|_{\mathsf{L}^2_\nu(S)} = \|\lim_{n\to\infty} f_n(x)\|_{\mathsf{L}^2_\nu(S)} = \|f\|_{\mathsf{L}^2_\nu(S)} \quad . \end{aligned} \tag{2.31}$$

Further, the fact that $\bullet : \mathcal{G} \times \mathsf{L}^2_\nu(S) \to \mathsf{L}^2_\nu(S)$ is an action on functions in $\mathsf{L}^2_\nu(S)$, leads to:

$$(\mathcal{T}_g \cdot \mathcal{T}_h)[f] = \mathcal{T}_g[\mathcal{T}_h[f]] = \mathcal{T}_g[h \bullet f] = g \bullet (h \bullet f) = (g \circ h) \bullet f = \mathcal{T}_{g\circ h}[f] \quad . \tag{2.32}$$

Also, $\mathcal{T}_e$ is the identity operator on $\mathsf{L}^2_\nu(S)$. Hence, the map $\zeta : \mathcal{G} \to L_\mathcal{G}$ is a homomorphism and so the operators $\mathcal{T}_g$ form a representation of $\mathcal{G}$ on $\mathsf{L}^2_\nu(S)$.

To see that each operator $\mathcal{T}_g$ is unitary, we consider $\phi, \psi \in \mathsf{L}^2_\nu(S)$ and the inner product $\langle \phi, \psi \rangle_{\mathsf{L}^2_\nu(S)} = \int_S \phi(x)\overline{\psi(x)}d\nu$. Let $\{\phi_m\}_{m\in\mathbb{N}}$ and $\{\psi_n\}_{n\in\mathbb{N}}$ be sequences in $\mathsf{C_c}(S)$ that converge to ϕ and ψ respectively. Then, by definition of the action on $\mathsf{L}^2_\nu(S)$ functions, continuity of the inner product and a change of variables, we have:

$$\begin{aligned}
&\langle \mathcal{T}_g\phi, \mathcal{T}_g\psi \rangle_{\mathsf{L}^2_\nu(S)} = \langle g \bullet \phi, g \bullet \psi \rangle_{\mathsf{L}^2_\nu(S)} = \langle \lim_{m\to\infty} \phi_m(g^{-1} \bullet x), \lim_{n\to\infty} \psi_n(g^{-1} \bullet x) \rangle_{\mathsf{L}^2_\nu(S)} \\
&= \lim_{m,n\to\infty} \langle \phi_n(g^{-1} \bullet x), \psi_m(g^{-1} \bullet x) \rangle_{\mathsf{L}^2_\nu(S)} = \lim_{m,n\to\infty} \int_S \phi_m(g^{-1} \bullet x)\, \overline{\psi_n(g^{-1} \bullet x)}\, d\nu \\
&= \lim_{m,n\to\infty} \int_{g\bullet S} \phi_m(g^{-1} \bullet (g \bullet y))\, \overline{\psi_n(g^{-1} \bullet (g \bullet y))}\, d\nu = \lim_{m,n\to\infty} \int_S \phi_m(y)\, \overline{\psi_n(y)}\, d\nu \\
&= \lim_{m,n\to\infty} \langle \phi_m, \psi_n \rangle_{\mathsf{L}^2_\nu(S)} = \langle \lim_{m\to\infty} \phi_m, \lim_{n\to\infty} \psi_n \rangle_{\mathsf{L}^2_\nu(S)} = \langle \phi, \psi \rangle_{L^2_\nu(S)} \quad .
\end{aligned} \tag{2.33}$$

Thus each $\mathcal{T}_g$ is an isometry. Furthermore, $(\mathcal{T}_g)^{-1} = \mathcal{T}_{g^{-1}}$ is well defined on and so, the range $\mathcal{T}_g$ is easily seen to be $\mathsf{L}^2_\nu(S)$. Hence, each $\mathcal{T}_g$ is a unitary operator [12] and $\zeta : \mathcal{G} \to L_{\mathcal{G}}$ forms a unitary representation of $\mathcal{G}$. ■

We now move onto ideas related to the irreducibility of representations.

2.3.3 Irreducible Representations and Completely Reducible Representations

Given two unitary representations ζ_1 and ζ_2 of $\mathcal{G}$ on the Hilbert spaces H_1 and H_2 respectively, we may introduce the set of intertwining operators for ζ_1 and ζ_2:

$$\mathcal{C}(\zeta_1, \zeta_2) = \{T \in \mathcal{L}(\mathsf{H}_1, \mathsf{H}_2) : T \cdot \zeta_1(g) = \zeta_2(g) \cdot T, \forall g \in \mathcal{G}\} \tag{2.34}$$

In particular, we refer to $\mathcal{C}(\zeta) = \mathcal{C}(\zeta, \zeta)$ as the commutant of the unitary representation $\zeta : \mathcal{G} \to \mathcal{L}(\mathsf{H}, \mathsf{H})$. Clearly, this is the set of bounded operators on H that commute with $\zeta(g)$ for every $g \in \mathcal{G}$.

We say that the representations ζ_1 and ζ_2 are unitarily equivalent if $\mathcal{C}(\zeta_1, \zeta_2)$ contains a unitary operator $U : \mathsf{H}_1 \to \mathsf{H}_2$ since in this case we have an isomorphism between the representations given as $\zeta_2(g) = U \cdot \zeta_1(g) \cdot U^{-1}, \forall g \in \mathcal{G}$. This motivates us to introduce an equivalence relation $\sim$ between unitary representations of $\mathcal{G}$ by specifying that $\zeta_1 \sim \zeta_2$ iff ζ_1 is unitarily equivalent to ζ_2. This equivalence relation clearly partitions the set of all unitary representations of $\mathcal{G}$ into equivalence classes of unitarily equivalent representations.

[12] A surjective linear isometry is a unitary map [Folland, 1999].

The question that arises at this point then, is that, given a particular equivalence class of unitary representations, is there a specific representative in the given equivalence class that has a relatively simpler structure than the others? It turns out that the answer to this question is intimately tied to the notion of invariant subspaces of representations. So we introduce:

Definition 2.3.7. Let $\zeta : \mathcal{G} \to \mathcal{U}(\mathsf{H}, \mathsf{H})$ be a unitary representation of the group $\mathcal{G}$ on the carrier space H and let $\mathcal{M}$ be a closed subspace of H. We say that $\mathcal{M}$ is an invariant subspace for the representation ζ or that $\mathcal{M}$ is group invariant if:

$$\zeta(g)[f] \in \mathcal{M}, \ \forall f \in \mathcal{M}, \forall g \in \mathcal{G}. \tag{2.35}$$

If $\mathcal{M} \neq \{0\}$ or H we say that the invariant subspace is non trivial and that the representation ζ is reducible. If ζ does not admit any non-trivial invariant subspaces, we say that the representation is irreducible. □

The above ideas lead us to the following important result:

Theorem 2.3.8. *Let $\zeta : \mathcal{G} \to \mathcal{U}(\mathsf{H}, \mathsf{H})$ be a unitary representation of the group $\mathcal{G}$ over the carrier space H and let $\mathcal{M}$ be a closed subspace of H. Let $\mathcal{P}^{\mathcal{M}}$ be the projection operator on H whose range is $\mathcal{M}$. Then:*

1. *The orthogonal complement $\mathcal{M}^{\perp}$ of $\mathcal{M}$ is group invariant if and only if $\mathcal{M}$ is group invariant.*
2. *Any $f \in \mathsf{H}$ admits the unique representation $f = f_1 + f_2$, with $f_1 \in \mathcal{M}, f_2 \in \mathcal{M}^{\perp}$.*
3. *$\mathcal{M}$ is group invariant if and only if $\mathcal{P}^{\mathcal{M}} \in \mathcal{C}(\zeta)$ i.e., $\mathcal{P}^{\mathcal{M}} \cdot \zeta(g) = \zeta(g) \cdot \mathcal{P}^{\mathcal{M}}, \ \forall g \in \mathcal{G}$.*
4. *The restriction of ζ to $\mathcal{M}$, that is, $\zeta^{\mathcal{M}}(g) = \zeta(g)|_{\mathcal{M}}$, defines a representation of $\mathcal{G}$ on $\mathcal{M}$. Similarly, the restriction of ζ to $\mathcal{M}^{\perp}$ defines a representation of $\mathcal{G}$ on $\mathcal{M}^{\perp}$. (These are the so called sub-representations of ζ over the invariant subspaces $\mathcal{M}$ and $\mathcal{M}^{\perp}$ respectively.)*

Proof: 1. We begin by recalling that $\mathcal{M}^{\perp} = \{f \in \mathsf{H} : \langle f, \phi \rangle_{\mathsf{H}} = 0, \ \forall \phi \in \mathcal{M}\}$. This definition automatically implies that $\mathcal{M}^{\perp}$ is closed, since for any convergent sequence $\{f_n\}_{n=1}^{\infty} \subset \mathcal{M}^{\perp}$ with $f = \lim_{n\to\infty} f_n$ and $\phi \in \mathcal{M}$, we have by the continuity of the inner product:

$$\langle f, \phi \rangle_{\mathsf{H}} = \langle \lim_{n\to\infty} f_n, \phi \rangle_{\mathsf{H}} = \lim_{n\to\infty} \langle f_n, \phi \rangle_{\mathsf{H}} = 0 \tag{2.36}$$

So $f \in \mathcal{M}^{\perp}$.

Now, if $\mathcal{M}$ is group invariant, then $\forall f \in \mathcal{M}, \forall \phi \in \mathcal{M}^{\perp}$ and $\forall g \in \mathcal{G}$ we have:

$$\langle \zeta(g)\phi, f \rangle_{\mathsf{H}} = \langle \phi, \zeta(g)^* f \rangle_{\mathsf{H}} = \langle \phi, \zeta(g^{-1}) f \rangle_{\mathsf{H}} = 0, \tag{2.37}$$

because $\zeta(g^{-1})f \in \mathcal{M}$ and ζ is a unitary representation. Hence, $\mathcal{M}^{\perp}$ is also group invariant. The opposite implication follows readily by exchanging the roles of $\mathcal{M}$ and $\mathcal{M}^{\perp}$ and noting that $\{\mathcal{M}^{\perp}\}^{\perp} = \bar{\mathcal{M}} = \mathcal{M}$ since $\mathcal{M}$ is closed.

2. This result is a consequence of the Hilbert projection theorem from linear functional analysis and it may be found in various standard references such as Folland [1999] and Naylor and Sell [1971]. However, because of the important role that this result plays, we derive a proof of it in Appendix C, Section C.1.

3. We first notice that for any $\phi \in \mathsf{H}$, we have $\phi \in \mathcal{M}$ if and only if $\mathcal{P}^{\mathcal{M}}\phi = \phi$. Now, if $\mathcal{P}^{\mathcal{M}} \in \mathcal{C}(\zeta)$ and if $f \in \mathcal{M}$ then $\mathcal{P}^{\mathcal{M}} f = f$ and so,

$$\forall g \in \mathcal{G},\ \zeta(g)f = \zeta(g)[\mathcal{P}^{\mathcal{M}} f] = \mathcal{P}^{\mathcal{M}}[\zeta(g)f]. \tag{2.38}$$

Thus $\zeta(g)f \in \mathcal{M},\ \forall g \in \mathcal{G}, \forall f \in \mathcal{M}$. Hence, $\mathcal{M}$ is a group invariant subspace.

Conversely, we suppose that $\mathcal{M}$ is a group invariant subspace and we let $f \in \mathsf{H}$. We use the result in part(2) to write $f = f_1 + f_2$ where, $f_1 \in \mathcal{M}, f_2 \in \mathcal{M}^{\perp}$. Now, for any $g \in \mathcal{G}$, we have $\zeta(g)[\mathcal{P}^{\mathcal{M}} f] = \zeta(g)f_1$. On the other hand,

$$\mathcal{P}^{\mathcal{M}}[\zeta(g)f] = \mathcal{P}^{\mathcal{M}}[\zeta(g)f_1] + \mathcal{P}^{\mathcal{M}}[\zeta(g)f_2]. \tag{2.39}$$

But since $\mathcal{M}^{\perp}$ is also group invariant, $\zeta(g)f_2 \in \mathcal{M}^{\perp}$ and so, $\mathcal{P}^{\mathcal{M}}(\zeta(g)f_2) = 0$. Finally, since $\mathcal{M}$ is group invariant, $\zeta(g)f_1 \in \mathcal{M}$ and so, $\mathcal{P}^{\mathcal{M}}[\zeta(g)f_1] = \zeta(g)f_1$. Hence, for any $f \in \mathsf{H}, g \in \mathcal{G}$, we have that:

$$(\mathcal{P}^{\mathcal{M}})[\zeta(g)f] = \zeta(g)[\mathcal{P}^{\mathcal{M}} f] = \zeta(g)f_1. \tag{2.40}$$

Hence $\mathcal{P}^{\mathcal{M}} \in \mathcal{C}(\zeta)$.

4. The definition of the map $\zeta^{\mathcal{M}}$ is such that for each $g \in \mathcal{G}$, we have a bounded linear operator $T_g^{\mathcal{M}} : \mathcal{M} \to \mathcal{M}$. The range of each T_g is $\mathcal{M}$ by group invariance. It is now easy to check that $\zeta^{\mathcal{M}}$ is an identity preserving homomorphism and so, it is a representation of $\mathcal{G}$ over $\mathcal{M}$. The proof for the case of $\mathcal{M}^{\perp}$ is exactly similar.

■

By part (2) of Theorem 2.3.8 above, since any $f \in \mathsf{H}$ admits the representation $f = f_1 + f_2$ with $f_1 \in \mathcal{M}$, $f_2 \in \mathcal{M}^\perp$, we may introduce the direct sum notation to write $\mathsf{H} = \mathcal{M} \oplus \mathcal{M}^\perp$. Part (4) of the theorem then motivates the notion of direct sums of representations and we may formally write $\zeta = \zeta^{\mathcal{M}} \oplus \zeta^{\mathcal{M}^\perp}$ to mean that the unitary representation $\zeta : \mathcal{G} \to \mathcal{U}(\mathsf{H}, \mathsf{H})$ has invariant subspaces $\mathcal{M}$ and $\mathcal{M}^\perp$ and that $\zeta^{\mathcal{M}}$ and $\zeta^{\mathcal{M}^\perp}$ are the restrictions of ζ to these invariant subspaces. We call $\zeta^{\mathcal{M}}$ and $\zeta^{\mathcal{M}^\perp}$ the sub-representations of ζ. We may now repeat this procedure by looking at the invariant subspaces of $\zeta^{\mathcal{M}}$ on $\mathcal{M}$ as well as the invariant subspaces of $\zeta^{\mathcal{M}^\perp}$ on $\mathcal{M}^\perp$ and so on. Thus, this recursive procedure can be used to yield a decomposition of the given Hilbert space in terms of group invariant subspaces. The usefulness of this arises from the fact that a problem posed on the original Hilbert space may often be solved more conveniently on the "smaller" invariant subspaces.

To make these ideas concrete, we first need to introduce the general notion of direct sums of Hilbert spaces. Since this involves an extra bit of work and so, we do it separately in Appendix C, Section C.2. With the ideas presented in the appendix in place, we are now ready to define the direct sum of representations:

Definition 2.3.9. For each $\alpha \in \mathcal{A}$, let ζ_α be a unitary representations of the group $\mathcal{G}$ on the Hilbert space H_α. Then the direct sum of representations is the representation ζ of $\mathcal{G}$ on $\mathsf{H} = \bigoplus_{\alpha \in \mathcal{A}} \mathsf{H}_\alpha$ defined by

$$\zeta(g)(\sum_{\alpha \in \mathcal{A}} v_\alpha) = \sum_{\alpha \in \mathcal{A}} \zeta_\alpha(g) v_\alpha \tag{2.41}$$

with $v_\alpha \in \mathsf{H}_\alpha$. We express this symbolically as $\zeta = \bigoplus_{\alpha \in \mathcal{A}} \zeta_\alpha$. □

We may easily verify that for each $g \in \mathcal{G}$, the operator $\zeta(g)$ defined in the above manner is indeed a unitary operator on H. Further, the H_α are invariant subspaces under the representation ζ and that each ζ_α is a sub-representation of ζ, i.e., $\zeta_\alpha(g) = \zeta(g)|_{\mathsf{H}_\alpha}$.

The above definition of direct sums of representations is from the perspective of building newer representations on "larger" spaces from given ones on "smaller spaces". As mentioned a little earlier, from the point of view of applications, we would in fact like to turn this procedure around by expressing a given representation on a "larger" space as the direct sum of sub-representations on "smaller" spaces. In fact, we may define:

Definition 2.3.10. Let $\zeta : \mathcal{G} \to \mathcal{U}(\mathsf{H}, \mathsf{H})$ be a unitary representation of the group $\mathcal{G}$ on the carrier space H and let us suppose that we have:

$$\mathsf{H} = \bigoplus_{\alpha \in \mathcal{A}} \mathcal{M}_\alpha, \quad \zeta = \bigoplus_{\alpha \in \mathcal{A}} \zeta_\alpha, \tag{2.42}$$

as defined in Appendix C and Definition 2.3.9. We say that the unitary representation ζ of $\mathcal{G}$ on H is completely reducible if each sub-representation ζ_α on $\mathcal{M}_\alpha$ is irreducible. □

From this perspective, it is apparent that irreducible unitary representations of a given $\mathcal{G}$ are the "building blocks" of all other (completely reducible) unitary representations of $\mathcal{G}$ since, the process of breaking down representations using invariant subspaces has to terminate when irreducible representations appear. Hence, irreducible representations assume a central role in the representation theory of $\mathcal{G}$.[13] Irreducible representations of many of the common discrete groups of isometries (particularly, the crystallographic space groups and point groups) are well known and are easily obtainable as tabulated data [Miller, 1967; Aroyo et al., 2006; Serre, 1977]. For the purpose of this work, we will have the occasion to refer to these tables when dealing with finite groups of isometries. We demonstrate in the next few sections that it is possible to prove a few qualitative features of irreducible representations of some particular groups without referring to these tables.

2.3.4 Reducibility and Irreducibility Criteria

Given a particular representation of $\mathcal{G}$ on $\mathcal{U}(\mathsf{H}, \mathsf{H})$ the results of Theorem 2.3.8 can be used to identify if the given representation is reducible or not. However, the criteria suggested in that theorem are not necessarily easy to verify and so we would like to formulate criteria which are easier to check. The following result for example, provides a characterization of completely reducible representations when the carrier space H is a finite dimensional and so this result is important from the perspective of numerical algorithms that employ symmetry:

Proposition 2.3.11. *A finite dimensional unitary representation of any group is completely reducible. In particular, there exists an orthonormal basis of* H *in which the (finite) matrix representation corresponding to any (and every) group element appears block diagonal.*

[13] Technical remark: It is not clear apriori however, that a given group will have any irreducible representations except the trivial identity representation. However, the Gelfand-Raikov Theorem [Folland, 1994] assures us that every locally compact group admits sufficiently many irreducible unitary representations on Hilbert spaces so that points can be separated. More specifically, for any locally compact group G and $x, y \in G, x \neq y$, there exists an irreducible representation ζ of G such that $\zeta(x) \neq \zeta(y)$. Thus, in case of discrete groups of isometries for example, we are assured of the existence of non-trivial representations.

Proof: If H_1 is a proper invariant subspace of H, then by part (1) of Theorem 2.3.8, $\mathsf{H}_1^\perp$ is also invariant and we have $\mathsf{H} = \mathsf{H}_1 \oplus \mathsf{H}_1^\perp$. If H_1 or $\mathsf{H}_1^\perp$ contains a proper invariant subspace, then we use the same result again, to obtain a decomposition and we continue this procedure until we obtain a decomposition of H into irreducible invariant subspaces. The finite dimensionality of H assures us that this procedure will terminate to yield the required decomposition.

Now, for the sake of definiteness, let $\dim.(\mathsf{H}) = n < \infty$. For some $m < n$, let $\{\mathcal{M}_j\}_{j=1}^m$, denote the collection of invariant subspaces of H obtained by the above procedure, i.e., $\mathsf{H} = \bigoplus_{j=1}^m \mathcal{M}_j$. For each $j = 1, \ldots, m$, let $\mathcal{E}_j = \{e_k^j\}_{k=1}^{n_j}$ be an orthonormal basis of $\mathcal{M}_j$. Clearly, the set $\mathcal{E} = \bigcup_j \mathcal{E}_j$ is an orthonormal basis of H and $\displaystyle\sum_{j=1}^{m} n_j = n$. We denote $\mathcal{E} = \{\tilde{e}_i\}_{i=1}^n$ and we let this be an ordering of $\mathcal{E}$ in which the first n_1 basis vectors belong to $\mathcal{E}_1$, the next n_2 basis vectors belong to $\mathcal{E}_2$ and so on. Thus, the first n_1 vectors in $\mathcal{E}$ are basis vectors of $\mathcal{M}_1$, the next n_2 vectors are basis vectors of $\mathcal{M}_2$, etc. For any $g \in \mathcal{G}$, we now consider the matrix representation of $\zeta(g) = \mathcal{T}_g$ in this basis. For any $i, k \in \{1, 2, \ldots, n\}$, if $\tilde{e}_i \in \mathcal{M}_j$ and $\tilde{e}_k \in \mathcal{M}_{j'}$, with $j \neq j'$, then $T_g\tilde{e}_i \in \mathcal{M}_j$ while $\tilde{e}_k \in \mathcal{M}_j^\perp$ and so, $D_{i,k}(g) = \langle T_g\tilde{e}_i, \tilde{e}_k\rangle_{\mathsf{H}} = 0$. On the other hand, if both $\tilde{e}_i, \tilde{e}_k \in \mathcal{M}_j$, then $T_g\tilde{e}_i \in \mathcal{M}_k$ as well, and so $D_{i,k}(g) \neq 0$ in general. Hence, in this basis, the matrix form of $\mathcal{T}_g$ assumes the following block diagonal form:

$$D_{n\times n}(g) = \begin{bmatrix} D^1_{n_1\times n_1}(g) & 0 & \ldots & 0 \\ 0 & D^2_{n_2\times n_2}(g) & \ldots & 0 \\ \vdots & \vdots & \vdots & \vdots \\ 0 & 0 & \ldots & D^m_{n_m\times n_m}(g) \end{bmatrix}, \tag{2.43}$$

with each $D^j(g)$ an irreducible block of size $n_j \times n_j$, for $j \in \{1, \ldots, m\}$. The rest of the entries of $D(g)$ are zero. In general however, some of the subspaces $\mathcal{M}_j$ may just be related to each other by orthogonal transformations. Thus, an irreducible representation can appear more than once in the given representation through unitarily equivalent representations. ■

Remark 2.3.12. If, in particular $\mathsf{H} = \mathbb{C}^n$, and we are working with a given basis $\mathcal{E}'$ of H such that the matrix representation of $\zeta(g)$ in this basis is $D(g)$, then the block diagonal structure of $D(g)$ is revealed by the change of basis to $\mathcal{E} = \{\tilde{e}_i\}_{i=1}^{i=n}$. This can be done by the unitary transformation $Q^\dagger D(g)Q$ with $Q = [\tilde{e}_1\ \tilde{e}_2\ \ldots\ \tilde{e}_n]$, with each $\tilde{e}_i$ expressed in the basis $\mathcal{E}'$. □

One of the most fundamental and widely used irreducibility criteria is Schur's Lemma [Folland, 1994; Barut and Raczka, 1986]. We will have the occasion to use this result quite extensively in some of the following material and so, we briefly outline a proof of this result here:

Theorem 2.3.13 (Schur's Lemma)**.** *A representation $\zeta : \mathcal{G} \to \mathcal{U}(\mathsf{H}, \mathsf{H})$ is irreducible if and only if the only operator commuting with all $\zeta(g), g \in \mathcal{G}$ is a scalar multiple of the identity operator (that is, $\mathcal{C}(\zeta)$ is one-dimensional).*

Proof: We suppose first that the given representation ζ is reducible. Then clearly, ζ has a non-trivial group invariant subspace $\mathcal{M}$. By part 3 of Theorem 2.3.8, the projection operator $\mathcal{P}^{\mathcal{M}} \in \mathcal{C}(\zeta)$ and so, $\mathcal{C}(\zeta)$ is not one-dimensional.

On the other hand, we suppose that ζ is irreducible and let $A \in \mathcal{C}(\zeta)$ such that $A \neq cI_{\mathsf{H}}$. First, let A be a symmetric (Hermitian) operator. Then, by the spectral theorem for such operators [Raskin, 2006; Folland, 1994], there exists a spectral measure E such that $A = \int \lambda \, dE_\lambda$. At this point, it simply remains to observe that $A \in \mathcal{C}(\zeta)$ would have to imply that $\zeta(g)$ commutes with all projections E_λ. This would violate irreducibility because the ranges of the projections E_λ would be left invariant by ζ. If A is not Hermitian, then $A_1 = \frac{A+A^*}{2}$ and $A_1 = \frac{A-A^*}{2i}$ are Hermitian and both lie in $\mathcal{C}(\zeta)$ since $A \in \mathcal{C}(\zeta)$. Applying the spectral theorem arguments presented above to both A_1 and A_2, we get:

$$A_1 = \lambda_1 I_{\mathsf{H}}, \quad A_2 = \lambda_2 I_{\mathsf{H}}, \quad A = (A_1 + iA_2) = (\lambda_1 + i\lambda_2) I_{\mathsf{H}} \quad . \tag{2.44}$$

This completes the proof. Further details of this calculation, using spectral measures and the spectral theorem for symmetric operators may be found in Raskin [2006]. ■

There is an immediate corollary of Schur's Lemma that turns out to be particularly useful in many situations. Its statement and proof are as follows:

Corollary 2.3.14. *If $\zeta_1 : \mathcal{G} \to \mathcal{U}(\mathsf{H}, \mathsf{H})$ and $\zeta_2 : \mathcal{G} \to \mathcal{U}(\mathsf{H}, \mathsf{H})$ are two irreducible representations of $\mathcal{G}$ then $\mathcal{C}(\zeta_1, \zeta_2) = \{0\}$ if ζ_1 and ζ_2 are inequivalent.*

Proof: If $T \in \mathcal{C}(\zeta_1, \zeta_2)$, then the adjoint $T^* \in \mathcal{C}(\zeta_1, \zeta_2)$ as for any $g \in \mathcal{G}$ we have:

$$T^* \cdot \zeta_2(g) = [\zeta_2(g^{-1}) \cdot T]^* = [T \cdot \zeta_1(g^{-1})]^* = \zeta_1(g) \cdot T^* \quad . \tag{2.45}$$

Hence we have that $T^* \cdot T \in \mathcal{C}(\zeta_1)$ while $T \cdot T^* \in \mathcal{C}(\zeta_2)$. By Schur's Lemma, we then have that $T \cdot T^* = T^* \cdot T = c\, I_{\mathsf{H}}$. Thus, either $T = 0$ or $c^{-\frac{1}{2}} T$ is unitary. In particular, therefore,

$\mathcal{C}(\zeta_1, \zeta_2) = \{0\}$ if ζ_1 and ζ_2 are inequivalent since in that case the possibility of $c^{-\frac{1}{2}}T$ being unitary is ruled out. ■

We will end this discussion by analyzing the consequences of Schur's Lemma for the particular case of finite (compact) groups of isometries which may or may not be Abelian.

2.3.5 Irreducible Representations of Finite Groups

Whether or not a finite group of isometries (which is necessarily discrete) is Abelian, it obeys the following result:

Proposition 2.3.15. *Let $\mathcal{G}$ be a finite group of isometries and let $\zeta : \mathcal{G} \to \mathcal{U}(\mathsf{H}, \mathsf{H})$ be an irreducible unitary representation of $\mathcal{G}$ on the carrier space H. Then, ζ is finite dimensional.*

Proof: We fix a unit vector $u \in \mathsf{H}$ and we define an operator T on H as follows:

$$\text{For any } v \in \mathsf{H}, Tv = \int_{\mathcal{G}} \langle v, \zeta(g)u\rangle_{\mathsf{H}}\, \zeta(g)\, u\, d\mu = \sum_{g\in\mathcal{G}} \langle v, \zeta(g)u\rangle_{\mathsf{H}}\, \zeta(g)\, u \quad . \tag{2.46}$$

We then notice the properties that $T \in \mathcal{L}(\mathsf{H}, \mathsf{H})$, T is a finite rank operator and $T \in \mathcal{C}(\zeta)$. Let us now prove each of these statements.

The linearity property of T is easily verified since the inner product is linear in it's first argument. Next, for any $v \in \mathsf{H}$, using the Cauchy Schwarz inequality,

$$\begin{aligned} \|Tv\|_{\mathsf{H}} &= \|\sum_{g\in\mathcal{G}} \langle v, \zeta(g)u\rangle_{\mathsf{H}}\, \zeta(g)\, u\|_{\mathsf{H}} \\ &\leq \sum_{g\in\mathcal{G}} |\langle v, \zeta(g)u\rangle_{\mathsf{H}}|\ \|\zeta(g)\, u\|_{\mathsf{H}} \leq \sum_{g\in\mathcal{G}} \|v\|_{\mathsf{H}} \|\zeta(g)u\|_{\mathsf{H}}^2 \end{aligned} \tag{2.47}$$

Since $\zeta(g)$ is unitary, we have that $\|\zeta(g)u\|_{\mathsf{H}} = \|u\|_{\mathsf{H}} = 1$ and so:

$$\|Tv\|_{\mathsf{H}} \leq |\mathcal{G}|\ \|v\|_{\mathsf{H}} \quad , \tag{2.48}$$

where $|\mathcal{G}|$ is the group order. Thus, $T \in \mathcal{L}(\mathsf{H}, \mathsf{H})$. Next, the operator T is of finite rank (that is, it's range is finite dimensional) since by construction, the v appears only as a complex coefficient and so:

$$\text{Ran}\,(T) \subset \text{span}\{\zeta(g)u : g \in \mathcal{G}\} \quad . \tag{2.49}$$

To check that $T \in \mathcal{C}(\zeta)$, we have for any $g \in \mathcal{G}$:

$$\begin{aligned}
\zeta(h)[Tv] &= \sum_{g\in\mathcal{G}} \langle v, \zeta(g)u\rangle_{\mathsf{H}}\, \zeta(h)[\zeta(g)\, u] = \sum_{g\in\mathcal{G}} \langle v, \zeta(g)u\rangle_{\mathsf{H}}\, \zeta(h\circ g)\, u \\
&= \sum_{(h^{-1}\circ g)\in\mathcal{G}} \langle v, \zeta(h^{-1}\circ g)u\rangle_{\mathsf{H}}\, \zeta(h\circ(h^{-1}\circ g))\, u \\
&= \sum_{g\in\mathcal{G}} \langle v, \zeta(h^{-1})[\zeta(g)u]\rangle_{\mathsf{H}}\, \zeta(g)\, u \\
&= \sum_{g\in\mathcal{G}} \langle v, \zeta(h)^*[\zeta(g)u]\rangle_{\mathsf{H}}\, \zeta(g)\, u \\
&= \sum_{g\in\mathcal{G}} \langle \zeta(h)v, \zeta(g)u\rangle_{\mathsf{H}}\, \zeta(g)\, u = T[\zeta(h)v] \quad . \qquad (2.50)
\end{aligned}$$

By Schur's Lemma (Theorem 2.3.13), since ζ is irreducible, it must be that $T = cI_{\mathsf{H}}$. But since T is of finite rank so must be I_{H} and hence, we must have that H is finite dimensional. Thus, ζ is a finite dimensional unitary representation. ■

The most important consequence of this result is that every unitary representation ζ of a finite group of isometries is completely reducible as the following result shows:

Theorem 2.3.16. *Let $\mathcal{G}$ be a finite group of isometries and let $\zeta : \mathcal{G} \to \mathcal{U}(\mathsf{H}, \mathsf{H})$ be a unitary representation of $\mathcal{G}$ on the carrier space H. Then, ζ is expressible as the direct sum of irreducible representations.*

Proof: Given an arbitrary unitary representation ζ of $\mathcal{G}$, we define the operator $T \in \mathcal{L}(H, H)$ as in Proposition 2.3.15. Then T is self-adjoint because for any $v, w \in \mathsf{H}$ we have:

$$\begin{aligned}
\langle Tv, w\rangle_{\mathsf{H}} &= \left\langle \sum_{g\in\mathcal{G}} \langle v, \zeta(g)u\rangle_{\mathsf{H}}\, \zeta(g)u\,, w \right\rangle_{\mathsf{H}} = \sum_{g\in\mathcal{G}} \langle v, \zeta(g)u\rangle_{\mathsf{H}}\, \langle \zeta(g)u, w\rangle_{\mathsf{H}} \\
&= \sum_{g\in\mathcal{G}} \langle \zeta(g)^*v, u\rangle_{\mathsf{H}}\, \langle u, \zeta(g)^*w\rangle_{\mathsf{H}} = \sum_{g\in\mathcal{G}} \langle \zeta(g^{-1})v, u\rangle_{\mathsf{H}}\, \langle u, \zeta(g^{-1})w\rangle_{\mathsf{H}} \\
&= \left\langle \sum_{g\in\mathcal{G}} \langle u, \zeta(g)w\rangle_{\mathsf{H}}\zeta(g)v\,, u \right\rangle_{\mathsf{H}} = \langle v, Tw\rangle_{\mathsf{H}} \quad , \qquad (2.51)
\end{aligned}$$

as well as the fact that both T and T^* are defined on all of H. Hence, T is a finite rank self adjoint operator on H. So the spectral theorem for compact self-adjoint operators [Naylor and Sell, 1971] says that T has a nonzero eigenvalue λ with a finite dimensional eigenspace $\mathcal{M}$. But $T \in \mathcal{C}(\zeta)$ by the calculations in Proposition 2.3.15 and so, $\mathcal{M}$ is a group invariant

subspace by part 3 of Theorem 2.3.8. Thus, ζ has a finite dimensional sub-representation on $\mathcal{M}$. By Proposition 2.3.11, every finite dimensional representation is completely reducible. Hence, ζ has an irreducible sub-representation.

Now we consider families of mutually orthogonal irreducible invariant subspaces of ζ. We can partially order these families by set inclusion and use Zorn's Lemma [Folland, 1999; Naylor and Sell, 1971] to conclude that there is a maximal family $\{\mathcal{M}_\alpha\}_{\alpha\in\mathcal{A}}$. Let $\mathsf{H}_\mathcal{A} = \oplus_{\alpha\in\mathcal{A}}\mathcal{M}_\alpha$ and let $\mathcal{N}$ be the orthogonal complement of $\mathsf{H}_\mathcal{A}$. By part 1 of Theorem 2.3.8, it must be that $\mathcal{N}$ is group invariant since $\mathsf{H}_\mathcal{A}$ is group invariant. By the maximality of $\{\mathcal{M}_\alpha\}_{\alpha\in\mathcal{A}}$, it must be that $\mathcal{N}$ is irreducible, otherwise it should have been part of the family $\{\mathcal{M}_\alpha\}_{\alpha\in\mathcal{A}}$. Hence it must be that $\mathcal{N} = \{0\}$. Thus, we are led to the conclusion $\mathsf{H} = \mathsf{H}_\mathcal{A} = \oplus_{\alpha\in\mathcal{A}}\mathcal{M}_\alpha$ with each $\mathcal{M}_\alpha$ a finite dimensional irreducible invariant subspace. Thus, introducing $\zeta_\alpha = \zeta|_{\mathcal{M}_\alpha}$ we see that ζ is expressible as $\zeta = \oplus_{\alpha\in\mathcal{A}}\zeta_\alpha$, with each ζ_α an irreducible representation of $\mathcal{G}$, thus proving the theorem. ■

We find it quite remarkable that there is in fact a systematic method to carry out the direct sum decomposition that the above theorem proves the existence of. That is, there is actually an explicit formula that one can use for constructing the invariant subspaces associated with the irreducible representations of a finite group. In the context of investigating the effects of symmetry on a boundary value problem, this is perhaps the single most useful result. To prove this result, we first need the following:

Lemma 2.3.17 (Orthogonality Relations)**.** *Let $\zeta : \mathcal{G} \to \mathcal{U}(\mathsf{H},\mathsf{H})$ and $\zeta' : \mathcal{G} \to \mathcal{U}(\mathsf{H},\mathsf{H})$ be any two irreducible unitary representations of $\mathcal{G}$ on the carrier space H. Let $D_{ij}(g)$ and $D'_{ij}(g)$ denote respectively, the the matrix elements of $\zeta(g)$ and $\zeta'(g)$. Let d_ζ be the matrix dimension of the representation D_{ij}. Then, the matrix elements satisfy the relations:*

$$\frac{1}{|\mathcal{G}|}\sum_{g\in\mathcal{G}} D_{ij}(g)\overline{D'_{mn}(g)} = \begin{cases} 0 & \text{if} \quad \zeta \text{ and } \zeta' \text{are not equivalent.} \\ \frac{1}{d_\zeta}\,\delta_{im}\delta_{jn} & \text{if} \quad \zeta \text{ and } \zeta' \text{are unitarily equivalent.} \end{cases} \tag{2.52}$$

Proof: We introduce the operators:

$$E_{ij} = \frac{1}{|\mathcal{G}|}\sum_{g\in\mathcal{G}} \zeta(g)\mathcal{E}_{ij}\zeta'(g^{-1}) \;, \tag{2.53}$$

with $(\mathcal{E}_{ij})^{mn} = \delta_{i,m}\delta_{j,n};\ i,m = 1,2,\ldots,d_\zeta$ and $j,n = 1,2,\ldots,d_{\zeta'}$. [14] For every $h \in \mathcal{G}$,

[14] Due to Proposition 2.3.15, we know that both ζ and ζ' must be equivalent to finite dimensional matrices of dimension d_ζ and $d_{\zeta'}$ respectively. The operator $\mathcal{E}_{ij}$ is a linear transformation on the space of $d_{\zeta'} \times d_{\zeta'}$ matrices, with range in the space of $d_\zeta \times d_\zeta$ matrices.

the operators (2.53) satisfy the relation:

$$\begin{aligned}\zeta(h)E_{ij} &= \frac{1}{|\mathcal{G}|}\sum_{g\in\mathcal{G}}\zeta(h\circ g)\mathcal{E}_{ij}\zeta'(g^{-1}) \\ &= \frac{1}{|\mathcal{G}|}\sum_{g\in\mathcal{G}}\zeta(g')\,\mathcal{E}_{ij}\,\zeta'(g'^{-1}\circ h) = E_{ij}\zeta'(h)\ . \end{aligned} \tag{2.54}$$

Hence, if ζ is not equivalent to ζ', then Schur's lemma (in the form of Corollary 2.3.14) implies $E_{ij}=0$, or in terms of matrix components:

$$\frac{1}{|\mathcal{G}|}\sum_{g\in\mathcal{G}}D_{li}(g)D'_{jk}(g^{-1}) = \frac{1}{|\mathcal{G}|}\sum_{g\in\mathcal{G}}D_{li}(g)\overline{D'_{jk}(g)} = 0\ . \tag{2.55}$$

On the other hand, if ζ and ζ' are equivalent, then by Schur's Lemma (Theorem 2.3.13), we have $E_{ij}=\lambda_{ij}I$. Thus, for $(l,i)\neq(k,j)$, the orthogonality relations (2.54) are still satisfied. If, however, $(l,i)=(k,j)$, then using (2.53) and $E_{ii}=\lambda_{ii}I$ (no summation), we obtain:

$$(E_{ii})_{ll} = \frac{1}{|\mathcal{G}|}\sum_{g\in\mathcal{G}}D_{li}(g)D_{il}(g^{-1}) = \frac{1}{|\mathcal{G}|}\sum_{g\in\mathcal{G}}|D_{li}(g)|^2 = \lambda_{ii}\ . \tag{2.56}$$

To evaluate the constant λ_{ii}, we set $i=j$ in (2.53) and take the trace on both sides to obtain:

$$\text{Tr.}(E_{ii}) = d_\zeta\,\lambda_{ii} = \frac{1}{|\mathcal{G}|}\sum_{g\in\mathcal{G}}\text{Tr.}(\zeta(g)\,\mathcal{E}_{ii}\,\zeta'(g^{-1})) = \text{Tr.}(\mathcal{E}_{ii}) = 1\ . \tag{2.57}$$

In the above, we have used the fact that the trace remains invariant under cyclic permutations. Thus, by (2.57), we finally conclude that $\lambda_{ii}=\frac{1}{d_\zeta}$, thus completing the proof. ■

A common statement of the above orthogonality relations [Bossavit, 1986] involves identifying equivalent representations by a Kronecker delta and then rewriting (2.52) as:

$$\frac{d_\nu}{|\mathcal{G}|}\sum_{g\in\mathcal{G}}D^\mu_{ij}(g)D^\nu_{lk}(g^{-1}) = \delta_{ik}\delta_{jl}\delta_{\mu\nu}\ . \tag{2.58}$$

Let us point out that the total number of inequivalent irreducible representations of a finite group equals the number of conjugacy classes [Serre, 1977] in the group, and so it is necessarily finite. Hence, we may think of numbering all the inequivalent irreducible representations associated with $\mathcal{G}$ by $\nu=1,\ldots,\ell$ and denoting them as ζ^ν, $\nu=1,\ldots,\ell$. We now have the following result:

Theorem 2.3.18 (Projection Operators)**.** *Let $\zeta : \mathcal{G} \to \mathcal{U}(\mathsf{H}, \mathsf{H})$ be an arbitrary unitary representation of the finite group of isometries $\mathcal{G}$ on the carrier space H. Let $\zeta^\nu : \mathcal{G} \to \mathcal{U}(\mathsf{H}, \mathsf{H})$ be an irreducible representation of $\mathcal{G}$ on the same carrier space and let d_ν be the dimension of the representation ζ^ν. Let the matrix elements of $\zeta^\nu(h)$ be denoted as $D^\nu_{ij}(h)$ and let us set:*

$$P^\nu_{ij} = \frac{d_\nu}{|\mathcal{G}|} \sum_{h \in \mathcal{G}} \overline{D^\nu_{ij}(h)} \zeta(h) \quad . \tag{2.59}$$

Then the P^ν_{ii} are projection operators on H, their ranges $V^\nu_{ii} = P^\nu_{ii}(\mathsf{H})$ are mutually orthogonal closed subspaces of H and we have the direct sum decomposition:

$$\mathsf{H} = \bigoplus_{\nu,i} V^\nu_{ii} \quad , \tag{2.60}$$

the direct sum being taken over $\nu = 1 \ldots, \ell$ and $i = 1, \ldots, d_\nu$.

Proof: We define P^ν_{ij} as in (2.59) and observe, that since $\zeta(g)$ and $D^\nu(g)$ are unitary operators, the operators P^ν_{ii} obey $P^\nu_{ii} = (P^\nu_{ii})^*$. Thus the operators P^ν_{ii} are self-adjoint. By direct computation, we have for every $g \in \mathcal{G}$:

$$\begin{aligned}
\zeta(g) P^\nu_{ij} &= \zeta(g) \, \frac{d_\nu}{|\mathcal{G}|} \sum_{h \in \mathcal{G}} D^\nu_{ji}(h^{-1}) \zeta(h) \\
&= \frac{d_\nu}{|\mathcal{G}|} \sum_{h \in \mathcal{G}} D^\nu_{ji}(h^{-1}) \zeta(g \circ h) = \frac{d_\nu}{|\mathcal{G}|} \sum_{h \in \mathcal{G}} D^\nu_{ji}(h^{-1} \circ g) \zeta(h) \\
&= \sum_{k=1}^{d_\nu} \frac{d_\nu}{|\mathcal{G}|} \sum_{h \in \mathcal{G}} D^\nu_{jk}(h^{-1}) D^\nu_{ki}(g) \zeta(h) = \sum_{k=1}^{d_\nu} D^\nu_{ki}(g) \, \frac{d_\nu}{|\mathcal{G}|} \sum_{h \in \mathcal{G}} D^\nu_{jk}(h^{-1}) \zeta(h) \\
&= \sum_{k=1}^{d_\nu} D^\nu_{ki}(g) \, P^\nu_{kj} \, .
\end{aligned} \tag{2.61}$$

Now, by use of the orthogonality relations (2.58) and (2.61), we conclude that:

$$P^\mu_{kl} P^\nu_{ij} = \frac{d_\mu}{|\mathcal{G}|} \sum_{g \in \mathcal{G}} D^\mu_{lk}(g^{-1}) \sum_{m=1}^{d_\mu} D^\nu_{mi}(g) P^\nu_{mj} = \delta_{li} \, \delta_{\mu\nu} \, P^\nu_{kj} \, . \tag{2.62}$$

The above expression immediately yields a few results. First, we conclude that $P^\mu_{ii} \, P^\nu_{jj} = \delta_{ij} \, \delta_{\mu\nu} \, P^\nu_{ij}$. Therefore, if V^ν_{ii} denotes the image of H under P^ν_{ii}, then the V^ν_{ii} are mutually orthogonal. The formulas also show that $P^\nu_{ii} P^\nu_{ii} = P^\nu_{ii}$ and since P^ν_{ii} are self-adjoint, we conclude that the P^ν_{ii} are in fact orthogonal projectors onto the ranges V^ν_{ii}.

To see that we actually obtain the decomposition (2.60), we can argue by contradiction. We introduce the projection operators associated with the irreducible representations, that is:

$$Q^{\nu} = \sum_{i=1}^{d_\nu} P_{ii}^{\nu} = \frac{d_\nu}{|\mathcal{G}|} \sum_{g \in \mathcal{G}} \overline{\text{Tr.}(\zeta^{\nu}(g))}\, \zeta(g) \quad . \tag{2.63}$$

clearly, for $\nu = 1, \ldots, \ell$, the range of the operators Q^{ν} is obtained as:

$$V^{\nu} = Q^{\nu}(\mathsf{H}) = \bigoplus_{i} V_{ii}^{\nu} \quad . \tag{2.64}$$

We may easily check using (2.62) that the operators Q^{ν} obey:

$$Q^{\nu} Q^{\mu} = \delta_{\mu\nu} Q^{\mu} \quad , \tag{2.65}$$

and so, V^{ν} form mutually orthogonal subspaces of H. Let us form:

$$W = \bigoplus_{\nu} V^{\nu} = \bigoplus_{i,\nu} V_{ii}^{\nu} \quad . \tag{2.66}$$

For the sake of contradiction, if $W \neq \mathsf{H}$, then the orthogonal complement $W^{\perp}$ of W in H would be an invariant subspace (by Theorem 2.3.8) and so the restriction of ζ to $W^{\perp}$ would be a sub-representation. Then, we would be able to find $Y \subseteq W^{\perp}$, such that Y is an irreducible subspace. But this would contradict the fact that the list of irreducible representations $\zeta^{\nu}, \nu = 1, \ldots, \ell$, which are the restrictions of ζ to all possible irreducible subspaces, is exhaustive.[15] ■

Remark 2.3.19. As a consequence of the above results, we may obtain an interpretation of the operators P_{ij}^{ν} as isomorphisms. Specifically, the operator P_{ji}^{ν} maps the space V_{ii}^{ν} onto the space V_{jj}^{ν} injectively. The proof of this result follows directly from the identities $P_{ii}^{\nu} P_{ij}^{\nu} = P_{ij}^{\nu}$, $P_{ij}^{\nu} P_{jj}^{\nu} = P_{ij}^{\nu}$ and $P_{ij}^{\nu} P_{ji}^{\nu} = P_{ii}^{\nu}$, all of which follow from (2.62). We note that these formulas also imply that the image of H under P_{ij}^{ν} is in V_{ii}^{ν} and that P_{ij}^{ν} maps to zero outside V_{jj}^{ν}. Thus, given $w \in \mathsf{H}$, we observe that P_{ij}^{ν} will "pick out" the component of w in V_{jj}^{ν} and it will map this component to its counterpart in V_{ii}^{ν}.

With these important ideas about group representations in place, our focus for the next chapter will be to use these tools for developing the cell problem associated with Density Functional Theory calculations of objective structures.

[15] In essence, this is a restatement of Theorem 2.3.16.

Chapter 3

Formulation of cell problems

In this chapter, we analyze the electronic structure computation problem of objective structures generated by finite groups of isometries and by helical groups. We use the tools developed in the previous chapter to characterize the effect of symmetry on a simplified version of the Kohn-Sham equations (2.19–2.21). We show that, like in the case of periodic Density Functional Theory for crystals, it is possible to formulate cell problems for Objective Structures. We first discuss the case of objective structures generated by finite groups and then later discuss the case of helical groups. The material in this chapter concerning results on objective structures generated by finite groups is directly adopted from our earlier work in Banerjee [2011].

3.1 Cell problem for Objective Structures generated by finite groups of isometries

3.1.1 Problem Set Up and Simplification

Let $\mathcal{S}$ be a fixed point free objective structure generated by the finite group of isometries $\mathcal{G}$ acting on the finite set $\mathcal{M}_0$. A finite group of isometries consists of (proper or improper) rotations which have at least one common fixed point Dayal et al. [2013], and we may assume that this fixed point is the origin, without any loss of generality.

We suppose that $\mathcal{M}_0$ consists of the points $\{\mathbf{x}_1, \mathbf{x}_2, \ldots, \mathbf{x}_{m_0}\} \subset \mathbb{R}^3$. We suppose further that $\{Z_1, Z_2, \ldots, Z_{m_0}\}$ are the respective nuclear charges associated with these points and we let $|\mathcal{G}|$ denote the group order. We are interested in computing the electronic structure of $\mathcal{S}$ and we intend to use the Kohn-Sham model of Density Function Theory (outlined in

Chapter 2, Section 2.2.3) for doing so. For the purpose of this calculation, we assume that the objective structure consists of $m_0|\mathcal{G}|$ nuclei and N electrons. The electronic structure associated with the objective structure is therefore obtained by the solving the minimization problem 2.17 or by solving the equations 2.19-2.21.

3.1.1.1 Simplification of domain

One of the key difficulties that one has to overcome while analyzing this probleme mathematically is that it is a locally compact problem posed on a noncompact domain in the following sense [Defranceschi and Le Bris, 1997]: if one restricts the problem to one posed on an open subset of $\mathbb{R}^3$ that has compact closure, then proving existence of solutions is relatively straightforward. The problem posed on the whole space on the other hand, is much more difficult to deal with. As far as numerical computations are concerned however, we will always be interested in computing solutions on a connected, bounded open set with a regular boundary. Hence, the first simplification that we will assume is that the objective structure $\mathcal{S}$ is embedded in a large sphere of radius R centered at the origin and we will apply the boundary condition $\rho(\mathbf{x}) = 0$ on the surface of the sphere to account for the fact that the electronic density of a finite system is known to have exponential decay far away from the system. This will automatically imply via eq. 2.21 that the $\phi_i(\mathbf{x})$ that appear in the Kohn-Sham model will also obey $\phi_i(\mathbf{x}) = 0$ whenever $|\mathbf{x}| = R$.

The particular choice of R is to be dictated by the decay properties of the exact electronic density (defined via equation 2.12) associated with the structure. Specifically, it is known from Hoffmann-Ostenhof et al. [1980] and Ahlrichs et al. [1981] for example, that at large distances from any nucleus the square root of the electronic density of an N-electron system with total nuclear charge Z and first ionization potential ϵ obeys:

$$\sqrt{\rho(\mathbf{x})} \leq C\,(1+|\mathbf{x}|)^{(Z-N+1)/\sqrt{2\epsilon}-1}\ \exp\left(-\sqrt{2\epsilon}\,|\mathbf{x}|\right) \quad . \tag{3.1}$$

Thus, as far as the analysis of the problem is concerned, we will not make any particular specification of R other than it has to be finite but "sufficiently large" in the sense that the $\rho(\mathbf{x}) = 0$ boundary condition is commensurate with (3.1). As far as the analysis of the problem is concerned, the choice of a spherical domain is particularly useful to us because such a domain possesses a C^∞ boundary and the isometric group action of any finite set of rotations is well defined for points belonging to a sphere.

3.1.1.2 Linearization via Self Consistent Field Iterations

Now, let $\mathcal{B}_R$ denote the open ball of radius R centered at the origin. Based on the above discussion, the problem at hand now reads as:

$$\tilde{I}_N^{KS} = \inf_{\phi_i \in \mathsf{H}_0^1(\mathcal{B}_R)} \left\{ \frac{1}{2} \sum_{i=1}^{N} \int_{\mathcal{B}_R} |\nabla \phi_i|^2 + \int_{\mathcal{B}_R} \rho V_{nu} + \frac{1}{2} \int_{\mathcal{B}_R} \int_{\mathcal{B}_R} \frac{\rho(\mathbf{x})\rho(\mathbf{y})}{|\mathbf{x}-\mathbf{y}|} \, d\mathbf{x}\, d\mathbf{y} \right.$$
$$\left. + E_{xc}(\rho) : \langle \phi_i, \phi_j \rangle_{L^2(\mathcal{B}_R)} = \delta_{ij} \right\} \quad . \tag{3.2}$$

Since each ϕ_i lies in the space $\mathsf{H}_0^1(\mathcal{B}_R)$ (this is simply the closure of $\mathsf{C}_c^\infty(\mathcal{B}_R)$ in the H^1 norm), we need to interpret the boundary conditions $\phi_i(\mathbf{x}) = 0, \forall \mathbf{x} \in \partial\mathcal{B}_R$ in the trace sense. Let us remark at this stage that a standard line of argument employing the direct method in the calculus of variations can be used to prove the existence of solutions to problem (3.2) for E_{xc} given by common parametrizations of the Local Density Approximation. Details of such an argument may be found in Suryanarayana et al. [2010].

Like many of the standard real space algorithms of Kohn-Sham Density Functional Theory (see for example Chelikowsky et al. [1994] or Martin [2004]), we now choose to work with the Euler-Lagrange equations of the minimization problem (3.2), that is the Kohn-Sham equations posed on the ball with Dirichlet boundary conditions:

$$\left(-\frac{1}{2}\Delta + V_{nu}(\mathbf{x}) + \left(\int_{\mathcal{B}(R)} \frac{\rho(\mathbf{x})}{|\mathbf{y}-\mathbf{x}|} \, d\mathbf{x} \right) + V_{xc}(\rho(\mathbf{x})) \right) \phi_i(\mathbf{x}) = \lambda_i \phi_i(\mathbf{x}) \quad , \tag{3.3}$$

$$\langle \phi_i, \phi_j \rangle_{L^2(\mathcal{B}(R))} = \delta_{ij}, \quad \rho(\mathbf{x}) = \sum_{i=1}^{N} |\phi_i(\mathbf{x})|^2 \quad , \tag{3.4}$$

$$\text{and for } \mathbf{x} \in \partial\mathcal{B}(R), \quad \phi_i(\mathbf{x}) = 0 \quad . \tag{3.5}$$

As we remarked earlier, the usual method of solution of this set of non-linear equations is to introduce a self-consistent iteration scheme. Let us make this a little more precise since this is effectively the process by which we achieve a linearization of (3.3). For the sake of simplicity, let us consider the case of linear mixing. First, we may lump all but the first term that appears on the left hand of (3.3) into a single term $\tilde{V}(\mathbf{x}, \rho(x))$ to write:

$$\left(-\frac{1}{2}\Delta + \tilde{V}(\mathbf{x}, \rho(x)) \right) \phi_i(\mathbf{x}) = \lambda_i \phi_i(\mathbf{x}) \quad . \tag{3.6}$$

To solve this iteratively, we suppose that we have a guess for the ground state electronic density of the system $\rho^k(\mathbf{x})$ at some stage of the iteration. We may now define the following

update scheme for $0 < \tilde{\alpha} < 1$:

$$V^k(\mathbf{x}) = \tilde{V}(\mathbf{x}, \rho^k(\mathbf{x})) \quad , \tag{3.7}$$

$$\Big(-\frac{1}{2}\Delta + V^k(\mathbf{x})\Big)\phi_i^{k+1}(\mathbf{x}) = \lambda_i^{k+1}\phi_i^{k+1}(\mathbf{x}),\ (\text{for } i = 1, \ldots, N) \quad , \tag{3.8}$$

$$\rho^{k+1}(\mathbf{x}) = \tilde{\alpha}\left(\sum_{i=1}^{N}|\phi_i^{k+1}(\mathbf{x})|^2\right) + (1-\tilde{\alpha})\,\rho^k(\mathbf{x}) \quad . \tag{3.9}$$

We could now hope that for a good enough initial guess $\rho^1(\mathbf{x})$, the above iteration would converge to an actual solution of (3.3-3.4) and satisfy the boundary condition (3.5). Thus, (3.7-3.9) form a linear approximation of the original problem in this sense. In an actual simulation, a typical choice for $\rho^1(\mathbf{x})$ would be to obtain it from the atomic orbitals of the constituent atoms [Le Bris, 2003].

The above discussion motivates the study of the following linearized eigenvalue problem (posed on the open ball of radius R) for a suitable class of "effective" potentials $V(\mathbf{x})$:

$$\Big(-\frac{1}{2}\Delta + V(\mathbf{x})\Big)\phi_i(\mathbf{x}) = \lambda_i\phi_i(\mathbf{x}), \quad \phi_i(\mathbf{x}) = 0 \text{ on } \partial\mathcal{B}_R \quad (i = 1, \ldots, N). \tag{3.10}$$

We aim to study how the above eigenvalue problem interacts with the symmetry group of a finite objective structure later in this chapter. First however, we need to characterize the relevant class of effective potentials and the generic properties of the above eigenvalue problem (3.10). We carry out this study next.

3.1.2 Characterization of the Effective Potential

Let us assume for the moment that the electronic density ρ is a known function and that ρ is continuous and compactly supported on the closure of $\mathcal{B}_R$, that is, we let $\rho \in \mathsf{C}_c^0(\mathcal{B}_R)$. The effective potential is given as:

$$V(\mathbf{x}) = \tilde{V}(\rho, \mathbf{x}) = V_{xc}(\rho(\mathbf{x})) + \int_{\mathcal{B}_R}\frac{\rho(\mathbf{y})}{|\mathbf{x}-\mathbf{y}|}\,d\mathbf{y} + V_{nu}(\mathbf{x}) \quad . \tag{3.11}$$

Let us examine the above expression term by term. One of the most common parametrizations of the Local Density Approximation form for V_{xc} is due to Perdew and Zunger [1981]

and Ceperley and Alder [1980] and it is of the following form:

$$
\begin{aligned}
V_{xc}(\rho) &= V_x(\rho) + V_c(\rho) \quad . \\
V_x(\rho) &= \Big(\epsilon_x(\rho) + \rho\frac{d\,\epsilon_x(\rho)}{d\rho}\Big), \quad V_c(\rho) = \Big(\epsilon_c(\rho) + \rho\frac{d\,\epsilon_c(\rho)}{d\rho}\Big) \quad . \\
\epsilon_x(\rho) &= -\frac{3}{4}\Big(\frac{3}{\pi}\Big)^{1/3}\rho^{1/3} \quad . \\
\epsilon_c(\rho) &= \begin{cases} \frac{\gamma}{1+\beta_1\sqrt{r_s}+\beta_2 r_s} & \text{for } r_s \geq 1 \quad . \\ A\log r_s + B + Cr_s\log r_s + Dr_s & \text{for } r_s < 1 \quad . \end{cases} \\
\text{where, } r_s &= \Big(\frac{3}{4\pi\rho}\Big)^{1/3} \quad .
\end{aligned} \tag{3.12}
$$

The coefficients $A, B, C, D, \gamma, \beta_1, \beta_2$ are chosen such that, among other things, $\epsilon_c(\rho)$ has a continuous first derivative at $r_s = 1$. It is quite clear that $V_x(\rho)$ is a continuous function. If we make the additional hypothesis that $\epsilon_c(0) = 0$, we see that $V_c(\rho)$ also becomes a continuous function thus making V_{xc} continuous in our region of interest. Unfortunately however, we can't say that V_{xc} is any more regular than this, since the first derivative of V_x blows up near zero.

The second term, that is, the Coulombic interaction between the electrons is better behaved. We may invoke results from potential theory [Gilbarg and Trudinger, 2001] to tell us that if ρ is Hölder continuous, then for $V_H(\mathbf{x}) = \int_{\mathcal{B}_R} \frac{\rho(\mathbf{y})}{|\mathbf{x}-\mathbf{y}|}\,dy$, we must have $V_H \in \mathsf{C}^2(\mathcal{B}_R)$ and and that it must satisfy the boundary value problem:

$$
\begin{aligned}
-\Delta V_H &= 4\pi\rho \quad \text{for } \mathbf{x} \in \mathcal{B}_R \quad , \\
V_H(\mathbf{x}) &= \int_{\mathcal{B}_R} \frac{\rho(\mathbf{y})}{|\mathbf{x}-\mathbf{y}|}\,d\mathbf{y} \quad \text{for } \mathbf{x} \in \partial\mathcal{B}_R \quad .
\end{aligned} \tag{3.13}
$$

Apart from demonstrating the above regularity property, this result is also quite useful to use at the numerical level, especially when large numerical simulations are involved: the integral expression for V_H is often much more expensive computationally, than solving the Poisson problem (3.13) by a conjugate gradient solver [Chelikowsky et al., 1994]. However, as we will see in Chapter 4, that there is a convenient way for us to deal with the integral expression for V_H.

The last term arises due to the nuclear interaction and it is also of a Coulombic nature. The standard Coulombic term is not continuous at the location of the nuclei. It is therefore, very common in the DFT simulations to replace this term by a smooth approximation [Le Bris,

2003; Martin, 2004].[1] One of the simplest ways to achieve this is to assume that a nuclear charge is not concentrated at a specific point but that it is smeared out as a smooth function supported on a small ball B_δ centered on the location of the nucleus. The expression for V_{nu} becomes:

$$V_{nu}(\mathbf{x}) = \sum_{\Upsilon \in \mathcal{G}} \sum_{i=1}^{m_0} \int_{B_\delta(\Upsilon(\mathbf{x}_i))} -\frac{Z_i \, b(|\mathbf{y} - \Upsilon(\mathbf{x}_i)|)}{|\mathbf{x} - \mathbf{y}|} \, d\mathbf{y} \quad , \tag{3.14}$$

where, $b(|\mathbf{y} - \mathbf{x}_i|)$ is a smooth radially symmetric charge distribution such that:

$$\int_{B_\delta(\mathbf{x}_i)} b(|\mathbf{y} - \mathbf{x}_i|) \, d\mathbf{y} = 1 \quad . \tag{3.15}$$

Since $b \in \mathsf{C}_c^\infty(B_\delta)$, it must be that $V_{nu}(\mathbf{x})$ is smooth [Gilbarg and Trudinger, 2001].

We will now prove a rather simple result which in some sense, forms the basis for the rest of the work presented in this section:

Lemma 3.1.1. *Let us suppose that the electronic density of the objective structure $\mathcal{S}$ is continuous, and that it inherits the symmetry of the structure, that is:*

$$\forall \mathbf{x} \in \mathcal{B}_R, \forall \Upsilon \in \mathcal{G}, \rho(\Upsilon(\mathbf{x})) = \rho(\mathbf{x}) \quad . \tag{3.16}$$

Then, the effective potential $V(x)$ is also continuous on $\mathcal{B}_R$ and it inherits the symmetry of the objective structure.

Proof: The continuity of V is required to ensure that we may investigate the behavior of $V(\mathbf{x})$ pointwise. From the preceding discussion, since V_{xc} is continuous in ρ, and ρ has been assumed continuous, $V_{xc}(\mathbf{x})$ must be a continuous function of $\mathbf{x}$. The nuclear contribution through (3.14) is also continuous. That, V_H is continuous if ρ is continuous, can be easily justified by potential theory results [Gilbarg and Trudinger, 2001]. Hence, the sum of V_{xc}, V_{nu} and V_H is a continuous function of $\mathbf{x}$.

Now, for arbitrary $\mathbf{x} \in \mathcal{B}_R, \forall \Upsilon \in \mathcal{G}$, we can investigate the effect of the change $\mathbf{x} \mapsto \Upsilon(\mathbf{x})$ by looking at how $V_{xc}(\mathbf{x}), V_H(\mathbf{x})$ and $V_{nu}(\mathbf{x})$ behave. From the parametrizations presented in (3.12), it is clear that V_{xc} respects the symmetry of the objective structure since

[1] This is the commonly referred to as the pseudopotential approximation. Another motivation for using a pseudopotential is that they can be formulated in a way such that only valence electrons have to be solved for in the resulting Kohn-Sham equations. The core electrons are usually chemically inert and do not play an important role in most chemical and physical processes. We will adopt this approximation in this work. See more details on this in Chapter 4

it is an explicit function of ρ and $\rho(\mathbf{x})$ respects the symmetry of the objective structure. Considering now, the representation formula for V_H, we have, by the change of variables $\mathbf{y} = \Upsilon(\mathbf{z})$:

$$\begin{aligned} V_H(\Upsilon(\mathbf{x})) = \int_{\mathcal{B}_R} \frac{\rho(\mathbf{y})}{|\Upsilon(\mathbf{x}) - \mathbf{y}|}\, d\mathbf{y} &= \int_{\Upsilon^{-1}(\mathcal{B}_R)} \frac{\rho(\Upsilon(\mathbf{z}))}{|\Upsilon(\mathbf{x}) - \Upsilon(\mathbf{z})|}\, d\mathbf{z} \\ &= \int_{\mathcal{B}_R} \frac{\rho(\mathbf{z})}{|\mathbf{x} - \mathbf{z}|}\, d\mathbf{z} = V_H(\mathbf{x}) \quad . \end{aligned} \tag{3.17}$$

This verifies that this contribution to the potential also inherits the symmetry of the objective structure. Finally, considering the nuclear contribution through (3.14), we have by the same change of variables $\mathbf{y} = \Upsilon(\mathbf{z})$:

$$\begin{aligned} V_{nu}(\Upsilon(\mathbf{x})) &= \sum_{\Upsilon_1 \in \mathcal{G}} \sum_{i=1}^{m_0} \int_{B_\delta(\Upsilon_1(\mathbf{x}_i))} -\frac{Z_i\, b(|\mathbf{y} - \Upsilon_1(\mathbf{x}_i)|)}{|\Upsilon(\mathbf{x}) - \mathbf{y}|}\, d\mathbf{y} \\ &= \sum_{\Upsilon_1 \in \mathcal{G}} \sum_{i=1}^{m_0} \int_{\Upsilon^{-1}(B_\delta(\Upsilon_1(\mathbf{x}_i)))} -\frac{Z_i\, b(|\Upsilon(\mathbf{z}) - \Upsilon(\Upsilon^{-1} \circ \Upsilon_1(\mathbf{x}_i))|)}{|\Upsilon(\mathbf{x}) - \Upsilon(\mathbf{z})|}\, d\mathbf{z} \\ &= \sum_{\Upsilon_1 \in \mathcal{G}} \sum_{i=1}^{m_0} \int_{(B_\delta(\Upsilon^{-1} \circ \Upsilon_1(\mathbf{x}_i)))} -\frac{Z_i\, b(|\mathbf{z} - \Upsilon^{-1} \circ \Upsilon_1(\mathbf{x}_i)|)}{|\mathbf{x} - \mathbf{z}|}\, d\mathbf{z} \\ &= \sum_{(\Upsilon^{-1} \circ \Upsilon_1) \in \mathcal{G}} \sum_{i=1}^{m_0} \int_{(B_\delta(\Upsilon^{-1} \circ \Upsilon_1(\mathbf{x}_i)))} -\frac{Z_i\, b(|\mathbf{z} - \Upsilon^{-1} \circ \Upsilon_1(\mathbf{x}_i)|)}{|\mathbf{x} - \mathbf{z}|}\, d\mathbf{z} \\ &= V_{nu}(\mathbf{x}) \quad . \end{aligned} \tag{3.18}$$

Thus, the effective potential $V(\mathbf{x})$ inherits the symmetry of the objective structure. ■

In our simplified framework therefore, we are led to the study of the a Schrödinger operator with an effective potential which is continuous and group invariant. We next summarize some results related to this eigenvalue problem.

3.1.3 Study of the simplified eigenvalue problem

The Kohn Sham equations (and its simplifications considered in this work) require that we evaluate the lowest n eigenvalues and corresponding eigenfunctions of the Kohn Sham operator. Even for the simplified eigenvalue problem however, it is not clear apriori that there exist eigenvalues and corresponding eigenfunctions since, from the material in Appendix C.3 there exist numerous possibilities in an infinite dimensional setting. In particular, it is quite possible to have linear operators that do not possess eigenfunctions at all. In the lan-

gauage of Appendix C.3, we find it necessary to investigate existence of a point spectrum in our simplified problem. The canonical approach to this, is to use the weak theory of elliptic equations [Gilbarg and Trudinger, 2001; Evans, 1998; Renardy and Rogers, 2004] as discussed below.

3.1.3.1 Existence of Eigenvalues & Eigenfunctions

In light of the discussion in the previous section, our starting point is the consideration of the operator $\mathfrak{H} = -\frac{1}{2}\Delta + V$, on the function space $\mathsf{L}^2(\mathcal{B}_R)$, with $V(\mathbf{x})$ a continuous and group invariant potential. It turns out that $\mathfrak{H}$ is an unbounded operator which is is densely defined on the domain $\mathsf{H}^2(\mathcal{B}_R) \cap \mathsf{H}^1_0(\mathcal{B}_R)$ [2]. The operator is clearly symmetric, since for any $u, v \in \mathsf{H}^2(\mathcal{B}_R) \cap \mathsf{H}^1_0(\mathcal{B}_R)$, we can show, using integration by parts:

$$\langle \mathfrak{H}u, v\rangle_{\mathsf{L}^2(\mathcal{B}_R)} = \langle u, \mathfrak{H}v\rangle_{\mathsf{L}^2(\mathcal{B}_R)} \, . \tag{3.19}$$

Study of the weak form of the eigenvalue problem (3.10) allows us to establish the existence of eigenvalues and associated eigenvectors. To interpret the eigenvalue problem associated with $\mathfrak{H}$ in a weak sense, we have to introduce the sesquilinear form $\mathfrak{B} : \mathsf{H}^1_0(\mathcal{B}_R) \times \mathsf{H}^1_0(\mathcal{B}_R) \to \mathbb{C}$ associated with $\mathfrak{H}$. For any $u, v \in \mathsf{H}^1_0(\mathcal{B}_R)$, we let:

$$\mathfrak{B}[u, v] = \int_{\mathcal{B}_R} \frac{1}{2}\nabla u.\nabla\overline{v} + Vu\overline{v}\, d\mathbf{x} \quad , \tag{3.20}$$

and we say that $\{\lambda \in \mathbb{C}, v \in \mathsf{H}^1_0(\mathcal{B}(R))\}$ is an eigenvalue-eigenvector pair for the operator $\mathfrak{H}$ in the weak sense if:

$$\mathfrak{B}[u, v] = \lambda\langle u, v\rangle_{\mathsf{L}^2(\mathcal{B}_R)} \quad \forall v \in \mathsf{H}^1_0(\mathcal{B}_R) \quad . \tag{3.21}$$

Using the Poincaré inequality, the Lax-Milgram lemma and the Rellich-Kondrachov theorem [Evans, 1998; Renardy and Rogers, 2004; Kato, 1995] we can show that the resolvent operator $R_\kappa = (\mathfrak{H} - \kappa I)^{-1}$ of $\mathfrak{H}$ (for κ belonging to the resolvent set of $\mathfrak{H}$), is a compact self-adjoint operator on $\mathsf{L}^2(\mathcal{B}_R)$. The spectral theorem for compact-self adjoint operators [Naylor and Sell, 1971; Kato, 1995] can therefore, be used on R_κ to prove the existence of an increasing sequence of real eigenvalues and associated eigenfunctions[3], which form an orthonormal basis of $\mathsf{L}^2(\mathcal{B}_R)$. This finally allows us to conclude that $\mathfrak{H}$ indeed has a point spectrum, and that there exist weak solutions to the problem (3.21). We may summarize

[2] Refer to Evans [1998] or Renardy and Rogers [2004] for the standard definitions of the Sobolev spaces $\mathsf{H}^2(\mathcal{B}_R)$ and $\mathsf{H}^1_0(\mathcal{B}_R)$

[3] Refer to Appendix C, section C.3 for some relevant definitions.

the above discussion as follows:

Theorem 3.1.2. *For $V(\mathbf{x}) \in \mathsf{C}(\mathcal{B}_R)$, the operator $\mathfrak{H} = -\frac{1}{2}\Delta + V$ has a compact self-adjoint resolvent $R_\kappa : \mathsf{L}^2(\mathcal{B}_R) \to \mathsf{H}^2(\mathcal{B}_R) \cap \mathsf{H}_0^1(\mathcal{B}_R)$. The operator $\mathfrak{H}$ therefore, has an increasing sequence of real eigenvalues of finite multiplicity $\lambda_1 \leq \lambda_2 \leq \ldots \leq \lambda_i \leq \ldots$ such that $\lambda_i \to \infty$ as $i \to \infty$. Further, there is an orthonormal basis $\{\phi_i\}_{i\in\mathbb{N}}$ of $\mathsf{L}^2(\mathcal{B}_R)$ consisting of the eigenfunctions $\{\phi_i\}_{i\in\mathbb{N}} \in \mathsf{H}_0^1(\mathcal{B}_R)$ such that $\mathfrak{H}\phi_i = \lambda_i\phi_i$ holds in the weak sense.*

We now move on to the issue of regularity of the eigenfunctions since they play some role in the self-consistent iterations.

3.1.3.2 Comments on the Regularity of Eigenfunctions

The next natural question that we need to concern ourselves with is, how regular the eigenfunctions of the operator $\mathfrak{H}$ are. In the light of self-consistent iterations, this is very important, since regularity of the eigenfunctions of $\mathfrak{H}$ dictate the regularity of the resulting density and hence, the regularity of the effective potential that appears in the next step of the self consistent iterations. Fortunately, theorems from the theory of elliptic partial differential equations can again be invoked to acquire this information. Since $V \in \mathsf{C}(\mathcal{B}_R) \subset \mathsf{L}^\infty(\mathcal{B}_R)$ and we are working on a domain with a smooth boundary, we may conclude that any eigenfunction $\phi \in \mathsf{H}^2(\mathcal{B}_R)$ [Theorem 4 in Chapter 6 of Evans, 1998]. We may then invoke general Sobolev inequalities [Theorem 6 in Chapter 5 of Evans, 1998] to conclude that ϕ Hölder continuous on $\mathcal{B}_R$ with the Hölder exponent $= 0.5$. As far as the self-consistent scheme is concerned, this is already quite good since this means that the density obtained from these eigenfunctions will be regular enough to yield a continuous effective potential for the next step of the iterations. We may however, sharpen the above regularity results considerably by using theorems from potential theory [specifically, Theorem 3.1 in Chapter 3 of Han and Lin, 2000] to conclude that even the gradient of ϕ is actually Hölder continuous. Among other things therefore, these theorems tell us that it makes sense to interpret values of the eigenfunctions and their gradients pointwise. This is useful from the perspective of implementation of boundary conditions in numerical methods as well as the analysis of convergence properties of these numerical methods.

3.1.4 Symmetry and the Simplified Eigenvalue Problem

We are now ready to analyze the interaction of the isometry group $\mathcal{G}$, of the given objective structure $\mathcal{S}$, with the simplified eigenvalue problem associated with electronic structure

calculation of $\mathcal{S}$. Most of the abstract theory worked out in Chapter 2 works for *any* unitary representations of a discrete group of isometries on *any* Hilbert space. As far as the simplified eigenvalue problem associated with electronic structure calculation is concerned, the function space that is of most interest to us is $\mathsf{L}^2(\mathcal{B}_R)$. Here again, results from Chapter 2 (specifically, Lemma 2.3.5 and Theorem 2.3.6) already tell us how to obtain group representations. We need to focus mainly on the consequences of Schur's Lemma (Theorem 2.3.13) as it applies to our problem.

3.1.4.1 Block Diagonalization of the Resolvent

In the context of Lemma 2.3.5 let us consider $S = \mathcal{B}_R$ and equip $\mathcal{B}_R$ with the Lebesgue measure[4]. Then Theorem 2.3.6 allows us to construct a unitary representation ζ of $\mathcal{G}$ on the carrier space $\mathsf{L}^2(\mathcal{B}_R)$. We denote the set of unitary operators associated with this unitary representation as $L_{\mathcal{G}} = \{T_g = \zeta(g) : g \in \mathcal{G}\}$. As in Chapter 2, let us denote the unitary irreducible representations of $\mathcal{G}$ as $\zeta^\nu, \nu = 1, \ldots, \ell$ and let us denote the matrix components of ζ^ν as D^ν_{ij} , $i, j = 1, \ldots, d_\nu$.

We will first show that for a potential that is associated with the objective structure, the operator $\mathfrak{H}$ on its domain $\text{Dom.}(\mathfrak{H}) = \mathsf{H}^2(\mathcal{B}_R) \cap \mathsf{H}^1_0(\mathcal{B}_R)$ commutes with each of the operators in $L_{\mathcal{G}}$. To see this, let us consider any $f \in \mathsf{C}^2_c(\mathcal{B}_R), g \in \mathcal{G}$ and observe that since the mapping $\mathbf{x} \mapsto \mathbf{R}^T_g\mathbf{x} - \mathbf{c}_g = g^{-1} \bullet \mathbf{x}$ leaves the Laplacian invariant. [5] The potential V is also group invariant by Lemma 3.1.1, and so we have:

$$\begin{aligned} T_g \cdot \mathfrak{H}[f(\mathbf{x})] &= T_g[(-\frac{1}{2}\Delta f)(\mathbf{x}) + (Vf)(\mathbf{x})] = (-\frac{1}{2}\Delta f)(g^{-1} \bullet \mathbf{x}) + (Vf)(g^{-1} \bullet \mathbf{x}) \\ &= (-\frac{1}{2}\Delta f)(g^{-1} \bullet \mathbf{x}) + V(\mathbf{x})f(g^{-1} \bullet \mathbf{x}) \quad . \end{aligned} \tag{3.22}$$

On the other hand, we also have:

$$\mathfrak{H} \cdot T_g[f(\mathbf{x})] = (-\frac{1}{2}\Delta + V)[f(g^{-1} \bullet \mathbf{x})] = (-\frac{1}{2}\Delta f)(g^{-1} \bullet \mathbf{x}) + V(\mathbf{x})f(g^{-1} \bullet \mathbf{x}) \quad . \tag{3.23}$$

Hence, $T_g \cdot \mathfrak{H}[f(\mathbf{x})] = \mathfrak{H} \cdot T_g[f(\mathbf{x})]$. By the density of $\mathsf{C}^2_c(\mathcal{B}_R)$ in $\text{Dom.}(\mathfrak{H}) = \mathsf{H}^2(\mathcal{B}_R) \cap \mathsf{H}^1_0(\mathcal{B}_R)$, we may now extend the above calculation to the domain of $\mathfrak{H}$ to conclude that $\mathfrak{H}$ commutes with each of the operators in $L_{\mathcal{G}}$. [6]

[4] The Lebesgue measure is a Radon measure and it is group invariant.

[5] This is easily verified by a change of variables calculation.

[6] Technically, to make the leap from $\mathsf{C}^2_c(\mathcal{B}_R)$ to $\text{Dom.}(\mathfrak{H}) = \mathsf{H}^2(\mathcal{B}_R) \cap \mathsf{H}^1_0(\mathcal{B}_R)$, it suffices to observe that the sesquilinear form $\mathfrak{B}[u, v]$ associated with $\mathfrak{H}$, obeys $\mathfrak{B}[u, v] = \mathfrak{B}[T_g(u), T_g(v)]$ for every $u, v \in \mathsf{H}^1_0(\mathcal{B}_R)$ and every $T_g \in L_{\mathcal{G}}$.This calculation is shown in (3.26).

At this point, we would like to invoke Schur's Lemma and its results from Chapter 2 to come to conclusions about the structure of $\mathfrak{H}$. The technical issue however, is that $\mathfrak{H}$ is an unbounded operator on $\mathsf{L}^2(\mathcal{B}_R)$. On the other hand Schur's Lemma concerns bounded operators. [7] We may avoid this annoying technicality by dealing with the resolvent operator of $\mathfrak{H}$[8]. This suits our purpose particularly well since the resolvent $R_\kappa : \mathsf{L}^2(\mathcal{B}_R) \to \mathsf{H}^2(\mathcal{B}_R) \cap \mathsf{H}^1_0(\mathcal{B}_R)$ of the operator $\mathfrak{H}$ is self-adjoint and compact for any κ belonging to the resolvent set (by Theorem 3.1.2). To proceed further, we first note the following result:

Proposition 3.1.3. *Let $A : Dom.(A) \subset \mathcal{X} \to \mathcal{X}$ be a closed linear operator[9] on the Banach space $\mathcal{X}$, such that the resolvent set of A is non-empty. Let B be a bounded linear operator on $\mathcal{X}$. Then, A commutes with B if and only if the resolvent $\mathcal{R}(\kappa, A)$ of A, commutes with B for some, and hence every κ in the resolvent set of A.*

Proof: Presented in Appendix C. ■

We now apply this abstract result to the operator $\mathfrak{H}$, to obtain:

Lemma 3.1.4. *For every κ in the resolvent set of $\mathfrak{H}$, the resolvent operator R_κ of $\mathfrak{H}$ commutes with every operator in $L_{\mathcal{G}}$.*

Proof: This result follows easily from the above proposition. It is not difficult to verify that the operator $\mathfrak{H}$, on $\mathcal{X} = \mathsf{L}^2(\mathcal{B}_R)$ is indeed, a closed operator, and that the resolvent set of $\mathfrak{H}$ is non-empty [Kato, 1995; Renardy and Rogers, 2004]. The calculations above already show that $\mathfrak{H}$ commutes with every operator in $L_{\mathcal{G}}$. Since each operator in $L_{\mathcal{G}}$ is a bounded operator on $\mathcal{X}$, the sought result follows. ■

With the above results in place, we are now in a position to use Schur's Lemma and it's consequences. Since R_κ is a bounded operator and $R_\kappa \in \mathcal{C}(\zeta)$, the basic idea is that we may perform a "block-diagonalization" of the operator R_κ in a precise sense described below.

Let us fix κ in the resolvent set of $\mathfrak{H}$ [10] and consider the resolvent operator R_κ. Let v be an eigenvector of R_κ and let $\sigma \in \mathbb{R}$ be the associated eigenvalue[11]. Since this implies

[7] In any case, it is quite awkward to interpret what commutation of an unbounded operator with a bounded operator such as T_g means and so it is customary in Functional Analysis to replace an unbounded operator by its resolvent while looking at commuting operators [Teschl, 2009]. This is what we do here as well.

[8] Refer to Appendix C for a definition of the resolvent operator and the resolvent set.

[9] As is customary in the literature, for an unbounded operator A on $\mathcal{X}$, the domain of A is denoted as Dom.(A)

[10] In particular, a detailed proof of Theorem 3.1.2 reveals that the resolvent set of $\mathfrak{H}$ is not empty. Any sufficiently large κ actually belongs to the resolvent set. The symmetry related arguments presented here work for any κ in the resolvent set.

[11] Since R_κ is self-adjoint, every eigenvalue of R_κ must be real.

that v is also an eigenvector of $\mathfrak{H}$ with the associated eigenvalue $1/\sigma$, many of the things which we discuss now hold for the operator $\mathfrak{H}$ as well. Now, since $R_\kappa v = \sigma v$, operating with any $T_g = \zeta(g), g \in \mathcal{G}$, we get that $T_g R_\kappa v = T_g \, \sigma v$. Lemma 3.1.4 implies that $R_\kappa(T_g v) = \sigma(T_g v)$, that is, $T_g v$ is also an eigenvector of R_κ, with the same eigenvalue. Thus, the eigen-space associated with a given eigenvalue σ, that is, the set $Y_\sigma = \{v : R_\kappa v = \sigma v\}$ carries a representation of the group $\mathcal{G}$. The natural question that arises, is if the representation carried by Y_σ reducible. The general belief, seems to be that such a representation will be irreducible in general [McWeeny, 2002; Bossavit, 1986]. Since the question of reducibility is basically the same as finding invariant subspaces, and in this case, the subspaces have already been distinguished according to eigenvalue, two non-symmetry related eigenvectors sharing the same eigenvalue are very unlikely to occur. Any such, non-symmetry related degeneracy is termed *accidental* in the literature [McWeeny, 2002], with the understanding that such degeneracies would vanish under small perturbations of the system[12]. Thus, assuming that accidental degeneracies do not exist, we may conclude that every degenerate group of eigenfunctions Y_σ of R_κ provides an irreducible representation of the group $\mathcal{G}$. Since the eigenvectors of R_κ provide a complete orthonormal basis of $\mathsf{L}^2(\mathcal{B}_R)$, we may now summarize the above discussions as follows:

Theorem 3.1.5. *Suppose, that the (unbounded) operator $\mathfrak{H} = -\frac{1}{2} + V(\mathbf{x})$ on $\mathsf{L}^2(\mathcal{B}_R)$ is such that the potential $V \in \mathsf{C}(\mathcal{B}_R)$ is invariant under the finite group of isometries $\mathcal{G}$. Then, for every d_ν-dimensional irreducible representation of the group $\mathcal{G}$, we can find d_ν-fold degenerate sets of eigenfunctions of $\mathfrak{H}$. Any further degeneracies should be viewed as accidental.*

Since a non-Abelian group necessarily has irreducible representations which have dimension more than one, we may conclude that in such cases, we would necessarily encounter symmetry related degenerate eigenfunctions.

As mentioned earlier, for a finite group $\mathcal{G}$, the dimension of irreducible representations of $\mathcal{G}$ is finite (Proposition 2.3.15) and the number of non-equivalent representations of $\mathcal{G}$ is finite as well. On the other hand, $\mathsf{L}^2(\mathcal{B}_R)$ is infinite dimensional. We therefore conclude that the number of degenerate sets of eigenfunctions must be infinite. Let us look at this a little more carefully from the point of view of the symmetry related projection operators introduced in Chapter 2.

Let S denote the spectrum of R_κ and as before, let $\mathsf{H} = \mathsf{L}^2(\mathcal{B}_R)$. Let Y_σ denote the

[12] If it is found that such "accidental" degeneracies are stable under perturbations, then the usual interpretation is that the system under question has generic un-accounted for symmetries [Bossavit, 1986].

eigenspace associated with $\sigma \in S$. The spectral theorem for compact operators [Naylor and Sell, 1971; Helmberg, 2008] tells us that we may write:

$$\mathsf{H} = \bigoplus_{\sigma \in S} Y_\sigma \quad . \tag{3.24}$$

On the other hand, from Chapter 2, we have the following projectors, for $\nu = 1, \ldots, \ell$:

$$\begin{aligned} \mathsf{H} &= \bigoplus_{\nu=1}^{l} V^\nu \ , \\ V^\nu = Q^\nu(\mathsf{H}) \ , \ Q^\nu &= \frac{d_\nu}{|\mathcal{G}|} \sum_{g \in \mathcal{G}} \overline{\mathrm{Tr.}(\zeta^\nu(g))}\, \zeta(g) \quad . \end{aligned} \tag{3.25}$$

The natural question is, how the subspaces V^ν are related to the subspaces Y_σ. As alluded to in the above discussion, the relationship is that, in the absence of accidental degeneracies, for every $\sigma \in S$, we have $Y_\sigma \subset V^\nu$ for some $\nu = 1, \ldots, \ell$. Provided there are no accidental degeneracies, this amounts to the claim that if $\exists v \in V^\nu \cap Y_\sigma$ with $v \neq 0$, then $Y_\sigma \subset V^\nu$. Thus, in the absence of accidental degeneracy, we have a partition of the spectrum S into the form $S = \cup_{\nu=1}^{d_\nu} S_\nu$, such that $Y_\sigma \subset V^\nu$ whenever $\sigma \in S_\nu$. The subspaces $V^\nu_{ii} \subset V^\nu, i = 1, \ldots, d_\nu, \nu = 1, \ldots, \ell$ correspond to choosing one eigenvector at a time (out of the d_ν ones available) from each $Y_\sigma \subset V^\nu$ (with $\sigma \in S_\nu$) and forming the closed linear span of these eigenvectors.[13]

Intuitively, it also makes sense to look at the matrix coefficients of R_κ in an orthonormal basis obtained from the basis functions of V^ν. First, we observe that R_κ commutes with each of the projectors Q^ν since it commutes with each operator in $L_\mathcal{G}$. This implies that R_κ has each V^ν as an invariant subspace. This is because, if $v \in V^\nu$, that is, if $Q^\nu v = v$, we have $R_\kappa v = R_\kappa(Q^\nu v) = Q^\nu(R_\kappa v) \in V^\nu$. Since R_κ has each V^ν as an invariant subspace, the matrix coefficient $\langle R_\kappa e_\alpha, e_\gamma \rangle_{\mathsf{L}^2(\mathcal{B}_R)}$ is non-zero or zero depending on whether e_α and e_γ are from the same invariant subspace or not. Since any compact operator is the norm limit of a sequence of finite rank operators [Naylor and Sell, 1971], we may think of R_κ as an "infinite matrix" with block diagonal entries corresponding to these non-zero matrix coefficients in the symmetry adapted basis.

We conclude therefore that the use of the theory developed in Chapter 2 allows the original

[13] We note however, that while the subspaces V^ν can be specified irrespective of the choice of basis vectors, the spaces V^ν_{ii} can only be obtained as the linear span of a set of basis vectors that are chosen specially. If accidental degeneracies are absent, the irreducible subspace associated with a particular eigenvalue can be specified without a particular choice of basis vectors as well.

eigenvalue problem to be broken into independent symmetry adapted subproblems. Specifically, there are ℓ subproblems, each associated with one of the irreducible representations of $\mathcal{G}$. The subproblems are obtained by restriction of the original problem to the subspaces $V^\nu, \nu = 1, \ldots, \ell$. In the next section, we will try to obtain a concrete formulation of these restricted subproblems. Later, we will show that see that these restricted subproblems can be interpreted as boundary value problems posed on the fundamental domain. [14]

3.1.5 Formulation of Symmetry Adapted Subproblems

Let us begin by observing that for every $T_g \in L_\mathcal{G}, g = (\mathbf{R}_g|\mathbf{0}) \in \mathcal{G}$ and for every $u, v \in \mathsf{H}^1_0(\mathcal{B}_R)$, the sesquilinear form $\mathfrak{B}[u, v]$ associated with our problem, obeys the condition:

$$
\begin{aligned}
&\mathfrak{B}[T_g u, T_g v] \\
&= \int_{\mathcal{B}_R} \frac{1}{2} \nabla u(g^{-1} \bullet \mathbf{x}) . \nabla \overline{v(g^{-1} \bullet \mathbf{x})} + V(\mathbf{x}) u(g^{-1} \bullet \mathbf{x}) \overline{v(g^{-1} \bullet \mathbf{x})} \, d\mathbf{x} \\
&= \int_{\mathcal{B}_R} \frac{1}{2} \big(\mathbf{R}_g^T \nabla u(\mathbf{x})\big) . \big(\mathbf{R}_g^T \nabla \overline{v(\mathbf{x})}\big) \, d\mathbf{x} + \int_{\mathcal{B}_R} V(g^{-1} \bullet \mathbf{x}) u(g^{-1} \bullet \mathbf{x}) \overline{v(g^{-1} \bullet \mathbf{x})} \, d\mathbf{x} \\
&= \int_{\mathcal{B}_R} \frac{1}{2} \big(\nabla u(\mathbf{x})\big) . \big(\mathbf{R}_g \mathbf{R}_g^T \nabla \overline{v(\mathbf{x})}\big) \, d\mathbf{x} + \int_{\mathcal{B}_R} V(g^{-1} \bullet \mathbf{x}) u(g^{-1} \bullet \mathbf{x}) \overline{v(g^{-1} \bullet \mathbf{x})} \, d\mathbf{x} \\
&= \int_{\mathcal{B}_R} \frac{1}{2} \nabla u(\mathbf{x}) . \nabla \overline{v(\mathbf{x})} \, d\mathbf{x} + \int_{\mathcal{B}_R} V(\mathbf{x}) u(\mathbf{x}) \overline{v(\mathbf{x})} \, d\mathbf{x} \\
&= \mathfrak{B}[u, v] \, .
\end{aligned} \tag{3.26}
$$

In the above calculation, we have used the group invariance of the potential V, the group invariance of the Lebesgue measure and the invariance of $\mathcal{B}_R$ under the group action. The property (3.26) is often referred to as equivariance in the literature [Bossavit, 1993] and we see that it implies:

$$
\mathfrak{B}[T_g u, v] = \mathfrak{B}[T_g u, T_g T_g^* v] = \mathfrak{B}[u, T_g^* v] = \mathfrak{B}[u, T_{g^{-1}} v] \, . \tag{3.27}
$$

[14] We recall, that every group action has a fundamental set (Proposition 2.3.2). However, usual formulations of boundary value problems require that the set on which the problem is being posed has some topological regularities. Therefore, we need to introduce the idea of a fundamental domain, since having a fundamental set is not adequate for discussing boundary value problems. This is done in Section 3.1.6.

This, in turn, by the sesquilinearity of $\mathfrak{B}$, implies that for each of the operators P^{ν}_{ij}, introduced in (2.59), we have:

$$\begin{aligned}\mathfrak{B}[P^{\nu}_{ij}u, v] &= \frac{d_\nu}{|\mathcal{G}|}\sum_{g\in\mathcal{G}}\overline{D^{\nu}_{ij}(g)}\mathfrak{B}[T_g u, v] = \sum_{g\in\mathcal{G}} D^{\nu}_{ji}(g^{-1})\mathfrak{B}[u, T_{g^{-1}}v] \\ &= \mathfrak{B}[u, \sum_{g\in\mathcal{G}}\overline{D^{\nu}_{ji}(g^{-1})}T_{g^{-1}}v] = \mathfrak{B}[u, P^{\nu}_{ji}v]\ . \end{aligned} \tag{3.28}$$

In particular, this implies that $\mathfrak{B}[P^{\nu}_{ii}u, v] = \mathfrak{B}[u, P^{\nu}_{ii}v]$. Summing over $i = 1, \ldots, d_\nu$, this also gives us, $\mathfrak{B}[Q^{\nu}u, v] = \mathfrak{B}[u, Q^{\nu}v]$. The fact that each operator T_g is unitary, implies that $\langle T_g u, T_g v\rangle_{\mathsf{L}^2(\mathcal{B}_R)} = \langle u, v\rangle_{\mathsf{L}^2(\mathcal{B}_R)}$ for every $u, v \in \mathsf{H}^1_0(\mathcal{B}_R)$. Since, the inner product is a sesquilinear form on $\mathsf{H}^1_0(\mathcal{B}_R)\times\mathsf{H}^1_0(\mathcal{B}_R)$, this automatically implies, $\langle P^{\nu}_{ij}u, v\rangle_{\mathsf{L}^2(\mathcal{B}_R)} = \langle u, P^{\nu}_{ji}v\rangle_{\mathsf{L}^2(\mathcal{B}_R)}$. Together, these results now imply the following about the weak form of the symmetry adapted subproblems[15]:

Proposition 3.1.6. *A function $u \in \mathsf{H}^1_0(\mathcal{B}_R)$ satisfies the eigenvalue problem* (3.21) *if and only if, for some $\nu = 1\ldots, \ell$, it satisfies:*

$$\mathfrak{B}[u, w] = \lambda\langle u, w\rangle_{\mathsf{L}^2(\mathcal{B}_R)}\,, \quad \forall w \in W^{\nu} = Q^{\nu}(\mathsf{H}^1_0(\mathcal{B}_R))\ . \tag{3.29}$$

Thus, solving the problem (3.21) *is equivalent to solving the ℓ subproblems listed in* (3.29)*.*

Proof: Given $u \in \mathsf{H}^1_0(\mathcal{B}_R)$ which satisfies $\mathfrak{B}[u, v] = \lambda\langle u, v\rangle_{\mathsf{L}^2(\mathcal{B}_R)},\ \forall v \in \mathsf{H}^1_0(\mathcal{B}_R)$, we must have that $u \in W^{\nu} = Q^{\nu}(\mathsf{H}^1_0(\mathcal{B}_R))$ for some $\nu = 1\ldots, \ell$.[16] Thus, we have, $Q^{\nu}u = u$, for this value of ν. So, we may write, $\forall v \in \mathsf{H}^1_0(\mathcal{B}_R)$:

$$\mathfrak{B}[u, v] = \mathfrak{B}[Q^{\nu}u, v] = \mathfrak{B}[u, Q^{\nu}v] = \lambda\langle u, Q^{\nu}v\rangle_{\mathsf{L}^2(\mathcal{B}_R)}\ . \tag{3.30}$$

In particular, if $v \in W^{\nu}$, this immediately gives us (3.29).

On the other hand, suppose that we have found $u \in \mathsf{H}^1_0(\mathcal{B}_R)$, which satisfies (3.29). It

[15] A technical point here is that the representation theory tools (projection operators, etc) developed were for functions in $\mathsf{L}^2(\mathcal{B}_R)$ and the result in Proposition 3.1.6 concerns functions in $\mathsf{H}^1_0(\mathcal{B}_R)$. This is alright, because the group action associated with the operators in $L_{\mathcal{G}}$ work for both the Hilbert spaces. Indeed, we may verify that $P^{\nu}_{ii}(\mathsf{H}^1_0(\mathcal{B}_R)) = P^{\nu}_{ii}(\mathsf{L}^2(\mathcal{B}_R))\cap\mathsf{H}^1_0(\mathcal{B}_R)$. As mentioned earlier, the operator theoretic interpretation of the eigenvalue problem is associated with the space $\mathsf{L}^2(\mathcal{B}_R)$, while it's equivalent weak interpretation is associated with the space $\mathsf{H}^1_0(\mathcal{B}_R)$.

[16] Following the discussion in Section 3.1.4.1, this assertion is certainly true provided accidental degeneracies are absent. In case an accidental degeneracy is present, we may choose our basis such that the eigenspace associated with a given eigenvalue σ, Y_σ can be written as $Y_\sigma = S_1 \cup S_2$, with $S_1 \subset W^{\nu_1}$ and $S_2 \subset W^{\nu_2}$. The rest of the theorem now works as outlined.

suffices to consider the case in which $u \in W^\nu = Q^\nu(\mathsf{H}^1_0(\mathcal{B}_R))$.[17] Given any $v \in \mathsf{H}^1_0(\mathcal{B}_R)$, we write, using Theorem 2.3.18 and equation (2.66), $v = v^\parallel + v^\perp$ with $v^\parallel \in W^\nu, v^\perp \in (W^\nu)^\perp$. We have therefore, using $\langle u, v^\perp\rangle_{\mathsf{L}^2(\mathcal{B}_R)} = 0$ and $Q^\nu v^\perp = 0$:

$$\begin{aligned}\mathfrak{B}[u,v] =& \mathfrak{B}[u,v^\parallel] + \mathfrak{B}[u,v^\perp] = \lambda\langle u, v^\parallel\rangle_{\mathsf{L}^2(\mathcal{B}_R)} + \mathfrak{B}[Q^\nu u, v^\perp] \\ =& \lambda\langle u, v^\parallel\rangle_{\mathsf{L}^2(\mathcal{B}_R)} + \lambda\langle u, v^\perp\rangle_{\mathsf{L}^2(\mathcal{B}_R)} + \mathfrak{B}[u, Q^\nu v^\perp] \\ =& \lambda\langle u, v\rangle_{\mathsf{L}^2(\mathcal{B}_R)} \ . \end{aligned} \tag{3.33}$$

Thus, (3.21) is established.[18] ■

Thus, we have obtained an interpretation of the symmetry adapted subproblems that can be obtained by restriction of the operator R_κ to the subspaces $V^\nu = Q^\nu(\mathsf{L}^2(\mathcal{B}_R)), \nu = 1, \ldots, \ell$, associated with the irreducible representations of $\mathcal{G}$.

3.1.6 Interpretation of Symmetry Adapted Subproblems

The naive interpretation of the use of symmetry in a boundary value problem would be that the problem can somehow be recast into smaller problems on the fundamental domain. It becomes necessary therefore, to interpret the problems associated with the symmetry adapted subspaces, mentioned in the earlier section, in terms of problems associated with the fundamental domain. As in Bossavit [1986, 1993], we use the notion of ν-symmetric families of vectors (functions in this case) to achieve this goal. We introduce:

Definition 3.1.7. A ν-symmetric set of vectors in H is a d_ν-tuple $\{v_i\}_{i=1}^{d_\nu} \subset \mathsf{H}$ such that $v_i = P^\nu_{ij}\, v_j, \forall i, j = 1, \ldots, d_\nu$. As a consequence of Remark 2.3.19, this definition requires that $v_i \in V^\nu_{ii}$. □

To systematically build a ν-symmetric set of vectors, we may start with any $v \in \mathsf{H}$ and we may set $v^\nu_{i,(j)} = P^\nu_{ij}\, v, \forall i, j = 1, \ldots, d_\nu$. Then, the set $\{v^\nu_{i,(j)}\}_{i=1}^{d_\nu}$ is ν-symmetric for every

[17] Absence of accidental degeneracy in fact, requires that $u \in W^\nu$, for some ν. In any case, the condition (3.29) implies that the part of u that lies in W^ν also obeys the same condition. To see this, we write for $u \in \mathsf{H}^1_0(\mathcal{B}_R), v \in W^\nu$:

$$\mathfrak{B}[u,v] = \mathfrak{B}[u, Q^\nu v] = \mathfrak{B}[Q^\nu u, v] \ . \tag{3.31}$$

On the other hand, we also have:

$$\langle u, Q^\nu v\rangle_{\mathsf{L}^2(\mathcal{B}_R)} = \langle Q^\nu u, v\rangle_{\mathsf{L}^2(\mathcal{B}_R)} \ . \tag{3.32}$$

Thus, we must have $\mathfrak{B}[Q^\nu u, v] = \lambda\langle Q^\nu u, v\rangle_{\mathsf{L}^2(\mathcal{B}_R)}$ for every $v \in W^\nu$.

[18] We may observe that the well posedness of problem (3.29) follows easily since the subspaces W^ν are closed and therefore they are Hilbert spaces in their own right.

fixed $j = 1, \ldots, d_\nu$. Thus, every $\nu = 1, \ldots, \ell$ contributes to d_ν ν-symmetric sets and each set is of size d_ν. The elements of the ν-symmetric sets so formed $v^\nu_{i,(j)}$, are referred to as the generalized Fourier components of $v \in \mathsf{H}$ [Bossavit, 1986, 1993]. Conversely, given d_ν ν-symmetric sets, $\{v^\nu_{i,(j)}\}_{i=1}^{d_\nu}, j = 1, \ldots, d_\nu$, we may reconstruct $v = \sum_{\nu=1}^{l} \sum_{i=1}^{d_\nu} v^\nu_{i,(i)}$. Next, we may use the relation (2.62) to verify that this vector $v \in \mathsf{H}$ will generate the same generalized Fourier components that it was created from.

A ν-symmetric set of vectors transforms in a very special way under the group action. In fact, we may show [Bossavit, 1986]:

Proposition 3.1.8. *A d_ν-tuple of vectors $\{v_j\}_{i=1}^{d_\nu} \subset \mathsf{H}$ is a ν-symmetric set if and only if for every $j = 1, \ldots, d_\nu$, we have:*

$$\zeta(g) v_j = \sum_{k=1}^{d_\nu} D^\nu_{kj}(g) v_k \ , \ \forall g \in \mathcal{G}. \tag{3.34}$$

Proof: Given a ν-symmetric set of vectors, we may use (2.61) to conclude that (3.34) holds. On the other hand, given a d_ν-tuple of vectors that obey (3.34), we may multiply by $d_\nu D^\nu_{ji}(g^{-1})$, sum over the group and use the orthogonality relations (2.58) to conclude that Definition 3.1.7 holds. ■

The above characterization of a ν-symmetric set basically tells us that the linear span of such a set is a group invariant subspace (in the sense of Definition 2.3.7) and that this subspace is in fact irreducible. Using this, and the discussion following Theorem 3.1.5, we are immediately led to the important result that, in the absence of accidental degeneracies, the eigenspace Y_σ associated with any eigenvalue of the resolvent R_κ is a ν-symmetric set.[19] We may conclude therefore that, degenerate eigenvectors of $\mathfrak{H}$ obey the relation (3.34). We will now see, how this special structure of the eigenvectors of $\mathfrak{H}$, can be used to simplify the boundary value problem associated with the computation of the eigenvectors.

To proceed, we will first show that a ν-symmetric set of functions posed on the ball $\mathcal{B}_R$ can be interpreted in terms of their restriction to the fundamental domain. We need to formalize the notion of a fundamental domain and therefore, we introduce the following[20]:

[19] If accidental degeneracies are present, the eigenspace Y_σ consists of the union over ν-symmetric sets.

[20] We use the standard notation cl.(Ω) to denote the closure, and $\partial\Omega$ to denote the boundary of a set Ω.

Definition 3.1.9. Suppose that $\mathcal{G}$ is a finite group of isometries. A fundamental domain (or symmetry cell) of $\mathcal{G}$ relative to the open ball $\mathcal{B}_R$ is a set $\mathcal{D} \subset \mathcal{B}_R$ such that it is open, connected, possesses a regular boundary[21] and has the properties:

$$\mathcal{B}_R \subset \text{cl.}\left(\bigcup_{\Upsilon \in \mathcal{G}} \Upsilon(\mathcal{D}) \right) \quad , \quad \Upsilon_1(\mathcal{D}) \cap \Upsilon_2(\mathcal{D}) = \emptyset \, , \, \forall \Upsilon_1, \Upsilon_2 \in \mathcal{G}, \Upsilon_1 \neq \Upsilon_2. \tag{3.35}$$

Given a fundamental domain $\mathcal{D}$, we will call the set $\partial_{\mathcal{O}}(\mathcal{D}) = \partial\mathcal{D} \backslash \partial\mathcal{B}_R$, the objective boundary of $\mathcal{D}$ and the set $\partial_D(\mathcal{D}) = \partial\mathcal{D} \cap \partial\mathcal{B}_R$, the original boundary of $\mathcal{D}$.

Roughly speaking, the fundamental domain is a well behaved set containing one point per orbit, with respect to the group action of $\mathcal{G}$ on points in $\mathcal{B}_R$. Based on the properties in (3.35), we may see that $\bigcup_{\Upsilon \in \mathcal{G}} \Upsilon\left(\partial_D(\mathcal{D}) \right) = \partial\mathcal{B}_R$. It follows that, whenever $\mathbf{x} \in \partial_{\mathcal{O}}(\mathcal{D})$, there exists $g \in \mathcal{G}, g \neq e$ such that $g \bullet \mathbf{x} \in \partial_{\mathcal{O}}(\mathcal{D})$ and that for almost every $\mathbf{x} \in \partial_{\mathcal{O}}(\mathcal{D})$, this $g \in \mathcal{G}$ must be unique [Bossavit, 1986]. To say this in a somewhat different way, we may define, for $g \in \mathcal{G}, g \neq e$:

$$\partial^g_{\mathcal{O}}(\mathcal{D}) = \left\{ \mathbf{x} \in \text{cl.}(\mathcal{D}) : g \bullet \mathbf{x} \in \text{cl.}(\mathcal{D}) \right\} , \tag{3.36}$$

and we may then notice that each point $\mathbf{x} \in \partial_{\mathcal{O}}(\mathcal{D})$ lies in $\partial^g_{\mathcal{O}}(\mathcal{D})$, for some $g \in \mathcal{G}, g \neq e$. Further, each point in $\mathbf{x} \in \partial_{\mathcal{O}}(\mathcal{D})$ lies in only one such $\partial^g_{\mathcal{O}}(\mathcal{D})$, except for a subset of $\partial\mathcal{D}$, of relative measure zero [Bossavit, 1993].

Now that we have established the notion of the fundamental domain, we may proceed further. We let $\mathcal{W}$ denote the restriction to $\mathcal{D}$, of functions in $\mathsf{H}^1(\mathcal{B}_R)$ and we further let:

$$\mathcal{W}_0 = \left\{ f \in \mathcal{W} : f = 0 \text{ on } \partial_D(\mathcal{D}) \right\} . \tag{3.37}$$

We introduce the space $\mathcal{W}_0$, so as to be able to establish an isomorphism between the subspaces $W^\nu_{ii} = P^\nu_{ii}(\mathsf{H}^1_0(\mathcal{B}_R)), \nu = 1, \ldots, \ell; i = 1, \ldots, d_\nu$ and the space:

$$\mathcal{W}_0^{d_\nu} = \mathcal{W}_0 \times \cdots \times \mathcal{W}_0 \ (d_\nu \text{ times}) \, . \tag{3.38}$$

We can define a natural trace operator on the d_ν-tuples of functions in $\mathcal{W}_0^{d_\nu}$. Specifically, let $\tilde{\mathbf{v}} \in \mathcal{W}_0^{d_\nu}$, with $\tilde{\mathbf{v}} = \{\tilde{v}_i\}_{i=1}^{d_\nu}$. For $\mathbf{x} \in \partial_{\mathcal{O}}(\mathcal{D})$, let $g \in \mathcal{G}, g \neq e$, be such that $\mathbf{x} \in \partial^g_{\mathcal{O}}(\mathcal{D})$.

[21] We say that a domain, that is, a bounded, connected, open subset of $\mathbb{R}^3$, has a regular boundary Γ, if Γ is the union of a finite number of differentiable closed surfaces.

We set:

$$\big(\Gamma_\nu \tilde{\mathbf{v}}\big)(\mathbf{x}) = \left\{ \tilde{v}_i(\mathbf{x}) - \sum_{k=1}^{d_\nu} D^\nu_{ki}(g)\tilde{v}_k(g \bullet \mathbf{x}) \right\}_{i=1}^{d_\nu}, \tag{3.39}$$

and we may now observe the following result:

Proposition 3.1.10 (Characterization of ν-symmetric sets using fundamental domain)**.** *A d_ν-tuple of functions $\tilde{\mathbf{v}} = \{\tilde{v}_i\}_{i=1}^{d_\nu}$ is the restriction of a ν-symmetric set to cl.$(\mathcal{D})$ if and only if $\big(\Gamma_\nu \tilde{\mathbf{v}}\big) = 0$. Hence, the space W^ν_{ii} is isomorphic to the space $\left\{ \tilde{\mathbf{v}} \in \mathcal{W}_0^{d_\nu} : \big(\Gamma_\nu \tilde{\mathbf{v}}\big) = 0 \right\}$.*

Proof: Since compactly supported continuous functions form a dense subspace of $\mathsf{H}^1_0(\mathcal{B}_R)$, it suffices to establish the above result for such functions. So, given $\tilde{\mathbf{v}}$, a d_ν-tuple of functions on $\mathcal{D}$, we may form $\mathbf{v}^\nu = \{v_i^\nu\}_{i=1}^{d_\nu}$, the continuous extension of this tuple of functions to all of $\mathcal{B}_R$ as follows: we define, for every $\mathbf{x} \in \mathcal{D}, g \in \mathcal{G}$:

$$\mathbf{v}^\nu(g \bullet \mathbf{x}) = \{v_i^\nu(g \bullet \mathbf{x})\}_{i=1}^{d_\nu} = \left\{ \sum_{k=1}^{d_\nu} D^\nu_{ki}(g^{-1})\tilde{v}_k(\mathbf{x}) \right\}_{i=1}^{d_\nu} \tag{3.40}$$

The condition $\big(\Gamma_\nu \tilde{\mathbf{v}}\big) = 0$, ensures that $\mathbf{v}^\nu$ is continuous across the boundaries $\partial_{\mathcal{O}}(\mathcal{D})$ and the conditions laid out in Proposition 3.1.8 now indicate that $\mathbf{v}^\nu$ forms a ν-symmetric set.

On the other hand, if $\mathbf{v} = \{v_i\}_{i=1}^{d_\nu}$ is a given ν-symmetric set, then, its components obey the conditions of Proposition 3.1.8. Therefore, (3.40) holds, and consequently, the restriction to cl.$(\mathcal{D})$ of these functions obey $\big(\Gamma_\nu \tilde{\mathbf{v}}\big) = 0$.

In the light of the above discussion, the isomorphism between the spaces W^ν_{ii} is and $\left\{ \tilde{\mathbf{v}} \in \mathcal{W}_0^{d_\nu} : \big(\Gamma_\nu \tilde{\mathbf{v}}\big) = 0 \right\}$ is easy to see. Starting form $v_i \in W^\nu_{ii}$, we may generate the corresponding ν-symmetric set (for instance, using the operators P^ν_{ji}) and then, consider the restrictions of these d_ν functions to cl.$(\mathcal{D})$. This way, we will end up with a vector of functions $\tilde{\mathbf{v}} \in \mathcal{W}_0^{d_\nu}$ which obeys the relation $\big(\Gamma_\nu \tilde{\mathbf{v}}\big) = 0$. On the other hand, given a vector of functions $\tilde{\mathbf{v}} \in \mathcal{W}_0^{d_\nu}$ which obey $\big(\Gamma_\nu \tilde{\mathbf{v}}\big) = 0$, we may extend this set of functions to all of $\mathcal{B}_R$ via (3.40) and consider the i^{th} component of the vector of functions so formed to get an element of W^ν_{ii}. ■

With the above result in place, we can interpret the symmetry adapted problems in Proposition 3.1.6 as problems posed on the fundamental domain. We have, for $u, v \in \mathsf{H}^1_0(\mathcal{B}_R)$,

the left hand side of (3.29):

$$\begin{aligned}
\mathfrak{B}[u,v] &= \int_{\mathcal{B}_R} \frac{1}{2}\nabla u(\mathbf{x}).\nabla\overline{v(\mathbf{x})}\,d\mathbf{x} + \int_{\mathcal{B}_R} V(\mathbf{x})u(\mathbf{x})\overline{v(\mathbf{x})}\,d\mathbf{x} \\
&= \sum_{g\in\mathcal{G}} \int_{g(\mathcal{D})} \frac{1}{2}\nabla u(\mathbf{x}).\nabla\overline{v(\mathbf{x})}\,d\mathbf{x} + \sum_{g\in\mathcal{G}} \int_{g(\mathcal{D})} V(\mathbf{x})u(\mathbf{x})\overline{v(\mathbf{x})}\,d\mathbf{x} \\
&= \sum_{g\in\mathcal{G}} \int_{\mathcal{D}} \frac{1}{2}\nabla u(g\bullet\mathbf{y}).\nabla\overline{v(g\bullet\mathbf{y})}\,d\mathbf{y} + \sum_{g\in\mathcal{G}} \int_{\mathcal{D}} V(g\bullet\mathbf{y})u(g\bullet\mathbf{y})\overline{v(g\bullet\mathbf{y})}\,d\mathbf{y} \\
&= \sum_{g\in\mathcal{G}} \int_{\mathcal{D}} \frac{1}{2}\nabla\big(\zeta(g)u(\mathbf{y})\big).\nabla\big(\overline{\zeta(g)v(\mathbf{y})}\big)\,d\mathbf{y} + \sum_{g\in\mathcal{G}} \int_{\mathcal{D}} V(\mathbf{y})\big(\zeta(g)u(\mathbf{y})\big)\overline{\big(\zeta(g)v(\mathbf{y})\big)}\,d\mathbf{y}
\end{aligned} \tag{3.41}$$

In the light of the discussion in Section 3.1.5, we know that the eigenvalue problem posed on $\mathsf{H}^1_0(\mathcal{B}_R)$ only needs to be posed on the symmetry adapted subspaces W^ν. Indeed, let $u, v \in W^\nu_{ii} \subset \mathsf{H}^1_0(\mathcal{B}_R)$ for some $\nu = 1,\dots,\ell$ and $i = 1,\dots,d_\nu$, and let $\{u_j\}_{j=1}^{d_\nu}, \{v_k\}_{k=1}^{d_\nu}$ be the corresponding ν-symmetric families. Since $u_i \equiv u$ and $v_i \equiv v$, using (3.34), we may rewrite (3.41) as:

$$\begin{aligned}
\mathfrak{B}[u,v] = \sum_{g\in\mathcal{G}} \int_{\mathcal{D}} \frac{1}{2}\nabla\Big(\sum_{j=1}^{d_\nu} D^\nu_{ji}(g)u_j\Big).\nabla\overline{\Big(\sum_{k=1}^{d_\nu} D^\nu_{ki}(g)v_k\Big)}\,d\mathbf{y} \\
+ \sum_{g\in\mathcal{G}} \int_{\mathcal{D}} V(\cdot)\Big(\sum_{j=1}^{d_\nu} D^\nu_{ji}(g)u_j\Big)\overline{\Big(\sum_{k=1}^{d_\nu} D^\nu_{ki}(g)u_k\Big)}\,d\mathbf{y}\ .
\end{aligned} \tag{3.42}$$

To be able to simplify (3.42) further, we need to introduce the sesquilinear form over the fundamental domain. Accordingly, for any $u, v \in \mathsf{H}^1_0(\mathcal{B}_R)$, let $\tilde{u}, \tilde{v}$ denote the restriction of these functions to $\mathcal{D}$. Then, let us define:

$$\tilde{\mathfrak{B}}[\tilde{u},\tilde{v}] = \int_{\mathcal{D}} \frac{1}{2}\nabla\tilde{u}(\mathbf{x}).\nabla\overline{\tilde{v}(\mathbf{x})}\,d\mathbf{x} + \int_{\mathcal{D}} V(\mathbf{x})\tilde{u}(\mathbf{x})\overline{\tilde{v}(\mathbf{x})}\,d\mathbf{x} \tag{3.43}$$

With this notation in hand, and denoting the restrictions of the ν-symmetric families associated with u and v to the fundamental domain as $\{\tilde{u}_j\}_{j=1}^{d_\nu}$ and $\{\tilde{v}_k\}_{k=1}^{d_\nu}$ respectively, we

rewrite (3.42) as:

$$\begin{aligned}\mathfrak{B}[u,v] =& \sum_{g\in\mathcal{G}}\sum_{j,k=1}^{d_\nu} D^\nu_{ji}(g)\overline{D^\nu_{ki}(g)}\tilde{\mathfrak{B}}[\tilde{u}_j,\tilde{v}_k] \\ =& \frac{|\mathcal{G}|}{d_\nu}\sum_{k=1}^{d_\nu}\tilde{\mathfrak{B}}[\tilde{u}_k,\tilde{v}_k]\ , \end{aligned} \tag{3.44}$$

using the orthogonality relations (2.58). A similar calculation for the right hand side of (3.29) yields:

$$\langle u,v\rangle_{\mathsf{L}^2(\mathcal{B}_R)} = \frac{|\mathcal{G}|}{d_\nu}\sum_{k=1}^{d_\nu}\langle\tilde{u}_k,\tilde{v}_k\rangle_{\mathsf{L}^2(\mathcal{D})} \tag{3.45}$$

Thus, for every irreducible representation of the the group, we arrive at d_ν coupled subproblems over the fundamental domain:

$$\sum_{k=1}^{d_\nu}\tilde{\mathfrak{B}}[\tilde{u}_k,\tilde{v}_k] = \lambda\sum_{k=1}^{d_\nu}\langle\tilde{u}_k,\tilde{v}_k\rangle_{\mathsf{L}^2(\mathcal{D})}\ . \tag{3.46}$$

If the eigenfunctions are sufficiently regular, we may perform integration by parts to obtain the strong form of the equations in (3.46). This calculation leads us to the following symmetry adapted version of the problem laid out in (3.10), over the fundamental domain:

$$\begin{aligned}&\text{For every irreducible representation } \nu = 1,\dots,\ell \text{ and } i = 1,\dots,d_\nu:\\ &-\frac{1}{2}\Delta\tilde{u}^i(\mathbf{x}) + V(\mathbf{x})\tilde{u}^i(\mathbf{x}) = \lambda\tilde{u}^i(\mathbf{x}) \text{ for } \mathbf{x}\in\mathcal{D}.\\ &\tilde{u}^i(\mathbf{x}) = 0\ \text{, for } \mathbf{x}\in\partial_D\big(\mathcal{D}\big),\\ &\text{and } \big(\Gamma_\nu\tilde{\mathbf{u}}\big) = 0 \text{ on } \partial_{\mathcal{O}}\big(\mathcal{D}\big), \text{with } \tilde{\mathbf{u}} = \{\tilde{u}^i\}_{i=1}^{d_\nu}.\end{aligned} \tag{3.47}$$

As before, each irreducible representation yields d_ν coupled subproblems. Once the above problems have been solved on the the fundamental domain, we may extend the solutions to all of $\mathcal{B}_R$ by means of (3.34).

3.1.7 Self Consistent Field Iterations and Symmetry Based Reduction

So far, we have seen that, if at some stage of the self-consistent field iterations, the electronic density ρ is continuous and it is invariant under a finite group of isometries $\mathcal{G}$, then the problem of computing the Kohn Sham eigenstates admits symmetry based simplifica-

tions through (3.47) or (3.29). The natural question to ask, then, is if the newly computed set of eigenfunctions yields an electronic density that is continuous and invariant under the same group of isometries $\mathcal{G}$. It is important for us to know the answer to this question because it gives us an indication whether the self consistent iterations can be carried out in a consistent manner while computing the electronic properties of an objective structure. In the absence of this consistency, it is quite possible that an objective structure with an underlying symmetry group $\mathcal{G}$ has a ground state electronic density that is not commensurate with $\mathcal{G}$, but with some subgroup of $\mathcal{G}$. Such examples of symmetry breaking in physical systems tends to occur whenever there are degenerate energy minima.

In the case of electronic structure computation using the Kohn-Sham equations, it is easy to appreciate why symmetry breaking is likely to be observed in some cases.[22] We recall, that the self consistent method of solution, requires us to form the electronic density using the lowest few eigenstates of the Kohn-Sham operator. If the highest occupied Kohn-Sham state happens to be degenerate, then each of the eigenfunctions associated with the degenerate level are likely to lead to different electronic densities. While studying objective structures, this might be particularly problematic, because objective structures with an underlying non-Abelian group of symmetries will always have symmetry related degeneracies.

There are special circumstances, under which, it can be guaranteed that the electronic density resulting from symmetry adapted schemes, are commensurate with the symmetry of the objective structure. Specifically, we have:

Theorem 3.1.11. *Let $\mathcal{G}$ denote the finite group of isometries underlying a given fixed point free objective structure $\mathcal{S}$. Suppose that, we are computing the ground state electronic properties of $\mathcal{S}$, by means of a self consistent field iteration scheme for the Kohn-Sham equations (as in 3.7-3.9) and that the starting guess for the electronic density, ρ^1, is continuous and commensurate with the group $\mathcal{G}$. If, at each stage of the iteration, the entire eigenspace associated with the highest occupied Kohn-Sham level, λ_N^k, is used for computing the electronic density, ρ^k, then, the ground state electronic density resulting from the above iteration scheme will be continuous and commensurate with the group $\mathcal{G}$.*

Proof: The continuity of the electronic density at each stage of the iteration, follows from Lemma 3.1.1 and the comments in Section 3.1.3.2. To see, that under the hypothesis of the theorem, the resulting electronic density is commensurate with the symmetry group $\mathcal{G}$, let

[22] See Prodan [2005] for a specific example.

us proceed by induction. Therefore, let ρ^{k-1} be commensurate with the symmetry group $\mathcal{G}$. Based on the results developed in Section 3.1.4, this now implies that the eigenspace $Y_{\lambda_N^k}$ associated with λ_N^k is a ν-symmetric set, if accidental degeneracies are absent; or that $Y_{\lambda_N^k}$ is a combination of more than one ν-symmetric set, if accidental degeneracies are present. We first assume, that the highest occupied level has no accidental degeneracy. The ν-symmetric eigenspace $Y_{\lambda_N^k}$, contributes a term of the form $\sum_{l=1}^{d_\nu} |\phi_l^k|^2$ to the electronic density ρ^k, with each $\phi_l^k \in Y_{\lambda_N^k}$. Now, for any $g \in \mathcal{G}$, the eigenspace $Y_{\lambda_N^k}$ must transform as in (3.34), and we may write this as:

$$\Phi(g^{-1} \bullet \mathbf{x}) = [\mathbf{D}^\nu(g)]^T \Phi(\mathbf{x}) \ . \tag{3.48}$$

Here, $\Phi(\cdot)$ is the d_ν dimensional vector field over the ball $\mathcal{B}_R$, formed by lining up the eigenfunctions $\{\phi_l^k\}_{l=1}^{d_\nu}$ that lie in $Y_{\lambda_N^k}$ and $\mathbf{D}^\nu(g)$ denotes the matrix of unitary irreducible representations that appears in (3.34). In this notation, the contribution to the electronic density can be expressed as:

$$\rho_{Y_{\lambda_N^k}}(\mathbf{x}) = \|\Phi(\mathbf{x})\|^2_{\mathbb{C}^{d_\nu}} = \langle \Phi(\mathbf{x}), \Phi(\mathbf{x}) \rangle_{\mathbb{C}^{d_\nu}} \ . \tag{3.49}$$

Hence, we have, for any $g \in \mathcal{G}$:

$$\begin{aligned} \rho_{Y_{\lambda_N^k}}(g^{-1} \bullet \mathbf{x}) &= \langle \Phi(g^{-1} \bullet \mathbf{x}), \Phi(g^{-1} \bullet \mathbf{x}) \rangle_{\mathbb{C}^{d_\nu}} \\ &= \langle [\mathbf{D}^\nu(g)]^T \Phi(\mathbf{x}), [\mathbf{D}^\nu(g)]^T \Phi(\mathbf{x}) \rangle_{\mathbb{C}^{d_\nu}} \\ &= \langle \Phi(\mathbf{x}), \overline{[\mathbf{D}^\nu(g)]} [\mathbf{D}^\nu(g)]^T \Phi(\mathbf{x}) \rangle_{\mathbb{C}^{d_\nu}} \\ &= \langle \Phi(\mathbf{x}), \Phi(\mathbf{x}) \rangle_{\mathbb{C}^{d_\nu}} = \rho_{Y_{\lambda_N^k}}(\mathbf{x}) \ . \end{aligned} \tag{3.50}$$

Thus, the contribution to the electronic density, at the highest occupied level is commensurate with the group $\mathcal{G}$, provided accidental degeneracy is absent at this level. On the other hand, if there is accidental degeneracy, we may apply the above argument to each of the ν-symmetric sets that constitute $Y_{\lambda_N^k}$, to reach the same conclusions as (3.50). For the Kohn-Sham states that lie below the highest occupied level, we are anyway forced to consider the entire eigenspace associated with any eigenvalue, and therefore, the above argument works for the contributions from these levels too. In summary therefore, provided the conditions of the theorem are met, we may always write $\sum_{i=1}^{N} |\phi_i^k|^2 (g \bullet \mathbf{x}) = \sum_{i=1}^{N} |\phi_i^k|^2(\mathbf{x})$ for any $g \in \mathcal{G}$. It follows by (3.9), that we have $\rho^k(g \bullet \mathbf{x}) = \rho^k(\mathbf{x}), \forall g \in \mathcal{G}$, thus proving the theorem. ■

The above result gives us an indication of the circumstances under which one might have to study symmetry breaking bifurcations in the ground state electronic properties of objective structures. If the conditions of the above theorem are not met, and the highest occupied Kohn-Sham level is degenerate at some stage of the Kohn-Sham iterations, it would, perhaps, be desirable to fork off multiple calculations, each one corresponding to the usage of one of the degenerate eigenstates. We find it useful to mention, that in the setting of the so called extended Kohn Sham scheme [Le Bris, 2003], these situations can never occur. In particular, finite temperature Kohn-Sham theory [Mermin, 1965; Martin, 2004] will always result in electronic densities commensurate with the symmetry of the objective structure[Prodan, 2005]. The reason for this is that these modified theories consider averaged out contributions from all degenerate eigenstates.

3.2 Cell problem for Objective Structures generated by helical groups

We now study the electronic structure calculation problem for infinite helical groups in this section. Following Defranceschi and Le Bris [2000]; Le Bris [2003] and using the case of infinite periodic systems as a guide, we realize that the first step in this process should be to set up a band theory for the electrons. Mathematically speaking therefore, our first task is to obtain the spectral decomposition of a Scrödinger operator with a potential that is invariant under a discrete helical group of isometries.

As mentioned in Chapter 2, the key player in the solution to the above problem for the case of crystals, is known as Bloch's Theorem in the physics literature [Ashcroft and Mermin, 1976]. The potential in that case is invariant under periodicity of the underlying crystal lattice. We encountered a wide range of work on the derivation of this theorem, starting from ones which are physics oriented and which tend to use group theoretic tools (such as: Ashcroft and Mermin [1976], Lax [2001] and Kittel [2004]), to ones which are more focused on the functional analysis aspects (such as: Reed and Simon [1978], Berezin and Shubin [1991], Odeh and Keller [1964] and Wilcox [1978]). We are of the opinion that the use of the so called Born-von Karman boundary conditions on the wavefunction in the aforementioned physics literature (which makes it possible to use the representation theory of finite cyclic groups) is not really the correct approach since one really has an infinite group at hand. In any case, the authors, in these works, do not rigorously demonstrate that the solution to the actual infinite problem can be obtained as the limit of their finite solutions. Our derviation of the Bloch theorem for helical groups therefore, will follow the rigorous functional analysis / operator theory approach.

3.2.1 Electronic Band Structure Theory for Helical Groups

For the purpose of derivation of a Bloch Theorem for helical groups, we will assume the simplest possible case of a helical group of isometries. So, we will work with an Abelian group of isometries genrated by powers of a single element, that is, $\mathcal{G} = \{\tilde{\Upsilon}^j : j \in \mathbb{Z}\}$.

3.2.1.1 Problem Set Up: Helical Coordinates

Let $(\mathbf{e}_1, \mathbf{e}_2, \mathbf{e}_3)$ be an orthonormal basis of $\mathbb{R}^3$. We denote the infinite cylinder in $\mathbb{R}^3$ of radius R and axis $\mathbf{e}_3$ as:

$$\mathcal{C} = \mathbb{R} \times \{\mathbf{x} \in \mathbb{R}^3 : \mathbf{x}.\mathbf{e}_3 = 0 \text{ and } |\mathbf{x}| < R\} \tag{3.51}$$

Let $\mathcal{S}$ denote a helical Objective Structure which sits inside $\mathcal{C}$ and whose axis is oriented parallel to $\mathbf{e}_3$ and let $\mathcal{G} = \{\tilde{\Upsilon}^j : j \in \mathbb{Z}\}$ be the discrete group of isometries that describes $\mathcal{S}$. Here, $\Upsilon = (\mathbf{R}_{2\pi\alpha}|\tau\mathbf{e}_3)$ is an isometry, $\alpha \in (0, 1]$ and $\mathbf{R}\mathbf{e}_3 = \mathbf{e}_3$, since $\mathbf{e}_3$ is the axis of $\mathbf{R}$. We note that the discreteness of $\mathcal{G}$ leads to the fact that $\mathcal{G}$ contains a subgroup of pure translations if and only if $\alpha \in \mathbb{Q}$ [Dayal et al., 2013].

We are interested in the study of the following eigenvalue problem posed on $\mathcal{C}$:

$$\begin{aligned} (-\frac{1}{2}\Delta + V)\,\psi &= \lambda\,\psi \\ \psi(\mathbf{x}) &= 0, \quad \text{for } \mathbf{x} \in \partial\mathcal{C} \quad . \end{aligned} \tag{3.52}$$

Here, $V : \mathcal{C} \to \mathbb{R}$ represents the "effective potential" perceived by an electron. As in the case of finite groups, we will assume that this eigenvalue problem and the potential $V(\mathbf{x})$ arise as the current iterate of the inner loop of a self-consistent Kohn Sham iteration. However, unlike the calculations in Section 3.1.2, we will not attempt to characterize the potential or prove it's group invariance at this stage. Instead, for now, we will assume that V is a continuous function on the cylinder and that for every $\mathbf{x} \in \mathcal{C}$, we have $V(\Upsilon(\mathbf{x})) = V(\mathbf{x}), \forall\Upsilon \in \mathcal{G}$.

As shown in Figure 3.1 schematically, the purpose of Bloch's Theorem for a helical group such as $\mathcal{G}$, is to enable us to reduce the problem (3.52) posed on the infinite cylinder to a problem posed on a finite fundamental domain. The first step in this direction therefore, is to introduce a fundamental domain for the group $\mathcal{G}$. It is easy to see in this case that the

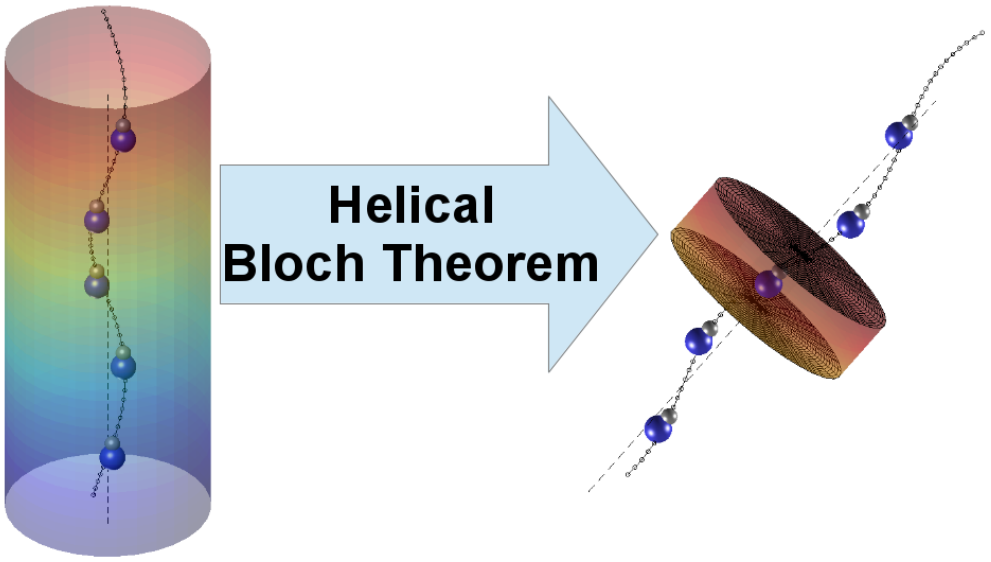

Figure 3.1: The Bloch theorem for helical groups reduces the problem problem on the infinite cylinder to one on the fundamental domain

following set (cylinder of height τ) serves as a fundamental domain:

$$\mathcal{D} = (0, \tau) \times \{\mathbf{x} \in \mathbb{R}^3 : \mathbf{x}.\mathbf{e}_3 = 0 \text{ and } |\mathbf{x}| < R\} \quad , \tag{3.53}$$

since we have:

$$\mathcal{C} \subset \text{cl.}\Big(\bigcup_{j\in\mathbb{Z}} \tilde{\Upsilon}^j(\mathcal{D})\Big) \quad \text{and} \quad \tilde{\Upsilon}^j(\mathcal{D}) \cap \tilde{\Upsilon}^k(\mathcal{D}) = \emptyset \quad \text{for} \quad j \neq k \quad . \tag{3.54}$$

Next, we note that there is a coordinate system that is naturally adapted to the group action by $\mathcal{G}$. For $\mathbf{x} \in \mathcal{C}$ with coordinates (x_1, x_2, x_3) in the $(\mathbf{e}_1, \mathbf{e}_2, \mathbf{e}_3)$ basis, we may introduce (r, θ_1, θ_2) as follows:

$$r = \sqrt{x_1^2 + x_2^2}, \quad \theta_1 = \frac{x_3}{\tau}, \quad \theta_2 = \frac{1}{2\pi}\arctan\left(\frac{x_2}{x_1}\right) - \alpha\frac{x_3}{\tau} \quad . \tag{3.55}$$

We may verify that these relations are onto and globally invertible on $\mathcal{C}\backslash\{\lambda\mathbf{e}_3 : \lambda \in \mathbb{R}\}$ and that the inverse relations

$$(r, \theta_1, \theta_2) \mapsto (x_1, x_2, x_3) = \big(r\cos(2\pi(\alpha\theta_1 + \theta_2)), r\sin(2\pi(\alpha\theta_1 + \theta_2)), \theta_1\tau\big) \tag{3.56}$$

map the open cuboid $(0, R) \times (0, 1) \times (0, 1)$ to the fundamental domain $\mathcal{D}$. We refer to the (r, θ_1, θ_2) coordinate system as Helical Coordinates. The group action in these coordinates can be easily computed as follows. For $\mathbf{x} = (x_1, x_2, x_3) \in \mathcal{C}$ with corresponding

transformed coordinates (r, θ_1, θ_2), the group action is $\mathbf{x}' = \tilde{\Upsilon}(\mathbf{x}) = \mathbf{R}_{2\pi\alpha}\mathbf{x} + \tau\mathbf{e}_3$, which in terms of the helical coordinates is:

$$\begin{aligned}
\mathbf{x}' &= (x_1', x_2', x_3') \\
&= \big(x_1\cos(2\pi\alpha) - x_2\sin(2\pi\alpha), x_2\cos(2\pi\alpha) + x_1\sin(2\pi\alpha), x_3 + \tau\big) \quad . \\
\implies r' &= \sqrt{(x_1\cos(2\pi\alpha) - x_2\sin(2\pi\alpha))^2 + (x_2\cos(2\pi\alpha) + x_1\sin(2\pi\alpha))^2} = r \quad , \\
\theta_1' &= \frac{x_3 + \tau}{\tau} = \theta_1 + 1 \quad , \\
\theta_2' &= \frac{1}{2\pi}\arctan\left[\frac{x_2\cos(2\pi\alpha) + x_1\sin(2\pi\alpha)}{x_1\cos(2\pi\alpha) - x_2\sin(2\pi\alpha)}\right] - \alpha\frac{x_3 + \tau}{\tau} \\
&= \frac{1}{2\pi}\arctan\left[\tan\left(2\pi\alpha + \arctan\left(\frac{x_2}{x_1}\right)\right)\right] - \alpha\frac{x_3}{\tau} - \alpha \\
&= \frac{1}{2\pi}\arctan\left(\frac{x_2}{x_1}\right) - \alpha\frac{x_3}{\tau} = \theta_2 \quad . \qquad (3.57)
\end{aligned}$$

So, $(r', \theta_1', \theta_2') = (r, \theta_1 + 1, \theta_2)$. Thus, the helical coordinates transform boundary conditions of the form $\phi(\mathbf{x}) = \phi(\tilde{\Upsilon}(\mathbf{x}))$, to periodic boundary conditions in θ_1 (with period 1). Also, these coordinates are naturally periodic in θ_2 in the sense that for any $r \in (0, R)$ and $\theta_1 \in (0, 1)$, the coordinates $(r, \theta_1, \theta_2 = 0)$ and $(r, \theta_1, \theta_2 = 1)$ refer to the same point in the cylinder.

3.2.1.2 Bloch's Theorem for Helical Groups and its consequences

We now move to the actual derivation of the Bloch Theorem. Our treatment is largely based on the approach in Wilcox [1978] and Odeh and Keller [1964]. First, we need to formalize the problem (3.52).

Proposition 3.2.1. *The operator $\mathfrak{H} = -\frac{1}{2}\Delta + V$ acting on the domain $\mathsf{H}^2(\mathcal{C})$ is a self-adjoint operator in $\mathsf{L}^2(\mathcal{C})$*

Proof: We know that $\mathfrak{H}_0 = -\frac{1}{2}\Delta$ acting on the domain $\mathsf{H}^2(\mathcal{C})$ is a self adjoint operator in $\mathsf{L}^2(\mathcal{C})$. We can prove, starting from Sobolev inequalies, that for any $u \in \mathsf{H}^2(\mathcal{C})$ and $r \geq 1$, the estimate:

$$\|Vu\|^2_{\mathsf{L}^2(\mathcal{C})} \leq C\|V\|_{\mathsf{L}^2(\mathcal{D})}\, r^{-1/2}\left(\|\Delta u\|^2_{\mathsf{L}^2(\mathcal{C})} + r^2\|u\|^2_{\mathsf{L}^2(\mathcal{C})}\right) \quad , \qquad (3.58)$$

holds. This allows us to view the operator $\mathfrak{H} = \mathfrak{H}_0 + V$ as a compact perturbation of the operator $\mathfrak{H}_0$ [Kato, 1995] and so the self-adjointness follows. ■

The Bloch waves for $\mathfrak{H}$ are solutions (3.52) that fit the ansatz $\psi(\mathbf{x}) = e^{2\pi i \frac{kx_3}{\tau}}\phi(\mathbf{x})$ with $\mathbf{x} \in \mathcal{C}$, and ϕ obeying $\phi(\partial\mathcal{C}) = 0, \phi(\tilde{\Upsilon}(\mathbf{x})) = \phi(\mathbf{x})$. To show the existence of such solutions, we prove the following fundamental result:

Theorem 3.2.2. *Under the aforementioned hypothesis on the potential $V(\mathbf{x})$ the following results hold:*

1. *(Existence theorem for Bloch Waves) For any $k \in \mathbb{R}$ there exist a countable number of solutions of* (3.52) *of the form $\psi_n(x,k) = e^{2\pi i \frac{kx_3}{\tau}}\phi_n(\mathbf{x},k)$, where $\phi_n(\mathbf{x},k)$ is a smooth function of $\mathbf{x}$ which is group invariant, i.e., $\forall \Upsilon \in \mathcal{G}, \forall \mathbf{x} \in \mathcal{C},\ \phi_n(\Upsilon(\mathbf{x}),k) = \phi_n(\mathbf{x},k)$ and which meets the Dirichlet boundary condition $\phi(\partial\mathcal{C}) = 0$. Further, it suffices to restrict $k \in [-1,1]$.*

2. *(Completeness) The set of Bloch waves $\{\psi_n(x,k) : n \in \mathbb{N}, k \in [-1,1]\}$ is dense in $\mathsf{L}^2_m(\mathcal{C})$.*

Proof. We substitute the Bloch wave ansatz (for a fixed k) into the governing PDE (3.52) to get an operator $\mathfrak{H}_k$ and we restrict this problem to the fundamental domain by imposing the boundary conditions $\phi(\mathbf{x}) = 0$ for $\mathbf{x} \in \partial\mathcal{C} \cap \partial\mathcal{D}$ and $\phi(\mathbf{x}) = \phi(\Upsilon(\mathbf{x})), \nabla\phi(\mathbf{x}) = \mathbf{R}^T_{2\pi\alpha}\nabla\phi(\Upsilon(\mathbf{x}))$ for $\mathbf{x} \in \partial\mathcal{D}\backslash\partial\mathcal{C}$. The operator $\mathfrak{H}_k$ is densely defined on $\mathsf{H}^2(\mathcal{D})$ and these boundary conditions are meaningful in the trace sense on $\mathsf{H}^2(\mathcal{D})$. The resulting restricted problem (with these boundary conditions) defines a self-adjoint operator with a compact resolvent and therefore the spectral theorem implies an increasing sequence of eigenvalues of finite multiplicity and associated eigenfunctions which are dense in $\mathsf{L}^2(\mathcal{D})$. We can then extend this solution by group invariance to all of $\mathcal{C}$ and thus establish the existence of Bloch waves. The density of the Bloch waves follows from [Odeh and Keller, 1964, Theorem 1] and by the earlier observation that helical coordinates map the current problem into a periodic one. ■

From the perspective of a computational algorithm, the above theorem actually tells us that instead of (3.52) one can investigate the following set of problems indexed by $\beta \in [-\frac{2\pi}{\tau}, \frac{2\pi}{\tau}]$

$$\begin{aligned} \tilde{\mathfrak{H}}_\beta\phi = -\frac{1}{2}(\Delta\phi - \beta^2\phi + i2\beta\frac{\partial\phi}{\partial x_3}) + V(\mathbf{x})\phi = \lambda\phi, \mathbf{x} \in \mathcal{D} \\ \phi(\mathbf{x}) = 0, \mathbf{x} \in \partial\mathcal{D} \cap \partial\mathcal{C};\ \ \phi(\mathbf{R}_{2\pi\alpha}\mathbf{x} + \tau\mathbf{e}_3) = \phi(\mathbf{x}), \mathbf{x} \in \partial\mathcal{D}\backslash\partial\mathcal{C} \end{aligned} \tag{3.59}$$

Since this is a problem posed on a finite domain, we can now try to solve it numerically by any of the common discretization methods. This is discussed in a later chapter.

Chapter 4

Spectral scheme for Kohn - Sham Density Functional Theory of clusters

4.1 Introduction

Over the past few decades, quantum mechanical calculations based on Kohn-Sham Density Functional Theory (KS-DFT) have provided important insights into a variety of material systems [Martin, 2004; Le Bris, 2003]. One of the most widely used and successful methods for numerical solution of the equations of Kohn Sham theory is the pseudopotential plane-wave method [Kresse and Furthmuller, 1996a,b; Marx and Hutter, 2009; Payne et al., 1992], currently available in a number of software packages [Kresse and Furthmuller, 1996a; Gonze et al., 2002; Segall et al., 2002; Giannozzi et al., 2009]. The focus of this chapter is to build a powerful suite of algorithms and methods which are analogous to the plane-wave method, but can be used to study objective structures generated by finite groups of isometries (i.e., cluster systems).

The advantages of plane-waves include the fact that they are orthornormal and therefore result in simple discretized expressions. Also, they form a complete basis, thus allowing for systematic convergence with increasing basis set size, governed by a single parameter, the energy cutoff. The global nature of the plane wave basis also results in minimum user intereference in terms of basis set choice. Being a Fourier basis, plane-waves allow for spectral convergence leading to highly accurate numerical solutions [Cancès et al., 2012]. Further, independence of the basis functions on atomic positions results in the absence of (the otherwise difficult to compute) Pulay forces [Segall et al., 2002]. On the downside, while the plane-wave method is ideally suited for the study of periodic systems such as

crystals, its application to non-periodic systems such as molecules and clusters is more limited due to the need for introducing artificial periodicity in the form of the supercell method [Martin, 2004; Marx and Hutter, 2009]. In addition, while studying such systems, the plane-wave methods only take advantage of symmetry groups which are commensurate with translational symmetry (such as some of the crystallographic point groups).

Alternatives to the plane-wave approach include the use of atom centered basis functions such as Gaussians and atomic orbitals [Hehre et al., 1969; Slater and Koster, 1954; Soler et al., 2002], as well as real space discretization approaches such as finite differences and finite elements [Chelikowsky et al., 1994; Castro et al., 2006; Pask and Sterne, 2005; Suryanarayana et al., 2010; Motamarri et al., 2013]. Atom centered basis functions generally require fewer basis functions per atom compared to plane-waves but these basis sets are usually incomplete and they suffer from basis set superposition errors Le Bris [2003]. Thus, they have issues with systematic convergence. Finite element methods, in contrast, have systematic convergence properties but often require a large amount of user involvment since the quality of the solution as well as the efficiency of the method is heavily dependent on the quality of the mesh as well as the type of element used for the calculation [Motamarri et al., 2013].

From the above discussion, it is quite clear that it would be highly desirable to have methods which are very similar to the plane-wave method but are designed for systems which are non-periodic (such as clusters and helical structures). Accordingly, in this work, we develop a scheme that is in many respects an exact analog of the plane-wave method but one which is designed with isolated systems such as clusters and molecules in mind. Ab-initio studies of clusters, including various fullerenes and nanostructures, has received and continue to receive a lot of attention in different contexts [Botti et al., 2009; Jing et al., 1995; Kronik et al., 2006; Zhou et al., 2006a; Scuseria, 1996; Gurin, 2005; Gonzalez Szwacki et al., 2007; Hakkinen, 2008; Castleman and Khanna, 2009; Castleman, 2011]. The methodology developed in this work therefore is likely to be useful for carrying out first principles studies of clusters in a consistent, systematic and efficient manner.

In order to formulate the appropriate basis functions for our method, we first make the observation that plane-waves are eigenfunctions of the periodic Laplacian. Using eigenfunctions of the Laplacian as basis functions leads to the natural advantage of having a basis in which the kinetic energy operator is diagonalized. Accordingly, our method also uses eigenfunctions of the Laplacian as the basis set. However, since the focus of the present work is on cluster systems, the physical domain is chosen to be a sphere (inside of which

the system under study is to be placed) and we enforce Dirichlet boundary conditions on the surface of the sphere. Our basis functions are eigenfunctions of the Dirichlet laplacian in a spherical domain and they are expressible as the product of spherical harmonics with spherical Bessel functions. Let us remark that the use of a spherical (or near spherical) domain for the study of cluster systems has been used earlier in finite difference and finite element methods Kronik et al. [2006]; Suryanarayana et al. [2010]. To the best of our knowledge however, this is the first work to make systematic use of Laplacian eigenfunction expansions in such non-periodic domains for computing solutions to the Kohn-Sham equations.

Spherical basis functions have been used in earlier works to compute electronic properties of small metallic clusters [Iñiguez et al., 1988; Mattei and Toigo, 1998] as well as that of C_{60} [Yabana and Bertsch, 1993; Alasia et al., 1994]. These basis functions have the distinct advantage that for many cluster systems, the Kohn-Sham eigenstates (molecular orbitals) and their symmetry properties are relatively easy to interpret using the quantum numbers associated with the basis functions themselves [Broglia et al., 2004]. As explained in [Alasia et al., 1994] the choice of spherical basis functions is motivated by the fact that the systems under study were nearly spherical. We show in this work however, that such a constraint on the system under study is unnecessary and that a wide variety of cluster systems including ones which are far from being spherical can be studied efficiently with our method. In contrast to our use of spherical Bessel functions, the radial part of the spherical basis functions used in the aforementioned works has typically been obtained by solving a one dimensional radial eigenvalue problem.

In order to avoid computational complexity, many of the aforementioned works use a simplified treatment of the electron-nucleus interaction in the form of simple-jellium or pseudo-jellium models [Mattei and Toigo, 1998]. The use of these simplied models however, can often lead to inaccuracies, even while studying simple metal clusters [Brack, 1993]. In our view, one of the main reasons behind the computational difficulties encountered by these authors is due to the formulation of their methods in which convolution sums are carried out in reciprocal space by means of coupling coefficients (e.g. Mattei and Toigo [1998] and Broglia et al. [2004]). This makes certain operations such as computation of the electronic density from the wavefunctions unmanageable beyond relatively small system sizes, unless approximations are used. In addition, these works also rely on setting up of the full Hamiltonian matrix and then performing diagonalization of this matrix using direct methods, at each self-consistent field iteration cycle. This is quite unlike the approach employed by modern plane-wave codes where a dual representation of various quantities is

employed for efficiency purposes and the Fast Fourier Transform (FFT) is used to switch between real and reciprocal space [Marx and Hutter, 2009]. In addition, instead of direct diagonalization methods, most plane-wave codes employ matrix free iterative diagonalization methods to compute the occupied eigenspace of the Hamiltonian [Kresse and Furthmuller, 1996a; Payne et al., 1992]. We adopt similar strategies in this work and show that this leads to a method where accurate ground state electronic structure calculations for cluster systems containing many hundreds of electrons can be done routinely using our code. In particular, employing widely used, accurate abinitio norm conserving pseudopotentials for modeling the electron-nucleus interaction, without resorting to any form of spherical averaging of the potentials [Mattei and Toigo, 1998], poses no difficulty in our method.

As mentioned earlier, one of the key aspects of the plane-wave method is the use of three dimensional FFTs to switch between quantities expressed in real and reciprocal space. Analogously, we require efficient transforms to switch between quantities expressed on an appropriate grid used to discretize our spherical domain and the expansion coefficients of that quantity when expanded using our basis set (i.e., reciprocal space). We accomplish this through a combination of separation of variables into radial and angular parts and handling the radial part using Gauss-Jacobi quadrature [Teodorescu et al., 2013] while handling the angular part using high performance Spherical Harmonics Transforms (SHTs)[Schaeffer, 2013].

Another key requirement for carrying out accurate Kohn-Sham calculations is the ability to accurately evaluate the electrostatics terms. We accomplish this task here by developing an expansion of the Green's function of the associated Poisson problem in terms of our basis functions. This is followed by computing the convolution of the Green's function with the electronic charge. This is somewhat similar in spirit to some of the Green's function based methods developed in the context of plane-wave codes [Marx and Hutter, 2009; Hockney, 1970; Eastwood and Brownrigg, 1979; Martyna and Tuckerman, 1999]. The calculation of the Green's function (in terms of its expansion) can be done ahead of time and does not have to be repeated.

Computation of the occupied eigenspace of the discretized Kohn-Sham eigenvalue problem is the most computationally demanding step in a typical self consistent field calculation. Accordingly, a number of strategies have been devised over the years for an efficient solution of this problem through iterative diagonalization methods [Payne et al., 1992; Kresse and Furthmuller, 1996a; Vömel et al., 2008; Marx and Hutter, 2009]. We have adopted the Locally Optimal Block Preconditioned Conjugate Gradient (LOBPCG)

algorithm [Knyazev, 2001] for this purpose in our code. This robust method has been implemented with success in other state of the art Kohn-Sham codes [Bottin et al., 2008; Lorenzen, 2006] and with the aid of a simple diagonal preconditioner (described later) we have found it to work well for a variety of systems. For relatively large system sizes however, especially while running under distributed memory environments, LOBPCG-like methods suffer from the need to repeatedly orthogonalize the computed eigenstates. For dealing with such situations, we have adopted a highly efficient Chebyshev polynomial filtered subspace iteration algorithm [Zhou et al., 2006b,a] which avoids explicit diagonlization and minimizes orthonormalizations.

Spectral methods like the plane-wave method and the method presented here are susceptible to suffer from scalability issues while running under distributed memory environments, since the global nature of the basis functions involved tends to induce communication between the processing elements. To ameliorate this difficulty, we have adopted a two-level parallelization scheme over electronic states as well as physical space, much in the spirit of some large scale plane-wave codes [Gygi et al., 2006]. This strategy has resulted in speed-critical portions of our code scaling well up to 1024 processing units.

The culmination of the various strategies outlined above is in the numerous example problems that are solved efficiently and accurately using our method. We employ norm conserving abinitio pseudopotentials for most of our calculations. Starting from light atoms, small molecules and clusters (metallic and non metallic), we move to some examples involving fullerenes and large face centered cubic (FCC) aluminum clusters. The largest example system considered here contains 1688 aluminum atoms (over 5000 electrons).

The rest of the chapter is organized as follows. Section 4.2 describes the formulation of our method while Section 4.3 describes various implementation aspects. Section 4.4 presents the example problems solved using our method and compares our results with the literature to assess the efficacy of our method.

4.2 Formulation

We describe the Kohn Sham equations and our discretization scheme for numerical solution of these equations in this section. The basis transforms as well as methods of dealing with various terms of the equation are discussed.

4.2.1 Problem set-up and discretization

Let us consider a system consisting of N_e electrons moving in the fields produced by M nuclei. The nuclei are assumed to have charges $(z_1, \ldots, z_M)$ and are assumed to be clamped to the positions $(\mathbf{x}_1, \ldots, \mathbf{x}_M) \in \mathbb{R}^3$. For the sake of simplicity, we will consider a system in which spin polarization effects are absent and consider N_e to be even. The extension of the present work to study spin-polarized systems is straight forward and therefore, we will not present the details.

As explained in Chapter 2, The Kohn-Sham equations [Kohn and Sham, 1965], are a set of coupled non-linear partial differential equations. The central quantities of interest in these equations are an $N_e/2$ tuple of complex valued scalar fields $\{\phi_i\}_{i=1}^{N_e/2}$ (the orbitals) and the electronic density that can be obtained from the orbitals. The equations are as follows:

$$K(\rho)\,\phi_i = \lambda_i\,\phi_i \;;\; \langle \phi_i, \phi_j \rangle_{\mathsf{L}^2(\mathbb{R}^3)} = \delta_{ij} \quad . \tag{4.1}$$

$$\text{with,} \quad K(\rho) = -\frac{1}{2}\Delta + V_{nu} + \int_{\mathbb{R}^3} \frac{\rho(\mathbf{y})}{|\mathbf{x}-\mathbf{y}|}\, d\mathbf{y} + V_{xc}(\rho) \quad . \tag{4.2}$$

$$\text{where,} \quad V_{xc}(\rho) = \frac{\partial E_{xc}(\rho)}{\partial \rho} \quad . \tag{4.3}$$

$$\text{and} \quad \rho(\mathbf{x}) = 2\sum_{i=1}^{N_e/2} |\phi_i(\mathbf{x})|^2 \quad . \tag{4.4}$$

The λ_i that appear in eq. 4.1 are the Lagrange multipliers of the orthonormality constraints on the orbitals and they are taken to be the lowest $N_e/2$ eigenvalues of the Kohn-Sham operator $K(\rho)$. The factor of two in eq. 4.4 is due to the assumption of dealing with a spin-unpolarized system, as a consequence of which, each orbital is doubly occupied. The orthonormalization condition on the orbitals implies that the electronic density ρ satisfies the normalization condition:

$$\int_{\mathbb{R}^3} \rho = N_e \; . \tag{4.5}$$

As before, the first term in eq. 4.2 (involving the Laplacian) models the kinetic energy of the electrons. The second term models the interaction of the nuclei with the electrons and it is usually presented in the form of the pseudopotential approximation [Le Bris, 2003; Martin, 2004] to smoothen out Coulombic singularities.[1] The third term in eq. 4.2 represents

[1] Coulombic singularities present in the nucleus electron interaction cause problems with efficient numerical solution of the equations. Spectral methods like the plane-wave method and the present one are particularly affected due to appearance of Gibbs phenomenon [Folland, 1999] in the neighborhood of singularities.

the Hartree potential which models the electrostatic repulsion of the electrons amongst themselves. Finally, $V_{xc}(\rho)$ denotes the exchange-correlation potential, that is, functional derivative of the exchange-correlation energy. We adopt here the commonly used Local Density Approximation (LDA) [Parr and Yang, 1994; Kohn and Sham, 1965] of this term. We remark that an extension of our method to other exchange correlation functionals, such as those involving density gradient corrections [Perdew et al., 1996] poses no particular difficulty. As also mentioned in Chapter 2, the Kohn-Sham equations as written above, are usually solved through Self-Consistent Field (SCF) iterations and this is the methodology we adopt for this work.

As in the previous chapter, let $\mathcal{B}_R$ denote the sphere of radius R centered at the origin. For the purpose of this work, we will restrict the physical domain to $\mathcal{B}_R$ instead of all of $\mathbb{R}^3$, while solving the Kohn-Sham equations (eq. 4.1 – 4.3). The cluster system will be embedded within this spherical region and we will apply Dirichlet boundary conditions to the electronic density on the surface of the sphere in accordance with the well-known spatially exponential decay of the electronic density [Hoffmann-Ostenhof et al., 1980; Ahlrichs et al., 1981]. The relation between the electronic density and the wavefunctions (eq. 4.3) automatically implies that the Dirichlet boundary conditions apply to the wavefunctions as well. Application of Dirichlet boundary conditions to the Kohn-Sham wavefunctions has been considered earlier in the context of real-space methods [Suryanarayana et al., 2010; Chelikowsky et al., 1994; Jing et al., 1994].

4.2.2 Basis set

The particular choice of a spherical domain allows for the Laplacian eigenfunctions in this domain to be represented analytically in spherical coordinates [2]. Specifically, in order to obtain our basis functions, we consider the $\mathsf{L}^2(\mathcal{B}_R)$ orthonormal eigenfunctions of the Laplacian operator in the spherical domain and we impose Dirichlet boundary conditions on the surface of the domain. In this setup, a simple separation of variables calculation shows that the eigenfunctions of the Laplacian which are regular at the origin are expressible in terms of spherical Bessel functions of the first kind and spherical harmonics. See

The bulk of the present work is devoted to pseudopotential calculations.

[2] In our notation for spherical coordinates, we denote $r \in [0, R]$ as the radial coordinate, $\vartheta \in [0, \pi]$ as the polar angle and $\varphi \in [0, 2\pi]$ as the azimuthal angle. The Cartesian coordinates (x, y, z) are obtained as $x = r \sin\vartheta \cos\varphi,\ y = r \sin\vartheta \sin\varphi,\ z = r \cos\vartheta$.

Appendix A for details of this calculation. Letting $(l, m, n) \in \Gamma_\infty$ with:

$$\Gamma_\infty = \left\{ (l, m, n) : l \in \{0, 1, \ldots\}, m \in \{-l, \ldots, l\}, n \in \{0, 1, \ldots\} \right\} , \tag{4.6}$$

the Laplacian eigenfunctions take the form:

$$F_{l,m,n}(r, \vartheta, \varphi) = \mathcal{R}_{l,n}(r)\, \mathcal{Y}_l^m(\vartheta, \varphi) , \tag{4.7}$$

with, the radial part being the spherical Bessel functions of the first kind:

$$\mathcal{R}_{l,n}(r) = \frac{1}{R J_{l+\frac{3}{2}}\left(b^n_{l+\frac{1}{2}}\right)} \sqrt{\frac{2}{r}} J_{l+\frac{1}{2}}\left(\frac{b^n_{l+\frac{1}{2}}}{R} r \right) , \tag{4.8}$$

and, the angular part being the spherical harmonics:

$$\mathcal{Y}_l^m(\vartheta, \varphi) = c_{l,m}\, \mathcal{P}_l^m(\cos\vartheta)\, e^{im\varphi} \text{ , with } c_{l,m} = \sqrt{\frac{(2l+1)}{4\pi} \frac{(l-m)!}{(l+m)!}} . \tag{4.9}$$

In eq. 4.8, $J_{l+\frac{1}{2}}(\cdot)$ denotes the (ordinary) Bessel function of the first kind of order $(l + \frac{1}{2})$, while $b^n_{l+\frac{1}{2}}$ is denotes its $(n+1)^{\text{th}}$ root. Thus, $\mathcal{R}_{l,n}(r)$ attains a value of zero $(n+1)$-times in the interval $[0, R]$. In eq. 4.9, $\mathcal{P}_l^m(\cdot)$ denotes the associated Legendre polynomial of degree l and order m. The eigenvalue associated with the eigenfunction $F_{l,m,n}$ is given by:

$$\Lambda_{l,m,n} = \left(\frac{b^n_{l+\frac{1}{2}}}{R} \right)^2 . \tag{4.10}$$

Since the Laplacian is a self-adjoint operator with a compact resolvent, the infinite collection of eigenfunctions $\mathcal{E}_{\Gamma_\infty} = \left\{ F_{l,m,n} : (l, m, n) \in \Gamma_\infty \right\}$ form an orthonormal basis of $\mathsf{L}^2(\mathcal{B}_R)$ [Evans, 1998; Kato, 1995]. Further, elliptic-regularity results [Evans, 1998] imply that each basis function $F_{l,m,n}$ is smooth. We now choose a finite subset of $\mathcal{E}_{\Gamma_\infty}$ as our basis set.

We fix $\mathcal{L}, \mathcal{N} \in \mathbb{N}$ (henceforth referred to as the angular and radial cutoff, respectively), and form $\Gamma \subset \Gamma_\infty$ by restricting[3] $l \in \{0, \ldots, \mathcal{L} - 1\}$ and $n \in \{0, \ldots, \mathcal{N} - 1\}$. Given any function $f \in \mathsf{L}^2(\mathcal{B}_R)$, for the purpose of numerical discretization, we approximate it using

[3] For each l, m is allowed to vary in $\{-l, \ldots, l\}$ as before.

the functions in $\mathcal{E}_\Gamma = \left\{F_{l,m,n} : (l,m,n) \in \Gamma\right\}$ as:

$$f = \sum_{(l,m,n)\in\Gamma} \hat{f}_{l,m,n}\, F_{l,m,n} \ . \tag{4.11}$$

We may observe that the span of the functions in $\mathcal{E}_{\tilde{\Gamma}}$ form a linear subspace of $\mathsf{L}^2(\mathcal{B}_R)$ of dimension $d = \mathcal{L}^2\mathcal{N}$. The expansion coefficients can be obtained by orthonormality of the basis functions as:

$$\hat{f}_{l,m,n} = \langle f, F_{l,m,n}\rangle_{\mathsf{L}^2(\mathcal{B}_R)} = \int_{\mathcal{B}_R} f\ \overline{F_{l,m,n}}\, d\mathbf{y} \ , \tag{4.12}$$

and the collection of expansion coefficients $\left\{\hat{f}_{l,m,n} : (l,m,n) \in \Gamma\right\}$ will often be interpreted interchangeably with vectors in $\mathbb{C}^d$. If the function f is real valued, as it is for example, in case of the electronic density, the expansion coefficients obey the additional condition[4] $\hat{f}_{l,-m,n} = \overline{\hat{f}_{l,m,n}}$.

4.2.3 Basis transforms

In order to perform the quadratures required for evaluation of the expansion coefficients via eq. 4.12 we introduce a discretization of the domain $B \subset \mathcal{B}_R$. Akin to the terminology used in the plane-wave literature, we will often refer to the representation of a given function in terms of its expansion coefficients as the *reciprocal space representation* while the representation of the same function on the grid points in B will be referred to as the *real space representation*. The operations that allow us to switch between these two representations will be referred to as *basis transforms*.

The specific choice of the grid points is made as follows. Let N_r, N_ϑ and N_φ denote the number of discretization points in the radial, polar and azimuthal directions respectively. In practice, these quantities are dependent on the radial and angular cutoffs and are chosen keeping the constraints of the sampling theorem in mind [Schaeffer, 2013]. We form a discretization of the unit sphere by choosing N_ϑ Gauss quadrature points in $\cos(\vartheta)$ over the interval $[-1,1]$ and N_φ equally spaced points in φ over the interval $[0, 2\pi]$. In the radial direction, we choose N_r Gauss-Jacobi quadrature nodes [Teodorescu et al., 2013] associated the quadrature weight of r^2 over the interval $[0, R]$. The set B is now taken to be a Cartesian product of the radial quadrature points and the unit sphere discretization points. This allows a separation of variables in the angular and radial directions while carrying out

[4] If the Condon-Shortley phase [Weisstein, a] is included, this becomes $\hat{f}_{l,-m,n} = (-1)^m \overline{\hat{f}_{l,m,n}}$. We do not make use of the Condon-Shortley phase in this work.

the basis transforms, thereby reducing computational complexity.[5]

Given a function $f : \mathcal{B}_R \to \mathbb{C}$ (in terms of its real space representation $\tilde{f} : B \to \mathbb{C}$), we obtain the reciprocal space representation by first computing spherical harmonic transforms holding the radial variable fixed:

$$\begin{aligned} A(r;\, l, m) &= \int_0^{2\pi} \int_0^{\pi} f(r; \vartheta, \varphi)\, \overline{\mathcal{Y}_l^m(\vartheta, \varphi)}\, \sin(\vartheta)\, d\vartheta\, d\varphi\ , \\ &= c_{l,m} \int_{-1}^{1} \mathcal{P}_l^m(t) \left[\int_0^{2\pi} f(r;\, \cos^{-1}(t), \varphi)\, e^{-im\varphi}\, d\varphi \right] dt \end{aligned} \tag{4.13}$$

and then performing radial quadratures:

$$\hat{f}_{l,m,n} = \int_0^R A(r;\, l, m)\, \mathcal{R}_{l,n}(r)\, r^2\, dr \approx \sum_{k_r=1}^{N_r} w_{k_r} A(r_{k_r};\, l, m)\, \mathcal{R}_{l,n}(r_{k_r})\ , \tag{4.14}$$

using the quadrature nodes $\{r_{k_r}\}_{k_r=1}^{N_r}$ and corresponding weights $\{w_{k_r}\}_{k_r=1}^{N_r}$. The spherical harmonic transform as expressed in eq. 4.13 itself consists of two steps: first holding ϑ fixed, the Fast Fourier Transform (FFT)[Cooley and Tukey, 1965] is used to evaluate the inner integral involving φ and then a quadrature in $t = \cos(\vartheta)$ is carried out on the result to evaluate the outer integral.

Similarly, given the reciprocal space representation $\hat{f} : \Gamma \to \mathbb{C}$, the inverse transform can be carried out by first computing:

$$G(l, m; r_{k_r}) = \sum_{n=0}^{\mathcal{N}-1} \hat{f}_{l,m,n}\, \mathcal{R}_{l,n}(r_{k_r})\,, \tag{4.15}$$

while holding l and m fixed and then, for each radial grid node r_{k_r}, performing inverse spherical harmonics transforms (using inverse FFTs and dot products as in [Schaeffer, 2013]).

The basis transforms as described above, have a time complexity of $O(\mathcal{L}^3\mathcal{N} + \mathcal{L}^2\mathcal{N}^2)$ in terms of the angular and radial cutoffs.[6] As far as practical implementation is concerned, the use of Gauss quadrature points as well as various numerical and implementation level optimizations [see Schaeffer, 2013, for e.g.] can be used to ensure that the prefactor for this

[5] A naive implementation of the transforms, that is, one that does not employ this separation of variables structure, would have a time complexity of $O(\mathcal{L}^4\mathcal{N}^2)$ in terms of the angular and radial cutoffs.

[6] Using more sophisticated techniques for carrying out the associated Legendre polynomial transforms [Mohlenkamp, 1999; Driscoll and Healy, 1994], this can be reduced to $O(\mathcal{L}^2(\log \mathcal{L})^2\mathcal{N} + \mathcal{L}^2\mathcal{N}^2)$.

asymptotic estimate is rather low. This allowed us to carry out basis transforms routinely and efficiently even with basis sets containing millions of basis functions in our code.

4.2.4 Set up of matrix eigen-value problem

Within the self-consistent field iterations, the governing equations (eq. 4.1 – 4.3) posed in the spherical domain take the form of the following linearized eigen-value problem with an effective potential V_{eff}:

$$\Big(-\frac{1}{2}\Delta + V_{eff}\Big)\phi_i = \lambda_i\,\phi_i \text{ for } i = 1, \ldots, N_e/2 \quad , \tag{4.16}$$

$$\phi_i = 0 \text{ on } \partial\mathcal{B}_R \ , \tag{4.17}$$

and the effective potential at a point $\mathbf{x} \in \mathcal{B}_R$ is given as:

$$V_{eff}(\mathbf{x}) = V_{xc}(\rho(\mathbf{x})) + \int_{\mathcal{B}_R} \frac{\rho(\mathbf{y})}{|\mathbf{x}-\mathbf{y}|}\, d\mathbf{y} + V_{nu}(\mathbf{x}) \quad . \tag{4.18}$$

For the purpose of this particular discussion, we choose to ignore any non-local contributions to the ionic pseudopotentials. The specific treatment of these non-local terms is discussed in a later section.

To discretize eq. 4.16 we set:

$$\phi_i = \sum_{(l,m,n)\in\Gamma} \hat{\phi}^i_{l,m,n}\, F_{l,m,n} \ , \tag{4.19}$$

noting that this ensures that the Dirichlet boundary conditions on the wavefunctions are satisfied automatically. This gives us:

$$\frac{1}{2}\sum_{\Gamma}\hat{\phi}^i_{l,m,n}\,\Lambda_{l,m,n}\,F_{l,m,n} + V_{eff}\sum_{\Gamma}\hat{\phi}^i_{l,m,n}\,F_{l,m,n} = \ \lambda_i\ \sum_{\Gamma}\hat{\phi}^i_{l,m,n}\,F_{l,m,n} \ . \tag{4.20}$$

Now, if the expansion coefficients of V_{eff} are known as $\{\hat{V}^{eff}_{\tilde{l},\tilde{m},\tilde{n}} : (\tilde{l},\tilde{m},\tilde{n}) \in \Gamma\}$, we may substitute the expansion of V_{eff} into eq. 4.20 to get:

$$\begin{aligned}\frac{1}{2}\sum_{\Gamma}\hat{\phi}^i_{l,m,n}\,\Lambda_{l,m,n}\,F_{l,m,n} + \sum_{\Gamma}\sum_{\Gamma}\ \hat{\phi}^i_{l,m,n}\,\hat{V}^{eff}_{\tilde{l},\tilde{m},\tilde{n}}\,F_{\tilde{l},\tilde{m},\tilde{n}}\,F_{l,m,n} \\ = \lambda_i \sum_{\Gamma}\ \hat{\phi}^i_{l,m,n} F_{l,m,n} \ .\end{aligned} \tag{4.21}$$

We now take the inner product of this equation with $F_{l',m',n'}$ and use orthonormality of the basis functions to obtain the following system of linear equations for $\hat{\phi}^i_{l',m',n'}$, with $(l', m', n') \in \Gamma$:

$$\frac{1}{2}\Lambda_{l',m',n'}\,\hat{\phi}^i_{l',m',n'} + \sum_{\Gamma}\sum_{\Gamma} \mathcal{W}^{(l',m',n')}_{(l,m,n)\,,\,(\tilde{l},\tilde{m},\tilde{n})}\,\hat{V}^{eff}_{\tilde{l},\tilde{m},\tilde{n}}\,\hat{\phi}^i_{l,m,n} = \lambda_i\,\hat{\phi}^i_{l',m',n'}\ , \tag{4.22}$$

where $\mathcal{W}^{(l',m',n')}_{(l,m,n)\,,\,(\tilde{l},\tilde{m},\tilde{n})}$ denote the coupling coefficients of the basis set, i.e.,

$$\mathcal{W}^{(l',m',n')}_{(l,m,n)\,,\,(\tilde{l},\tilde{m},\tilde{n})} = \left\langle F_{\tilde{l},\tilde{m},\tilde{n}}\,F_{l,m,n}\,,\,F_{l',m',n'}\right\rangle_{\mathsf{L}^2(\mathcal{B}_R)}\ . \tag{4.23}$$

It is possible to express these coupling coefficents in terms of Wigner 3-j symbols [Messiah, 1962] and the integral of the product of three spherical basis functions taken together [Banerjee, 2011]. Such an expression allows us to see that the coupling coefficients are non-zero only when $|l - \tilde{l}| \leq l' \leq l + \tilde{l}$, $m + m' + \tilde{m} = 0$ and $l + l' + \tilde{l}$ is odd.

To recognize the finite dimensional linear eigen-value problem expressed in eq. 4.22, we may introduce an indexing map $\mathcal{I} : \Gamma \to \{1, 2, \ldots, d\}$ and let $\mathcal{J}$ denote its inverse[7]. We may then rewrite eq. 4.22 using the map $\mathcal{J}$ to obtain a matrix problem of the form:

$$\mathbf{H}\,\mathbf{X} = \mathbf{X}\,\mathfrak{D}\ , \tag{4.24}$$

where $\mathbf{H} \in \mathbb{C}^{d\times d}$, $\mathbf{X} \in \mathbb{C}^{d\times(N_e/2)}$ and $\mathfrak{D} \in \mathbb{R}^{(N_e/2)\times(N_e/2)}$. Denoting $\delta_{\alpha,\beta}$ as the Kronecker delta, we see that matrices $\mathbf{H}, \mathbf{X}$ and $\mathfrak{D}$ have entries of the following form:

$$\mathbf{H}_{\alpha,\beta} = \frac{1}{2}\delta_{\alpha,\beta}\,\Lambda_{\mathcal{J}(\alpha)} + \sum_{(\tilde{l},\tilde{m},\tilde{n})\in\Gamma} \hat{V}^{eff}_{\tilde{l},\tilde{m},\tilde{n}}\;\mathcal{W}^{\mathcal{J}(\alpha)}_{\mathcal{J}(\beta)\,,\,(\tilde{l},\tilde{m},\tilde{n})}\,, \tag{4.25}$$

$$\mathbf{X}_{\alpha,\beta} = \hat{\phi}^{\beta}_{\mathcal{J}(\alpha)} \text{ and } \mathfrak{D}_{\alpha,\beta} = \delta_{\alpha,\beta}\,\lambda_{\mathcal{J}(\beta)}\,, \tag{4.26}$$

with α, β varying within the relevant matrix dimensions.

As we mentioned earlier, setting up of the matrix eigen-value problem followed by direct diagonalization are both expensive operations, although this approach seems to have been adopted by earlier works involving spherical basis functions [see e.g. Broglia et al., 2004]. From eq. 4.25, for instance, we can see that the matrix H is dense and therefore, the asymptotic computational complexity of the matrix setup is of cubic order in the total number of basis functions. Direct diagonalization of the Hamiltonian, even by the most

[7] A simple indexing map might be, for instance, $(l, m, n) \mapsto (l^2 + l + m) * \mathcal{N} + (n + 1)$.

efficient algorithms available today [see e.g. Dhillon et al., 2006], will have the same cubic computational complexity in the number of basis functions due to the necessity of reducing the matrix to tridiagonal form. In addition, the memory storage requirement of the full Hamiltonian matrix scales as the square of the number of basis functions and therefore this becomes an additional constraint while trying to deal with even moderate sized systems.

4.2.5 Set up of matrix-vector products

To avoid the above mentioned computational difficulties, we choose to employ matrix-free iterative methods for computing the occupied eigen space of the Hamiltonian matrix [see Saad, 2011, for a detailed discussion of this class of methods]. As the name suggests, these methods do not need access to the individual matrix entries but only require matrix vector products to be specified. To see how the product of a given vector with the Hamiltonian matrix may be calculated efficiently, without explicit involvement of the coupling coefficients, we proceed as follows.

Let $\mathbf{Y} \in \mathbb{C}^d$ be a given vector and let $\mathbf{Z} \in \mathbb{C}^d$ be the result of the matrix vector product, that is, $\mathbf{Z} = \mathbf{H}\,\mathbf{Y}$. In terms of components we have :

$$\begin{aligned}\mathbf{Z}_\alpha = \sum_{\beta=1}^{d} \mathbf{H}_{\alpha,\beta}\,\mathbf{Y}_\beta &= \sum_{\beta=1}^{d} \left(\frac{1}{2}\delta_{\alpha,\beta}\,\Lambda_{\mathcal{J}(\alpha)} + \sum_{(\tilde{l},\tilde{m},\tilde{n})\in\Gamma} \hat{V}^{eff}_{\tilde{l},\tilde{m},\tilde{n}}\; \mathcal{W}^{\mathcal{J}(\alpha)}_{\mathcal{J}(\beta)\,,\,(\tilde{l},\tilde{m},\tilde{n})} \right) \mathbf{Y}_\beta \\ &= \frac{1}{2}\Lambda_{\mathcal{J}(\alpha)}\mathbf{Y}_\alpha + \sum_{\beta=1}^{d} \left(\sum_{(\tilde{l},\tilde{m},\tilde{n})\in\Gamma} \hat{V}^{eff}_{\tilde{l},\tilde{m},\tilde{n}}\; \mathcal{W}^{\mathcal{J}(\alpha)}_{\mathcal{J}(\beta)\,,\,(\tilde{l},\tilde{m},\tilde{n})} \right) \mathbf{Y}_\beta\,. \end{aligned} \tag{4.27}$$

The second term, by making use of eq. 4.23 and the linearity of the inner product, can be written as:

$$\begin{aligned} &= \sum_{\beta=1}^{d} \sum_{(\tilde{l},\tilde{m},\tilde{n})\in\Gamma} \hat{V}^{eff}_{\tilde{l},\tilde{m},\tilde{n}}\; \mathbf{Y}_\beta \left\langle F_{\tilde{l},\tilde{m},\tilde{n}}\, F_{\mathcal{J}(\beta)}\,,\, F_{\mathcal{J}(\alpha)} \right\rangle_{\mathsf{L}^2(\mathcal{B}_R)} \\ &= \left\langle \left(\sum_{(\tilde{l},\tilde{m},\tilde{n})\in\Gamma} \hat{V}^{eff}_{\tilde{l},\tilde{m},\tilde{n}} F_{\tilde{l},\tilde{m},\tilde{n}} \right) \left(\sum_{\beta=1}^{d} \mathbf{Y}_\beta F_{\mathcal{J}(\beta)} \right), F_{\mathcal{J}(\alpha)} \right\rangle_{\mathsf{L}^2(\mathcal{B}_R)}. \end{aligned}$$

We recognize the first term in parentheses as the expansion of the effective potential in our basis set, and therefore, the final expression for $\mathbf{Z}_\alpha$ becomes:

$$\mathbf{Z}_\alpha = \frac{1}{2}\Lambda_{\mathcal{J}(\alpha)}\mathbf{Y}_\alpha + \left\langle V^{eff}\left(\sum_{\beta=1}^{d}\mathbf{Y}_\beta F_{\mathcal{J}(\beta)}\right), F_{\mathcal{J}(\alpha)}\right\rangle_{\mathsf{L}^2(\mathcal{B}_R)}. \tag{4.28}$$

The above equation suggests that the computation of the Hamiltonian times vector product should be carried out in two stages. First, the action of the kinetic energy operator is carried out in reciprocal space because of the diagonal structure of that operator in that space. In the second stage, the action of the operator expressing the action of the effective potential has to be computed. This operator however, is diagonal in real space. Thus, given the vector $\mathbf{Y}$, we imagine its components $\{\mathbf{Y}_\alpha\}_{\alpha=1}^{d}$ to represent expansion coefficients and we perform an inverse basis transform to obtain a function Y defined on the gridpoints in B. We then perform a pointwise multiplication of Y with the effective potential (also defined over B) and we finally compute a forward basis transform of the product $(V^{eff}\cdot Y)$ to obtain the result of the second stage. We have to keep in mind however, the restrictions arising from the sampling theorem while carrying out the matrix vector product in this fashion, so that aliasing errors can be avoided.

The principal computational cost of the process described above arises from a pair of basis transforms and therefore the associated time and space complexities are $O(\mathcal{L}^3\mathcal{N}+\mathcal{L}^2\mathcal{N}^2)$ and $O(\mathcal{L}^2\mathcal{N})$ respectively. In contrast, a direct matrix vector product, once the Hamiltonian matrix has been set up, would involve $O(\mathcal{L}^4\mathcal{N}^2)$ complexity both in memory and speed.

4.2.6 Computation of the electronic density

Using the expansion of the wavefunctions (eq. 4.19) as well as the expression in eq. 4.4, we see that the electron density admits expansion coefficients of the form:

$$\tau_{l',m',n'} = 2\sum_{j=1}^{N_e/2}\sum_{\Gamma}\sum_{\Gamma}\mathcal{W}^{(l',m',n')}_{(l,m,n),(\tilde{l},\tilde{m},\tilde{n})}\,\hat{\phi}^{i}_{\tilde{l},\tilde{m},\tilde{n}}\,\overline{\hat{\phi}^{i}_{l,-m,n}}. \tag{4.29}$$

Two comments are in order at this stage. First, since the coupling coefficients are non-zero only when $|l-\tilde{l}| \leq l' \leq l+\tilde{l}$ and we have $0 \leq l, \tilde{l} \leq (\mathcal{L}-1)$, we see that $\tau_{l',m',n'}$ may have non-zero values for all l' satisfying $0 \leq l' \leq 2(\mathcal{L}-1)$. Thus, due to the quadratic nonlinearity in eq. 4.4, the electronic density needs to be represented using a basis set that is larger than the one used to represent the wavefunctions. A similar situation also arises in the context of the plane-wave method, where sometimes, compared to the wavefunctions, the

electronic density expansion employs a larger energy cutoff [Bylaska et al., 2011; Marx and Hutter, 2009]. Often however, plane wave codes allow the so called *dualing approximation* to be engaged, as a result of which, the electronic density is expanded using the same basis set as the wavefunctions [Bylaska et al., 2011]. We have kept these points in mind during the design and implementation of our code, in which a larger basis set (as well as a denser real space grid) for the electronic density may or may not be employed based on user choice.

The second comment is that the computation of the expansion coefficients of the electronic density through eq. 4.29 should actually be avoided because the associated time complexity, in terms of the basis set size and the number of electrons involved, is $O(N_e d^3)$. Instead, starting from the expansion coefficients of the wavefunctions, we may compute the real space representations of the wavefunctions using inverse basis transforms. We may then use eq. 4.4 to compute the electronic density at the grid points in B and finally apply a forward basis transform to obtain the required expansion coefficients of the density. This method results in the reduced time complexity of $O(N_e(\mathcal{L}^3\mathcal{N} + \mathcal{L}^2\mathcal{N}^2))$ and is therefore, much more efficient.

4.2.7 Computation of the Hartree potential

The Hartree potential at a point $\mathbf{x} \in \mathcal{B}_R$ is given as:

$$V_H(\mathbf{x}) = \int_{\mathcal{B}_R} \frac{\rho(\mathbf{y})}{|\mathbf{x}-\mathbf{y}|}\, d\mathbf{y} \ . \tag{4.30}$$

One of the most popular approaches to solving this equation is by employing Poisson solvers [Suryanarayana et al., 2010; Genovese et al., 2008; Chelikowsky et al., 1994][8]. Our approach to the computation of V_H is to directly deal with eq. 4.30 by exploiting the so called Laplace expansion [Jackson, 1975] of the Green's kernel:

$$\frac{1}{|\mathbf{x}-\mathbf{y}|} = \sum_{l=0}^{\infty} \frac{4\pi}{2l+1} \sum_{m=-l}^{m=l} \frac{r_<^l}{r_>^{l+1}}\, \overline{\mathcal{Y}_l^m(\vartheta_\mathbf{x}, \varphi_\mathbf{x})}\, \mathcal{Y}_l^m(\vartheta_\mathbf{y}, \varphi_\mathbf{y}) \ . \tag{4.31}$$

[8] In the finite element setting for example, the Poission equation for $V_{es} = V_H + V_{nu}$ is solved, often in conjunction with Dirichlet boundary conditions on V_{es} [Suryanarayana et al., 2010; Motamarri et al., 2013]. Solving the Poisson problem for V_H with Dirichlet boundary conditions is more problematic because of the much slower decay of V_H compared to V_{es}. Since V_{nu} is known apriori, it can then be subtracted from the solution V_{es} to obtain V_H. This turns out to be a particularly fruitful approach (in the finite-element setting) because a rapid coarsening of the mesh allows one to reach rather large domain sizes. This allows V_{es} to decay sufficiently, thus making the Dirichlet boundary conditions appropriate and applicable. It is quite clear that such a methodology is not applicable to our setting.

In the equation above, $r_< = \min(r_\mathbf{x}, r_\mathbf{y}), r_> = \max(r_\mathbf{x}, r_\mathbf{y})$ and $(r_\mathbf{x}, \vartheta_\mathbf{x}, \varphi_\mathbf{x})$ and $(r_\mathbf{y}, \vartheta_\mathbf{y}, \varphi_\mathbf{y})$ denote $\mathbf{x}$ and $\mathbf{y}$ in spherical coordinates respectively. Now, for a typical point $\mathbf{y} \in \mathcal{B}_R$, the electronic density ρ is available through a basis expansion as:

$$\rho(r_\mathbf{y}, \vartheta_\mathbf{y}, \varphi_\mathbf{y}) = \sum_{\hat{\Gamma}} \tau_{\hat{l},\hat{m},\hat{n}}\, \mathcal{R}_{\hat{l},\hat{n}}(r_\mathbf{y})\, \mathcal{Y}_{\hat{l}}^{\hat{m}}(\vartheta_\mathbf{y}, \varphi_\mathbf{y})\ , \tag{4.32}$$

with $\hat{\Gamma}$ denoting the same basis set as Γ, or a larger one, depending on whether the dualing approximation has been used or not. Now, if $d\breve{\mathbf{y}}$ denotes the volume element in the sphere $\mathcal{B}_R$, that is, $d\breve{\mathbf{y}} = r_\mathbf{y}^2 \sin\vartheta_\mathbf{y}\, dr_\mathbf{y} d\vartheta_\mathbf{y} d\varphi_\mathbf{y}$, then substituting eqs. 4.31 and 4.32 in eq. 4.30 and using orthonormality of the spherical harmonics, we get:

$$\begin{aligned}
V_H(r_\mathbf{x}, \vartheta_\mathbf{x}, \varphi_\mathbf{x}) &= \sum_{l=0}^{\infty} \frac{4\pi}{2l+1} \sum_{m=-l}^{m=l} \sum_{\hat{\Gamma}} \tau_{\hat{l},\hat{m},\hat{n}} \mathcal{Y}_l^m(\vartheta_\mathbf{x}, \varphi_\mathbf{x}) \\
&\quad \times \int_{\mathcal{B}_R} \frac{r_<^l}{r_>^{l+1}} \overline{\mathcal{Y}_l^m(\vartheta_\mathbf{y}, \varphi_\mathbf{y})} \mathcal{R}_{\hat{l},\hat{n}}(r_\mathbf{y})\, \mathcal{Y}_{\hat{l}}^{\hat{m}}(\vartheta_\mathbf{y}, \varphi_\mathbf{y})\, d\breve{\mathbf{y}}\ , \\
&= \sum_{l=0}^{\infty} \frac{4\pi}{2l+1} \sum_{m=-l}^{m=l} \sum_{\hat{\Gamma}} \tau_{\hat{l},\hat{m},\hat{n}}\, \mathcal{Y}_l^m(\vartheta_\mathbf{x}, \varphi_\mathbf{x})\, \delta_{l,\hat{l}}\, \delta_{m,\hat{m}} \\
&\quad \times \int_{r_\mathbf{y}=0}^{r_\mathbf{y}=R} \frac{r_<^{\hat{l}}}{r_>^{\hat{l}+1}} \mathcal{R}_{\hat{l},\hat{n}}(r_\mathbf{y})\, r_\mathbf{y}^2\, dr_\mathbf{y}\ ,
\end{aligned}$$

which we may rewrite as,

$$:= \sum_{\hat{\Gamma}} \frac{4\pi}{2\hat{l}+1}\, \tau_{\hat{l},\hat{m},\hat{n}}\, \mathcal{Y}_{\hat{l}}^{\hat{m}}(\vartheta_\mathbf{x}, \varphi_\mathbf{x})\, \mathfrak{Z}_{\hat{l},\hat{n}}(r_\mathbf{x})\ . \tag{4.33}$$

This suggests that computing the Hartree potential from the electronic density expansion coefficients is very much like performing an inverse basis transform except that the functions $\mathfrak{Z}_{\hat{l},\hat{n}}(r)$ need to be used, instead of the usual radial basis functions $\mathcal{R}_{l,n}(r)$, while carrying out the radial part of the calculation. If the $\mathfrak{Z}_{\hat{l},\hat{n}}(r)$ are pre-computed and stored, the method described here turns out to be extremely efficient: in our implementation, the entire calculation of obtaining the real space representation of V_H, starting from the real space representation of ρ, consumes less than 0.03% of the total time of a typical SCF cycle.

The functions $\mathfrak{Z}_{\hat{l},\hat{n}}(r_{\mathbf{x}})$ may be written as follows:

$$\begin{aligned}
\mathfrak{Z}_{\hat{l},\hat{n}}(r_{\mathbf{x}}) &= \frac{1}{RJ_{\hat{l}+\frac{3}{2}}(b^{\hat{n}}_{\hat{l}+\frac{1}{2}})} \int_{r_{\mathbf{y}}=0}^{r_{\mathbf{y}}=R} \frac{r_<^{\hat{l}}}{r_>^{\hat{l}+1}} \sqrt{\frac{2}{r_{\mathbf{y}}}}\, J_{\hat{l}+\frac{1}{2}}\left(\frac{b^{\hat{n}}_{\hat{l}+\frac{1}{2}}}{R} r_{\mathbf{y}}\right) r_{\mathbf{y}}^2\, dr_{\mathbf{y}} \\
&= \frac{\sqrt{2}}{RJ_{\hat{l}+\frac{3}{2}}(b^{\hat{n}}_{\hat{l}+\frac{1}{2}})} \left[\frac{1}{r_{\mathbf{x}}^{\hat{l}+1}} \int_0^{r_{\mathbf{x}}} r_{\mathbf{y}}^{\hat{l}+2} \frac{1}{\sqrt{r_{\mathbf{y}}}} J_{\hat{l}+\frac{1}{2}}\left(\frac{b^{\hat{n}}_{\hat{l}+\frac{1}{2}}}{R} r_{\mathbf{y}}\right) dr_{\mathbf{y}} \right. \\
&\qquad \left. + r_{\mathbf{x}}^{\hat{l}} \int_{r_{\mathbf{x}}}^{R} \frac{1}{r_{\mathbf{y}}^{\hat{l}-1}\sqrt{r_{\mathbf{y}}}} J_{\hat{l}+\frac{1}{2}}\left(\frac{b^{\hat{n}}_{\hat{l}+\frac{1}{2}}}{R} r_{\mathbf{y}}\right) dr_{\mathbf{y}} \right] \\
&:= \sqrt{2R}\; \tilde{\mathfrak{Z}}_{\hat{l},\hat{n}}(s)\,, \text{with } s = r_{\mathbf{x}}/R \text{ and } s \in [0,1] \text{ and} \\
\tilde{\mathfrak{Z}}_{\hat{l},\hat{n}}(s) &= \frac{1}{J_{\hat{l}+\frac{3}{2}}(b^{\hat{n}}_{\hat{l}+\frac{1}{2}})} \left[s^{\hat{l}+1} \int_0^s r_1^{\hat{l}+\frac{3}{2}} J_{\hat{l}+\frac{1}{2}}\left(b^{\hat{n}}_{\hat{l}+\frac{1}{2}} r_1\right) dr_1 \right. \\
&\qquad \left. + s^{\hat{l}} \int_s^1 \frac{1}{r_1^{\hat{l}-\frac{1}{2}}} J_{\hat{l}+\frac{1}{2}}\left(b^{\hat{n}}_{\hat{l}+\frac{1}{2}} r_1\right) dr_1 \right], \qquad (4.34)
\end{aligned}$$

and r_1 simply denotes an integration variable. The integrals in eq. 4.34 can be carried out numerically using Gauss quadrature. In our implementation, we have computed $\tilde{\mathfrak{Z}}_{\hat{l},\hat{n}}(s)$ accurately for a large number of values of $\hat{l}$ and $\hat{n}$ over a fine grid of values over $[0,1]$ and stored the results. The values of $\tilde{\mathfrak{Z}}_{\hat{l},\hat{n}}(s)$ at other values of $s \in [0,1]$ are computed using cubic spline interpolation as and when required. During an actual simulation, this procedure is used to quickly set up the functions $\mathfrak{Z}_{\hat{l},\hat{n}}(r_{\mathbf{x}})$ at the different radial grid points before the first SCF step.

In our experience, it is rather important to do the Hartree calculation accurately in order to obtain well converged and accurate answers. As is evident from a Lagrangian formulation of the Kohn-Sham problem [Suryanarayana et al., 2010], inaccurate computation of the electrostatics terms might even lead to the variational property of a basis set being lost (that is, the total energy need not decrease monotonically to the converged value with increasing basis set size). This is something we seem to have observed when, for example, too few radial gridpoints were used or when the integrals in eq. 4.34 were not computed accurately.

4.2.8 Computation of the local pseudopotential terms

The total local pseudopotential at a point $\mathbf{x}$ is a combination of terms of the form:

$$V_{nu}(\mathbf{x}) = \sum_{j=1}^{M} V_{nu}^{j}(|\mathbf{x} - \mathbf{x}_j|)\,, \qquad (4.35)$$

where each of the functions V_{nu}^{j} is radially symmetric and reasonably smooth.[9] Let us look at how the expansion coefficients for an individual term $V_{nu}^{j}(|\mathbf{x}-\mathbf{x}_j|)$ might be computed. The primary issue is that this term is centered at $\mathbf{x}_j$ while the basis functions are centered at the origin. To overcome this problem, we now make use of a Löwdin transformation [Löwdin, 1956] as suggested in [Broglia et al., 2004].

Let us consider a rotated coordinate system (x', y', z') centered on the origin such that the axis z' points along the vector $\mathbf{x}_j$. In this new coordinate system, the atom at $\mathbf{x}_j$ has Cartesian coordinates $(0, 0, r_j = |\mathbf{x}_j|)$. We denote its position vector as $\mathbf{y}_0$. Let $\mathbf{Q} \in SO(3)$ be a rotation that takes the original coordinate system into the new one. The definition of $\mathbf{Q}$ is ambiguous at this point since the orientation of the x' and y' axes have not been specified as yet. To fix this, let φ_j and ϑ_j denote the azimuthal and polar angles associated with $\mathbf{x}_j$ and let us assume that the x' and y' axes result from rotating the natural axis with Euler angles $\alpha = \varphi_j, \beta = \vartheta_j, \gamma = 0$.

The expansion coefficient $\hat{V}_{nu,(l,m,n)}^{j}$ can be obtained as:

$$\hat{V}_{nu,(l,m,n)}^{j} = \int_{\mathcal{B}_R} V_{nu}^{j}(|\mathbf{x}-\mathbf{x}_j|)\,\overline{F_{l,m,n}(\mathbf{x})}\,d\mathbf{x}\,, \tag{4.36}$$

which, on making the change of variables $\mathbf{x} = \mathbf{Q}^T\,\mathbf{y}$ becomes:

$$= \int_{\mathcal{B}_R} V_{nu}^{j}(|\mathbf{y}-\mathbf{y}_0|)\,\overline{F_{l,m,n}(\mathbf{Q}^T\,\mathbf{y})}\,d\mathbf{y}\,. \tag{4.37}$$

Since the angular part of the basis functions is composed of spherical harmonics, their transformation under rotations can be formulated in terms of the Wigner D-Matrices [Edmonds, 1996]. The radial part of the basis functions remains unchanged. Therefore, we may write:

$$F_{l,m,n}(\mathbf{Q}^T\,\mathbf{y}) = \sum_{m'=-l}^{l} \mathsf{D}_{m,m'}^{l}(\mathbf{Q}^T)\,F_{l,m,n}(\mathbf{y})\;, \tag{4.38}$$

which, for the particular Euler angles associated with $\mathbf{Q}^T$ becomes:

$$= \sum_{m'=-l}^{l} \sqrt{\frac{4\pi}{2l+1}}\,\mathcal{Y}_{l}^{m'}(\vartheta_j, \varphi_j)\,F_{l,m',n}(\mathbf{y}) \tag{4.39}$$

[9] These functions are actually in $\mathsf{C}^{\infty}(\mathbb{R})$ for the pseudopotentials considered in this work. They have a somewhat lower regualrity for the popular Troullier-Martins pseudopotentials [Troullier and Martins, 1991].

Substituting eq. 4.39 into eq. 4.37 and using spherical coordinates $(r_{\mathbf{y}}, \vartheta_{\mathbf{y}}, \varphi_{\mathbf{y}})$ we get $\hat{V}^j_{nu,(l,m,n)}$ as:

$$= \sqrt{\frac{4\pi}{2l+1}} \sum_{m'=-l}^{l} \Bigg[\overline{\mathcal{Y}_l^{m'}(\vartheta_j, \varphi_j)} \int_{r_{\mathbf{y}}=0}^{R} \int_{\vartheta_{\mathbf{y}}=0}^{\pi} \int_{\varphi_{\mathbf{y}}=0}^{2\pi} V^j_{nu}\big(\sqrt{r_{\mathbf{y}}^2 + r_0^2 - 2r_{bfy} r_0 \cos(\vartheta_{\mathbf{y}})}\big) \times \mathcal{R}_{l,n}(r_{\mathbf{y}})\, r_{\mathbf{y}}^2\, \mathcal{P}_l^{m'}(\cos\vartheta_{\mathbf{y}})\, e^{-im'\varphi_{\mathbf{y}}} \sin(\vartheta_{\mathbf{y}})\, dr_{\mathbf{y}}\, d\vartheta_{\mathbf{y}}\, d\varphi_{\mathbf{y}} \Bigg] . \quad (4.40)$$

Since there is only $\varphi_{\mathbf{y}}$ dependent term in the integrand, only the $m' = 0$ term survives in the summation and so, we get:

$$\hat{V}^j_{nu,(l,m,n)} = \sqrt{\frac{4\pi}{2l+1}}\, \overline{\mathcal{Y}_l^m(\vartheta_j, \varphi_j)} \int_{r_{\mathbf{y}}=0}^{R} \hat{v}^j_{nu}(l;\ r_{\mathbf{y}})\, \mathcal{R}_{l,n}(r_{\mathbf{y}})\, r_{\mathbf{y}}^2\, dr_{\mathbf{y}} \,, \quad (4.41)$$

with:

$$\hat{v}^j_{nu}(l;\ r_{\mathbf{y}}) = \int_{-1}^{1} V^j_{nu}\big(\sqrt{r_{\mathbf{y}}^2 + r_0^2 - 2r_{\mathbf{y}} r_0 s}\big)\, \mathcal{P}_l^0(s)\, ds \,. \quad (4.42)$$

Equations 4.41 and 4.42 suggest the following method for dealing with the local pseudopotential term. For each atom, we first compute $\hat{v}^j_{nu}(l;\ r_{\mathbf{y}})$ via eq. 4.42 by using Gauss quadrature over the interval $[-1, 1]$. The results from each atom may be used to form a weighted sum to obtain:

$$\hat{v}_{nu}(l, m;\ r_{\mathbf{y}}) = \sum_{j=1}^{M} \sqrt{\frac{4\pi}{2l+1}}\, \overline{\mathcal{Y}_l^m(\vartheta_j, \varphi_j)}\, \hat{v}^j_{nu}(l;\ r_{\mathbf{y}}) \,. \quad (4.43)$$

Thereafter, if we require the real space representation of V_{nu}, we simply carry out inverse spherical harmonics transforms of $\hat{v}_{nu}(l, m;\ r_{\mathbf{y}})$ at each value of $r_{\mathbf{y}}$. On the other hand, if we require the reciprocal space reprsentation, it suffices to perform radial quadratures holding l and m fixed.

4.2.9 Computation of the non-local pseudopotential terms

Non-local pseudopotentials are used in electronic structure methods in order to account for the effect of the inert core electrons on the chemically active valence electrons, without directly introducing these core states into the calculation [Martin, 2004; Le Bris, 2003]. In the Kohn-Sham setting, for example, this results in computational savings since it reduces the total number of orbitals involved in the calculation, with the added benefit that the

highly oscillatory core states (which require many basis functions to resolve) are absent. From a computational point of view, inclusion of non local pseudopotential means that a projection operator needs to be added to the Hamiltonian while performing matrix vector products or while computing the total energies / forces. In general, this projection operator can be written as the sum of atom centered rank one operators, and therefore, we now look into how these rank one operators can be handled using our basis set.

The action of a rank one operator $\mathcal{O} = p_1 \otimes p_2$ on a function $f \in \mathsf{L}^2(\mathcal{B}_R)$ is simply given as $\mathcal{O}\, f = \langle p_2, f \rangle_{\mathsf{L}^2(\mathcal{B}_R)}\ p_1$. The functions p_1, p_2 are atom centered and are usually short ranged. A straightforward method of computing the action of such an operator on a function whose expansion coefficients are known, would be to expand the functions p_1 and p_2 in our basis set and to then perform the inner product of p_2 and f in reciprocal space. The resulting scalar can be used to multiply the expansion coefficents of p_2 to obtain the answer. If the total number of projectors (from all the atoms) to be used in the simulation is $\mathcal{P}$, then action of the projectors on a single electronic state can be carried out in $O(\mathcal{P}d)$ time by matrix multiplications, provided of course that the expansion coefficients of p_1 and p_2 are known apriori. Instead of this reciprocal space formulation, it is possible to do this calculation more efficiently in real space by making use of the short ranges of the functions p_1 and p_2, while ensuring some extra care so as to avoid aliasing errors [King-Smith et al., 1991]. We intend to look into this aspect in future work and we adopt the reciprocal space approach in the present one.

We remark in passing that the functions p_1 or p_2 are typically of the form[10] [see, for e.g., Hartwigsen et al., 1998]:

$$p(\mathbf{x}) = \mathcal{Y}_l^m(\widehat{\mathbf{x} - \mathbf{x}_0})\, g(|\mathbf{x} - \mathbf{x}_0|) \tag{4.44}$$

and this allows us to use the Löwdin transformation technique described earlier in section 4.2.8 to arrive at the expansion coefficents. The additional direction dependent factor in eq. 4.44 can be easily handled by using well known results on the translations of spherical harmonics [see for e.g., Tikochinsky, 1967], specifically:

$$\mathcal{Y}_l^m(\widehat{\mathbf{x} - \mathbf{x}_0}) = \sum_{l_1,l_2} \mathfrak{g}^l_{l_1,l_2}\big(|\mathbf{x}|/|\mathbf{x}_0|\big) \sum_{m_1,m_2} \mathcal{G}(l_1, l_2, l;\ m_1, m_2, m)\, \mathcal{Y}_{l_1}^{m_1}(\widehat{\mathbf{x}})\, \mathcal{Y}_{l_2}^{m_2}(\widehat{\mathbf{x}}_0)\,, \tag{4.45}$$

with $\mathcal{G}$ denoting the vector-coupling coefficients [Messiah, 1962; Edmonds, 1996] and $\mathfrak{g}$ being expressible in terms of the hypergeometric function.

[10] The hat in eq. 4.44 is used to denote the unit vector in order to emphasize direction dependence.

4.2.10 Brief remarks on convergence

For any numerical method, it is highly desirable to have mathematically rigorous demonstrations of the convergence of the method, and in particular, to have theoretical estimates of the rates of convergence. In the context of the present numerical scheme, we remark that convergence to the correct ground states follows directly from recent work by Chen et al. [2013]. Regarding rates of convergence, we may conjecture, based on [Cancès et al., 2012; Cancès, 2013] that the Kohn-Sham ground state will converge, for the energy form (i.e., the $\mathsf{H}_0^1(\mathcal{B}_R)$ Sobolev norm), at the rate of convergence of the best approximation of the Kohn-Sham ground state in the discretization space (still using the $\mathsf{H}_0^1(\mathcal{B}_R)$ norm). Further, the ground state energy, as well as the Kohn-Sham eigenvalues, are likely to converge with a rate that is twice as high. The rate of convergence of the best approximation then depends on the decay rate of the coefficients of the expansion of the Kohn-Sham ground state orbitals in our spectral basis, and this in turn, is likely to be directly related to the smoothness of the pseudopotential employed. A full scale investigation of these theoretical issues is the scope of future work.

4.3 Implementation

We outline various implementation related issues and solution strategies in this section. In particular, we discuss methods of obtaining the occupied eigenspace of the Hamiltonian as well as aspects of parallelization.

4.3.1 Diagonalization using LOBPCG

As remarked earlier, efficient eigensolvers for iterative diagonalization of the Hamiltonian matrix are necessary for dealing with large systems. Perhaps, the most commonly used diagonalization method in abinitio calculations is the band-by-band conjugate gradient algorithm for direct minimization of the total energy [Teter et al., 1989; Payne et al., 1992], later modified to fit the iterative diagonalization framework [Bylander et al., 1990]. In this work, we have adopted the Locally Optimal Block Preconditioned Conjugate Gradient (LOBPCG) method [Knyazev, 2001]. The LOBPCG algorithm is much better supported theoretically [Knyazev and Neymeyr, 2003] and has been shown to outperform the traditional preconditioned conjugate gradient method [Bottin et al., 2008]. It has found applications in other electronic structure methods both with and without modifications [Yang et al., 2006; Lin et al., 2013; Lorenzen, 2006; Bottin et al., 2008]. In addition to the above mentioned reasons, our choice of this method is also determined by its simplicity, robustness

and relative ease of implementation.

For computing the smallest eigenpair $\{\lambda_0, \mathbf{z}_0\}$ of the Hamiltonian, the LOBPCG method takes the form of a 3-term recurrence:

$$\begin{aligned} \mathbf{z}_0^{k+1} &= \mathbf{w}^k + \tau^k \mathbf{z}_0^k + \gamma^k \mathbf{z}_0^{(k-1)} \,, \\ \mathbf{w}^k = \mathbf{T_p} \left(\mathbf{H}\, \mathbf{z_0^k} - \lambda_\mathbf{0}^\mathbf{k}\, \mathbf{z_0^k} \right) &, \; \lambda_\mathbf{0}(\mathbf{z_0^k}) = \langle \mathbf{z_0^k}, \mathbf{H}\, \mathbf{z_0^k} \rangle / \langle \mathbf{z_0^k}, \mathbf{z_0^k} \rangle \,, \end{aligned} \tag{4.46}$$

with $\mathbf{T_p}$ denoting a preconditioner. The parameters τ^k and γ^k are chosen based on the idea of *local optimality*, that is, they are such that they minimize the Rayleigh quotient $\lambda_0(\mathbf{z}_0^{(k+1)})$ by using the Rayleigh Ritz procedure in the 3 dimensional trial subspace spanned by $\mathbf{w}^k$, $\mathbf{z}_0^k$ and $\mathbf{z}_0^{(k-1)}$. For computing the lowest $\mathfrak{m}$ eigenstates, the above method is applied in a block fashion and the Raleigh-Ritz procedure is carried out on a trial subspace of dimension $3\mathfrak{m}$. Thus, a relatively small $3\mathfrak{m} \times 3\mathfrak{m}$ generalized eigenvalue problem needs to be solved on every LOBPCG iteration step, through a direct diagonalization method. From the description above, it is apparent that an implementation of the LOBPCG method needs access to the Hamiltonian only through matrix vector products.

When dealing with relatively small sized example systems (approx. up to a couple of hundred electrons), we have used the LOBPCG method exclusively to carry out diagonalization in all SCF steps. For some of the larger example systems described later, we used the LOBPCG method only in the first SCF step so as to generate a good guess for the Chebyshev polynomial filtered subspace iteration algorithm that was used in the subsequent SCF steps. This algorithm and its implementation is described in a later section.

4.3.1.1 Important implementation details

Our implementation of the LOBPCG method follows the algorithmic steps outlined in Knyazev et al. [2007]. We find it worthwhile to mention the following three implementation details. First, in the block setting, when multiple eigenvectors are being converged in parallel, some eigenvectors may converge faster than others. In order to gain computational efficiency, eigenvectors that have already converged within a required tolerance should be "locked" while iteration on the non-converged ones should continue. Following Knyazev et al. [2007], our implementation allows for this behavior via *soft locking*: this is based on the idea of removing the residuals of the locked vectors from the computation but continuing to use the vectors themselves in the Rayleigh-Ritz procedure, which can change them.

Second, in calculations on large systems, the total number of electronic states may be too numerous to fit all required eigenstates into one LOBPCG block due to the large computational demand (both memory and processing power) of the Raleigh-Ritz method. This situation can be handled by partitioning up the total number of required eigenstates into smaller LOBPCG blocks and using deflation (or *hard locking*): we loop over each block and use previously computed eigenstates (from the previously iterated blocks) as orthonormal constraints to the block that is being currently iterated.

Finally, the third detail is related to the use of Cholesky factorization for orthonormalization (of the residual vectors and cojugate directions) in the implementation. This technique is more computationally efficient but also known to be less reliable than the traditional approach involving QR factorization [Knyazev et al., 2007]. In particular, since the matrices plugged into the Cholesky decomposition are poorly scaled, it is crucial to either use a Cholesky decomposition that is numerically invariant with respect to matrix scaling, or to scale the columns of the matrix before performing the factorization [Knyazev, 2013].[11] In addition, our experience has been that numerical noise or round off errors can sometimes cause the Cholesky factorization or the Raleigh-Ritz procedure to fail. In these situations, we have always found it useful to restart the LOBPCG iterations (discarding the computed conjugate direction and residual vectors) by using the most recently computed block of eigenvectors as the initial guess of a fresh set of iterations. This simple strategy seems to result in a much more robust implementation and does not introduce any computational bottlenecks.

4.3.1.2 Parallel implementation strategy

Our strategy for parallelization of the LOBPCG method is to carry out relevant linear algebra operations using a distributed memory dense linear algebra library. For this purpose, we have adopted the state of the art numerical library Elemental [Poulson et al., 2013]. This library has been designed to be a more scalable and easier to interface successor of the ScaLAPACK [Blackford et al., 1997; Choi et al., 1992] and PLAPACK [Van de Geijn, 1997; Alpatov et al., 1997] libraries that have already found widespread use in other electronic sturcture codes. Elemental uses an element-wise block-cyclic distribution of matrices over a two-dimensional grid of processors. The Message Passing Interface (MPI) is used for interprocess communication while linear algebra operations that are local to each

[11] We are grateful to Andrew Knyazev for his consistent support and suggestions during our implementation of LOBPCG, and in particular for pointing out the issue related to Cholesky factorization.

process are carried out by making calls to (serial) BLAS and LAPACK libraries.[12]

The dimensions of the process grid that underlies the operations in Elemental can have an impact on the resulting parallel efficiency of the LOBPCG routine. We have used square process grids in most cases. In some cases however, we found that the use of rectangular process grids, in which the height of the grid was twice that of the width of the grid seemed to result in better performance. Also, for every LOBPCG step, depending on the problem size (specifically, the value of $\mathfrak{m}$), we carried out the Cholesky factorization and the solution to the generalized eigenvalue problem (from the Raleigh-Ritz step), either locally on every process or using a subset of processes from the process grid. This tends to reduce wasteful inter-process communication.

As a preliminary check of the correctness of our implementation, we applied our LOBPCG routine to randomly generated dense Hermitian matrices and attempted to compute a few eigenstates. No preconditioner was used, as a result of which convergence was slow.[13] Nevertheless, as can be seen from Figure 4.1, the errors, computed by comparing LOBPCG results aginst the results obtained by using the direct parallel solver PMRRR [Bientinesi et al., 2005] (available in Elemental), do decrease over the number of iterations, confirming convergence to the correct results.

4.3.1.3 Scaling behavior

We studied the scaling behavior of our LOBPCG implementation under the somewhat stringent setting of using dense matrices. For studying the strong scaling behavior, we generated a random hermitian matrix and computed the first few hundred eigenstates. We used between 16 and 256 cpu cores[14] and we then measured the average time per LOBPCG step. The results are plotted in Figure 4.2a. At 256 cpu-cores, the parallel efficiency drops to a little less than 40%.

As discussed in Knyazev et al. [2007], it is more appropriate to look at the weak scaling behavior, which we studied next. We generated random hermitian matrices of various sizes and computed the first few hundred eigenstates. We used between 16 and 512 cpu cores and the matrix sizes were increased in proportion to the number of cores used. The average time per LOBPCG step was again measured and the results are plotted in Figure

[12] To ensure maximum use of hardware resources, our code was linked to machine optimized BLAS and LAPACK libraries.

[13] The slow convergence behavior of LOBPCG in the absence of a preconditioner has also been reported in [Zhou, 2010]

[14] The computational platform details are described in a later section.

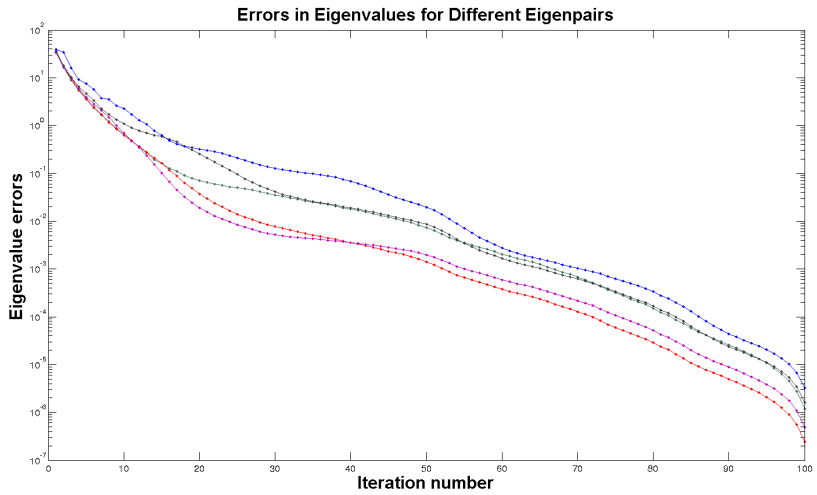

(a) Convergence of eigenvalues.

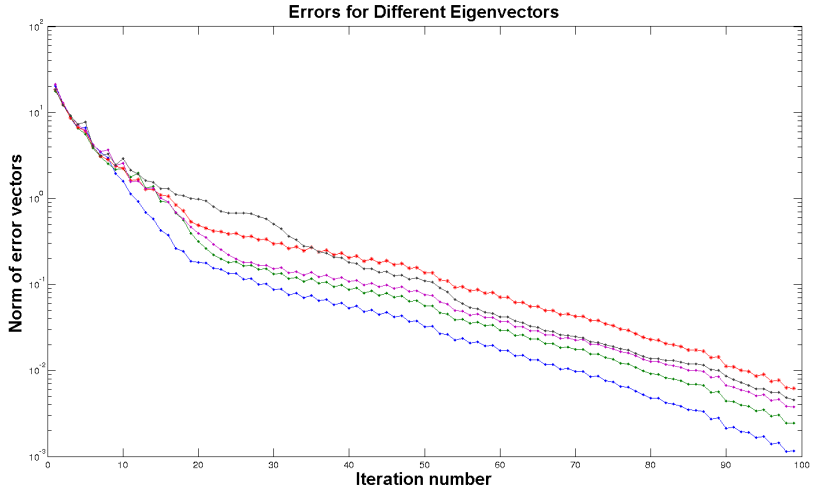

(b) Convergence of eigenvectors.

Figure 4.1: Basic checks on the LOBPCG routine : Convergence to PMRRR results.

4.2b. At first sight, the scaling of our implementation seems to be much worse than what would be expected based on the results in Knyazev et al. [2007]. However, we need to keep in mind that the most computationally expensive step in the dense matrix setting is due to matrix vector multiplication. Thus, the problem size actually grows by a factor of 4 on doubling the matrix dimensions. Therefore, also plotted in Figure 4.2b is the efficiency after adjusting for the quadratic computational complexity of the matrix vector multiplication step. Clearly, this indicates that our routine scales very well: the adjusted parallel efficiency remains above 90% up to 256 cpu cores and drops to a little less than 80% at 512 cpu cores.

These scaling studies make it very apparent that an optimized and scalable matrix vector

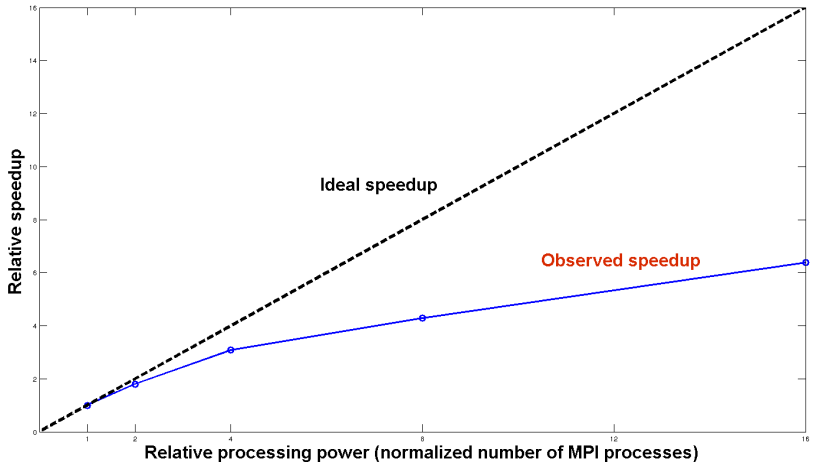

(a) Strong scaling behavior.

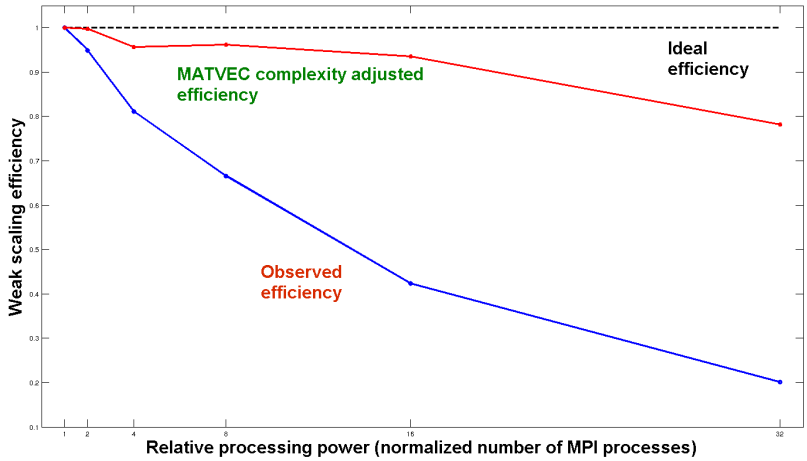

(b) Weak scaling behavior.

Figure 4.2: Parallel scaling behavior of the LOBPCG implementation measured by time taken per LOBPCG step vs. the relative number of MPI processes employed.

product routine is the key ingredient for carrying out large scale computations with the present approach. In particular, it also suggests the use of diagonalization methods where the majority of the time is spent on computing matrix vector products so that the time spent on other dense linear algebra operations (such as orthogonormalization) is minimized. As we discuss in a later section, the Chebyshev polynomial filtering approach has these desirable properties and is therefore the dominantly used solver in most of our example computations.

4.3.1.4 Use of the Teter-Payne-Allan preconditioner

The need for a good preconditioner for use with the LOBPCG method been emphasized in [Knyazev et al., 2007; Knyazev and Neymeyr, 2003]. A good majority of the generic

preconditioners that have been developed over the years however, are aimed towards sparse systems. This is problematic for us because our method is matrix free, and moreover, the underlying matrix involved is dense. Fortunately, as observed in [Teter et al., 1989; Payne et al., 1992] the structure of the Kohn-Sham eigenvalue problem, particularly, the presence of the Laplacian operator, itself suggests a viable preconditioner.

The basic point is that, for pseudopotential calculations, the ill-conditioning (i.e., a large spread in the eigenvalue spectrum) of the discretized Kohn-Sham operator is associated with the wide range of energies of the basis functions. Basis functions, which have high kinetic energies tend to dominate the higher energy eigen-states of the operator, since the high kinetic energy is close to the eigenvalue of the state. In conjugate-gradient like methods therefore, the diagonal dominance of the Hamiltonian (due to the Laplacian operator in the Kinetic energy) produces steepest-descent vectors that are biased towards high energy states. Therefore, in order to improve the conditioning of the Kohn-Sham Hamiltonian, we must remove the effect of the kinetic-energy operator, thus rendering states whose eigenvalues are dominated by their kinetic energy nearly degenerate.

A naive solution to the above problem might be to use the inverse of the kinetic-energy operator as a diagonal preconditioner. However, this will cause a problem for the lower energy eigenstates because the potential and kinetic energies are similar for those states and thus, the potential can cause basis functions of different energies to mix into the eigenstates. Thus, the preconditioner should interpolate between being the inverse Laplacian for basis functions with a high energy and a constant for basis functions with low energy.

Following [Teter et al., 1989; Payne et al., 1992] therefore, we write the interpolated diagonal preconditioner as:

$$\mathbf{T}_{p_{\alpha,\beta}} = \frac{27 + 18g + 12g^2 + 8g^3}{27 + 18g + 12g^2 + 8g^3 + 16g^4}\ \delta_{\alpha,\beta} \tag{4.47}$$

where g is the ratio of the Laplacian eigenvalue $\Lambda_{\mathcal{J}(\alpha)}$ to the kintetic energy of the residual vector on which the preconditioner is being applied. As g approaches zero, the preconditioner elements approach one with zero derivatives upto third order. Thus, $\mathbf{T}_p$ leaves the low energy states unchanged. On the other hand, above $g = 1$, $\mathbf{T}_p$ asymptotically approaches the inverse Laplacian as required.

As can be seen from Figure 4.3, this simple and inexpensive preconditioner seems to make a marked difference in the rate of convergence of the residuals in LOBPCG. The particular system under test was an 18 atom Barium cluster, 4000 basis functions were used and only

the linear part of the Kohn-Sham equations was solved. This preconditioner was therefore adopted in all further calculations wherever the LOBPCG solver was employed.

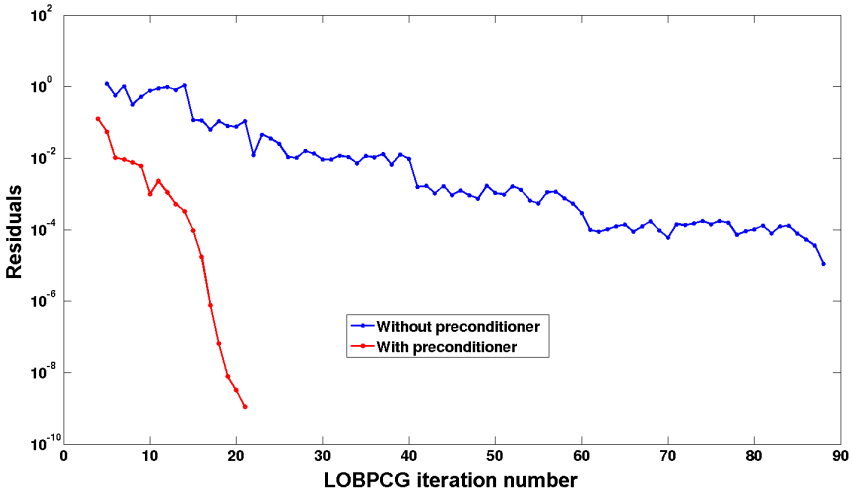

Figure 4.3: Effect of the diagonal preconditioner on LOBPCG iterations. The average residual for a few eigenvectors has been plotted against the iteration number.

4.3.2 Chebyshev polynomial filter accelarated subspace iterations

4.3.2.1 Subspace Iterations

Subspace iteration algorithms constitute a generalization of the classical power iterations approach to computation of eigenpairs [Saad, 2011; Gu, 2000]. These methods allow the computation of multi-dimensional invariant subspaces rather than one eigenvector at a time. Since the electronic density or the total Kohn-Sham energy do not depend explicitly on the eigenvcetors of the Hamiltonian, but only on the occupied subspace, subspace iterations have often been used for electronic structure calculations [Stephan et al., 1998; Bekas et al., 2005; Baroni and Giannozzi, 1992].

In order to make the simple subspace iterations efficient and practically applicable, several modifications are typically needed. As pointed out earlier, it is important to reduce orthonormalizations as much as possible because this operation does not scale linearly with problem size. In addition, in distributed computing environments, this operation typically involves large communication overheads. Thus, we may perform several subspace iterations before performing an orthogonalization. Secondly, if we operate on a subspace whose dimension is larger than the number of required eigen-pairs, the Rayleigh-Ritz method can be used to get better approximations to the eigen-pairs.[15] Finally, effects of ill conditioning

[15]This is often referred to as the *subspace rotation technique* in the materials science literature.

may be reduced by using accelaration techniques. This is the precise reason for employing Chebyshev polynomial filters.

4.3.2.2 Chebyshev polynomial filtered SCF iterations

The Chebyshev polynomial filtered SCF iteration technique for computing the occupied eigenspace of the Kohn-Sham operator was introduced by Zhou et al. [2006b,a] and can be thought of as a form of nonlinear subspace iterations. This approach takes advantage of the fact that eigenvectors of the Hamiltonian do not need to be computed accurately at every SCF step since the Hamiltonians involved are approximate as well. This allows one to exploit the nonlinear nature of the problem in the sense that the resulting technique removes emphasis on the accurate solution of the intermediate linearized Kohn-Sham eigenvalue problems.

In our implementation of this method, we first obtain a guess for the initial electronic density and for the Kohn-Sham orbitals. Typically, we do this by linearly superposing the electronic densities and wavefunctions of the individual atoms that constitute the system of interest; these atomic solutions having been computed apriori and stored. Next, having computed the potentials, we use the LOBPCG method to obtain a good eigen-basis of the Hamiltonian for the first SCF step. This is used to serve as a good guess for the occupied subspace of the Hamiltonian at self-consistency.[16] The Chebyshev polynomial filtered subspace iterations begin after this first SCF step – the main idea behind the iterations is to adaptively improve the initial guess subspace by polynomial filtering. The polynomials change on every SCF step since the Hamiltonian itself changes (due to updates to the electronic density and potentials). The filtering prcoess is such that the sequence of subspaces from the individual SCF steps form progressively closer approximations of the wanted eigensubspace of the final Hamiltonian when self-consistency is reached.

The main use of the Chebyshev polynomials in this method is to exploit the exponential growth property of these polynomials outside the region $[-1, 1]$. On every SCF step, the unwanted part of the spectrum is mapped to $[-1, 1]$ for damping, so that the wanted part can be magnified in comparison. Similar to the observations of [Zhou et al., 2006a], we found that polynomial degrees of relatively low order (within 15) are enough for most calculations . Recursive formulas for the Chebyshev polynomials enable rapid computation of the filtered susbapces as long as one has access to efficient Hamiltonian times vector products.

[16] Typically, a few extra states (about 10 – 20) are included from the LOBPCG calculation so that the Raleigh-Ritz step and finite-temperature Fermi-Dirac smearing (for metallic systems) can be employed.

Mapping of the spectrum as described above requires knowledge of the upper and lower bounds of the unwanted part of the spectrum. As in [Zhou et al., 2006b,a], we do this by using Ritz values from the previous step to estimate the lower bound and a few iterations of the Lanczos algorithm to estimate the upper bound. In every SCF step, after the approximation to the occupied eigenspace has been obtained, we orthonormalize the basis functions of the subspace and then carry out a Raleigh-Ritz step to compute the explicit eigenvalues and eigenvectors that are required for computing the total energies and occupation numbers.

4.3.2.3 Important implementation details

In the original presentation of the Chebyshev filtering method, the authors used the DGKS algorithm [Daniel et al., 1976] for orthonormalization of the basis vectors. In the sprit of the LOBPCG method as well as the RMM-DIIS method [Kresse and Furthmuller, 1996a], we have used the faster (but less stable) Cholesky factorization method instead. This helped speed up the orthonormalization calculation (by a factor of 2–3) and we have not witnessed any problematic side effects.

The bulk of the Chebyshev filtering algorithm consists of evaluating the polynomial filter using matrix vector products. The only linear algebra operations involved are in the form of scaling and shifting (AXPY operation in BLAS terminology), orthonormalization and the Raleigh-Ritz step. Therefore, as in the LOBPCG method we used the Elemental package and its underlying process grid structure for carrying out all dense linear algebra operations in parallel. Once again, depending on the problem size, we carried out the Cholesky factorization and the eigenvalue problem from the Raleigh-Ritz step, either locally on every process or using a subset of processes from the process grid.

4.3.2.4 Comparison with LOBPCG: Computation time and accuracy

To test the basic correctness of our implementation, we looked at a couple of test problems: an 172 atom face centered cubic (F.C.C.) aluminum cluster and the C_{60} buckyball. Anderson mixing was used to expedite convergence of the SCF iterations for both material systems and in addition, Fermi-Dirac occupations were used to stabilize the SCF iterations for the metallic Aluminum system.[17] For each material system, an equal number of basis functions was used for both LOBPCG based SCF iterations and Chebyshev filtering based SCF iterations.

[17] Details of the mixing and occupation schemes as well as the pseudopotentials used, follow in later sections.

In both material systems, the Chebyshev filtering based method reached the same converged answers for the total ground state energy of the system as the LOBPCG based SCF iterations. This ensures the basic accuracy of the implementation. Both methods used very nearly the same number of SCF steps. However, each Chebyshev filtered SCF step is found to be upto 20 times faster than each LOBPCG based SCF step. This results in an enormous amount of savings for the total computation time. The results are summarized in Table 4.1. It seems likely that for larger material systems, the savings are even more.

Material System	172 atoms Al F.C.C. cluster	C_{60}
No. of Basis functions	512000	343000
No. of states used	280	136
No. of LOBPCG SCF steps	21	10
No. of Chebyshev SCF steps	22	10
(LOBPCG SCF time) / (Chebyshev SCF time)	20.2	12.3

Table 4.1: Performance of Chebyshev Filtered SCF iterations compared against LOBPCG based SCF iterations.

4.3.3 Parallelization of Matrix vector products and electronic density computation

4.3.3.1 Two-level parallelization scheme

The Hamiltonian matrix times vector computation routine is one of the main computationally intensive steps in the LOBPCG method and it is the principle one in the Chebyshev filtering method. In order to implement a scalable and efficient version of this routine, we first need to keep in mind that for the LOBPCG and the Chebyshev filtering routines, the product of the Hamiltonian with a block of vectors (and not an individual vector) is actually required. Since this operation can be done by applying the Hamiltonian to each of the individual vectors that make up the block of vectors, it is natural to parallelize the matrix vector product over the different Kohn-Sham states (or bands, as they are often called in the plane-wave literature). The second thing to keep in mind is that the inverse basis transform requires access to all the expansion coefficients that constitute an entire band (eq. 4.15) while the forward basis transform requires access to function values at all the grid points (eq. 4.13, 4.14). However, the bulk of the operations involved within the basis transforms can be performed independently over the various radial grid points. This is true of the operation involving the pointwise multiplication of the effective potential with the forward transformed state (refer to Section 4.2.5) as well as the forward and inverse spherical harmonics transforms which need to be carried out during the forward and in-

verse basis transforms, respectively. The third thing to keep in mind is that, due to the use of the process grid for carrying out linear algebra operations, the block of vectors that need to be multiplied with the Hamiltonian, already appear distributed over the two dimensional process grid. In particular, they are distributed band wise over the process grid columns and each state is further distributed over the process grid rows.

These factors taken together seem to suggest that a two dimensional parallelization scheme [Bylaska et al., 2011; Gygi et al., 2006], for the matrix vector products is ideally suited in this scenario: the states already happen to be distributed over the process grid columns thus offering one level of parallelization. For the second level, we distribute real space quantities over different values of the radial gridpoints. Then, the only communication involved during the matrix vector product calculations will be over process grid rows: once during the broadcast of the different portions of a particular state while the inverse basis transform occurs and a second time during computation of the radial quadratures while the forward basis transform occurs. The important point however is that the communication load has been reduced from the total number of processors involved, to roughly the square root of the total number of processors, if a square process grid is in use. Also, due to the distribuion of various real space quantities over the radial grid points, the memory overhead is reduced as well.

The computation of the electronic density from the Kohn-Sham states can be parallelized in an exactly similar manner. In this case, while computing the electronic density in real space from the bands in reciprocal space, the communication involved will be once during the broadcast of the different portions of a particular state, while the inverse basis transform occurs and a second time in order to sum the results from the different individual bands according to eq. 4.4. Once again, this means that the communication load scales roughly as the square root of the number of processors.

4.3.3.2 Scaling of the two-level parallelization scheme

We now perform a scaling study of this two level parallelization scheme. We look at the particular case of the matrix-vector product by looking at a computation involving 1-million basis functions and 128 Kohn-Sham states. As we may expect, the process grid geometry plays an important role in this study and so we studied the scalability from 8 to 1024 processors using different process grid geometries. The results are plotted in Figure 4.4.

From the figure, we see that once the process grid height is fixed, the matrix vector products scale very nearly linearly with the number of processing elements. This is due to the

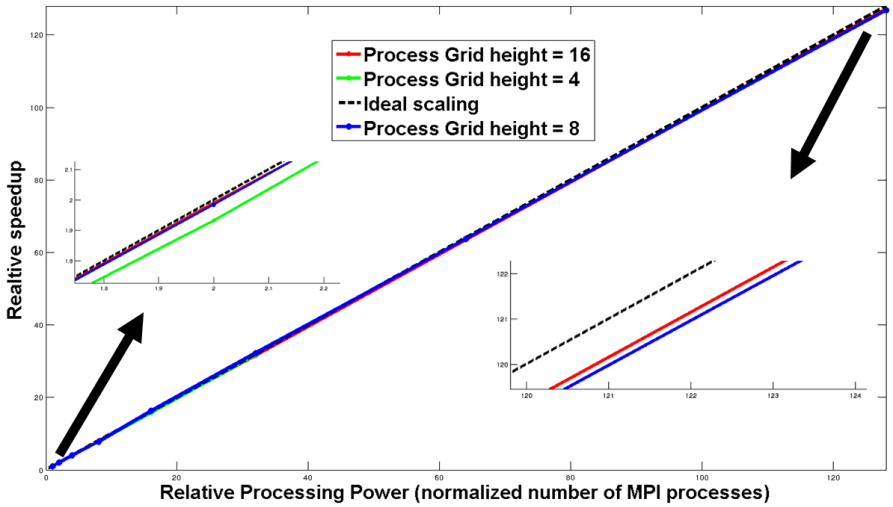

Figure 4.4: Strong parallel scaling of the Hamiltonian matrix times vector product routine, keeping the process grid height fixed, for different process grid heights.

fact that the problem is embarrassingly parallel in the number of Kohn-Sham states and the process grid based methodology allows us to take advantage of this. However, evident from the few examples on Table 4.2 is the fact that keeping the number of processors fixed, it is often possible to get even better performance than what the scaling results suggest, by changing the process grid, usually in favor of a grid with shorter height. On the other hand, as alluded to earlier, due to the fact that the various linear algebra operations involved in the diagolnalization routines operate on tall and skinny matrices, it is often more advantageous to have process grids in which the height exceeds the width. Since these two factors compete, we have found that square process grids often result in optimum performance of the LOBPCG and Chebyshev filtering routines.

Case	Normalized timing 1	Normalized timing 2	Normalized timing 3
8 vs. 16	1.00 (8×1)	0.510 (8×2)	0.3601 (4×4)
16 vs. 32	1.00 (8×2)	0.502 (8×4)	0.3454 (4×8)
32 vs. 64	1.00 (8×4)	0.509 (8×8)	0.3641 (4×16)
64 vs. 256	1.00 (16×4)	0.2625 (16×16)	0.1441 (8×32)
256 vs. 1024	1.00 (32×8)	0.2528 (32×32)	0.1314 (16×64)

Table 4.2: Some examples showing how the process grid geometry can enhance performance of the matrix vector product routine: It is often possible to achieve better timings by reducing the process grid height.

4.3.4 Miscellaneous implementation details

4.3.4.1 Mixing scheme

As mentioned earlier, SCF iterations typically employ mixing schemes in order to accelarate convergence towards the fixed point of the Kohn-Sham map [Martin, 2004]. The importance of mixing schemes in SCF iterations has been recognized both empirically and theoretically [Dederichs and Zeller, 1983], leading to the development of various methods over the years [Anderson, 1965; Broyden, 1965; Pulay, 1980; Johnson, 1988; Kudin et al., 2002; Fang and Saad, 2009]. We employed the multiple stage Anderson mixing scheme [Anderson, 1965] in this work, using the particular formulation available in Kohanoff [2006].[18]

In Anderson mixing, the quantity being mixed (such as the electronic density or the effective total potential) that is to be used at a given SCF step, is expressed as a linear combination of the same quantity from the previous SCF steps. The coefficients are determined by a norm minimization condition [see for e.g. Motamarri et al., 2013, for a more detailed presentation]. The implementation of an N_{mix} - stage Anderson mixing scheme requires the storage of $2N_{\text{mix}}$ variables from the most recent SCF steps. We implemented this using double ended queues and decided to use real space representations of the quantities to be mixed. To reduce memory requirements, these quantites were stored by distribution over all processing elements. Inner products were computed using quadrature over the real space grid points and global reduction operations.

Our implementation allows for mixing of the total effective potentials or of the electronic density. We have found that potential mixing tends to result in faster convergence of the total energies in most systems. The associated linear mixing parameter used was between 0.1 and 0.3 for all metallic system examples, while for non-metallic systems, a higher mixing parameter of 0.5 was used. A complete mixing history was used for these metallic systems while 3-5 mixing stages were used for most non-metallic ones.

4.3.4.2 Thermalization and Fermi-Dirac occupations

Regardless of the solution procedure, materials systems which have small or no band gaps tend to experience convergence issues in the SCF iterations. This occurs due to degenerate energy levels near the Fermi surface in these systems, and it usually manifests itself as *charge sloshing*. This means that the spatial distribution of the electronic density oscil-

[18] This is sometimes referred to as the Direct Inversion of the Iterative Subspace (DIIS) method.

lates rapidly in between SCF iterations although the ground state energy might converge [Kresse and Furthmuller, 1996a]. The usual solution to this issue is to thermalize the system, that is, to introduce a temperature dependent orbital occupation factor. Very often, these occupations are generated in accordance with the Fermi-Dirac distribution:[19]

$$f_i = \frac{1}{1 + \exp\left(\frac{\lambda_i - \epsilon_F}{K_B \Theta}\right)}\,, \tag{4.48}$$

the electronic density is computed through the expression:

$$\rho(\mathbf{x}) = 2 \sum_{i=1}^{N_e/2} f_i \left|\phi_i(\mathbf{x})\right|^2\,, \tag{4.49}$$

and the Fermi level ϵ_F is determined through the constraint:

$$\int_{\mathbb{R}^3} \rho = N_e \quad \Longrightarrow \sum_{i=1}^{N_e/2} f_i = N_e/2\,. \tag{4.50}$$

We implemented thermalization in our code for dealing with the various metallic system examples. The Fermi level was determined by solving equation 4.50 using Brent's method [Brent, 1973]. The electronic temperature Θ was set to 100 or 200 Kelvin for all simulations where thermalization was used.

4.3.4.3 The ClusterES package

We have incorporated all the methods and algorithms discussed so far into an efficient and reliable package called ClusterES (Cluster Electronic Structure). The package is written in the C++ programing language and makes heavy use of various Object Oriented Programing features. User inputs to the pacakage are made with the aid of scripts written using the Perl programing language. Parallelization was carried out by use of the Message Passing Interface (MPI).

Since our package makes heavy use of Spherical Harmonics Transforms, access to optimized and efficient routines for carrying out these transforms is quite essential for good performance of our code. We adopted the state of the art SHTns library [Schaeffer, 2013] for this purpose. In spite of using a traditional cubic order algorithm for computation (as

[19] Effectively, this amounts to replacing the minimization of the Kohn-Sham functional by minimization of the electronic free energy given accroding to the Mermin functional [Mermin, 1965]. The Kohn-Sham functional can be recovered in the limit of zero electronic temperature.

opposed to algorithms which are asymptotically faster, e.g. Mohlenkamp [1999]) this library has been shown to far outperform other Spherical Harmonics Transform routines because of its use of various hardware level optimizations [Schaeffer, 2013].

The spherical Bessel functions and the Associated Legendre polynomials required for various computations in our code were generated using routines from the GNU Scentific Library [Galassi et al., 2009]. Evaluation of the Gauss quadrature weights and nodes were carried out using the algorithm presented in [Golub and Welsch, 1969]. Computation of the roots of the Bessel functions was carried out by Halley's method [Weisstein, b].

4.4 Example systems

We finally move to some examples. We compute the ground states of various metallic and non-metallic materials systems using our code.

The computational platform details are as follows. All computations were carried out on the Itasca cluster of the Minnesota Supercomputing Institute. Itasca is an HP Linux cluster with 1,091 HP ProLiant BL280c G6 blade servers, each with two-socket, quad-core 2.8 GHz Intel Xeon X5560 "Nehalem EP" processors sharing 24 GB of system memory, with a 40 gigabit QDR InfiniBand (IB) interconnect. In total, Itasca consists of 8,728 computing cores and 24 TB of main memory.[20] The GNU g++ compiler (ver. 4.8.1) was used and the Linear Algebra and FFT operations were carried out using the hardware optimized Intel Math Kernel Library.

4.4.1 All-electron claculations of light atoms

We begin by computing the ground state electronic structures of the first few elements of the periodic table. This serves as a simple test of our implementation. No pseudopotential was used that is, these are all electron calculations. We used the parametrization of the Local Density Approximation as presented in Perdew and Zunger [1981]; Ceperley and Alder [1980]. The results of our computations are shown in Table 4.3 and compared with values from the literature.

The results illustrate the difficulty that our code faces when dealing with all-electron calculations. In spite of the spherical symmetry of the ground state, the Coulombic singularity at the origin makes it necessary to use a large number of radial basis functions to converge towards expected results. As the atomic numbers increase, so does strength of the singular-

[20] Quoted directly from the Minnesota Supercomputing Institute web page.

Element	Spectral code	Kotochigova et al. [1997]	Suryanarayana et al. [2011]
Hydrogen	-0.445	-0.445	-0.445
Helium	-2.833	-2.834	-2.830
Lithium	-7.310*	-7.335	-7.338
Beryllium	-14.165*	-14.447	-14.434

(*Unconverged, due to large radial basis set requirements.)

Table 4.3: Ground state energies of a few light atoms (Hartree units used).

ity and hence the increased difficulty of the computation. Therefore, we did not pursue the Lithium and Beryllium atom calculations after we ascertained that our results were within 1-2% of the values from the literature.

Figure 4.5 shows the plots of the ground wavefunction and radial probability distribution of the hydrogen atom as computed using our code. Since the hydrogen atom is a single electron atom and DFT is a many body theory, a generic discrepancy between analytical solution of the Schrodinger equation for hydrogen and Kohn-Sham DFT results is expected. Indeed, the theoretical groundstate energy of -0.5 Hartrees is different from the Kohn-Sham results. Nevertheless, there is general agreement between the plots and even the point of maximum probability density nearly coincides. What is more important to note however, is the behavior of the wavefunctions (theoretical and computed) near the origin. The theoretical solution shows a cusp at the origin due to the Coulombic singularity, as expected [Le Bris, 2003], but the numerical solution does not approximate this cusp so well. This helps to explain why so many radial basis functions are required.

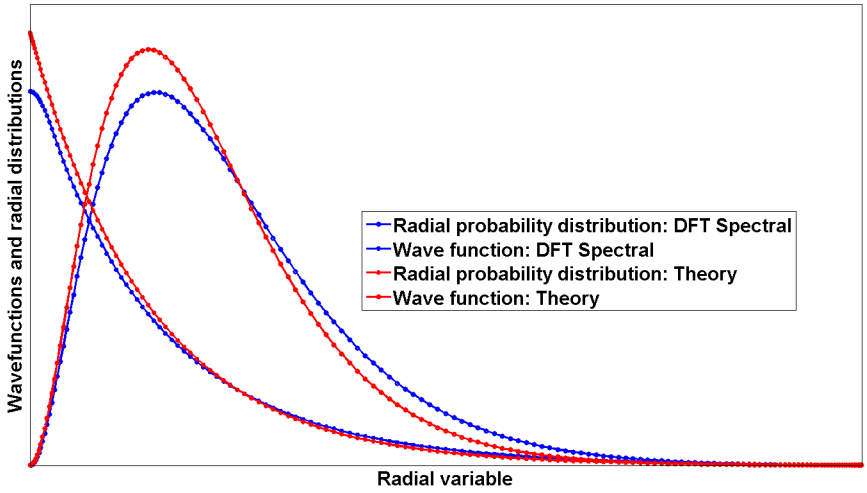

Figure 4.5: Ground state wave function and radial probability distribution of the Hydrogen atom: analytical solution vs. DFT results using the spectral code.

4.4.2 Local pseudopotential calculations

Having validated the basic correctness of our methodology and implementation, we now move to pseudopotential calculations. We first work with the smooth local 'Evanescent Core' pseudopotential [Fiolhais et al., 1995]. This pseudopotential has been designed to deal with various simple metallic systems and because of the lack of non-local projectors, it is relatively computationally inexpensive. Due to the smoothness of the pseudopotential, we witnessed rapid convergence of our code with increasing basis set size in all the examples that follow.

We first compute the ground state energies of various pseudo-atoms using the pseudopotential and compare with the values from the literature. The results displayed in Table 4.4 show excellent agreement.

Element	Spectral code	[Nogueira et al., 1996]	Suryanarayana et al. [2010]
Lithium	-5.97	-5.97	-5.97
Sodium	-5.21	-5.21	-5.21
Magnesium	-23.06	-23.06	-23.05

Table 4.4: Ground state energies of a few light atoms (Electron volt units used).

Next, we computed the ground state properties of lithium and sodium dimers and octahedral clusters. We computed the binding energy (in electron volts per atom units) and the bond length (in atomic units) of these systems. For the octahedral clusters, as in [Suryanarayana et al., 2011], we did not perform any geometry optimization but only sought minima in terms of the nearest neighbor bond length. The results are shown in Table 4.5.

Cluster	Parameters	Spectral	[Suryanarayana et al., 2011]	[Nogueira et al., 1996]
Li_2	B. E.	-0.50	-0.49	-0.52
	B. L.	4.86	4.86	4.92
Na_2	B.E.	-0.42	-0.37	-0.46
	B.L.	5.73	5.72	5.77
Li_6	B.E.	-0.52	-0.50	-0.72
	B.L.	5.68	5.69	5.79
Na_6	B.E.	-0.43	-0.42	-0.53
	B.L.	6.81	6.80	6.87

Table 4.5: Binding energy (B.E.) in electron volts per atom and bond length (B.L) in atomic units for sodium and lithium dimers and octahedral clusters.

We see that our results agree to within 1-2% of the values in the literature. The somewhat larger discrepancy with the results of [Nogueira et al., 1996] is probably because of the use of the LCAO method by the authors. Mid plane electron density contour plots for the Li_2 and Na_6 systems is shown in Figure 4.6

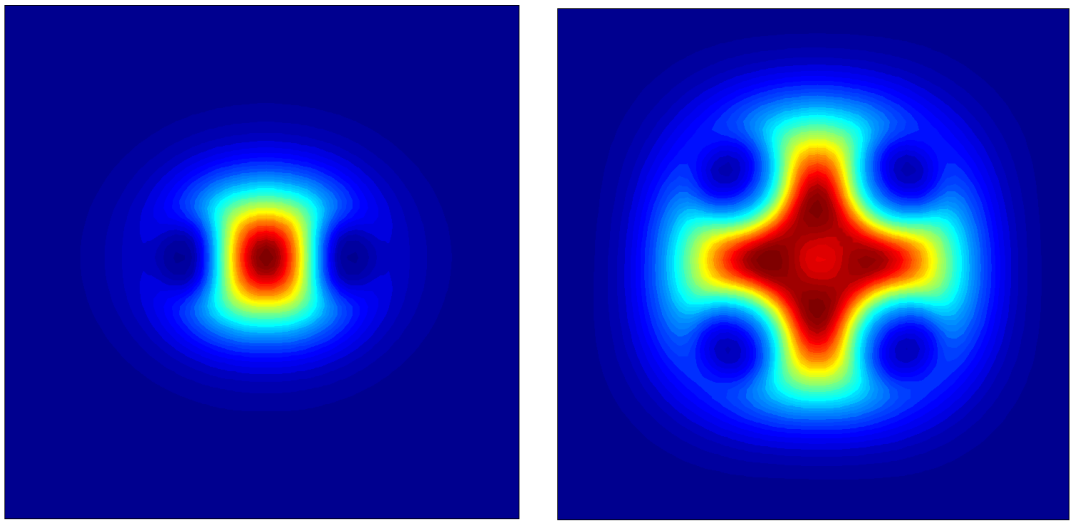

(a) Lithium dimer.

(b) Octahedral sodium cluster.

Figure 4.6: Mid plane electron density contour plots.

Next, we study the properties of a few clusters of sodium consisting of $1\times1\times1$, $2\times2\times2$, and $3\times3\times3$ body centered cubic unit cells. We calculated the binding energy per atom and lattice constant for these clusters by computing the total energy for various values of the lattice parameter and then fitting this data to a cubic polynomial. Our results, as compared to the values in the literature are shown in Table 4.6. Once again, the agreement is very good, assuring us of the efficacy of our method. Figure 4.7 shows the mid-plane contour plot of the electron density of the $2\times2\times2$ cluster, as well as the ground state energy curve.

Cluster	Parameters	Spectral	[Suryanarayana et al., 2010]
$1\times1\times1$	Binding Energy (e.v./atom)	-0.54	-0.54
	Bond Length (a.u.)	7.20	7.20
$2\times2\times2$	Binding Energy (e.v./atom)	-0.70	-0.71
	Bond Length (a.u.)	7.60	7.55
$3\times3\times3$	Binding Energy (e.v./atom)	-0.81	-0.80
	Bond Length (a.u.)	7.79	7.75

Table 4.6: Binding energy per atom and lattice constant of sodium BCC unit cells.

4.4.3 Non-local pseudopotential calculations

In order to deal with a wider variety of materials systems, we now turn to calculations involving norm-conserving non-local pseudopotentials. This class of pseudopotentials is attractive because the pseuopotentials are accurate and transferable and at the same time, they are availabile for all elements in the periodic table (including ones which require relativistic treatment of the core electrons). Here, we look at the results obtained using the separable dual space Gaussian pseudopotentials introduced in Goedecker et al. [1996]; Hartwigsen et al. [1998]. This pseudopotential is available in analytical form with a small set of parameters for every element (thus allowing for easy implementation) and it satisfies an optimality criterion for the real-space integration of the nonlocal part. While this pseudopotential is known to be harder (i.e., it requires many more basis functions per atom for converged results) as compared to other norm conserving pseudopotentials, it is also known to be more accurate and transferable than other pseudopotentials [Goedecker et al., 1996]. In the examples that follow, we chose the rational polynomial form of the local density approximation introduced in [Goedecker et al., 1996] for all calculations.

We computed the bond lengths of a few small molecules using our spectral code and compared our results with values from literature. This is displayed in Table 4.7. Our results all agree to within 1% of values obtained by the authors in Goedecker et al. [1996].

Molecule	Bond length: Spectral	Bond length: [Goedecker et al., 1996]
CH_4	2.078 a.u.	2.072 a.u.
NH_3	1.924 a.u.	1.931 a.u.
H_2O	1.819 a.u.	1.835 a.u.
C_2H_6 (C-C)	2.895 a.u.	2.910 a.u.

Table 4.7: Bond lengths of a few small molecules using the Goedecker-Teter-Hutter pseudopotentials.

Next, we computed the ground state of the C_{60} fullerene molecule. This is a system containing 240 electrons. Our results are compared to the results obtained by [Fang et al., 2012] in Table 4.8. Once again, the agreement is excellent, thereby confirming the efficacy of our method.

4.4.4 Benchmark calculations on large systems

Finally, in order to demonstrate the capabilities of our method in dealing with large systems efficiently, we now carry out computations of the ground states of large aluminum clusters.

Cluster	Properties	Spectral	[Fang et al., 2012]
C_{60}	Binding Energy (e.v./atom)	-155.0225	-155.0206
	HOMO-LUMO gap (e.v.)	1.7050	1.7048

Table 4.8: Properties of the C_{60} fullerene molecule.

We looked at 3×3×3, 5×5×5 and 7×7×7 face centered cubic clusters for this study. The lattice spacing was fixed at 7.45 a.u. for all the clusters. We used the 'Evanescent Core' pseudopotential for these calculations. A thermalization temperature of 100 Kelvin was used. For the 3×3×3 and 5×5×5 clusters, in order to assess the efficacy of our method, we aimed to converge our ground state energies to within 1-2 milli electron volts of the plane wave and higher order finite element method (FEM) results presented in Motamarri et al. [2013]. For the 7×7×7 cluster, due to computational resource constraints, we used a somewhat smaller basis set than what would be required to achieve this same level of convergence. So we present here results in which the total energy was within 0.01 electron volts per atom of the higher order finite element method (FEM) results. The results are shown in Table 4.9

System	No. atoms	No. electrons	Spectral	Planewave*	FEM*
3×3×3	172	516	-56.01809	-56.01814	-56.01776
5×5×5	666	1998	-56.05057	-56.05068	-56.04906
7×7×7	1688	5064	-56.05712	–	-56.06826

(*From Motamarri et al. [2013].)

Table 4.9: Ground state energy per atom of large aluminum clusters. Electron-volt units used.

To show that our methodology and its implementation is highly competitive with existing methods, we display in Table 4.10 timing results of the 3×3×3 and 5×5×5 systems and compare it with the results presented in Motamarri et al. [2013]. The computational platforms in both systems was quite similar. However, due to the fast convergence of our spectral basis set and the various algorithmic methodologies adopted, our code was able to well outperform the plane-wave and finite element codes.

System	Spectral	FEM*	Planewave*
3×3×3	18	371	646
5×5×5	1948	6619	7307

(*From Motamarri et al. [2013].)

Table 4.10: Computational run times of ClusterES compared against existing plane-wave and FEM codes. All run times are presented in cpu hours.

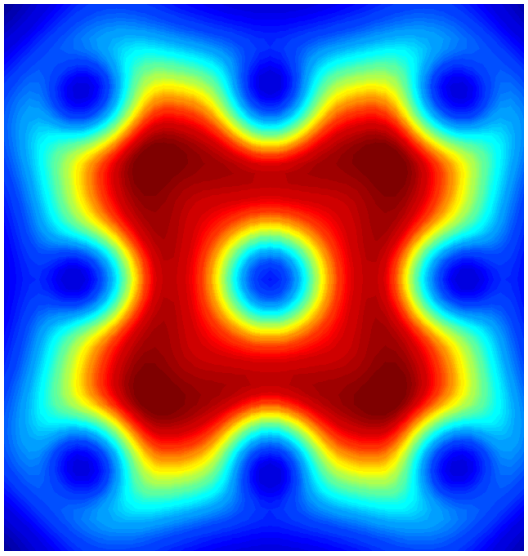

(a) Mid-plane contour plot of the electron density.

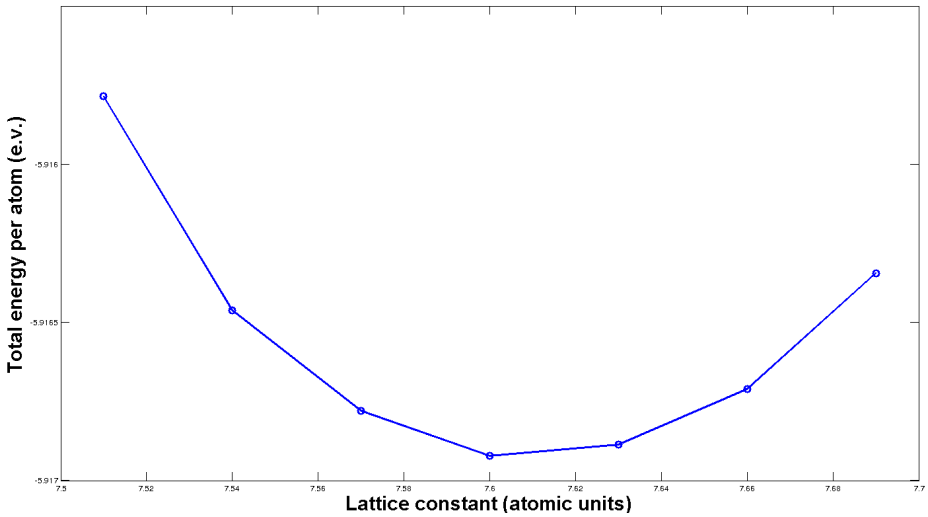

(b) Ground state energy curve.

Figure 4.7: Electron density and ground state energy curve of the 2×2×2 BCC sodium cluster.

Chapter 5

Symmetry adapted spectral schemes

In the previous chapter, we formulated and implemented a spectral scheme for cluster systems. In this chapter, we look at how symmetry adaptation may be carried out within the framework of that methodology. We also present a spectral scheme for helical groups.

5.1 Symmetry adapted subspace iterations

As described in Chapter 3, the interpretation of symmetry adaptatation for the case of eigenvalue problems can be understood in terms of block diagonalization or, equivalently, in terms of problems posed on the fundamental domain (symmetry cell). The basis set described in Chapter 5 interacts well with arbitrary point group symmetries because of the intimate connection of spherical harmonics with the group of rotations: indeed, spherical harmonics form the basis functions of the irreducible subspaces of the group of rotations in three dimensions. Even with the choice of such a basis set however, the set up and solution of problems on the fundamental domain can be non-trivial whenever non-Abelian groups are involved. To illustrate this point, we may consider the case of the simplest non-Abelian group D_3 which is associated with the symmetries of an equilateral triangle [Bossavit, 1986]. As detailed in Figure 5.1, since this group has three irreducible representations, the original problem can be broken into three subproblems, each assoiciated with one irreducible representation. One of the irreducible representations happens to be two dimensional, thus leading to a pair of coupled boundary value problems over the symmetry cell. It is not clear at the outset however, how the use of the spherical harmonics basis might allow for an efficient solution of the coupled sub-problems.

The alternative to the symmetry cell reduction is to exploit block diagonalization of the

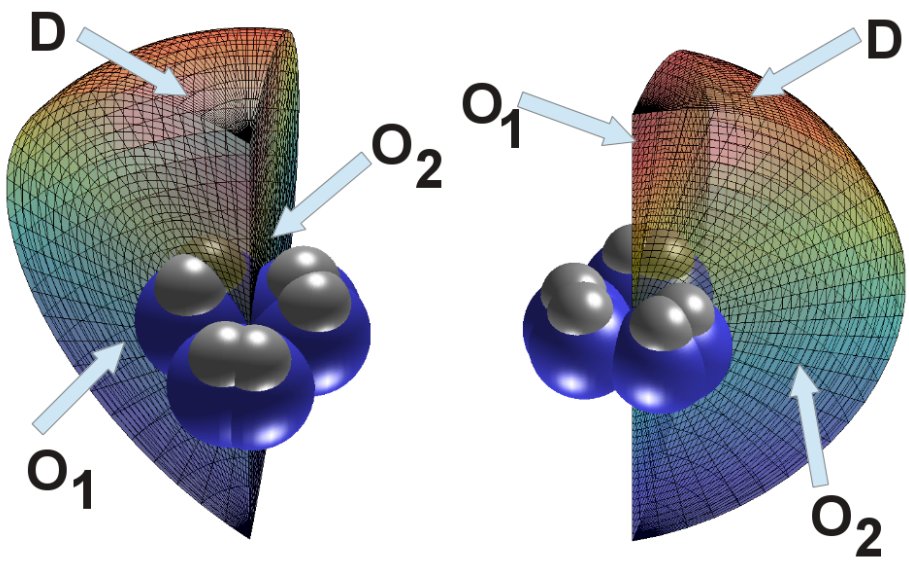

Figure 5.1: Symmetry adapted boundary value problems on the fundamental domain for the group D_3: Three problems ($\nu = 1, 2, 3$) arise, the boundary conditions of which are as follows. For $\nu = 1$, $\tilde{u}^1$: $\partial_n \tilde{u}^1 = 0$ on $\mathsf{O}_1, \mathsf{O}_2$ and $\tilde{u}^1 = 0$ on D. For $\nu = 2$, $\tilde{u}^2$: $\tilde{u}^2 = 0$ on $\mathsf{O}_1, \mathsf{O}_2$ and $\tilde{u}^2 = 0$ on D. For $\nu = 3$, a pair of coupled problems arise. On O_1, we have $\partial_n(\tilde{u}^3_1 - \sqrt{3}\tilde{u}^3_2) = 0$ and $\tilde{u}^3_2 + \sqrt{3}\tilde{u}^3_1 = 0$. On O_2 we have, $\partial_n \tilde{u}^3_1 = 0$ and $\tilde{u}^3_2 = 0$. On D, we have $\tilde{u}^3_k = 0, (k = 1, 2)$.

Hamiltonian in the symmetry adapted basis. In order to obtain the block diagonal form of the matrix for which symmetry based reduction is to be carried out, a commonly suggested approach [see for e.g. Healey and Treacy, 1991] is to compute the matrix of orthonormalized symmetry adapted basis vectors $\mathfrak{R}$ and to then compute $\mathfrak{R}^* \mathbf{H} \mathfrak{R}$. This casts the matrix $\mathbf{H}$ to the sought block diagonal form. The individual blocks can be diagonalized subsequently by using standard diagonalization techniques. The symmetry adapted basis vectors that are required for the construction of the matrix $\mathfrak{R}$, may be computed as eigenvectors of the projection operators to the symmetry adapted invariant subspaces (described in Chapter 2) [Chang and Healey, 1988].

There are several issues in trying to directly adopt this methodology to the numerical frame work described in Chapter 4. First, the Hamiltonian matrix is never explicitly constructed in the methods described in that chapter for reasons of speed and efficiency. Computation and storage of the symmetry adapted blocks arising from the Hamiltonian is likely to result in large memory demands in most computations since there is no straightforward way of representing these blocks in a matrix free manner. Secondly, the storage and manipulation of the matrix $\mathfrak{R}$ is inefficient and cumbersome since this matrix, like the Hamiltonian, is dense (in general) and of the same dimension as the Hamiltonian itself (i.e., $d \times d$). Compu-

tation of the action of the Hamiltonian on each of the d columns of this matrix is far more demanding than for example, the application of several steps of the Chebyshev polynomial filter to the collection of the Kohn-Sham orbitals.[1] Thirdly, the symmetry adaptation methodology is not designed with the SCF iteration cycles in mind. Thus the computational difficulties described in the first two points are going to be encountered on each SCF step.

The discussion above, points out that a naive adoption of the usual methods of symmetry adaptation to the iterative methods of solution of the Kohn-Sham eigenvalue problem, is likely to result in performance degradation. Indeed, a large majority of the computation time is likely to be spent on extraction of the symmetry adapted blocks from the Hamiltonian, instead of computation of the required eigenstates. In contrast, the techniques described in Chapter 4 could be employed in computing the required eigenstates directly in a much more efficient manner. The underlying theoretical issue is that the naive symmetry adaptation approach deals with symmetry adapted basis sets of the space $\mathbb{C}^d$, whereas iterative diagonalization schemes for the Kohn-Sham equations (like the Chebyshev filtering approach described in Chapter 4) work with the occupied subspace only.

In order to avoid these computational issues, our recipe is to carry out symmetry adaptation in the occupied subspace of the Hamiltonian. Provided that the conditions of Theorem 3.1.11 are met, the occupied subspace is an invariant subspace of the Hamiltonian. As pointed out in earlier chapters, the symmetry adapted subspaces are invariant subspaces of the Hamiltonian as well. Thus, a natural way to perform a symmetry adapted computation of the occupied subspace would be to perform subspace iterations after projecting the occupied eigenspace to each of the invariant subspaces. More specifically, we may proceed as follows. For the first SCF step, we may compute an initial guess for the occupied subspace of the Hamiltonian by linearly superposing atomic orbitals and then refining this guess by a few steps of the LOBPCG algorithm. This leaves us with a set of basis vectors for the invariant subspace of the Hamiltonian. Thereafter, we may apply projection operators associated with the group invariant subspaces (Chapters 2, 3) to this collection of basis vectors and orthonormalize the results to obtain a symmetry adapted decomposition of the occupied subspace of the Hamiltonian. A quick look into the steps involved in the Chebyshev filtering algorithm [Zhou et al., 2006a,b] now tells us that this algorithm can be used to independently extract relevant eigenpairs from each of the individual symmetry adapted subspaces.[2] To continue with the SCF cycle, we may now collect and sort the relevant

[1] This is because, in most typical computations, the ratio of the number of basis functions d, to the number of Kohn-Sham orbitals is 100-1000 (or more in high fidelity calculations).

[2] The fact that we are dealing with invariant subspaces of the Hamiltonian ensures that the starting and ending vectors of the Chebyshev filtering algorithm span the same invariant susbapces.

eigenpairs and compute the electronic density from this sorted collection. For subsequent SCF steps, we may use the Chebyshev filtered symmetry adapted subspaces from previous steps to act as the initial guess for the current Chebyshev filtering step. This ensures that we continue to get relevant eigenpairs from the individual symmetry adapted subspaces independently on each SCF step.

This methodology can be carried out for any symmetry group in general. It is particularly simple to apply for the case of point group symmetries using the spherical basis set described in Chapter 4 because the action of the projection operators on a generic function expanded using the spherical basis may be computed analytically (using Wigner D-matrices). The asymptotic computational savings occur in the orthonormalization and Rayleigh-Ritz projection steps of the Chebyshev filtering algorithms. It is easy to see that if $\mathfrak{N}$ symmetry adapted subspaces are involved, then these two steps can be performed faster by a factor of $\mathfrak{N}$ overall since the computationjal cost of these steps scales quadratically in the number of states involved. Further optimizations and savings are possible for the case of cyclic groups and this is described in the next section.

5.2 Optimal scheme for cyclic groups

The issue with the methodology presented in the previous section is that the savings are not perfectly linear in the number of irreducible representations of the group involved. This is because only the orthonormalization and Rayleigh-Ritz projection step lead to savings; the Chebyshev filtering step (the bulk of which is matrix-vector products) is carried out over the complete set of real space points and all the basis functions are involved in this process. We show in this section how this can be avoided for the case of cyclic groups and we obtain a scheme that has linear savings in the order of the cyclic group involved. The basic idea is that for the case of cyclic groups, the abelian structure of the group allows us to reformulate the problem completely in terms of its projection on to the subspace associated with the identity representation.

Let $\mathcal{G}$ denote the cyclic group of order $\mathfrak{N}$ generated by the single element g, that is,

$$\mathcal{G} = \{g, g^2, \ldots, g^{\mathfrak{N}} = id\}. \tag{5.1}$$

The inverse element to $g^\gamma \in \mathcal{G}$, is the element $g^{\mathfrak{N}-\gamma}$. A physical realization of this abstract group can be obtained by considering a discrete group of rotations about a common axis.

Let $(\mathbf{e}_1, \mathbf{e}_2, \mathbf{e}_3)$ denote the standard basis of $\mathbb{R}^3$. Then, the matrices:

$$\{\mathfrak{R}^\gamma : \gamma = 1, \ldots, \mathfrak{N}\}, \quad \text{with} \quad \mathfrak{R}^\gamma = \begin{pmatrix} \cos\frac{2\pi\gamma}{\mathfrak{N}} & -\sin\frac{2\pi\gamma}{\mathfrak{N}} & 0 \\ \sin\frac{2\pi\gamma}{\mathfrak{N}} & \cos\frac{2\pi\gamma}{\mathfrak{N}} & 0 \\ 0 & 0 & 1 \end{pmatrix}, \tag{5.2}$$

form a faithful representation of $\mathcal{G}$ on $\mathbb{R}^3$. Since, $\mathcal{G}$ is a finite Abelian group, the representation theory of $\mathcal{G}$ over any separable Hilbert spaces H, is particularly simple. Indeed, following the developments in Chapter 2, it is easy to see that $\mathcal{G}$ has $\mathfrak{N}$ distinct irreducible representations $\chi_\nu : \mathcal{G} \to \mathbb{C}$, each of dimension one. These are expressible as, for $\nu = 0, 1, \ldots, \mathfrak{N} - 1$:

$$\chi_\nu(\mathfrak{R}^\gamma) = e^{i\frac{2\pi\gamma\nu}{\mathfrak{N}}}. \tag{5.3}$$

The irreducible representations $\{\chi_\nu\}_{\nu=0}^{\mathfrak{N}-1}$, can be used to perform a direct sum decomposition of the form $\mathsf{H} = \bigoplus_{\nu=0}^{\mathfrak{N}-1} V^\nu$. A function F^ν belonging to the irreducible subspace V^ν transforms[3] under the group as:

$$g^\gamma \circ \hat{F}^\nu(r, \vartheta, \varphi) = \hat{F}^\nu(r, \vartheta, \varphi - \frac{2\pi\gamma}{\mathfrak{N}}) = e^{i\frac{2\pi\gamma\nu}{\mathfrak{N}}} \hat{F}^\nu(r, \vartheta, \varphi)\,. \tag{5.4}$$

This immediately suggests that $\hat{F}^\nu(r, \vartheta, \varphi)$ is expressible as:

$$\hat{F}^\nu(r, \vartheta, \varphi) \equiv e^{-i\nu\varphi}\, \hat{u}^\nu(r, \vartheta, \varphi)\,, \tag{5.5}$$

with $\hat{u}^\nu(r, \vartheta, \varphi)$ group invariant, that is, $\hat{u}^\nu(r, \vartheta, \varphi + \frac{2\pi\gamma}{\mathfrak{N}}) = \hat{u}^\nu(r, \vartheta, \varphi)$, for each $\gamma = 1, 2, \ldots, \mathfrak{N}$.

5.2.1 Eigenvalue problem and its discretization

In the setting of Chapters 3 and 4, we consider the Hamiltonian operator $\mathfrak{H} = -\frac{1}{2}\Delta + V$ on the Hilbert space $\mathsf{L}^2(\mathcal{B}_R)$ and we suppose that the potential $V(\mathbf{x})$ is invariant under $\mathcal{G}$. Then, the eigenfunctions of $\mathfrak{H}$ transform as the irreducible subspaces of $\mathcal{G}$ in H (Chapter 3) and therefore, they admit the ansatz introduced in eq. 5.5.

[3]Here and later, a function $f(\mathbf{x})$, when expressed in polar coordinates is written as $\hat{f}(r, \vartheta, \varphi)$. The point $\mathbf{x} = (x, y, z)$ has spherical polar coordinates (r, ϑ, φ) and $x = r\sin\vartheta\cos\varphi, y = r\sin\vartheta\sin\varphi, z = r\cos\vartheta$.

To see what this implies for the eigenvalue problem associated with $\mathfrak{H}$, we observe that:

$$\frac{\partial \hat{F}^\nu}{\partial \varphi} = -i\nu\, e^{-i\nu\varphi}\, \hat{u}^\nu + e^{-i\nu\varphi}\, \frac{\partial \hat{u}^\nu}{\partial \varphi}\ ,$$
$$\frac{\partial^2 \hat{F}^\nu}{\partial \varphi^2} = -\nu^2\, e^{-i\nu\varphi}\, \hat{u}^\nu - 2i\nu\, e^{-i\nu\varphi}\, \frac{\partial \hat{u}^\nu}{\partial \varphi} + e^{-i\nu\varphi} \frac{\partial^2 \hat{u}^\nu}{\partial \varphi^2}\ , \tag{5.6}$$

and therefore:

$$\Delta \hat{F}^\nu = e^{-i\nu\varphi} \left(\Delta \hat{u}^\nu - \nu^2\, \hat{u}^\nu - 2i\nu\, \frac{\partial \hat{u}^\nu}{\partial \varphi} \right). \tag{5.7}$$

The eigenvalue problem $\mathfrak{H} F^\nu = \lambda F^\nu$ becomes:

$$-\frac{1}{2} \left(\Delta \hat{u}^\nu - \nu^2\, \hat{u}^\nu - 2i\nu\, \frac{\partial \hat{u}^\nu}{\partial \varphi} \right) + \hat{V}\, \hat{u}^\nu = \lambda \hat{u}^\nu\ , \tag{5.8}$$

with $\hat{u}^\nu$ group invariant. Thus, there are $\nu = 0, \ldots, (\mathfrak{N} - 1)$ problems to solve, but each problem only involves functions belonging to the group invariant subspace.

We now discretize this problem using the spherical basis set introduced in Chapter 4. However, we only require basis functions which are group invariant. To identify these invariant basis functions, we may construct the projection operator to the subspace associated with the identity representation. This calculation reveals that a basis function $F_{l,m,n}$ is invariant under $\mathcal{G}$ if and only if m is an integer multiple of $\mathfrak{N}$. To choose a basis set $\mathcal{V} \subset \mathsf{H}$ for the solution of (5.8) therefore, we set $\mathcal{L}, \mathcal{N} \in \mathbb{N}$,

$$\Gamma^{\mathfrak{N}} = \left\{ (l,m,n) : l \in \{0,1,\ldots,\mathcal{L}-1\}, m \in \{-l,\ldots,l\} \cap \mathfrak{N}\mathbb{Z}, n \in \{1,\ldots,\mathcal{N}\} \right\}, \tag{5.9}$$

$$\text{and } \mathcal{V} = \left\{ F_{l,m,n} \right\}_{(l,m,n)\in\Gamma}\ . \tag{5.10}$$

To obtain the discretized form of the governing equation (5.8) when expanded in these basis functions, let us write:

$$\hat{u}^\nu = \sum_{\Gamma} a^\nu_{l,m,n} \hat{F}_{l,m,n}\ . \tag{5.11}$$

This implies that:

$$\frac{\partial \hat{u}^{\nu}(r,\vartheta,\varphi)}{\partial \varphi} = \sum_{\Gamma} a^{\nu}_{l,m,n} \frac{\partial \hat{F}_{l,m,n}(r,\vartheta,\varphi)}{\partial \varphi} = i \sum_{\Gamma} m\, a^{\nu}_{l,m,n}\, \hat{F}_{l,m,n}(r,\vartheta,\varphi)\ . \tag{5.12}$$

Using the above expressions, as well as:

$$-\Delta \hat{F}_{l,m,n} = \tilde{\lambda}_{l,m,n} \hat{F}_{l,m,n}\ , \tag{5.13}$$

and writing:

$$\hat{V}(r,\vartheta,\varphi) = \sum_{\Gamma} v_{\tilde{l},\tilde{m},\tilde{n}}\ \hat{F}_{\tilde{l},\tilde{m},\tilde{n}}(r,\vartheta,\varphi)\ , \tag{5.14}$$

we arrive at:

$$\begin{aligned} -\frac{1}{2}\Bigg(-\sum_{\Gamma} a^{\nu}_{l,m,n} \tilde{\lambda}_{l,m,n} \hat{F}_{l,m,n} - \nu^2 \sum_{\Gamma} a^{\nu}_{l,m,n} \hat{F}_{l,m,n} - 2i\nu \sum_{\Gamma} a^{\nu}_{l,m,n} (im) \hat{F}_{l,m,n} \Bigg) \\ + \sum_{\Gamma} \sum_{\Gamma} v_{\tilde{l},\tilde{m},\tilde{n}} a^{\nu}_{l,m,n} \hat{F}_{\tilde{l},\tilde{m},\tilde{n}} \hat{F}_{l,m,n} = \lambda \sum_{\Gamma} a^{\nu}_{l,m,n} \hat{F}_{l,m,n}\ . \end{aligned} \tag{5.15}$$

We take the inner product of this equation with $\hat{F}_{l',m',n'}$ and use the orthonormality of the basis functions to obtain obtain the following system of linear equations for $a_{l',m',n'}$:

$$\left(\frac{1}{2}\tilde{\lambda}_{l',m',n'} + \frac{\nu^2}{2} - \nu\, m'\right) a_{l',m',n'} + \sum_{\Gamma}\sum_{\Gamma} \mathcal{W}^{(l',m',n')}_{(l,m,n)\,,\,(\tilde{l},\tilde{m},\tilde{n})}\ v_{\tilde{l},\tilde{m},\tilde{n}}\ a_{l,m,n} = \lambda\, a_{l',m',n'}\ , \tag{5.16}$$

$$\text{where as in Chapter 4,} \quad \mathcal{W}^{(l',m',n')}_{(l,m,n)\,,\,(\tilde{l},\tilde{m},\tilde{n})} = \langle \hat{F}_{\tilde{l},\tilde{m},\tilde{n}}\ \hat{F}_{l,m,n}\ , \hat{F}_{l',m',n'} \rangle_{\mathsf{L}^2(\mathcal{B}_R)}\ . \tag{5.17}$$

Based on the methods of the previous chapter, this immediately lends itself to solution by iterative solution schemes. Specifically, for each ν, a problem similar to the one solved in Chapter 4 is needed to be solved. However, since the total number of occupied eigenstates are likely to be distributed more or less equally over all values of ν, we need to compute roughly $N_e/(2 * \mathfrak{N})$ eigenstates for every value of ν (instead of $N_e/2$ eigenstates). Matrix vector products can be carried out by the techniques mentioned in Section 4.2.5 with the following two added considerations. First, the action of the kinetic energy on a given vector requires the inclusion of the additional term $(\frac{\nu^2}{2} - \nu\, m')$. Indeed, this term also needs to be included while computing for instance the entries of the preconditioner described in 4.3.1.4.

Secondly, since only group invariant functions are involved, (that is, roughly speaking, the angular basis set size is $\mathcal{L}^2/\mathfrak{N}$ instead of $\mathcal{L}^2$) the spherical harmonics transforms required for the matrix vector products can be computed faster by a factor of $\mathfrak{N}$. Also, the pointwise multiplication of the total effective potential with the Kohn–Sham orbitals can be carried out with the same speedup since the underlying real space grid in the azimuthal direction only needs to contain points in the interval $[0, 2\pi/\mathfrak{N}]$. The fact that $N_e/(2 * \mathfrak{N})$ eigenstates need to be computed for each value of ν and the matrix vector products are cheaper by a factor of $\mathfrak{N}$, together contribute to the fact that an overall savings factor of $\mathfrak{N}$ can be achieved. Thus, for a diagonalization algorithm like Chebyshev filtering, an overall speed up factor of $\mathfrak{N}$ can be achieved by making use of the cyclic symmetry.

5.2.2 Implementation and results

We have implemented the scheme described above within the framework of the ClusterES package. As a preliminary test of the basic correctness of our method, we set up a molecular ring with 16 fold cyclic symmetry. We used the model local pseudopotential described in [Garcia-Cervera et al., 2009] and we used two different values of the parameters for that pseudopotential to represent two distinct species of atoms. We verified that our code with cyclic symmetry imposed converged to the ground state energies obtained by the code which had no cyclic symmetry imposed (i.e., the original ClusterES code). What is more interesting however, is that consistent with the discussion in the previous section, our computational time reduced almost linearly with increase of the group order. A schematic of this ring systems along with computational scaling behavior is shown in Figure 5.2

We next applied our cyclic groups code for the study of hydrogen passivated silicon nano dot cluster systems.[4] For silicon, we used the bulk-fitted local pseudopotentials as described in Huang and Carter [2008]. The configuration for the silicon atoms for one of these clusters is shown in Figure 5.3. We computed the ground state configurations of a number of large nano dot systems. The ground state energies so computed are shown in Table 5.1. Without the use of our spectral method and the cyclic symmetries, accurate computation of the ground states of these very large systems would not have been feasible.

5.3 A spectral solution scheme for helical groups

We recall that the Bloch theorem for helical groups 3.2.2 allows us to reduce the problem posed on the infinite helical structure, to one posed on the fundamental domain (eq.

[4] Atomic position coordinates obtained from Suryanarayana [2013] and Zhou [2013].

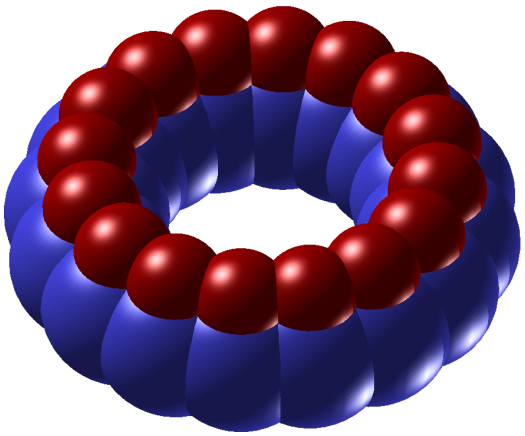

(a) Schematic of the cyclic molecular system used for verification of the cyclic symmetry code.

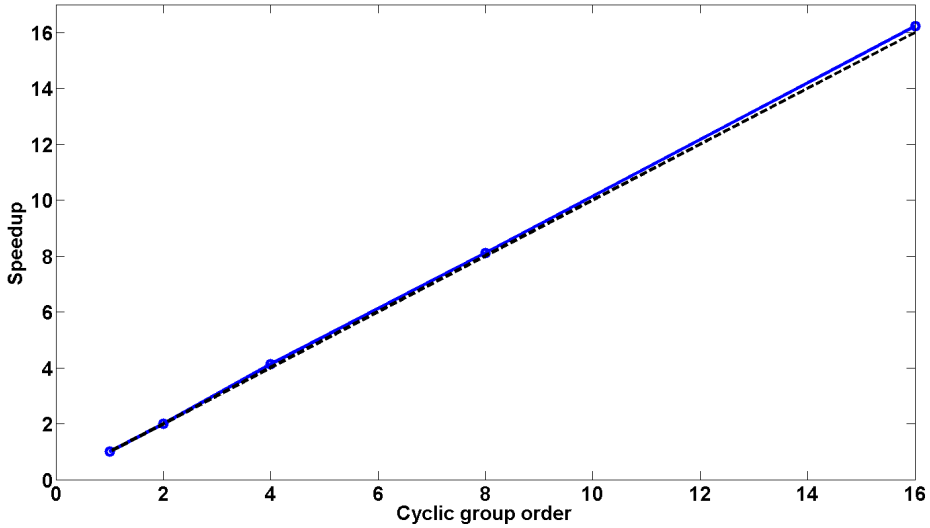

(b) Speedup obtained on increasing cyclic group order

Figure 5.2: Cyclic symmetry group code: Example system and scaling with group order.

(3.59)). The first step in trying to solve (3.59) by any discretization method is to choose a finite subset $\mathcal{B} \subset [-\frac{2\pi}{\tau}, \frac{2\pi}{\tau}]$ and to restricts β to lie in $\mathcal{B}$. We may think of this as an analog of *Brillouin Zone Sampling*. A straightforward choice for be would be to use Gauss weights and nodes. For each fixed $\beta \in \mathcal{B}$, we may then solve (3.59) by some appropriate discretization method. It is quite clear however, that helical objective boundary conditions are unlike any of the usual boundary conditions usually encountered in the numerical solution of PDEs and therefore, regular finite difference or finite element methods are likely to face issues in trying to satisfy this boundary condition.

The straight forward way to overcome the issue of the boundary conditions is to use helical

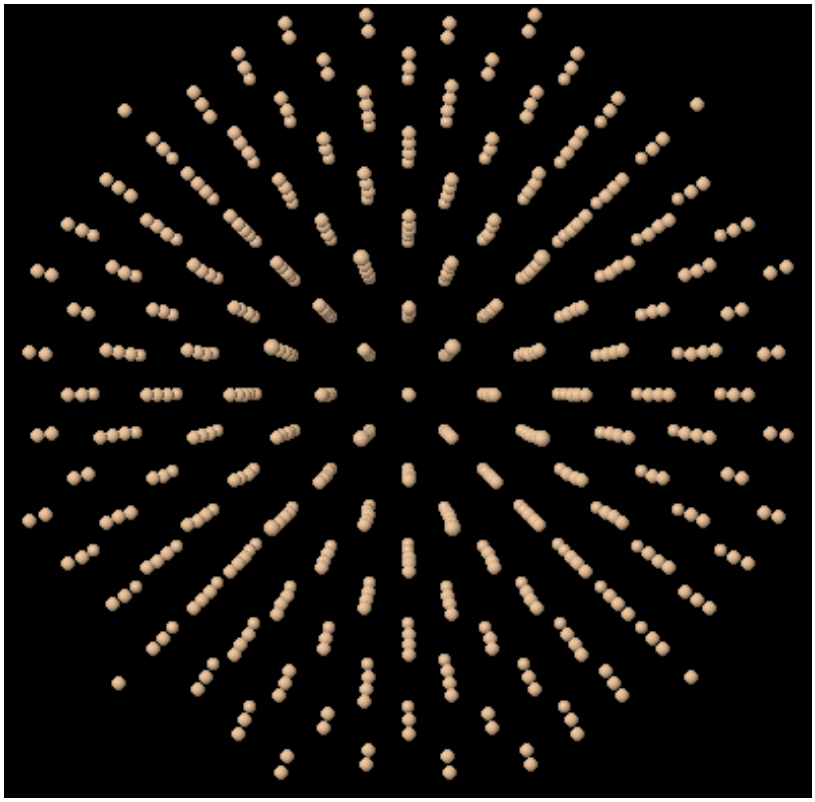

Figure 5.3: A typical silicon nanodot configuration containing 525 silicon atoms.

No. of Silcon atoms in nanodot system	Ground state energy (e.v./atom)
525	-77.3220
2713	-86.2789
4001	-89.2360
6047	-92.3615

Table 5.1: Ground state energies of a few hydrogen passivated silicon nano dot systems.

coordinates (3.55) in $\mathcal{D}\backslash\{\lambda \mathbf{e}_3 : \lambda \in (0,\tau)\}$ to get (with a mild abuse of notation), $\phi(\mathbf{x}) = \phi(r,\theta_1,\theta_2)$ as well as $V(\mathbf{x}) = V(r,\theta_1,\theta_2)$. Using the calculations in the Appendix B we see that the equations to be solved in the helical coordinates become:

$$-\frac{1}{2}\Big(\phi_{rr}+\frac{1}{r}\phi_r+\frac{1}{\tau^2}\phi_{\theta_1\theta_1}-\frac{2\alpha}{\tau^2}\phi_{\theta_1\theta_2}+\frac{1}{4\pi^2}(\frac{1}{r^2}+\frac{4\pi^2\alpha^2}{\tau^2})\phi_{\theta_2\theta_2}-\beta^2\phi$$
$$+i\frac{2\beta}{\tau}(\phi_{\theta_1}-\alpha\phi_{\theta_2})\Big)+V\phi=\lambda\phi,\quad (r,\theta_1,\theta_2)\in(0,R)\times(0,1)\times[0,1) \tag{5.18}$$

With the boundary conditions: $\phi(R,\theta_1,\theta_2)=0,\quad (\theta_1,\theta_2)\in[0,1]^2$ (5.19)

$$\phi(r,0,\theta_2)=\phi(r,1,\theta_2),\quad (r,\theta_2)\in(0,R)\times[0,1] \tag{5.20}$$

$$\phi(r,\theta_1,0)=\phi(r,\theta_1,1),\quad (r,\theta_1)\in(0,R)\times[0,1] \tag{5.21}$$

We have deliberately omitted the $r = 0$ line of points in the above set of equations because these points are actually problematic in the helical coordinate system and we need some extra care in handling them: The solution to (3.59) is regular at $r = 0$, but (5.18) clearly has a singularity at $r = 0$. This singularity of course, is an artifact of this coordinate system and is related to the non-invertibility of (3.55) along the axis. Thus, our formulation of a numerical method should have a way of handling the pole singularity built into it. The new boundary conditions to be enforced are zero Dirichlet in r and periodic in θ_1 and θ_2 and these can be implemented more readily. We now move onto specific solution approaches.

5.3.1 Finding a good basis set

We recall that in a standard plane-wave approach, the functions $\{e^{i2\pi\mathbf{k}.\mathbf{x}} : \mathbf{k} \in \mathbb{Z}^3\}$ serve as the basis functions. The underlying reason is that these functions are eigenfunctions of the Laplace operator with periodic boundary conditions. In a similar vein, we have the following result:

Theorem 5.3.1. *The eigenfunctions of the Laplace operator form an orthonormal basis for functions in $\mathsf{L}^2(\mathcal{D})$ with objective boundary conditions.*

Proof. Appropriately posed, the Laplace operator with the boundary conditions in 3.2.2 is self adjoint and has a compact resolvent and therefore it's eigenfunctions form an orthonormal basis. ■

Thus, we only need to figure out the eigenfunctions of the Laplace operator with helical objective boundary conditions to obtain a good basis set. Let $\{\lambda_k; f_k\}_{k\in\mathbb{N}}$ denote the eigenpairs of the Laplace operator with these boundary conditions on $\mathcal{D}$. Thus for each $k \in \mathbb{N}$ we have that $-\Delta f_k = \lambda_k f_k$ in $\mathcal{D}$ and the boundary conditions $f_k(\mathbf{x}) = 0, \mathbf{x} \in \partial\mathcal{D} \cap \partial\mathcal{C}$; $\quad f_k(\mathbf{R}_{2\pi\alpha}\mathbf{x} + \tau\mathbf{e}_3) = f_k(\mathbf{x}), \mathbf{x} \in \partial\mathcal{D}\backslash\partial\mathcal{C}$. In line with the discussion in the previous section, using (3.55) we introduce the helical coordinates $f_k(\mathbf{x}) = \hat{f}_k(r, \theta_1, \theta_2)$ in $\mathcal{D}\backslash\{\lambda\mathbf{e}_3 : \lambda \in (0, \tau)\}$. To guess the form of $\hat{f}_k$, we first introduce the separation of variables $\hat{f}_k(r, \theta_1, \theta_2) = \gamma_k(r)\eta_k(\theta_1)\zeta_k(\theta_2)$. The boundary conditions now become:

$$\gamma_k(R) = 0,\ \eta_k(0) = \eta_k(1),\ \zeta_k(0) = \zeta_k(1). \tag{5.22}$$

The periodic boundary conditions in η_k and ζ_k and the fact that $f_k \in \mathsf{L}^2(\mathcal{D})$ suggest that we

expand these functions as Fourier series and we write:

$$\eta_k(\theta_1) = \sum_{m\in\mathbb{Z}} a_m^k e^{i2\pi m\theta_1},\ \zeta_k(\theta_2) = \sum_{n\in\mathbb{Z}} b_n^k e^{i2\pi n\theta_2}. \tag{5.23}$$

We still need to determine the function $\gamma_k(r)$. We therefore consider the ansatz:

$$\hat{f}(r,\theta_1,\theta_2) = \gamma(r)e^{i2\pi(m\theta_1+n\theta_2)}; m,n\in\mathbb{Z}, \tag{5.24}$$

and we try to determine the conditions under which this function becomes an eigenfunction of the Laplace operator with objective boundary conditions. The condition $\gamma(R) = 0$ is enough to ensure the objective boundary conditions hold. We still need to ensure that γ is finite at the origin however. Next, we compute the Laplace operator in the (r,θ_1,θ_2) coordinate system. From Appendix B we have:

$$\Delta\hat{f} = \hat{f}_{rr} + \frac{1}{r}\hat{f}_r + \frac{1}{\tau^2}\hat{f}_{\theta_1\theta_1} - \frac{2\alpha}{\tau^2}\hat{f}_{\theta_1\theta_2} + \frac{1}{4\pi^2}(\frac{1}{r^2} + \frac{4\pi^2\alpha^2}{\tau^2})\hat{f}_{\theta_2\theta_2} \quad .$$

So the eigenvalue problem for the Laplace operator reduces to the following parametrized ODE in $\gamma(r)$ for $r\in(0,R)$:

$$\gamma_{rr} + \frac{1}{r}\gamma_r - \Big(\frac{4\pi^2}{\tau^2}(m-\alpha n)^2 + \frac{n^2}{r^2}\Big)\gamma = -\lambda\gamma\ ;\ m,n\in\mathbb{Z} \tag{5.25}$$

Since this is a second order ODE, we need two boundary conditions and these are:

$$\gamma(R) = 0 \text{ and } \gamma(0) \text{ is finite.} \tag{5.26}$$

The ODE is not exactly in a standard form as yet. To get to a more recognizable, standard form, we multiply throughout by r^2 $(r\neq 0)$ and denote $\nu_{m,n} = |\frac{2\pi}{\tau}(m-\alpha n)|$ to get:

$$r^2\gamma_{rr} + r\gamma_r + ((\lambda-\nu_{m,n}^2)r^2 - n^2)\gamma = 0\ ;\ m,n\in\mathbb{Z}\ ;\ r\in(0,R). \tag{5.27}$$

For $\lambda - \nu_{m,n}^2 > 0$, we let $c = \sqrt{\lambda-\nu_{m,n}^2}$. We now, let $y = cr, \gamma(r) = \tilde{\gamma}(y)$ so that we get $\gamma_r = c\tilde{\gamma}_y, \gamma_{rr} = c^2\tilde{\gamma}_{yy}$ and so (5.27) and (5.26) become:

$$y^2\tilde{\gamma}_{yy} + y\tilde{\gamma}_y + (y^2-n^2)\tilde{\gamma} = 0\ ;\ y\in(0,cR). \tag{5.28}$$

$$\tilde{\gamma}(cR) = 0 \text{ and } \tilde{\gamma}(0) \text{ is finite.} \tag{5.29}$$

Equation (5.28) is simply Bessel's differential equation. Since the order of the Bessel

equation is an integer, the general solution is given by:

$$\tilde{\gamma}(y) = c_1 J_n(y) + c_2 Y_n(y), \tag{5.30}$$

where, J_n is the Bessel Function of the first kind (often simply called Bessel Function in literature) of order n and Y_n is the Bessel Function of the second kind (also called Neumann function in literature) of order n. The condition of finiteness of $\tilde{\gamma}(y)$ at the origin implies $c_2 = 0$ since the Neumann functions Y_n have a singularity at 0 while the Bessel functions J_n are regular at 0. The constant c_1 can be fixed later using a normalization condition. The first boundary condition at $y = cR$ can be used to evaluate the eigenvalue λ that was absorbed into the constant c. To do so, let b_k^n denote the k^{th} zero of the Bessel function of order n, that is, $J_n(b_k^n) = 0$ and $0 < b_k^n < b_{k+1}^n$ for each $k \in \mathbb{N}$. These values have been well studied in literature and are quite easily obtainable. The boundary conditions (5.29) imply $cR = R\sqrt{\lambda - \nu_{m,n}^2} = b_k^n$ and so, we get:

$$\lambda = \big(\frac{b_k^n}{R}\big)^2 + \nu_{m,n}^2 \quad . \tag{5.31}$$

The above calculations suggest that one should really parametrize the eigenvalue eigenfunction pairs of the Laplacian by the numbers $k \in \mathbb{N}; m, n \in \mathbb{Z}$ as:

$$\left\{ (\lambda_{m,n,k}, \hat{f}_{m,n,k}) : \lambda_{m,n,k} = \big(\frac{b_k^n}{R}\big)^2 + \nu_{m,n}^2, \right. \\ \left. \hat{f}_{m,n,k}(r, \theta_1, \theta_2) = c_{m,n,k}\ J_n(\frac{b_k^n}{R} r) e^{i2\pi(m\theta_1 + n\theta_2)} \right\} \tag{5.32}$$

with each $c_{m,n,k}$ a normalization constant and the parameter $\nu_{m,n} = |\frac{2\pi}{\tau}(m - \alpha n)|$. Thus, we have obtained a set of eigenpairs of the Laplace operator on $\mathcal{D}$ with objective boundary conditions. For $k \in \mathbb{N}$ and $m, n \in \mathbb{Z}$, we now let

$$\mathcal{E} = \left\{ f_{m,n,k}(\mathbf{x}) \ : \ \hat{f}_{m,n,k}(r, \theta_1, \theta_2) = c_{m,n,k}\ J_n(\frac{b_k^n}{R} r) e^{i2\pi(m\theta_1 + n\theta_2)} \right\} \tag{5.33}$$

and we let $\mathcal{E}$ be our proposed basis set.

We may directly check for the orthonormality of the basis functions in $\mathcal{E}$. Indeed, from the calculations in Appendix B we first note that the Jacobian of the coordinate transformation $(x_1, x_2, x_3) \mapsto (r, \theta_1, \theta_2)$ as given by (3.55) is

$$\mathcal{J}(r, \theta_1, \theta_2) = |\frac{\partial(x_1, x_2, x_3)}{\partial(r, \theta_1, \theta_2)}| = 2\pi r\tau \quad . \tag{5.34}$$

Hence, we have the integral identity:

$$\begin{aligned}&\int_{(x_1,x_2,x_3)\in\mathcal{D}} f(x_1,x_2,x_3)dx_1dx_2dx_3\\&=\int_{r=0}^{r=R}\int_{\theta_1=0}^{\theta_1=1}\int_{\theta_2=0}^{\theta_2=1}\hat{f}(r,\theta_1,\theta_2)2\pi r\tau d\theta_2 d\theta_1 dr \quad .\end{aligned} \tag{5.35}$$

where, $\hat{f}(r,\theta_1,\theta_2) = f(x_1(r,\theta_1,\theta_2), x_2(r,\theta_1,\theta_2), x_3(r,\theta_1,\theta_2))$. Next, we compute the inner product: Let $(m,n,k),(m',n',k,) \in \mathbb{Z}\times\mathbb{Z}\times\mathbb{N}$. We have that:

$$\begin{aligned}&\langle f_{m,n,k}, f_{m',n',k'}\rangle_{\mathsf{L}^2(\mathcal{D})}\\&=\int_{\mathbf{x}\in\mathcal{D}} f_{m,n,k}(\mathbf{x})\overline{f_{m',n',k'}(\mathbf{x})}\,d\mathbf{x}\\&=\int_{(x_1,x_2,x_3)\in\mathcal{D}} f_{m,n,k}(x_1,x_2,x_3)\overline{f_{m',n',k'}(x_1,x_2,x_3)}\,dx_1dx_2dx_3\\&=2\pi\tau\int_{r=0}^{r=R}\int_{\theta_1=0}^{\theta_1=1}\int_{\theta_2=0}^{\theta_2=1}\hat{f}_{m',n',k'}(r,\theta_1,\theta_2)\,\overline{\hat{f}_{m',n',k'}(r,\theta_1,\theta_2)}\,r d\theta_2 d\theta_1 dr\\&=c\int_0^R rJ_n(\frac{b_k^n}{R}r)J_{n'}(\frac{b_{k'}^{n'}}{R}r)\,dr\int_0^1 e^{i2\pi m\theta_1}e^{-i2\pi m'\theta_1}d\theta_1\int_0^1 e^{i2\pi n\theta_2}e^{-i2\pi n'\theta_2}d\theta_2,\end{aligned} \tag{5.36}$$

where, $c = 2\pi\tau c_{m,n,k}\overline{c_{m',n',k'}}$. Now, we recall the usual orthogonality relations for Fourier basis functions:

$$\int_0^1 e^{i2\pi m\theta_1}e^{-i2\pi m'\theta_1}d\theta_1 = \delta_{m,m'}\ ,\ \int_0^1 e^{i2\pi n\theta_2}e^{-i2\pi n'\theta_2}d\theta_2 = \delta_{n,n'}, \tag{5.37}$$

to conclude that the inner product vanishes if either $m \neq m'$ or $n \neq n'$ (the radial integral is just a finite number in these cases). In case, $m = m', n = n'$, the integral in the radial direction needs to be evaluated:

$$\begin{aligned}&\int_0^R rJ_n(\frac{b_k^n}{R}r)J_n(\frac{b_{k'}^n}{R}r)\,dr = R^2\int_0^R \frac{r}{R}J_n(b_k^n\frac{r}{R})J_n(b_{k'}^n\frac{r}{R})\,d(r/R)\\&=R^2\int_0^1 \bar{r}J_n(b_k^n\bar{r})J_n(b_{k'}^n\bar{r})\,d\bar{r} = \frac{R^2J_{n+1}^2(b_k^n)}{2}\delta_{k,k'} \quad .\end{aligned} \tag{5.38}$$

where we have used the orthogonality property of Bessel functions that follows from standard Sturm-Liouville theory. Hence, once again the inner product reduces to 0 unless $k = k'$. The above calculation also gives us a way of normalizing the basis set, since we

get from (5.42), (5.37) and (5.38) that:

$$\|f_{m,n,k}\|^2_{\mathsf{L}^2(\mathcal{D})} = 2\pi\tau|c_{m,n,k}|^2\frac{R^2J^2_{n+1}(b^n_k)}{2}, \tag{5.39}$$

and so, we may take $c_{m,n,k} = \frac{RJ_{n+1}(b^n_k)}{\sqrt{\pi\tau}}$ for the purpose of normalization.

5.3.2 Expansion in basis set and discretization

Let $\phi \in \mathsf{L}^2(\mathcal{D})|_{Obj}$, that is, square integrable functions on the domain $\mathcal{D}$ with objective boundary conditions. For the purpose of a numerical approximation, we fix $\mathcal{M}, \mathcal{N}, \mathcal{K} \in \mathbb{N}$ and we let $\Gamma = \{-\mathcal{M}, \ldots, \mathcal{M}\} \times \{-\mathcal{N}, \ldots, \mathcal{N}\} \times \{1, \ldots, \mathcal{K}\}$. We may then expand:

$$\phi(\mathbf{x}) = \sum_{(m,n,k)\in\Gamma} a_{m,n,k}\ f_{m,n,k}(\mathbf{x}) \tag{5.40}$$

To determine the coefficients, we will use the orthonormaility of the basis functions. To do this, we consider the inner product of ϕ with $f_{m',n',k'}$ in (5.40) and we obtain by orthonormality:

$$a_{m',n',k'} = \langle\phi, f_{m',n',k'}\rangle_{\mathsf{L}^2(\mathcal{D})}. \tag{5.41}$$

Since the inner product of ϕ and $f_{m',n',k'}$ can be evaluated in helical coordinates by the expression:

$$\langle\phi, f_{m',n',k'}\rangle_{\mathsf{L}^2(\mathcal{D})} = 2\pi\tau\int_{r=0}^{r=R}\int_{\theta_1=0}^{\theta_1=1}\int_{\theta_2=0}^{\theta_2=1}\phi(r,\theta_1,\theta_2)\ \overline{\hat{f}_{m',n',k'}(r,\theta_1,\theta_2)}\ r d\theta_2 d\theta_1 dr \quad , \tag{5.42}$$

we get, by substituting the expression for $\hat{f}_{m',n',k'}(r,\theta_1,\theta_2)$:

$$\begin{aligned} a_{m',n',k'} =& 2RJ_{n'+1}(b^{n'}_k)\sqrt{\pi\tau} \\ &\times\int_{r=0}^{r=R}\int_{\theta_1=0}^{\theta_1=1}\int_{\theta_2=0}^{\theta_2=1}\phi(r,\theta_1,\theta_2)J_{n'}(\frac{b^{n'}_k}{R}r)e^{-i2\pi(m'\theta_1+n'\theta_2)}r\ d\theta_2 d\theta_1 dr, \end{aligned} \tag{5.43}$$

Now, to obtain a discretization of (5.18), we substitute (5.40) expressed in helical coordinates into (5.18). Since the boundary conditions are automatically satisfied by the form of the basis set, we only need to worry about the governing equation. Using the fact that we designed the basis functions to be eigenfunctions of the Laplace operator in helical

coordinates, we get:

$$
\begin{aligned}
&-\frac{1}{2}\Big(\sum_{\Gamma} a_{m,n,k}\ (-\lambda_{m,n,k}\ \hat{f}_{m,n,k}(r,\theta_1,\theta_2)) - \beta^2 \sum_{\Gamma} a_{m,n,k}\ \hat{f}_{m,n,k}(r,\theta_1,\theta_2) \\
&-\frac{4\pi\beta}{\tau}\sum_{\Gamma} a_{m,n,k}\ (m-\alpha n)\ \hat{f}_{m,n,k}(r,\theta_1,\theta_2)\Big) + \hat{V}(r,\theta_1,\theta_2)\sum_{\Gamma} a_{m,n,k}\ \hat{f}_{m,n,k}(r,\theta_1,\theta_2) \\
&= \lambda \sum_{\Gamma} a_{m,n,k}\ \hat{f}_{m,n,k}(r,\theta_1,\theta_2) \quad . \qquad (5.44)
\end{aligned}
$$

Now we consider the inner product of the above equation with $\hat{f}_{m',n',k'}(r,\theta_1,\theta_2)$, and with $(m',n',k') \in \Gamma$ and we use orthonormality to get:

$$
\frac{1}{2}\big(a_{m',n',k'}\lambda_{m',n',k'} + \beta^2 a_{m',n',k'} + \frac{4\pi\beta}{\tau} a_{m',n',k'}(m' - \alpha n')\big) + \tilde{V}_{m',n',k'} = \lambda\ a_{m',n',k'}, \qquad (5.45)
$$

where, $\tilde{V}_{m',n',k'} = \langle V \sum_{\Gamma} a_{m,n,k} f_{m,n,k},\, f_{m',n',k'} \rangle_{\mathsf{L}^2(\mathcal{D})}$, which using (5.42) yields the following expression:

$$
\begin{aligned}
&\tilde{V}_{m',n',k'} \\
&= 2\pi\tau \int_0^R \int_0^1 \int_0^1 \hat{V}(r,\theta_1,\theta_2) \sum_{\Gamma} a_{m,n,k}\ \hat{f}_{m,n,k}(r,\theta_1,\theta_2) \overline{\hat{f}_{m',n',k'}(r,\theta_1,\theta_2)}\ r d\theta_2 d\theta_1 dr
\end{aligned} \qquad (5.46)
$$

The above expression for $\tilde{V}_{m',n',k'}$ needs to be simplified. First we observe that since V is group invariant and $V \in \mathsf{L}^2(\mathcal{D})$, we may expand it as:

$$
\begin{aligned}
V(\mathbf{x}) &= \sum_{\Gamma} b_{m*,n*,k*}\ f_{m*,n*,k*}(\mathbf{x}), \\
\text{that is, } \ V(r,\theta_1,\theta_2) &= \sum_{\Gamma} b_{m*,n*,k*}\ \hat{f}_{m*,n*,k*}(r,\theta_1,\theta_2), \qquad (5.47)
\end{aligned}
$$

with $b_{m*,n*,k*}$ to be determined by performing the quadratures in (5.43) with $\hat{\varphi}(r,\theta_1,\theta_2)$ set equal to $\hat{V}(r,\theta_1,\theta_2)$. Substitution of (5.47) into (5.46) gives us:

$$
\tilde{V}_{m',n',k'} = 2\pi\tau\ \Big(\sum_{(m,n,k)\in\Gamma} a_{m,n,k} \sum_{(m*,n*,k*)\in\Gamma} b_{m*,n*,k*}\ I_{m,n,k}^{m*,n*,k*}\Big) \qquad (5.48)
$$

where, $I^{m*,n*,k*}_{m,n,k}$

$$
\begin{aligned}
&= \int_{r=0}^{r=R} \int_{\theta_1=0}^{\theta_1=1} \int_{\theta_2=0}^{\theta_2=1} \hat{f}_{m,n,k}(r,\theta_1,\theta_2)\hat{f}_{m*,n*,k*}(r,\theta_1,\theta_2)\overline{\hat{f}_{m',n',k'}(r,\theta_1,\theta_2)}\; r d\theta_2 d\theta_1 dr \\
&= \kappa \int_0^R r J_n(b_k^n \frac{r}{R}) J_{n*}(b_{k*}^{n*}\frac{r}{R}) J_{n'}(b_{k'}^{n'}\frac{r}{R})\; dr \\
&\times \int_0^1 e^{i2\pi(m+m*-m')\theta_1}\; d\theta_1 \int_0^1 e^{i2\pi(n+n*-n')\theta_2}\; d\theta_2
\end{aligned} \tag{5.49}
$$

and,

$$
\kappa = c_{m,n,k}\; c_{m*,n*,k*}\; \overline{c_{m',n',k'}} = \Big(\frac{R}{\sqrt{\pi\tau}}\Big)^3 J_{n+1}(b_k^n) J_{n*+1}(b_{k*}^{n*}) J_{n'+1}(b_{k'}^{n'}) \tag{5.50}
$$

The last two integrals in θ_1 and θ_2 and a scaling change of variables in the first integral in r imply that:

$$
I^{m*,n*,k*}_{m,n,k} = \kappa R^2 \int_0^1 \bar{r} J_n(b_k^n \bar{r}) J_{n*}(b_{k*}^{n*}\bar{r}) J_{n'}(b_{k'}^{n'}\bar{r})\; d\bar{r} \quad , \tag{5.51}
$$

if $m + m* = m'$ and $n + n* = n'$ and $I^{m*,n*,k*}_{m,n,k} = 0$ otherwise. This allows us to re-write (5.48) as:

$$
\tilde{V}_{m',n',k'} = \sum_{(m,n,k)\in\Gamma} \Big(2\pi\tau \sum_{k*=1}^{k*=\mathcal{K}} b_{(m'-m),(n'-n),k*}\; I^{(m'-m),(n'-n),k*}_{m,n,k}\Big) a_{m,n,k} \tag{5.52}
$$

Thus, (5.45) now simply becomes a finite dimensional linear eigenvalue problem:

$$
\begin{aligned}
&\frac{1}{2}\big(\lambda_{m',n',k'} + \beta^2 + \frac{4\pi\beta}{\tau}(m' - \alpha n')\big) a_{m',n',k'} \\
&+ \sum_{(m,n,k)\in\Gamma} \Big(2\pi\tau \sum_{k*=1}^{k*=\mathcal{K}} b_{(m'-m),(n'-n),k*}\; I^{(m'-m),(n'-n),k*}_{m,n,k}\Big) a_{m,n,k} = \lambda\; a_{m',n',k'},
\end{aligned} \tag{5.53}
$$

keeping in mind that the summation appearing in (5.53) above should be such that the indices $((m'-m),(n'-n),k*) \in \Gamma$ since $b_{(m'-m),(n'-n),k*}$ is only defined for these indices. Note that since the dimension of this system is $(2\mathcal{M}+1)(2\mathcal{N}+1)\mathcal{K}$, and in a Density Functional Theory calculation therefore, this number should far exceed the number of electrons per unit cell.

5.3.3 Implementation details

We are currently in the process of implementing the spectral discretization scheme suggested above into a reliable and efficient computer code. Many of the computational strategies introduced in Chapter 4 can be directly adopted for this purpose.

The set $\mathcal{B}$ is discretized using Gauss quadrature nodes. The radial basis functions are discretized using Gauss-Jacobi quadrature weights and nodes while the integrals in θ_1 and θ_2 are carried out using Fast Fourier Transforms. As in Chapter 4 and Section 5.2.1, the form of the discretized eigenvalue problem in (eq. 5.53) immediately suggests that matrix vector products for use in diagonalization schemes can be carried out by splitting the computation partly in real space and partly in reciprocal space. The two-level parallelism described in Chapter 4 can be extended to form a highly scalable 3 level parallelism – the additional level of parallelism comes from the independent calculations at each point $\beta \in \mathcal{B}$. On the first SCF step, the LOBPCG routine is used, for each $\beta \in \mathcal{B}$ to compute the lowest few eigenstates commensurate with the number of electrons in the fundamental domain. In subsequent SCF steps, the Chebyshev filtering algorithm is employed independently for each $\beta \in \mathcal{B}$. The computation of the electronic density (carried out by first transforming the orbitals to real space) involves computing a sum over the electronic states (or bands) as well as over the points $\beta \in \mathcal{B}$. The computation of the Hartree potential requires special care due to the infinite extent of the system [Defranceschi and Le Bris, 1997]. We have been looking into the use of a modification of the Ewald summation technique (usually used for periodic structures) for helical groups for this purpose. Among numerous possibilities, (such as transforming a one-dimensional periodic Ewald summation to a helical one by use of the helical coordinates), the approach recently developed in Nikiforov et al. [2013] seems particularly promising.

Chapter 6

Conclusions and Future Directions

6.1 Summary

In this work, we have taken important steps toward formulating and implementing density functional theory methods for studying objective structures. We have achieved a good theoretical understanding of the role that symmetry plays in the electronic structure computation problem for objective structures. We have also formulated powerful numerical schemes for the solution of the electronic structure problem associated with certain objective structures.

In Chapter 3 we formulated rigorously, the cell problem that arises in the electronic structure computation of objective structures generated by finite and helical groups. Our basic tool for this was the harmonic analysis of the isometry groups that generate these objective structures (We deveopled these tools earlier in Chapter 2). One of the important outcomes of this enterprise was the recognition of symmetry related degeneracies in the eigenstates of the Kohn-Sham Hamiltonian in terms of the dimension of the irreducible reprsentations of the symmetry group involved. Yet another outcome was Theorem 3.1.11, which provides sufficient conditions under which symmetry adapted cell problem reductions can be carried out at each self consistent field iteration step. While the basic content of the theorem might have been known in the literature within the context of atoms, to our knowledge, this is the first and only general demonstration of this result for molecular systems with symmetry. Finally, a third outcome was the demonstration of the equivalence of the symmetry cell problems and a block diagonalization of the Hamiltonian in terms of group invariant subspaces. This result has important bearings on some of the symmetry adapted numerical schemes that we formulate later in the thesis.

In Chapter 4, we recognized the importance of developing a general spectral scheme that can be used to study various cluster systems and at the same time, exploit their underlying symmetries. We arrived at a suitable spectral basis set and formulated numerical solution schemes for solution of the discretized equations. We investigated and implemented various algorithmic strategies and methods that allow for efficient solution of the discretized solutions. We also investigated the parallelization issues of our numerical method. The resulting product of the methods developed in Chapter 4 is an efficient and reliable computer package that allows the study of electronic properties of clusters with high accuracy and systematic convergence properties without the use of the plane-wave basis set or artificial super cells. As a demonstration of the capabilities of our method, we computed ground state properties of a wide variety of cluster systems and compared our results with the literature. Benchmark calculations showed that our method is highly competitive in performance: it well outperformed other codes based on finite elements and plane-waves.

In Chapter 5, we formulated symmetry adapted spectral schemes. We discussed how traditional symmetry adaptation methods require modification in the context of the methods we developed in Chapter 4. We then formulated alternate methods for carrying out symmetry adaptation based on subspace iterations. A particular example application of these methods is the symmetry adaptation technique that we developed for the case of cyclic groups. We formulated and implemented this method in the framework of the software package developed in Chapter 4 and we were able to obtain savings that are linear in the order of the cyclic group employed. We then used this method to carry out ground state energies of large silicon nano dot clusters. Without the use of our spectral scheme and the symmetry adaptation techniques, highly accurate and systematic computations on such large cluster systems is unlikely to have been possible. We also formulated a spectral scheme for the case of helical structures. The implementation of this scheme is the focus of ongoing and future work.

6.2 Applications

We end with a short discussion of some of the applications of the various methods developed in this thesis.

One important application is the abinitio discovery of novel materials and structures by use of the objective structures framework. Using the first principles methods for objective structures generated by finite groups (described in Chapter 5) for instance, we could perform a systematic search for new materials among various cluster systems by involving

different elements across the periodic table. Symmetry adapted branch following and bifurcation algorithms are likely to be useful for the discovery of stable structures for these purposes.

Another potential application is in the field of nano-mechanics. The methods developed here allow for the simulation of the bending and twisting of nano-structures by using cyclic and helical groups respectively. A bent nano beam for instance, is well approximated by a cyclic objective structure and therefore, structural relaxation of the atoms in the fundamental domain of such a system (with energies and forces coming from the abinitio methods described in this thesis) would allow us to compute the energy curvature relationship for such a nanobeam system. This is shown schematically in Figure 6.1. Having access to computations which can predict, from first principles, bending behavior in nano systems, opens up the door to the reliable investigation of several important material phenomena such as flexoelectricity.

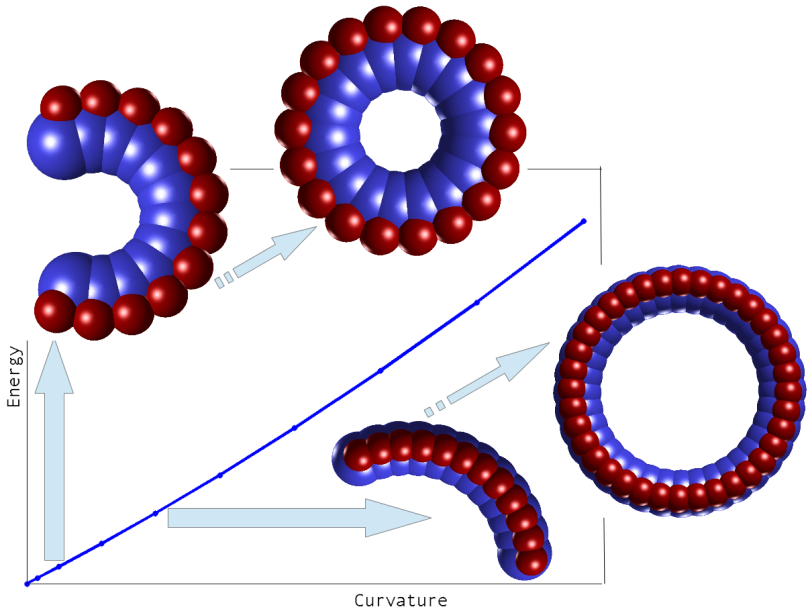

Figure 6.1: Schematic of the abinitio simulation of nano beam bending by using Objective DFT for cyclic groups: Each bent configuration is approximated by a cyclic objective structure whose energy and structural relaxation may be computed using the methods developed in this thesis.

Bibliography

K. Ahlander and H. Munthe-Kaas. Applications of the generalized Fourier transform in numerical linear algebra. *BIT Numerical Mathematics*, 45(4):819–850, 2005.

K. Ahlander and H. Munthe-Kaas. Eigenvalues for equivariant matrices. *Journal of Computational and Applied Mathematics*, 192(1):89–99, 2006. Special Issue on Computational and Mathematical Methods in Science and Engineering (CMMSE-2004).

R. Ahlrichs, M. Hoffmann-Ostenhof, T. Hoffmann-Ostenhof, and J. D. Morgan. Bounds on the decay of electron densities with screening. *Physical Review A*, 23(5):2106–2117, 1981.

R. Ahlrichs, M. Br, M. Hser, H. Horn, and C. Klmel. Electronic structure calculations on workstation computers: The program system turbomole. *Chemical Physics Letters*, 162 (3):165 – 169, 1989.

F. Alasia, R. A. Broglia, H. E. Roman, L. Serra, G. Colo, and J. M. Pacheco. Single-particle and collective degrees of freedom in C_{60}. *Journal of Physics B: Atomic, Molecular and Optical Physics*, 27(18):L643, 1994.

M. Allen and D. Tildesley. *Computer Simulation of Liquids*. Oxford University Press, 1987.

E. L. Allgower and K. Georg. Exploiting symmetry in numerical solving. In *Proceedings of the Seventh Workshop on Differential Equations and its Applications*, 1999. Preprint obtained from http://www.math.colostate.edu/∼georg/Preprints/taiwan.ps.Z.

E. L. Allgower, K. Georg, R. Miranda, and J. Tausch. Numerical exploitation of equivariance. *Zeitschrift für Angewandte Mathematik und Mechanik*, 78(12):795–806, 1998.

P. Alpatov, G. Baker, C. Edwards, J. Gunnels, G. Morrow, J. Overfelt, R. van de Geijn, and Y.-J. J. Wu. Plapack: parallel linear algebra package design overview. In *Proceedings*

of the 1997 ACM/IEEE conference on Supercomputing (CDROM), pages 1–16. ACM, 1997.

D. G. Anderson. Iterative procedures for nonlinear integral equations. *Journal of the ACM (JACM)*, 12(4):547–560, 1965.

M. I. Aroyo, A. Kirov, C. Capillas, J. M. Perez-Mato, and H. Wondratschek. Bilbao Crystallographic Server. II. Representations of crystallographic point groups and space groups. *Acta Crystallographica Section A*, 62(2):115–128, 2006.

N. W. Ashcroft and N. D. Mermin. *Solid State Physics*. Brooks Cole, first edition, 1976.

A. S. Banerjee. Harmonic analysis on isometry groups of objective structures and its applications to objective density functional theory. Master's thesis, University of Minnesota, Minneapolis, 2011.

A. S. Banerjee, R. S. Elliott, and R. D. James. Abinitio simulation of the bending of nano structures via objective density functional theory. (In preparation), 2014a.

A. S. Banerjee, R. S. Elliott, and R. D. James. A spectral scheme for kohn-sham density functional theory of clusters. (To be submitted), 2014b.

S. Baroni and P. Giannozzi. Towards very large-scale electronic-structure calculations. *EPL (Europhysics Letters)*, 17(6):547, 1992.

A. O. Barut and R. Raczka. *Theory of Group Representations and Applications*. World Scientific Publishing Company, second revised edition, 1986.

C. Bekas, Y. Saad, M. L. Tiago, and J. R. Chelikowsky. Computing charge densities with partially reorthogonalized lanczos. *Computer Physics Communications*, 171(3):175–186, 2005.

F. A. Berezin and M. A. Shubin. *The Schrödinger Equation*. Mathematics and its Applications. Springer, 1991.

P. Bientinesi, I. S. Dhillon, and R. A. Van De Geijn. A parallel eigensolver for dense symmetric matrices based on multiple relatively robust representations. *SIAM Journal on Scientific Computing*, 27(1):43–66, 2005.

L. S. Blackford, J. Choi, A. Cleary, E. D'Azevedo, J. Demmel, I. Dhillon, J. Dongarra, S. Hammarling, G. Henry, A. Petitet, K. Stanley, D. Walker, and R. C. Whaley. *ScaLAPACK Users' Guide*. Society for Industrial and Applied Mathematics, Philadelphia, PA, 1997.

F. Bloch. Über die quantenmechanik der elektronen in kristallgittern. *Zeitschrift für Physik A Hadrons and Nuclei*, 52:555–600, 1929.

M. Bockstedte, A. Kley, J. Neugebauer, and M. Scheffler. Density-functional theory calculations for poly-atomic systems: electronic structure, static and elastic properties and ab initio molecular dynamics. *Computer Physics Communications*, 107(1-3):187 – 222, 1997.

A. Bossavit. Symmetry, groups, and boundary value problems. a progressive introduction to noncommutative harmonic analysis of partial differential equations in domains with geometrical symmetry. *Computer Methods in Applied Mechanics and Engineering*, 56 (2):167–215, 1986.

A. Bossavit. Boundary value problems with symmetry and their approximation by finite elements. *SIAM Journal on Applied Mathematics*, 53(5):1352–1380, 1993.

S. Botti, A. Castro, N. N. Lathiotakis, X. Andrade, and M. A. L. Marques. Optical and magnetic properties of boron fullerenes. *Phys. Chem. Chem. Phys.*, 11:4523–4527, 2009.

F. Bottin, S. Leroux, A. Knyazev, and G. Zérah. Large-scale ab initio calculations based on three levels of parallelization. *Computational Materials Science*, 42(2):329 – 336, 2008.

L. P. Bouckaert, R. Smoluchowski, and E. Wigner. Theory of brillouin zones and symmetry properties of wave functions in crystals. *Phys. Rev.*, 50:58–67, 1936.

M. Brack. The physics of simple metal clusters: self-consistent jellium model and semiclassical approaches. *Rev. Mod. Phys.*, 65:677–732, 1993.

R. P. Brent. *Algorithms for Minimization Without Derivatives*. Courier Dover Publications, 1973.

R. Broglia, G. Coló, G. Onida, and H. Roman. *Solid State Physiscs of Finite Systems: Metallic Clusters, Fullerenes, Atomic Wires*. Advanced Texts in Physics. Springer, first edition, 2004.

C. G. Broyden. A class of methods for solving nonlinear simultaneous equations. *Mathematics of computation*, 19(92):577–593, 1965.

D. Bylander, L. Kleinman, and S. Lee. Self-consistent calculations of the energy bands and bonding properties of $B_{12}C_3$. *Physical Review B*, 42(2):1394, 1990.

E. Bylaska, K. Tsemekhman, N. Govind, and M. Valiev. Large-Scale Plane-Wave-Based Density Functional Theory: Fomalism, Parallelization and Applications. In J. R. Reimers, editor, *Computational Methods for Large Systems: Electronic Structure Approaches for Biotechnology and Nanotechnology*, pages 77–116. John Wiley & Sons, Inc., 2011.

E. Cancès. private communication, 2013.

E. Cancès, R. Chakir, and Y. Maday. Numerical analysis of the planewave discretization of some orbital-free and kohn-sham models. *ESAIM: Mathematical Modelling and Numerical Analysis*, 46:341–388, 3 2012. ISSN 1290-3841.

A. W. Castleman. From elements to clusters: The periodic table revisited. *The Journal of Physical Chemistry Letters*, 2(9):1062–1069, 2011.

A. W. Castleman and S. N. Khanna. Clusters, superatoms, and building blocks of new materials. *The Journal of Physical Chemistry C*, 113(7):2664–2675, 2009.

A. Castro, H. Appel, M. Oliveira, C. Rozzi, X. Andrade, F. Lorenzen, M. Marques, E. Gross, and A. Rubio. Octopus: A tool for the application of time-dependent density functional theory. *Physica Status Solidi (B) Basic Research*, 243(11):2465–2488, 2006.

D. M. Ceperley and B. J. Alder. Ground state of the electron gas by a stochastic method. *Physical. Review Letters*, 45(7):566–569, 1980.

P. Chang and T. Healey. Computation of symmetry modes and exact reduction in nonlinear structural analysis. *Computers & structures*, 28(2):135–142, 1988.

J. R. Chelikowsky, N. Troullier, K. Wu, and Y. Saad. Higher order finite difference pseudopotential method: An application to diatomic molecules. *Phys. Rev. B*, 50:11355–11364, 1994.

H. Chen, X. Gong, L. He, Z. Yang, and A. Zhou. Numerical analysis of finite dimensional approximations of kohn–sham models. *Advances in Computational Mathematics*, pages 1–32, 2013.

J. Choi, J. J. Dongarra, R. Pozo, and D. W. Walker. Scalapack: A scalable linear algebra library for distributed memory concurrent computers. In *Frontiers of Massively Parallel Computation, 1992., Fourth Symposium on the*, pages 120–127. IEEE, 1992.

J. W. Cooley and J. W. Tukey. An algorithm for the machine calculation of complex fourier series. *Mathematics of Computation*, 19(90):297–301, 1965.

B. Dakić, M. Damnjanović, and I. Milosević. Generalized bloch states and potentials of nanotubes and other quasi-1d systems ii. *Journal of Physics A: Mathematical and Theoretical*, 42(12):125202, 2009.

J. W. Daniel, W. B. Gragg, L. Kaufman, and G. Stewart. Reorthogonalization and stable algorithms for updating the gram-schmidt QR factorization. *Mathematics of Computation*, 30(136):772–795, 1976.

K. Dayal and R. D. James. Nonequilibrium molecular dynamics for bulk materials and nanostructures. *Journal of the Mechanics and Physics of Solids*, 58(2):145 – 163, 2010.

K. Dayal and R. D. James. Design of viscometers corresponding to a universal molecular simulation method. *Journal of Fluid Mechanics*, (submitted), 2011.

K. Dayal, R. S. Elliott, and R. D. James. Objective formulas. (In preparation), 2013.

P. Dederichs and R. Zeller. Self-consistency iterations in electronic-structure calculations. *Physical Review B*, 28(10):5462, 1983.

M. Defranceschi and C. Le Bris. Computing a molecule: A mathematical viewpoint. *Journal of Mathematical Chemistry*, 21(1):1–30, 1997.

M. Defranceschi and C. Le Bris, editors. *Mathematical Models and Methods for Ab Initio Quantum Chemistry*, volume 74 of *Lecture Notes in Chemistry*. Springer, 2000.

I. S. Dhillon, B. N. Parlett, and C. Vömel. The design and implementation of the MRRR algorithm. *ACM Trans. Math. Softw.*, 32(4):533–560, 2006.

J. R. Driscoll and D. Healy. Computing fourier transforms and convolutions on the 2-sphere. *Advances in Applied Mathematics*, 15(2):202 – 250, 1994.

T. Dumitrica and R. D. James. Objective molecular dynamics. *Journal of the Mechanics and Physics of Solids*, 55(10):2206 – 2236, 2007.

J. Eastwood and D. Brownrigg. Remarks on the solution of poisson's equation for isolated systems. *Journal of Computational Physics*, 32(1):24 – 38, 1979.

A. R. Edmonds. *Angular Momentum in Quantum Mechanics*. Princeton University Press, fourth printing edition, 1996.

L. C. Evans. *Partial Differential Equations*, volume 19 of *Graduate Studies in Mathematics*. American Mathematical Society, 1998.

R. A. Evarestov and V. P. Smirnov. Special points of the brillouin zone and their use in the solid state theory. *Physica Status Solidi (b)*, 119(1):9–40, 1983.

R. Fahmi and M. Potier-Ferry. The group representation theory and vibrations of cyclic structures. In H. Amann, C. Bandle, M. Chipot, F. Conrad, and I. Shafrir, editors, *Progress in Partial Differential Equations: Pont-A-Mousson 1997*, volume 384, pages 88–97. 1998.

H.-r. Fang and Y. Saad. Two classes of multisecant methods for nonlinear acceleration. *Numerical Linear Algebra with Applications*, 16(3):197–221, 2009.

J. Fang, X. Gao, and A. Zhou. A kohn–sham equation solver based on hexahedral finite elements. *Journal of Computational Physics*, 231(8):3166–3180, 2012.

J. Fang, X. Gao, and A. Zhou. A symmetry-based decomposition approach to eigenvalue problems. *Journal of Scientific Computing*, pages 1–32, 2013.

C. Fiolhais, J. P. Perdew, S. Q. Armster, J. M. MacLaren, and M. Brajczewska. Dominant density parameters and local pseudopotentials for simple metals. *Physical Review B*, 51 (20):14001, 1995.

G. B. Folland. *A Course in Abstract Harmonic Analysis*. Studies in Advanced Mathematics. Taylor & Francis, first edition, 1994.

G. B. Folland. *Real Analysis: Modern Techniques and Their Applications*. Wiley, second edition, 1999.

M. Galassi, J. Davies, J. Theiler, B. Gough, G. Jungman, P. Alken, M. Booth, and F. Rossi. *GNU Scientific Library Reference Manual*. Network Theory Ltd., third edition, 2009.

J. D. Gale. Gulp: A computer program for the symmetry-adapted simulation of solids. *J. Chem. Soc., Faraday Trans.*, 93:629–637, 1997.

C. Garcia-Cervera, J. Lu, Y. Xuan, and E. Weinan. Linear-scaling subspace-iteration algorithm with optimally localized nonorthogonal wave functions for kohn-sham density functional theory. *Physical Review B*, 79(11):115110, 2009.

L. Genovese, A. Neelov, S. Goedecker, T. Deutsch, S. A. Ghasemi, A. Willand, D. Caliste, O. Zilberberg, M. Rayson, A. Bergman, et al. Daubechies wavelets as a basis set for density functional pseudopotential calculations. *The Journal of chemical physics*, 129: 014109, 2008.

K. Georg and J. Tausch. A generalized fourier transform for boundary element methods with symmetries. Technical report, Department of Mathematics, Colorado State University, Ft. Collins, Colorado 80523, USA, 1994.

P. Giannozzi, S. Baroni, N. Bonini, M. Calandra, R. Car, C. Cavazzoni, D. Ceresoli, G. L. Chiarotti, M. Cococcioni, I. Dabo, A. D. Corso, S. de Gironcoli, S. Fabris, G. Fratesi, R. Gebauer, U. Gerstmann, C. Gougoussis, A. Kokalj, M. Lazzeri, L. Martin-Samos, N. Marzari, F. Mauri, R. Mazzarello, S. Paolini, A. Pasquarello, L. Paulatto, C. Sbraccia, S. Scandolo, G. Sclauzero, A. P. Seitsonen, A. Smogunov, P. Umari, and R. M. Wentzcovitch. QUANTUM ESPRESSO: a modular and open-source software project for quantum simulations of materials. *Journal of Physics: Condensed Matter*, 21(39), 2009.

D. Gilbarg and N. S. Trudinger. *Elliptic Partial Differential Equations of Second Order*. Classics in Mathematics. Springer, 2001.

S. Goedecker, M. Teter, and J. Hutter. Separable dual-space gaussian pseudopotentials. *Physical Review B*, 54:1703–1710, 1996.

G. H. Golub and J. H. Welsch. Calculation of gauss quadrature rules. *Mathematics of Computation*, 23(106):221–230, 1969.

N. Gonzalez Szwacki, A. Sadrzadeh, and B. I. Yakobson. B_{80} fullerene: An *Ab Initio* prediction of geometry, stability, and electronic structure. *Phys. Rev. Lett.*, 98:166804, 2007.

X. Gonze, J.-M. Beuken, R. Caracas, F. Detraux, M. Fuchs, G.-M. Rignanese, L. Sindic, M. Verstraete, G. Zerah, F. Jollet, M. Torrent, A. Roy, M. Mikami, P. Ghosez, J.-Y. Raty, and D. Allan. First-principles computation of material properties: the ABINIT software project. *Computational Materials Science*, 25(3):478 – 492, 2002.

M. Gu. Single- and multiple-vector iterations. In Z. Bai, J. Demmelc, J. Dongarra, A. Ruhe, and H. van der Vorst, editors, *Templates for the Solution of Algebraic Eigenvalue Problems: A Practical Guide*. SIAM, Philadelphia, 2000.

V. Gurin. Small metal clusters: Ab initio calculated bare clusters and models within fullerene cages. In E. Buzaneva and P. Scharff, editors, *Frontiers of Multifunctional Integrated Nanosystems*, volume 152 of *NATO Science Series II: Mathematics, Physics and Chemistry*, pages 31–38. Springer Netherlands, 2005. ISBN 978-1-4020-2171-8.

M. E. Gurtin. *An Introduction to Continuum Mechanics*, volume 158 of *Mathematics in Science and Engineering*. Academic Press, 1981.

F. Gygi, E. W. Draeger, M. Schulz, B. R. de Supinski, J. A. Gunnels, V. Austel, J. C. Sexton, F. Franchetti, S. Kral, C. W. Ueberhuber, and J. Lorenz. Large-scale electronic structure calculations of high-z metals on the bluegene/l platform. In *Proceedings of the 2006 ACM/IEEE conference on Supercomputing*, SC '06, New York, NY, USA, 2006. ACM. ISBN 0-7695-2700-0.

T. Hahn. International tables for crystallography: volumes A,E. In V. Kopsky and D. B. Litvin, editors, *International Tables for Crystallography.* Kluwer Academic Publishers, 2003.

H. Hakkinen. Atomic and electronic structure of gold clusters: understanding flakes, cages and superatoms from simple concepts. *Chem. Soc. Rev.*, 37:1847–1859, 2008.

M. Hammermesh. *Group Theory and Its Application to Physical Problems*. Dover, first edition, 1989.

Q. Han and F. Lin. *Elliptic Partial Differential Equations*. Courant Lecture Notes. American Mathematical Society, 2000.

C. Hartwigsen, S. Goedecker, and J. Hutter. Relativistic separable dual-space gaussian pseudopotentials from h to rn. *Physical Review B*, 58:3641–3662, 1998.

T. J. Healey. A group-theoretic approach to computational bifurcation problems with symmetry. *Computer Methods in Applied Mechanics and Engineering*, 67(3):257–295, 1988.

T. J. Healey. Symmetry and equivariance in nonlinear elastostatics, Part I. *Archive for Rational Mechanics and Analysis*, 105(3):205–228, 1989.

T. J. Healey and H. Kielhöfer. Symmetry and nodal properties in the global bifurcation analysis of quasi-linear elliptic equations. *Archive for Rational Mechanics and Analysis*, 113(4):299–311, 1991.

T. J. Healey and J. A. Treacy. Exact block diagonalization of large eigenvalue problems for structures with symmetry. *International Journal for Numerical Methods in Engineering*, 31(2):265–285, 1991.

W. Hehre, R. Stewart, and J. Pople. Self-consistent molecular-orbital methods. i. use of gaussian expansions of slater-type atomic orbitals. *The Journal of Chemical Physics*, 51 (6):2657–2664, 1969.

G. Helmberg. *Introduction to Spectral Theory in Hilbert Space*. Dover Books on Mathematics. Dover Publications, 2008.

R. Hockney. Potential calculation and some applications. *Journal Name: Methods Comput. Phys. 9: 135-211(1970).*, 1970.

M. Hoffmann-Ostenhof, T. Hoffmann-Ostenhof, R. Ahlrichs, and J. Morgan. On the exponential fall off of wavefunctions and electron densities. In K. Osterwalder, editor, *Mathematical Problems in Theoretical Physics*, volume 116 of *Lecture Notes in Physics*, pages 62–67. Springer Berlin / Heidelberg, 1980.

P. C. Hohenberg and W. Kohn. Inhomogenous electron gas. *Physical Review*, 136(3B): 864–871, 1964.

C. Huang and E. A. Carter. Transferable local pseudopotentials for magnesium, aluminum and silicon. *Physical Chemistry Chemical Physics*, 10(47):7109–7120, 2008.

M. Iñiguez, M. Lopez, J. Alonso, and J. Soler. Electronic and atomic structure of Na, Mg, Al and Pb clusters. *Zeitschrift für Physik D Atoms, Molecules and Clusters*, 11(2): 163–174, 1988.

J. D. Jackson. *Classical Electrodynamics*. John Wiley & Sons, New York, 1975.

R. D. James. Objective structures. *Journal of the Mechanics and Physics of Solids*, 54(11): 2354–2390, 2006.

X. Jing, N. Troullier, D. Dean, N. Binggeli, J. R. Chelikowsky, K. Wu, and Y. Saad. Ab initio molecular-dynamics simulations of si clusters using the higher-order finite-difference-pseudopotential method. *Physical Review B*, 50(16):12234–12237, 1994.

X. Jing, N. Troullier, J. R. Chelikowsky, K. Wu, and Y. Saad. Vibrational modes of silicon nanostructures. *Solid State Communications*, 96(4):231 – 235, 1995.

D. Johnson. Modified broydens method for accelerating convergence in self-consistent calculations. *Physical Review B*, 38(18):12807, 1988.

T. Kato. On the eigenfunctions of many-particle systems in quantum mechanics. *Communications on Pure and Applied Mathematics*, 10(2):151–177, 1957.

T. Kato. *Perturbation Theory for Linear Operators*. Classics in Mathematics. Springer, 1995.

E. Kaxiras. *Atomic and Electronic Structure of Solids*. Cambridge University Press, first edition, 2003.

R. King-Smith, M. Payne, and J. Lin. Real-space implementation of nonlocal pseudopotentials for first-principles total-energy calculations. *Physical Review B*, 44(23):13063, 1991.

C. Kittel. *Introduction to Solid State Physics*. Wiley, eighth edition, 2004.

A. Knyazev. Toward the optimal preconditioned eigensolver: Locally optimal block preconditioned conjugate gradient method. *SIAM Journal on Scientific Computing*, 23(2): 517–541, 2001.

A. Knyazev. private communication, 2013.

A. V. Knyazev and K. Neymeyr. A geometric theory for preconditioned inverse iteration iii: A short and sharp convergence estimate for generalized eigenvalue problems. *Linear algebra and its applications*, 358(1):95–114, 2003.

A. V. Knyazev, M. E. Argentati, I. Lashuk, and E. Ovtchinnikov. Block locally optimal preconditioned eigenvalue xolvers (blopex) in hypre and petsc. *SIAM Journal on Scientific Computing*, 29(5):2224–2239, 2007.

J. Kohanoff. *Electronic Structure Calculations for Solids and Molecules: Theory and Computational Methods*. Cambridge University Press, 2006.

W. Kohn and L. J. Sham. Self-consistent equations including exchange and correlation effects. *Physical Review*, 140(4A):1133–1138, 1965.

S. Kotochigova, Z. H. Levine, E. L. Shirley, M. Stiles, and C. W. Clark. Local-density-functional calculations of the energy of atoms. *Physical Review A*, 55(1):191, 1997.

G. Kresse and J. Furthmuller. Efficient iterative schemes for ab initio total-energy calculations using a plane-wave basis set. *Physical Review B*, 54:11169–11186, 1996a.

G. Kresse and J. Furthmuller. Efficiency of ab-initio total energy calculations for metals and semiconductors using a plane-wave basis set. *Computational Materials Science*, 6 (1):15 – 50, 1996b.

L. Kronik, A. Makmal, M. L. Tiago, M. M. G. Alemany, M. Jain, X. Huang, Y. Saad, and J. R. Chelikowsky. Parsec the pseudopotential algorithm for real-space electronic structure calculations: recent advances and novel applications to nano-structures. *Physica Status Solidi (b)*, 243(5):1063–1079, 2006.

K. N. Kudin, G. E. Scuseria, and E. Cancès. A black-box self-consistent field convergence algorithm: One step closer. *The Journal of chemical physics*, 116:8255, 2002.

M. Lax. *Symmetry Principles in Solid State and Molecular Physics*. Dover Publications, 2001.

C. Le Bris, editor. *Computational Chemistry*, volume X of *Handbook of Numerical Analysis*. North-Holland, 2003.

C. Le Bris. Computational chemistry from the perspective of numerical analysis. *Acta Numerica*, 14:363–444, 2005.

E. H. Lieb. Density functionals for Coulomb systems. *International Journal of Quantum Chemistry*, XXIV:243–277, 1983.

E. H. Lieb and B. Simon. The hartree-fock theory for Coulomb systems. *Communications in Mathematical Physics*, 53:185–194, 1977a.

E. H. Lieb and B. Simon. The thomas-fermi theory of atoms, molecules and solids. *Advances in Mathematics*, 23(1):22 – 116, 1977b.

L. Lin, S. Shao, and W. E. Efficient iterative method for solving the dirac-kohn-sham density functional theory. *Journal of Computational Physics*, 245(15):205–217, 2013.

P. L. Lions. Solutions of hartree-fock equations for Coulomb systems. *Communications in Mathematical Physics*, 109:33–97, 1987.

F. Lorenzen. Massively-parallel eigensolver for the Octopus code. (Online article), 2006.

P.-O. Löwdin. Quantum theory of cohesive properties of solids. *Advances in Physics*, 5 (17):1–171, 1956.

R. M. Martin. *Electronic Structure: Basic Theory and Practical Methods*. Cambridge University Press, first edition, 2004.

G. J. Martyna and M. E. Tuckerman. A reciprocal space based method for treating long range interactions in ab initio and force-field-based calculations in clusters. *The Journal of Chemical Physics*, 110(6):2810–2821, 1999.

D. Marx and J. Hutter. *Ab initio molecular dynamics: basic theory and advanced methods*. Cambridge University Press, first edition, 2009.

G. Mattei and F. Toigo. Spherical averaged jellium model with norm-conserving pseudopotentials. *The European Physical Journal D − Atomic, Molecular, Optical and Plasma Physics*, 3(3):245–256, 1998.

R. McWeeny. *Symmetry:An Introduction to Group Theory and Its Applications*. Dover, first edition, 2002.

N. D. Mermin. Thermal properties of the inhomogeneous electron gas. *Physical Review*, 137:A1441–A1443, 1965.

A. Messiah. Appendix C - Clebsch-Gordan coefficients and 3j symbols. In *Quantum Mechanics, Volume 2*, pages 1054–1060. North-Holland, 1962.

S. C. Miller. *Tables of irreducible representations of space groups and co-representations of magnetic space groups*. Pruett Press, first edition, 1967.

W. Miller. *Symmetry Groups and Their Applications*, volume 50 of *Pure and Applied Mathematics Series*. Elsevier Science & Technology Books, 1972.

I. Milosević, B. Dakić, and M. Damnjanović. Generalized bloch states and potentials of nanotubes and other quasi-1d systems. *Journal of Physics A: Mathematical and General*, 39(38):11833, 2006.

M. Mohlenkamp. A fast transform for spherical harmonics. *Journal of Fourier Analysis and Applications*, 5(2-3):159–184, 1999.

P. Motamarri, M. Nowak, K. Leiter, J. Knap, and V. Gavini. Higher-order adaptive finite-element methods for kohnsham density functional theory. *Journal of Computational Physics*, 253(0):308 – 343, 2013.

A. W. Naylor and G. R. Sell. *Linear Operator Theory in Engineering and Science*, volume 40 of *Applied Mathematical Sciences*. Springer, 1971.

I. Nikiforov, B. Hourahine, B. Aradi, T. Frauenheim, and T. Dumitrică. Ewald summation on a helix: A route to self-consistent charge density-functional based tight-binding objective molecular dynamics. *The Journal of chemical physics*, 139(9):094110, 2013.

Y. Noel, P. D'arco, R. Demichelis, C. M. Zicovich-Wilson, and R. Dovesi. On the use of symmetry in the ab initio quantum mechanical simulation of nanotubes and related materials. *Journal of Computational Chemistry*, 31(4):855–862, 2010.

F. Nogueira, C. Fiolhais, J. He, J. P. Perdew, and A. Rubio. Transferability of a local pseudopotential based on solid-state electron density. *Journal of Physics: Condensed Matter*, 8(3):287, 1996.

F. Odeh and J. B. Keller. Partial differential equations with periodic coefficients and bloch waves in crystals. *Journal of Mathematical Physics*, 5:1499–1504, 1964.

W. Opechowski. *Crystallographic and metacrystallographic groups*. North Holland, 1986.

R. G. Parr and W. Yang. *Density-Functional Theory of Atoms and Molecules*, volume 16 of *International Series of Monographs on Chemistry*. Oxford University Press, USA, 1994.

M. Parrinello and A. Rahman. Crystal structure and pair potentials: A molecular-dynamics study. *Physical Review Letters*, 45(14):1196–1199, 1980.

J. E. Pask and P. A. Sterne. Finite element methods in ab initio electronic structure calculations. *Modelling and Simulation in Materials Science and Engineering*, 13(3), 2005.

M. C. Payne, M. P. Teter, D. C. Allan, T. A. Arias, and J. D. Joannopoulos. Iterative minimization techniques for *ab initio* total-energy calculations: molecular dynamics and conjugate gradients. *Rev. Mod. Phys.*, 64:1045–1097, 1992.

J. P. Perdew and A. Zunger. Self-interaction correction to density-functional approximations for many-electron systems. *Physical Review B*, 23(10):5048–5079, 1981.

J. P. Perdew, K. Burke, and M. Ernzerhof. Generalized gradient approximation made simple. *Phys. Rev. Lett.*, 77:3865–3868, Oct 1996.

W. E. Pickett. Pseudopotential methods in condensed matter applications. *Computer Physics Reports*, 9(3):115 – 197, 1989.

J. Poulson, B. Marker, R. A. .van de Geijn, J. R. Hammond, and N. A. Romero. Elemental: A new framework for distributed memory dense matrix computations. *ACM Trans. Math. Softw.*, 39(2):13:1–13:24, Feb. 2013.

E. Prodan. Symmetry breaking in the self consistent kohn-sham equations. *Journal of Physics A: Mathematical and General*, 38(25):5647–5657, 2005.

P. Pulay. Convergence acceleration of iterative sequences. the case of scf iteration. *Chemical Physics Letters*, 73(2):393–398, 1980.

S. Raskin. Spectral measures and the spectral theorem, 2006.

M. Reed and B. Simon. *Analysis of Operators*, volume IV of *Methods of Modern Mathematical Physics*. Academic Press, 1978.

M. Renardy and R. C. Rogers. *An Introduction to Partial Differential Equations*, volume 13 of *Texts in Applied Mathematics*. Springer, second edition, 2004.

C. C. J. Roothaan. Self-consistent field theory for open shells of electronic systems. *Reviews of Modern Physics*, 32:179–185, 1960.

Y. Saad. *Numerical Methods for Large Eigenvalue Problems*. SIAM, Revised edition, 2011.

N. Schaeffer. Efficient spherical harmonic transforms aimed at pseudospectral numerical simulations. *Geochemistry, Geophysics, Geosystems*, 14(3):751–758, 2013.

G. E. Scuseria. Ab initio calculations of fullerenes. *Science*, 271(5251):942–945, 1996.

M. D. Segall, P. J. D. Lindan, M. J. Probert, C. J. Pickard, P. J. Hasnip, S. J. Clark, and M. C. Payne. First-principles simulation: ideas, illustrations and the CASTEP code. *Journal of Physics: Condensed Matter*, 14(11):2717, 2002.

J. P. Serre. *Linear Representations of Finite Groups*. Springer-Verlag, Berlin, 1977.

J. C. Slater and G. F. Koster. Simplified lcao method for the periodic potential problem. *Phys. Rev.*, 94:1498–1524, 1954.

J. Soler, E. Artacho, J. Gale, A. Garca, J. Junquera, P. Ordejn, and D. Snchez-Portal. The SIESTA method for ab initio order-n materials simulation. *Journal of Physics Condensed Matter*, 14(11):2745–2779, 2002.

U. Stephan, D. A. Drabold, and R. M. Martin. Improved accuracy and acceleration of variational order-n electronic-structure computations by projection techniques. *Physical Review B*, 58(20):13472, 1998.

P. Suryanarayana. private communication, 2013.

P. Suryanarayana, V. Gavini, T. Blesgen, K. Bhattacharya, and M. Ortiz. Non-periodic finite-element formulation of kohn-sham density functional theory. *Journal of the Mechanics and Physics of Solids*, 58(2):256–280, 2010.

P. Suryanarayana, K. Bhattacharya, and M. Ortiz. A mesh-free convex approximation scheme for kohn–sham density functional theory. *Journal of Computational Physics*, 230(13):5226–5238, 2011.

A. Szabo and N. S. Ostlund. *Modern Quantum Chemistry: Introduction to advanced Electronic structure theory*. Dover Publications, first edition, 1996.

E. B. Tadmor and R. E. Miller. *Modeling Materials: Continuum, Atomistic and Multiscale Techniques*. Cambridge University Press, 2011.

G. te Velde and E. Baerends. Numerical integration for polyatomic systems. *Journal of Computational Physics*, 99(1):84 – 98, 1992.

P. P. Teodorescu, N.-D. Stanescu, and N. Pandrea. *Numerical Analysis with Applications in Mechanics and Engineering*. John Wiley & Sons, first edition, 2013.

G. Teschl. *Mathematical Methods in Quantum Mechanics*. Graduate Studies in Mathematics. American Mathematical Society, 2009.

M. P. Teter, M. C. Payne, and D. C. Allan. Solution of schrödinger's equation for large systems. *Physical Review B*, 40:12255–12263, 1989.

Y. Tikochinsky. An addition theorem for spherical harmonics. *Mathematical Proceedings of the Cambridge Philosophical Society*, 63:127, 1967.

N. Troullier and J. L. Martins. Efficient pseudopotentials for plane-wave calculations. *Physical Review B*, 43(3):1993, 1991.

R. A. Van de Geijn. *Using PLAPACK: parallel linear algebra package*. The MIT Press, 1997.

C. Vömel, S. Z. Tomov, O. A. Marques, A. Canning, L.-W. Wang, and J. J. Dongarra. State-of-the-art eigensolvers for electronic structure calculations of large scale nano-systems. *Journal of Computational Physics*, 227(15):7113 – 7124, 2008.

E. W. Weisstein. Condon-Shortley phase. MathWorld–A Wolfram Web Resource., a. URL `http://mathworld.wolfram.com/Condon-ShortleyPhase.html`.

E. W. Weisstein. Halley's method. MathWorld–A Wolfram Web Resource., b. URL http://mathworld.wolfram.com/HalleysMethod.html.

C. T. White, D. H. Robertson, and J. W. Mintmire. Helical and rotational symmetries of nanoscale graphitic tubules. *Physical Review B*, 47:5485–5488, 1993.

C. Wilcox. Theory of bloch waves. *Journal d'Analyse Mathmatique*, 33:146–167, 1978.

K. Yabana and G. F. Bertsch. Electronic structure of C_{60} in a spherical basis. *Physica Scripta*, 48(5):633, 1993.

C. Yang, J. C. Meza, and L.-W. Wang. A constrained optimization algorithm for total energy minimization in electronic structure calculations. *Journal of Computational Physics*, 217(2):709–721, 2006.

D.-B. Zhang, M. Hua, and T. Dumitrica. Stability of polycrystalline and wurtzite si nanowires via symmetry-adapted tight-binding objective molecular dynamics. *The Journal of Chemical Physics*, 128(8):084104, 2008.

D.-B. Zhang, R. D. James, and T. Dumitrica. Electromechanical characterization of carbon nanotubes in torsion via symmetry adapted tight-1054-1060binding objective molecular dynamics. *Physical Review B*, 80(11):115418, 2009.

Y. Zhou. A block Chebyshev–Davidson method with inner–outer restart for large eigenvalue problems. *Journal of Computational Physics*, 229(24):9188–9200, 2010.

Y. Zhou. private communication, 2013.

Y. Zhou, Y. Saad, M. L. Tiago, and J. R. Chelikowsky. Parallel self-consistent-field calculations via chebyshev-filtered subspace acceleration. *Phys. Rev. E*, 74:066704, 2006a.

Y. Zhou, Y. Saad, M. L. Tiago, and J. R. Chelikowsky. Self-consistent-field calculations using chebyshev-filtered subspace iteration. *Journal of Computational Physics*, 219: 172–184, 2006b.

C. M. Zicovich-Wilson and R. Dovesi. On the use of symmetry-adapted crystalline orbitals in scf-lcao periodic calculations. i. the construction of the symmetrized orbitals. *International Journal of Quantum Chemistry*, 67(5):299–309, 1998a.

C. M. Zicovich-Wilson and R. Dovesi. On the use of symmetry-adapted crystalline orbitals in scf-lcao periodic calculations. ii. implementation of the self-consistent-field scheme and examples. *International Journal of Quantum Chemistry*, 67(5):311–320, 1998b.

Appendix A

Laplacian Eigenfunctions in Spherical Coordinates

For the sake of completness, we now derive the basis functions that were used for dealing with all finite structures.[1] As described earlier, these basis functions are essentially eigenfunctions of the Laplacian in a ball with Dirichlet boundary conditions. The eigenvalue problem for the Laplacian in the sphere $\mathcal{B}_R$, with Dirichlet boundary conditions is as follows:

$$-\Delta F = \Lambda F \ , \tag{A.1}$$

$$F = 0 \ \text{ on } x \in \partial\mathcal{B}_R \ . \tag{A.2}$$

We first introduce spherical coordinates for $r \in (0, R], \vartheta \in [0, \pi]$ and $\varphi \in [0, 2\pi]$:

$$\begin{aligned} x &= r \sin\vartheta \cos\varphi \\ y &= r \sin\vartheta \sin\varphi \\ z &= r \cos\vartheta \end{aligned} \tag{A.3}$$

Here, r denotes the radial coordinate, ϑ denotes the polar angle and φ denotes the azimuthal angle. The Cartesian coordinates (x, y, z) are obtained as $x = r\sin\vartheta\cos\varphi,\ y = r\sin\vartheta\sin\varphi,\ z = r\cos\vartheta$.

We set $\Lambda = k^2$ for convenience[2] and note that, the above problem posed in terms of

[1] This material is directly adopted from [Banerjee, 2011]

[2] Note that the Rayleigh quotient form allows us to write the lowest eigenvalue of the Dirichlet Laplace

$\hat{F}(r,\vartheta,\varphi)$, that is, $F(\mathbf{x})$ expressed in spherical coordinates reads as:

$$\frac{1}{r^2}\frac{\partial}{\partial r}\left(r^2\frac{\partial \hat{F}}{\partial r}\right)+\frac{1}{r^2\sin\vartheta}\frac{\partial}{\partial \vartheta}\left(\sin\vartheta\frac{\partial \hat{F}}{\partial \vartheta}\right)+\frac{1}{r^2\sin^2\vartheta}\frac{\partial^2 \hat{F}}{\partial \varphi^2}+k^2\hat{F}=0\ , \tag{A.5}$$

$$\hat{F}(r=R,\vartheta,\varphi)=0\ . \tag{A.6}$$

We use the canonical approach of separation of variables to write:

$$\hat{F}(r,\vartheta,\varphi)=\mathcal{R}(r)\,\Theta(\vartheta)\,\Phi(\varphi)\ .$$

Substituting this ansatz into (A.5) and multiplying by $r^2/(\mathcal{R}\vartheta\varphi)$ gives us:

$$\frac{1}{\mathcal{R}}\frac{d}{dr}\left(r^2\frac{d\mathcal{R}}{dr}\right)+k^2r^2+\frac{1}{\Theta\sin\vartheta}\frac{d}{d\vartheta}\left(\sin\vartheta\frac{d\Theta}{d\vartheta}\right)+\frac{1}{\Phi\sin^2\vartheta}\frac{d^2\Phi}{d\varphi^2}=0\ . \tag{A.7}$$

We multiply (A.7) by $\sin^2\vartheta$ and observe that the last term $\dfrac{1}{\Phi}\left(\dfrac{d^2\Phi}{d\varphi^2}\right)$ only involves φ while the first two terms only depend on r and ϑ. This implies, that the last term must be a constant and so we write:

$$\frac{1}{\Phi}\left(\frac{d^2\Phi}{d\varphi^2}\right)=-m^2\ , \tag{A.8}$$

The solution to (A.8) is $\Phi(\varphi)=e^{im\varphi}$ and to ensure the solution is continuous across the XZ plane, we must have $\Phi(\varphi)=\Phi(\varphi+2\pi s)$ for $s\in\mathbb{Z}$. Thus, we get:

$$\Phi(\varphi)=e^{im\varphi}\ ,\ m\in\mathbb{Z}. \tag{A.9}$$

We substitute this solution into (A.7) and we get:

$$\frac{1}{\mathcal{R}}\frac{d}{dr}\left(r^2\frac{d\mathcal{R}}{dr}\right)+k^2r^2+\frac{1}{\Theta\sin\vartheta}\frac{d}{d\vartheta}\left(\sin\vartheta\frac{d\Theta}{d\vartheta}\right)-\frac{m^2}{\sin^2\vartheta}=0\ . \tag{A.10}$$

Now, we observe that the last two terms in the above equation are a function of ϑ only while the first two depend on r only. Thus, the last two terms must equal a constant, which

---

as:

$$\tilde{\lambda}_1=\inf_{f\in \mathsf{H}^1_0(\mathcal{B}_R)}\frac{\int_{\mathcal{B}_R}|\nabla f|^2}{\int_{\mathcal{B}_R}|f|^2} \tag{A.4}$$

Hence, the lowest eigenvalue is non-negative. Since the only solution to $-\Delta f=0$ with Dirichlet boundary conditions is $f=0$, it must be that $\tilde{\lambda}_1>0$. Hence, all eigenvalues of the Dirichlet Laplacian are positive.

we write as $l(l+1)$ (to ensure no divergence for $\cos\vartheta = 1$ or $\cos\vartheta = -1$) and we get:

$$\frac{1}{\Theta \sin\vartheta}\frac{d}{d\vartheta}\left(\sin\vartheta\frac{d\Theta}{d\vartheta}\right) - \frac{m^2}{\sin^2\vartheta} = -l(l+1)\ . \tag{A.11}$$

We let $\eta = \cos\vartheta$ in the above and obtain the ordinary differential equation:

$$\frac{d}{d\eta}\left[(1-\eta^2)\frac{d\tilde{\Theta}}{d\eta}\right] + \left(l(l+1) - \frac{m^2}{1-\eta^2}\right)\tilde{\Theta}(\eta) = 0\,, \tag{A.12}$$

where $\tilde{\Theta}(\eta) = \Theta(\cos^{-1}\eta)$. Equation (A.12) above is the Associated Legendre equation and so, its solutions are the Associated Legendre Polynomials:

$$\tilde{\Theta}(\eta) = \mathcal{P}_l^m(\eta)\ ,\ l = 0, 1, 2, \ldots \text{ and } m = -l, -(l-1), \ldots, (l-2), (l-1), l\ . \tag{A.13}$$

The functions Θ and Φ are often combined and normalized on the unit sphere to yield the spherical harmonics for $l = 0, 1, 2, \ldots$ and $m = -l, -(l-1), \ldots, (l-1), l$:

$$\mathcal{Y}_l^m(\vartheta, \varphi) = \sqrt{\frac{(2l+1)}{4\pi}\frac{(l-m)!}{(l+m)!}}\,\mathcal{P}_l^m(\cos\vartheta)\, e^{im\varphi}\ . \tag{A.14}$$

Finally it remains to look at the radial equation, which from (A.10) and (A.11) is:

$$\frac{d}{dr}\left(r^2\frac{d\mathcal{R}}{dr}\right) + [k^2r^2 - l(l+1)]\mathcal{R} = 0\ . \tag{A.15}$$

To see this equation in a more recognizable form, we let $\tilde{r} = kr$ and we set $\mathcal{R}(r) = \tilde{\mathcal{R}}(\tilde{r})$. This gives us:

$$\tilde{r}^2\frac{d^2\tilde{\mathcal{R}}}{d\tilde{r}^2} + 2\tilde{r}\frac{d\tilde{\mathcal{R}}}{d\tilde{r}} + [\tilde{r}^2 - l(l+1)]\tilde{\mathcal{R}} = 0\,, \tag{A.16}$$

which is simply, spherical Bessel's differential equation. It's solutions are the so called spherical Bessel and Neumann functions. These functions admit expressions in terms of (the usual) Bessel and Neumann functions (that is, solutions to the usual Bessel equation) and for the purpose of implementation, it is important for us to obtain these expressions. We let $\tilde{\mathcal{R}}(\tilde{r}) = \kappa(\tilde{r})/\sqrt{\tilde{r}}$ and substitute this into the above equation to arrive at (after a bit of algebra):

$$\tilde{r}^2\frac{d^2\kappa}{d\tilde{r}^2} + \tilde{r}\frac{d\kappa}{d\tilde{r}} + [\tilde{r}^2 - (l+\frac{1}{2})^2]\kappa = 0\ . \tag{A.17}$$

This is Bessel's equation of order $(l + \frac{1}{2})$. The general solution is:

$$\kappa(\tilde{r}) = c_1 J_{l+\frac{1}{2}}(\tilde{r}) + c_2 N_{l+\frac{1}{2}}(\tilde{r}) \ , \tag{A.18}$$

where $J_\nu(\cdot)$ and $N_\nu(\cdot)$, denote Bessel functions of the first and second kind respectively. Thus, the solutions to the equation (A.16) are given as:

$$\tilde{\mathcal{R}}(\tilde{r}) = c_1 \frac{J_{l+\frac{1}{2}}(\tilde{r})}{\sqrt{\tilde{r}}} + c_2 \frac{N_{l+\frac{1}{2}}(\tilde{r})}{\sqrt{\tilde{r}}} \ , \tag{A.19}$$

and the solutions to the radial equation (A.15) are given by:

$$\mathcal{R}(r) = c_1 \frac{J_{l+\frac{1}{2}}(kr)}{\sqrt{kr}} + c_2 \frac{N_{l+\frac{1}{2}}(kr)}{\sqrt{kr}} \ . \tag{A.20}$$

The boundary conditions for the problem (A.15) are:

$$\mathcal{R}(R) = 0 \text{ and } \mathcal{R}(0) \text{ is finite.} \tag{A.21}$$

The second condition in the above eliminates the second term from (A.20) while keeping the first term since Bessel functions of the first kind are regular at the origin while the Bessel functions of the second kind are not. The first condition, on the other hand gives us:

$$\mathcal{R}(R) = c_1 \frac{J_{l+\frac{1}{2}}(kR)}{\sqrt{kR}} = 0 \ . \tag{A.22}$$

Thus, we must have $J_{l+\frac{1}{2}}(kR) = 0$, that is, $kR = b^n_{l+\frac{1}{2}}$, where $b^n_{l+\frac{1}{2}}$ is the n^{th} zero of the Bessel function of order $(l + \frac{1}{2})$. We may fix the constant c_1 in (A.20) by using a

normalization condition. In this case, we require:

$$c_1^2 \int_0^R r^2 \left[J_{l+\frac{1}{2}}\left(\frac{b^n_{l+\frac{1}{2}}}{R} r\right) \Big/ \sqrt{\frac{b^n_{l+\frac{1}{2}}}{R} r} \right]^2 dr = 1 \ , \tag{A.23}$$

$$\text{which implies} \ , \quad c_1^2 \frac{R^3}{b^n_{l+\frac{1}{2}}} \int_0^R (r/R) \left[J_{l+\frac{1}{2}}\left(b^n_{l+\frac{1}{2}} \frac{r}{R}\right) \right]^2 d(r/R) = 1 \ ,$$

$$\text{which for } r_1 = r/R \text{ becomes:} \quad c_1^2 \frac{R^3}{b^n_{l+\frac{1}{2}}} \int_0^1 r_1 \left[J_{l+\frac{1}{2}}\left(b^n_{l+\frac{1}{2}}\, r_1\right) \right]^2 dr_1 = 1 \ ,$$

$$\text{and using properties of Bessel functions this becomes:} \quad c_1^2 \frac{R^3}{b^n_{l+\frac{1}{2}}} \frac{1}{2} J^2_{(l+\frac{3}{2})}\left(b^n_{l+\frac{1}{2}}\right) = 1 \ . \tag{A.24}$$

So, we get finally:

$$\mathcal{R}(r) = \frac{1}{R J_{l+\frac{3}{2}}\left(b^n_{l+\frac{1}{2}}\right)} \sqrt{\frac{2}{r}} J_{l+\frac{1}{2}}\left(\frac{b^n_{l+\frac{1}{2}}}{R} r\right) \ , \tag{A.25}$$

$$\text{and} \quad \Lambda_{l,m,n} = k^2 = \left(\frac{b^n_{l+\frac{1}{2}}}{R}\right)^2 . \tag{A.26}$$

Thus, a normalized eigenfunction of the Dirichlet Laplacian on the ball $\mathcal{B}_R$ has the form:

$$\hat{F}_{l,m,n}(r, \vartheta, \varphi) = c_{l,m,n} \frac{1}{\sqrt{r}} J_{l+\frac{1}{2}}\left(\frac{b^n_{l+\frac{1}{2}}}{R} r\right) \mathcal{P}_l^m(\cos\vartheta)\, e^{im\varphi} \ , \tag{A.27}$$

$$\text{with} \quad c_{l,m,n} = \frac{1}{R J_{l+\frac{3}{2}}\left(b^n_{l+\frac{1}{2}}\right)} \sqrt{\frac{(2l+1)}{2\pi} \frac{(l-m)!}{(l+m)!}} \ . \tag{A.28}$$

Appendix B

Laplace Operator in Helical Coordinates

We compute the Laplace operator in Helical coordinates in this Appendix. This is a straightforward but somewhat long calculation and so, we reproduce it here for the sake future reference. With $i, j = 1, \ldots, 3$ and for:

$$\phi(x_1, x_2, x_3) = \hat{\varphi}(r(x_1, x_2, x_3), \theta_1(x_1, x_2, x_3), \theta_2(x_1, x_2, x_3)) \quad , \tag{B.1}$$

we have by the chain rule:

$$\frac{\partial \phi}{\partial x_i} = \frac{\partial \hat{\varphi}}{\partial r}\frac{\partial r}{\partial x_i} + \frac{\partial \hat{\varphi}}{\partial \theta_1}\frac{\partial \theta_1}{\partial x_i} + \frac{\partial \hat{\varphi}}{\partial \theta_2}\frac{\partial \theta_2}{\partial x_i} \quad , \tag{B.2}$$

and further,

$$\begin{aligned}\frac{\partial^2 \phi}{\partial x_i \partial x_j} =& \frac{\partial \hat{\varphi}}{\partial r}\frac{\partial^2 r}{\partial x_i \partial x_j} + \frac{\partial \hat{\varphi}}{\partial \theta_1}\frac{\partial^2 \theta_1}{\partial x_i \partial x_j} + \frac{\partial \hat{\varphi}}{\partial \theta_2}\frac{\partial^2 \theta_2}{\partial x_i \partial x_j} \\ &+ \frac{\partial(\frac{\partial \hat{\varphi}}{\partial r})}{\partial x_j}\frac{\partial r}{\partial x_i} + \frac{\partial(\frac{\partial \hat{\varphi}}{\partial \theta_1})}{\partial x_j}\frac{\partial \theta_1}{\partial x_i} + \frac{\partial(\frac{\partial \hat{\varphi}}{\partial \theta_2})}{\partial x_j}\frac{\partial \theta_2}{\partial x_i} \quad .\end{aligned} \tag{B.3}$$

Clearly, the chain rule applied again to the last 3 terms gives us:

$$\begin{aligned}\frac{\partial(\frac{\partial \hat{\varphi}}{\partial r})}{\partial x_j}\frac{\partial r}{\partial x_i} &= \frac{\partial r}{\partial x_i}\left(\frac{\partial^2 \hat{\varphi}}{\partial r^2}\frac{\partial r}{\partial x_j} + \frac{\partial^2 \hat{\varphi}}{\partial r \partial \theta_1}\frac{\partial \theta_1}{\partial x_j} + \frac{\partial^2 \hat{\varphi}}{\partial r \partial \theta_2}\frac{\partial \theta_2}{\partial x_j}\right) \quad . \\ \frac{\partial(\frac{\partial \hat{\varphi}}{\partial \theta_1})}{\partial x_j}\frac{\partial \theta_1}{\partial x_i} &= \frac{\partial \theta_1}{\partial x_i}\left(\frac{\partial^2 \hat{\varphi}}{\partial \theta_1 \partial r}\frac{\partial r}{\partial x_j} + \frac{\partial^2 \hat{\varphi}}{\partial \theta_1^2}\frac{\partial \theta_1}{\partial x_j} + \frac{\partial^2 \hat{\varphi}}{\partial \theta_1 \partial \theta_2}\frac{\partial \theta_2}{\partial x_j}\right) \quad . \\ \frac{\partial(\frac{\partial \hat{\varphi}}{\partial \theta_2})}{\partial x_j}\frac{\partial \theta_2}{\partial x_i} &= \frac{\partial \theta_2}{\partial x_i}\left(\frac{\partial^2 \hat{\varphi}}{\partial \theta_2 \partial r}\frac{\partial r}{\partial x_j} + \frac{\partial^2 \hat{\varphi}}{\partial \theta_2 \partial \theta_1}\frac{\partial \theta_1}{\partial x_j} + \frac{\partial^2 \hat{\varphi}}{\partial \theta_2^2}\frac{\partial \theta_2}{\partial x_j}\right) \quad .\end{aligned} \tag{B.4}$$

Note that for $i = j$, the above three expressions can be combined to yield:

$$\frac{\partial^2\hat{\varphi}}{\partial x_i^2} = \frac{\partial^2\hat{\varphi}}{\partial r^2}(\frac{\partial r}{\partial x_i})^2 + \frac{\partial^2\hat{\varphi}}{\partial\theta_1^2}(\frac{\partial\theta_1}{\partial x_i})^2 + \frac{\partial^2\hat{\varphi}}{\partial\theta_2^2}(\frac{\partial\theta_2}{\partial x_i})^2 + 2(\frac{\partial^2\hat{\varphi}}{\partial r\partial\theta_1}\frac{\partial r}{\partial x_i}\frac{\partial\theta_1}{\partial x_i} + \frac{\partial^2\hat{\varphi}}{\partial\theta_1\partial\theta_2}\frac{\partial\theta_1}{\partial x_i}\frac{\partial\theta_2}{\partial x_i} + \frac{\partial^2\hat{\varphi}}{\partial\theta_2\partial r}\frac{\partial\theta_2}{\partial x_i}\frac{\partial r}{\partial x_i}) \quad . \tag{B.5}$$

Let us compute term by term now. The helical coordinates and the first derivatives are computed as:

$$\begin{aligned} r(x_1,x_2,x_3) &= \sqrt{x_1^2+x_2^2} \\ \theta_1(x_1,x_2,x_3) &= \frac{x_3}{\tau} \\ \theta_2(x_1,x_2,x_3) &= \frac{1}{2\pi}\arctan(\frac{x_2}{x_1}) - \alpha\frac{x_3}{\tau} \\ \frac{\partial r}{\partial x_1} = \frac{x_1}{\sqrt{x_1^2+x_2^2}} = \frac{x_1}{r}\ ,\ \frac{\partial r}{\partial x_2} &= \frac{x_2}{\sqrt{x_1^2+x_2^2}} = \frac{x_2}{r}\ ,\ \frac{\partial r}{\partial x_3} = 0 \\ \frac{\partial\theta_1}{\partial x_1} = 0\ ,\ \frac{\partial\theta_1}{\partial x_2} &= 0\ ,\ \frac{\partial\theta_1}{\partial x_3} = \frac{1}{\tau} \\ \frac{\partial\theta_2}{\partial x_1} = -\frac{1}{2\pi}\frac{x_2}{x_1^2+x_2^2} = -\frac{1}{2\pi}\frac{x_2}{r^2}\ ,\ \frac{\partial\theta_2}{\partial x_2} &= \frac{1}{2\pi}\frac{x_1}{x_1^2+x_2^2} = \frac{1}{2\pi}\frac{x_1}{r^2}\ ,\ \frac{\partial\theta_2}{\partial x_3} = -\frac{\alpha}{\tau} \quad . \end{aligned} \tag{B.6}$$

We now compute the second derivatives of r, θ_1, θ_2 but we restrict ourselves only to the ones which would appear in the Laplacian:

$$\begin{aligned} \frac{\partial^2 r}{\partial x_1^2} = \frac{1}{r} - \frac{x_1^2}{r^3},\quad \frac{\partial^2\theta_1}{\partial x_1^2} = 0,\quad \frac{\partial^2\theta_2}{\partial x_1^2} &= \frac{1}{2\pi}\frac{2x_1x_2}{r^4}, \\ \frac{\partial^2 r}{\partial x_2^2} = \frac{1}{r} - \frac{x_2^2}{r^3},\quad \frac{\partial^2\theta_1}{\partial x_2^2} = 0,\quad \frac{\partial^2\theta_2}{\partial x_2^2} &= -\frac{1}{2\pi}\frac{2x_1x_2}{r^4}, \\ \frac{\partial^2 r}{\partial x_3^2} = 0,\quad \frac{\partial^2\theta_1}{\partial x_3^2} = 0,\quad \frac{\partial^2\theta_2}{\partial x_3^2} &= 0 \quad . \end{aligned} \tag{B.7}$$

We are now ready to evaluate (B.3) through (B.5), (B.6) and (B.7):

$$\begin{aligned} \frac{\partial^2\phi}{\partial x_1^2} &= \frac{\partial\hat{\varphi}}{\partial r}\frac{\partial^2 r}{\partial x_1^2} + \frac{\partial\hat{\varphi}}{\partial\theta_1}\frac{\partial^2\theta_1}{\partial x_1^2} + \frac{\partial\hat{\varphi}}{\partial\theta_2}\frac{\partial^2\theta_2}{\partial x_1^2} + \frac{\partial^2\hat{\varphi}}{\partial r^2}(\frac{\partial r}{\partial x_1})^2 + \frac{\partial^2\hat{\varphi}}{\partial\theta_1^2}(\frac{\partial\theta_1}{\partial x_1})^2 + \frac{\partial^2\hat{\varphi}}{\partial\theta_2^2}(\frac{\partial\theta_2}{\partial x_1})^2 \\ &\quad + 2(\frac{\partial^2\hat{\varphi}}{\partial r\partial\theta_1}\frac{\partial r}{\partial x_1}\frac{\partial\theta_1}{\partial x_1} + \frac{\partial^2\hat{\varphi}}{\partial\theta_1\partial\theta_2}\frac{\partial\theta_1}{\partial x_1}\frac{\partial\theta_2}{\partial x_1} + \frac{\partial^2\hat{\varphi}}{\partial\theta_2\partial r}\frac{\partial\theta_2}{\partial x_1}\frac{\partial r}{\partial x_1}) \\ &= \hat{\varphi}_r(\frac{1}{r} - \frac{x_1^2}{r^3}) + \hat{\varphi}_{\theta_2}(\frac{x_1x_2}{\pi r^4}) + \hat{\varphi}_{rr}\frac{x_1^2}{r^2} + \hat{\varphi}_{\theta_1\theta_2}(\frac{x_2^2}{4\pi^2r^4}) - \hat{\varphi}_{\theta_2 r}(\frac{x_1x_2}{\pi r^3}) \quad . \end{aligned} \tag{B.8}$$

Similarly,

$$\begin{aligned}\frac{\partial^2\phi}{\partial x_2^2} &= \frac{\partial\hat{\varphi}}{\partial r}\frac{\partial^2 r}{\partial x_2^2} + \frac{\partial\hat{\varphi}}{\partial\theta_1}\frac{\partial^2\theta_1}{\partial x_2^2} + \frac{\partial\hat{\varphi}}{\partial\theta_2}\frac{\partial^2\theta_2}{\partial x_2^2} + \frac{\partial^2\hat{\varphi}}{\partial r^2}(\frac{\partial r}{\partial x_2})^2 + \frac{\partial^2\hat{\varphi}}{\partial\theta_1^2}(\frac{\partial\theta_1}{\partial x_2})^2 + \frac{\partial^2\hat{\varphi}}{\partial\theta_2^2}(\frac{\partial\theta_2}{\partial x_2})^2 \\ &\quad + 2(\frac{\partial^2\hat{\varphi}}{\partial r\partial\theta_1}\frac{\partial r}{\partial x_2}\frac{\partial\theta_1}{\partial x_2} + \frac{\partial^2\hat{\varphi}}{\partial\theta_1\partial\theta_2}\frac{\partial\theta_1}{\partial x_2}\frac{\partial\theta_2}{\partial x_2} + \frac{\partial^2\hat{\varphi}}{\partial\theta_2\partial r}\frac{\partial\theta_2}{\partial x_2}\frac{\partial r}{\partial x_2}) \\ &= \hat{\varphi}_r(\frac{1}{r} - \frac{x_2^2}{r^3}) - \hat{\varphi}_{\theta_2}(\frac{x_1x_2}{\pi r^4}) + \hat{\varphi}_{rr}\frac{x_2^2}{r^2} + \hat{\varphi}_{\theta_2\theta_2}\frac{x_1^2}{4\pi^2r^4} + \hat{\varphi}_{\theta_2 r}\frac{x_1x_2}{\pi r^3} \quad . \end{aligned} \tag{B.9}$$

and,

$$\begin{aligned}\frac{\partial^2\phi}{\partial x_3^2} &= \frac{\partial\hat{\varphi}}{\partial r}\frac{\partial^2 r}{\partial x_3^2} + \frac{\partial\hat{\varphi}}{\partial\theta_1}\frac{\partial^2\theta_1}{\partial x_3^2} + \frac{\partial\hat{\varphi}}{\partial\theta_2}\frac{\partial^2\theta_2}{\partial x_3^2} + \frac{\partial^2\hat{\varphi}}{\partial r^2}(\frac{\partial r}{\partial x_3})^2 + \frac{\partial^2\hat{\varphi}}{\partial\theta_1^2}(\frac{\partial\theta_1}{\partial x_3})^2 + \frac{\partial^2\hat{\varphi}}{\partial\theta_2^2}(\frac{\partial\theta_2}{\partial x_3})^2 \\ &\quad + 2(\frac{\partial^2\hat{\varphi}}{\partial r\partial\theta_1}\frac{\partial r}{\partial x_3}\frac{\partial\theta_1}{\partial x_3} + \frac{\partial^2\hat{\varphi}}{\partial\theta_1\partial\theta_2}\frac{\partial\theta_1}{\partial x_3}\frac{\partial\theta_2}{\partial x_3} + \frac{\partial^2\hat{\varphi}}{\partial\theta_2\partial r}\frac{\partial\theta_2}{\partial x_3}\frac{\partial r}{\partial x_3}) \\ &= \hat{\varphi}_{\theta_1\theta_1}\frac{1}{\tau^2} + \hat{\varphi}_{\theta_2\theta_2}\frac{\alpha^2}{\tau^2} - 2\hat{\varphi}_{\theta_1\theta_2}\frac{\alpha}{\tau^2} \quad . \end{aligned} \tag{B.10}$$

So we have finally:

$$\begin{aligned}\Delta\phi &= \frac{\partial^2\phi}{\partial x_1^2} + \frac{\partial^2\phi}{\partial x_2^2} + \frac{\partial^2\phi}{\partial x_3^2} \\ &= \hat{\varphi}_{rr} + \frac{1}{r}\hat{\varphi}_r + \frac{1}{\tau^2}\hat{\varphi}_{\theta_1\theta_1} - \frac{2\alpha}{\tau^2}\hat{\varphi}_{\theta_1\theta_2} + \frac{1}{4\pi^2}(\frac{1}{r^2} + \frac{4\pi^2\alpha^2}{\tau^2})\hat{\varphi}_{\theta_2\theta_2} \quad . \end{aligned} \tag{B.11}$$

Appendix C

Hilbert Space Miscellany

We present miscellaneous useful concepts and results related to Hilbert spaces in this Appendix.

C.1 Hilbert Projection Theorem

Here we state and prove the Hilbert projection theorem:

Theorem C.1.1. *Let* H *be a Hilbert space with a closed subspace* $\mathcal{M}$*. Let* $\mathcal{M}^\perp$ *denote the orthogonal subspace of* $\mathcal{M}$*. Then any* $f \in \mathsf{H}$ *admits the unique representation* $f = f_1 + f_2$*, with* $f_1 \in \mathcal{M}, f_2 \in \mathcal{M}^\perp$*.*

Proof: Let $f \in \mathsf{H}$ be given. To find $f_1 \in \mathcal{M}, f_2 \in \mathcal{M}^\perp$ such that $f = f_1 + f_2$, we define:

$$f_1 = \text{argmin}_{y \in \mathcal{M}} \|f - y\|_{\mathsf{H}}, \quad f_2 = f - f_1. \tag{C.1}$$

To see the existence and uniqueness of such $f_1 \in \mathcal{M}$, we consider a minimizing sequence $\{y_n\}_{n=1}^\infty \subset \mathcal{M}$ and let $\alpha = \inf_{y \in \mathcal{M}} \|f - y\|_{\mathsf{H}}$. Then by definition of a minimizing sequence, $\|f - y_n\|_{\mathsf{H}} \to \alpha$ as $n \to \infty$ and each $y_n \in \mathcal{M}$. We actually intend to show that $\{y_n\}_{n=1}^\infty$ is a Cauchy sequence since that would imply by the closedness of $\mathcal{M}$ in the complete space H that there exists $x_0 \in \mathcal{M}$ such that $\{y_n\} \to x_0$. The continuity of the norm would then imply that $\|f - x_0\|_{\mathsf{H}} = \lim_{n \to \infty} \|f - y_n\|_{\mathsf{H}} = \alpha$, thus establishing existence. Now, to see that $\{y_n\}_{n=1}^\infty$ is Cauchy, we first observe that $\forall m, n \in \mathbb{N}$, $\frac{y_m + y_n}{2} \in \mathcal{M}$ and so,

$\|f - \frac{y_m+y_n}{2}\|_{\mathsf{H}} \geq \alpha$. We then have, by the parallelogram identity:

$$\begin{aligned}\|y_m - y_n\|_{\mathsf{H}}^2 &= \|(y_m - f) - (y_n - f)\|_{\mathsf{H}}^2 \\ &= 2(\|(y_m - f)\|_{\mathsf{H}}^2 + \|(y_n - f)\|_{\mathsf{H}}^2) - \|(y_m - f) + (y_n - f)\|_{\mathsf{H}}^2 \\ &= 2(\|(y_m - f)\|_{\mathsf{H}}^2 + \|(y_n - f)\|_{\mathsf{H}}^2) - 4\|(f - \frac{y_m + y_n}{2})\|_{\mathsf{H}}^2 \\ &\leq 2(\|(y_m - f)\|_{\mathsf{H}}^2 + \|(y_n - f)\|_{\mathsf{H}}^2) - 4\alpha^2 \end{aligned} \tag{C.2}$$

Clearly, as $m, n \to \infty$ in (C.2) above, we get:

$$\lim_{m,n\to\infty} \|y_m - y_n\|_{\mathsf{H}}^2 = 2(\alpha^2 + \alpha^2) - 4\alpha^2 = 0. \tag{C.3}$$

We can also see easily that uniqueness holds since if x_0, x_0^* are both solutions to the minimization problem, then $\|f - x_0\|_{\mathsf{H}} = \|f - x_0^*\|_{\mathsf{H}} = \alpha$. Then, by a calculation similar to the one above:

$$\begin{aligned}\|x_0 - x_0^*\|_{\mathsf{H}}^2 &= \|(x_0 - f) - (x_0^* - f)\|_{\mathsf{H}}^2 \\ &\leq 2(\|(x_0 - f)\|_{\mathsf{H}}^2 + \|(x_0^* - f)\|_{\mathsf{H}}^2) - 4\alpha^2 = 0. \end{aligned} \tag{C.4}$$

Thus, we have, $x_0 = x_0^*$. It now remains to show that $f_2 = f - f_1$ lies in $\mathcal{M}^\perp$. To see this, we observe that f_1 being the solution of the minimization problem $f_1 = \text{argmin}_{y\in\mathcal{M}}\|f - y\|_{\mathsf{H}}$ implies the first variation condition:

$$\begin{aligned}&\frac{d}{d\eta}\|f - (f_1 + \eta y)\|_{\mathsf{H}}\Big|_{\eta=0} = 0,\ \forall y \in \mathcal{M} \\ &\implies \text{Re}(\langle f - f_1, y\rangle_{\mathsf{H}}) = 0,\ \forall y \in \mathcal{M} \\ &\implies \langle f - f_1, y\rangle_{\mathsf{H}} = 0,\ \forall y \in \mathcal{M} \end{aligned} \tag{C.5}$$

Hence $f_2 \in \mathcal{M}^\perp$. The last step follows since we can multiply y with suitable scalars and make the inner product real valued and since $\mathcal{M}$ is a subspace, it is closed under multiplication by arbitrary scalars. We would also like to point out that the orthogonality condition (C.5) actually characterizes the minimizer: For given $f \in \mathsf{H}$, if $f_1 \in \mathcal{M}$ satisfies (C.5), then f_1 is the unique minimizer to the minimization problem $\inf_{y\in\mathcal{M}} \|f - y\|_{\mathsf{H}}$. This is because, for an arbitrary $y \in \mathcal{M}$, we have that $f_1 - y \in \mathcal{M}$. Now,

$$\begin{aligned}\|f - y\|_{\mathsf{H}}^2 &= \|(f - f_1) - (y - f_1)\|_{\mathsf{H}}^2 \\ &= \|f - f_1\|_{\mathsf{H}}^2 + \|y - f_1\|_{\mathsf{H}}^2 + \langle f - f_1, y - f_1\rangle_{\mathsf{H}} + \langle y - f_1, f - f_1\rangle_{\mathsf{H}}. \end{aligned} \tag{C.6}$$

Since the last two terms are zero by (C.5) we have

$$\forall y \in \mathcal{M}, \|f - y\|_{\mathsf{H}} \geq \|f - f_1\|_{\mathsf{H}}, \tag{C.7}$$

with the equality holding if and only if $y = f_1$.

Finally, if $f = f_1 + f_2 = \tilde{f}_1 + \tilde{f}_2$ with $f_1, \tilde{f}_1 \in \mathcal{M}$ and $f_2, \tilde{f}_2 \in \mathcal{M}^{\perp}$, then $f_1 - \tilde{f}_1 = \tilde{f}_2 - f_2 \in \mathcal{M} \cap \mathcal{M}^{\perp} = \{0\}$. Hence, $f_1 = \tilde{f}_1$ and $f_2 = \tilde{f}_2$, making the decomposition unique. ■

C.2 Direct Sums of Hilbert Spaces

Our primary sources for this material are Folland [1999] and Folland [1994]. We begin by recalling that given an arbitrary collection of sets $\{S_\alpha\}, \alpha \in \mathcal{A}$, the Cartesian product of the sets $S = \prod_{\alpha \in \mathcal{A}} S_\alpha$ is the collection of all functions $f : \mathcal{A} \to \bigcup_{\alpha \in \mathcal{A}} S_\alpha$ such that $f(\alpha) \in S_\alpha, \forall \alpha \in \mathcal{A}$. We may now deifne:

Definition C.2.1. Let $\{\mathsf{H}_\alpha\}_{\alpha \in \mathcal{A}}$ be a family of Hilbert spaces. The direct sum $\bigoplus_{\alpha \in \mathcal{A}} \mathsf{H}_\alpha$ is the set of all $v = (v_\alpha)_{\alpha \in \mathcal{A}}$ in the Cartesian product $\Pi_{\alpha \in \mathcal{A}} \mathsf{H}_\alpha$ such that $\sum_{\alpha \in \mathcal{A}} \|v_\alpha\|^2_{\mathsf{H}_\alpha} < \infty$. Since any uncountable sum of positive quantities is necessarily infinite, it must be that $v_\alpha = 0$ for all but countably many α. □

We express this relationship as $\mathsf{H} = \bigoplus_{\alpha \in \mathcal{A}} \mathsf{H}_\alpha$ and we note that H itself is a Hilbert space with inner product:

$$\langle u, v \rangle_{\mathsf{H}} = \sum_{\alpha \in \mathcal{A}} \langle u_\alpha, v_\alpha \rangle_{\mathsf{H}_\alpha} \tag{C.8}$$

The summands H_α are embedded in H as mutually orthogonal closed subspaces. Conversely, if H is a Hilbert space and $\{\mathcal{M}_\alpha\}_{\alpha \in \mathcal{A}}$ is a family of mutually orthogonal closed subspaces of H whose linear span is dense in H, we may identify $\mathsf{H} = \bigoplus_{\alpha \in \mathcal{A}} \mathcal{M}_\alpha$. Henceforth, when we speak of direct sums of subspaces of a Hilbert space, we will always assume that the subspaces are mutually orthogonal.

C.3 Classification of the Spectra of Operators

We find it instructive to elaborate on the various possibilities that one can encounter while discussing the spectral properties of an arbitrary operator on a Banach Space. We hope that this presentation will also elucidate some of the technical terms used in the thesis. The material in this Appendix has been taken from Renardy and Rogers [2004].

Let $\mathcal{X}$ be a non-empty Banach space over the field of complex numbers. Let A be an arbitrary operator on $\mathcal{X}$ with domain Dom.$(A) \subset \mathcal{X}$ and let I denote the identity operator on $\mathcal{X}$. For any $\lambda \in \mathbb{C}$, we may define the operator $A_\lambda = A - \lambda I$ on $\mathcal{X}$ also with domain Dom.(A). If A_λ has an inverse that is, if it is one to one, then we call the inverse the resolvent of A and we denote it as $R_\lambda(A)$. We now consider the following three conditions:

1. $R_\lambda(A)$ exists.
2. $R_\lambda(A)$ is a bounded operator.
3. The domain of $R_\lambda(A)$ is dense in $\mathcal{X}$.

Accordingly, decompose the complex plane as per the following rules:

1. The resolvent set of A is the set:

$$\mathcal{R}(A) = \{\lambda \in \mathbb{C} : (1),(2) \text{ and } (3) \text{ hold true}\} \quad . \tag{C.9}$$

   We say λ is a regular value of A if $\lambda \in \mathcal{R}(A)$. The operator valued map $R(\lambda, A) : \mathcal{R}(A) \to \mathcal{L}(\mathcal{X})$ is often called the resolvent map.

2. The spectrum of A is the set:

$$\sigma(A) = \mathbb{C} \backslash \mathcal{R}(A) \quad . \tag{C.10}$$

   The spectrum of A can be decomposed into three disjoint sets. The point spectrum of A is the set:

$$\sigma_p(A) = \{\lambda \in \sigma(A) : (1) \text{ does not hold}\} \quad . \tag{C.11}$$

   This is by far the most important set as far as the work in this thesis is concerned. Clearly, if $\lambda \in \sigma_p(A)$, then the null space of $R_\lambda(A)$ is non-trivial. We call the elements of the nullspace of $R_\lambda(A)$ the eigenfunctions of A for the eigenvalue $\lambda \in \sigma_p(A)$ and the dimension of the null space is called the multiplicity of the eigenvalue λ. Finally, continuous spectrum of A is the set:

$$\sigma_c(A) = \{\lambda \in \sigma(A) : (1) \text{ and } (3) \text{ hold, but } (2) \text{ does not hold}\} \quad , \tag{C.12}$$

   while the residual spectrum of A is the set:

$$\sigma_r(A) = \{\lambda \in \sigma(A) : (1) \text{ holds, but } (3) \text{ does not hold}\} \quad . \tag{C.13}$$

C.4 Proof of Proposition 3.1.3

We recall that A commutes with B means that $B\big(\text{Dom.}(A)\big) \subset \text{Dom.}(A)$ and that for every $y \in \text{Dom.}(A)$, we have $BAy = ABy$. Clearly, this happens if and only if $(A - \kappa I)$ and B commute for any $\kappa \in \mathbb{C}$. Now, for $y \in \text{Dom.}(A)$, and any κ in the resolvent set of A, we consider the expression $(A - \kappa I)By = B(A - \kappa I)y$. Since κ is in the resolvent set, $(A - \kappa I)^{-1}$ is a bounded linear operator. So we may operate on the above expression with $(A-\kappa I)^{-1}$ to conclude that A commutes with B if and only if $By = (A-\kappa I)^{-1}B(A-\kappa I)y$ for every $y \in \text{Dom.}(A)$. Now, since A is a closed operator, the closed graph theorem [Folland, 1999] can be used to extend $(A - \kappa I)^{-1} : \text{Ran.}(A - \kappa I) \to \text{Dom.}(A)$ to $(A - \kappa I)^{-1} : \mathcal{X} \to \text{Dom.}(A)$. Hence, we may express every $y \in \text{Dom.}(A)$ as $y = (A - \kappa I)^{-1}z$ for some $z \in \mathcal{X}$. Hence by expressing y in this form, we conclude that A commutes with B if and only if $B(A-\kappa I)^{-1}z = (A-\kappa I)^{-1}Bz$ for every $z \in \mathcal{X}$. Thus, we conclude, that A and B commute if and only if the resolvent $\mathcal{R}(\kappa, A)$ of A, commutes with B for some κ in the resolvent set of A. Since nothing special about κ, other than that it belongs to the resolvent set of A, we may infer that A commutes with B if and only if $\mathcal{R}(\kappa, A)$ commutes with B for every κ in the resolvent set of A. This completes the proof. ■